IAHR 2017

37th IAHR WORLD CONGRESS

13-18 August, 2017

Kuala Lumpur, Malaysia

GREEN INFRA AS DISASTER RISK REDUCTION MEASURES IN THE ASIAN-PACIFIC REGION

Lead Speaker: Hyoseop Woo

A SMALL MULTIPURPOSE RETARDING BASIN IN UGM CAMPUS AREA

JOKO SUJONO[(1)], MUHAMMAD SULAIMAN[(2)] & RACHMAD JAYADI[(3)]

[(1,3)]Department of Civil and Environmental Engineering, Faculty of Engineering, Universitas Gadjah Mada, Yogyakarta, Indonesia
jsujono@ugm.ac.id; [(3)]rjayadi@ugm.ac.id
[(2)]Civil Engineering, Vocational School, Universitas Gadjah Mada, Yogyakarta, Indonesia
muhammad.sulaiman@ugm.ac.id

ABSTRACT

Flood events and magnitude of Belik River, which flows through Universitas Gadjah Mada (UGM) campus area, is expected to become more frequent in coming years. On December 30, 2012, there was a big flood causing a school dormitory wall at Sagan village to collapse. In 2013 alone, at least three times that flooding have occurred in the area. Floods due to overflowing Belik River inundate some villages located at downstream of the UGM area. For flood mitigation, efforts involving the managing and control of flood are required for reducing flood impacts. One possibility to be done is to build a new retention and detention ponds in the UGM area as an addition of the existing retention pond. In line with the UGM plans to become an educopolis campus, a multipurpose detention pond is more suitable, which also can serve as a means of learning, sports and recreation. Hydrologic analysis that consists of hydrograph inflow and routing through the pond at certain return periods were done by using HEC-HMS software. The analysis showed that the addition of an existing retention pond, a new detention pond is only able to reduce the 2 and 5 years flood return period up to 28.4% and 22.3%, respectively. The simulation result indicates that despite construction of both detention and retention ponds, flooding still occurs downstream due to small size of the ponds and small carrying capacity of the river. However, during dry season or low water flow, the retention and detention ponds may give additional advantages such as for raw water sources, recreation and sport as well as outdoor lectures.

Keywords: Retarding basin; retention basin; flood mitigation.

1 INTRODUCTION

Belik river is a very small river that flows from just north of the Universitas Gadjah Mada (UGM) Yogyakarta-Indonesia to the south through the valley of the campus. In the rainy season, the river often causes flooding in some places because the river capacity is smaller than the discharge flow. The flood occurs several times a year. A major flood occurred on December 28, 2012 which causing inundation in some area just downstream of the campus area. Belik river flood's frequency and magnitude over the years has been increasing. In the year 2013, at least three (3) times major flood events has been recorded affecting the resident areas along the river Belik, especially south of the UGM. Recently, Belik river flood occurs more frequently. Beside heavy storms in the area, these floods also indicate that there is remarkable change in land use characteristics in the Belik catchment area, especially in the north of the UGM campus, so the surface runoff has become higher than before. In addition to land use change and heavy storm, other problems emerge in the Belik river, i.e. water polution and river ecology especially during dry season where the river flow is very small.

Belik river restoration project in the UGM campus area that started from 2014 has been doing wroks including constructing a new retention and detention ponds in additon to the existing retention pond. The retention pond has a function as a main raw water source for dringking water entirely the campus area as well as for groundwater recharge, whereas the detention pond or retarding pond as a temporary storage is used for reducing flood flow downstream for a certain period of time. A good example of retarding pond is Tsurumi river, which is a multipurpose retarding basin in Japan. This retarding basin has a storage capacity of 3.9 milion m^3 and it can reduce flood peak downstream up to 25% (Japanriver, 2013). Beside flood reduction, the retarding basin has other functions including recreation, sport, nature and health facilities.
.

2 METHODS

2.1 Study sites

The Belik river is a located in the UGM campus area, Yogyakarta, Indonesia, whereas the headwater area is located just north of the campus as depicted in Figure 1. The Belik river at the campus has a catchment area of 1.38 km^2 and main length of the river is 2.05 km. Belik river restoration in terms of ponds is given in Figure 1, where as the Belik river condition is given in Figure 2 (Sujono, 2015). These figures explain that the river is small, but the flood often destroyed the downstream area. On the other hand, during dry season, there is not enough flow water and quality of water is low.

 / ISSN 1562-6865 (Online) - ISSN 1063-7710 (Print)

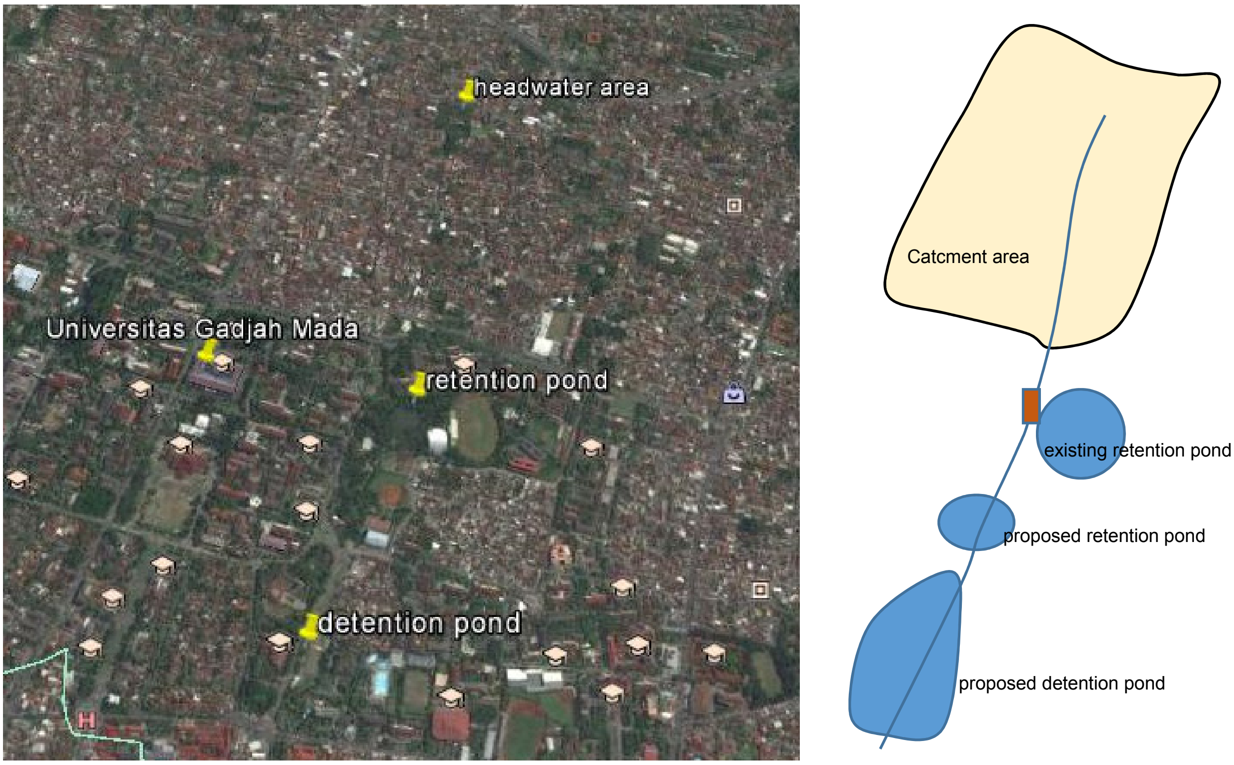

Figure 1. Study location in the UGM campus area

Figure 2. The Belik river condition

2.2 Data availability

Data needed for simulation include rainfall data, landuse and pond characteristics. Daily rainfall data from 1986-2004 was obtained from a rainfall station located in campus area (Directorate of Planning and Development UGM, 2006), whereas the rainfall distribution patern is based on storm event on January 24, 2017 (CEED UGM, 2017) as given in Table 1. This event was selected due to the storm causing flood in several parts of Yogyakarta city. Landuse and soil type were used to estimate the Curve Number (CN) value used for computing runoff volume. The pond characteristics are presented in Table 2 (Sujono, 2015). In the Belik river there is no water level recorder, thus flood hydrographs were computed through rainfall-runoff transformation.

Table 1. Rainfall pattern in the study area

Time	Rainfall intensity (mm/hr)	Rainfall depth (mm)	Percentage (%)
12:35	0.00	0.00	0.00
12:40	0.00	0.00	0.00
12:45	5.75	0.48	0.49
12:50	57.48	4.79	4.90
12:55	114.96	9.58	9.80
13:00	155.20	12.93	13.24
13:05	149.45	12.45	12.75
13:10	172.44	14.37	14.71
13:15	149.45	12.45	12.75
13:20	86.22	7.19	7.35
13:25	86.22	7.19	7.35
13:30	86.22	7.19	7.35
13:35	45.98	3.83	3.92
13:40	11.50	0.96	0.98
13:45	5.75	0.48	0.49
13:50	5.75	0.48	0.49
13:55	5.75	0.48	0.49
14:00	17.24	1.44	1.47
14:05	11.50	0.96	0.98
14:10	5.75	0.48	0.49
14:15	0.00	0.00	0.00
	Total	97.72	100.00

Table 2. Retention and detention pond characteristics

Existing retention pond		Proposed retention pond		Proposed detention pond	
Elevation (+m)	Volume ($1000m^3$)	Elevation (+m)	Volume ($1000m^3$)	Elevation (+m)	Volume ($1000m^3$)
129.5	0.00	126.0	0.00	120.1	0.00
130.0	2.62	126.5	0.33	120.5	0.48
130.5	5.39	127.0	1.55	121.0	2.41
131.0	8.42	127.5	3.00	121.5	4.99
131.5	11.71	128.0	4.45	122.0	8.40
132.0	15.15	128.5	5.90	122.5	12.49

2.3 Rainfall-runoff transformation

Rainfall-runoff transformation was carried out by using HEC-HMS version 4.2 (Ford et al., 2008). This transformation requires input data as follows:

a. Design rainfall for several of return periods were obtained from the nearest location. The design rainfall as given in Table 3 was analyzed based on annual maximum daily rainfall for the period of 1986-2004. The design rainfall is then distributed according to rainfall distribution pattern as given in Table 1
b. SCS-CN method (Chow et al.,1988) is selected for loss model for computing volume runoff. Based on landuse and soil data, it is estimated that CN(II) equal to 77.0 and for wet condition CN(III) is 88.5. Instead of using 0.2 for initial abstraction ratio in the SCS-CN method, the value of 0.05 was applied. This value is more appropriate for the study area (Sujono, 2011).
c. Nakayasu synthetic unit hydrograph (Soemarto, 1995; Jung and Moon, 2001) is used for transform method.
d. Constant baseflow of 0.5 m3/s is applied for the simulation.
e. Flood routing through ponds is carried out using level pool routing approach. Pond characteristics are given in Table 3, whereas broad crested spillway with orifice is chosen for detention pond spillway.

Table 3. Design rainfall

Return period (year)	Design rainfall (mm)
1.1	68
2	95
5	120
10	137

3 RESULTS AND DISCUSSIONS

3.1 Rainfall-runoff simulation

Simulation results show that both retention and detention ponds could reduce flood peak up to 28.4%, 22.3% and 18.5% for 2, 5, and 10 years return period, respectively as given in Table 4, whereas the inflow and outflow hydrographs through the series of ponds for 2 and 5 years return period are given in Figure 3 and Figure 4. Those flood reductions are quite small due to limited storage capacity of the ponds. The peak outflow from the detention pond still causes flood at downstream, since the carrying capacity of the river is quite small, i.e. about 4.0 m^3/s.

Table 4. Flood peak reduction through series of ponds

Return period (year)	Peak inflow (m^3/s)	Peak outflow (m^3/s)	Peak reduction (%)
2	8.18	5.86	28.4
5	11.35	8.82	22.3
10	13.88	11.31	18.5

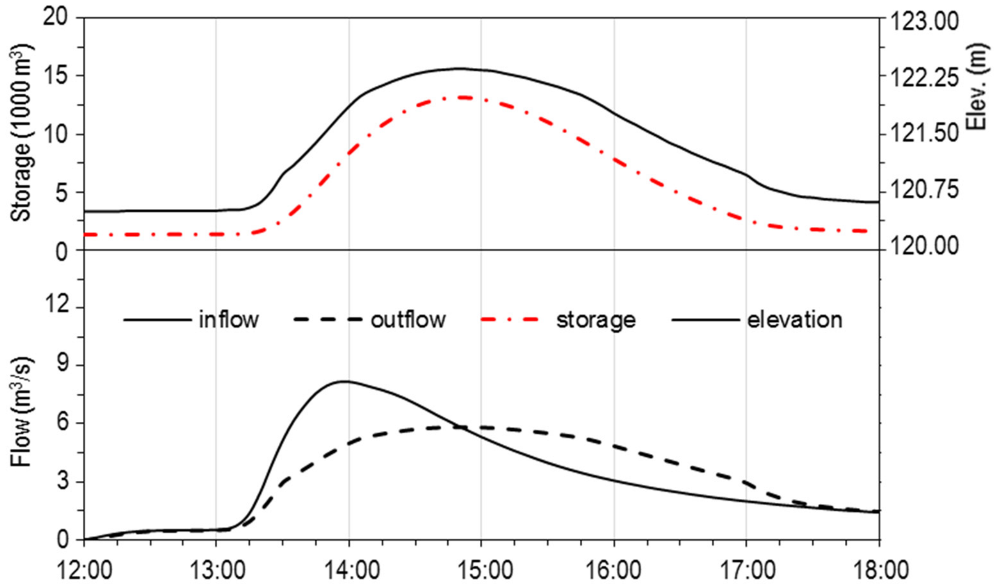

Figure 3. Flood routing through series of ponds for 2 year return period

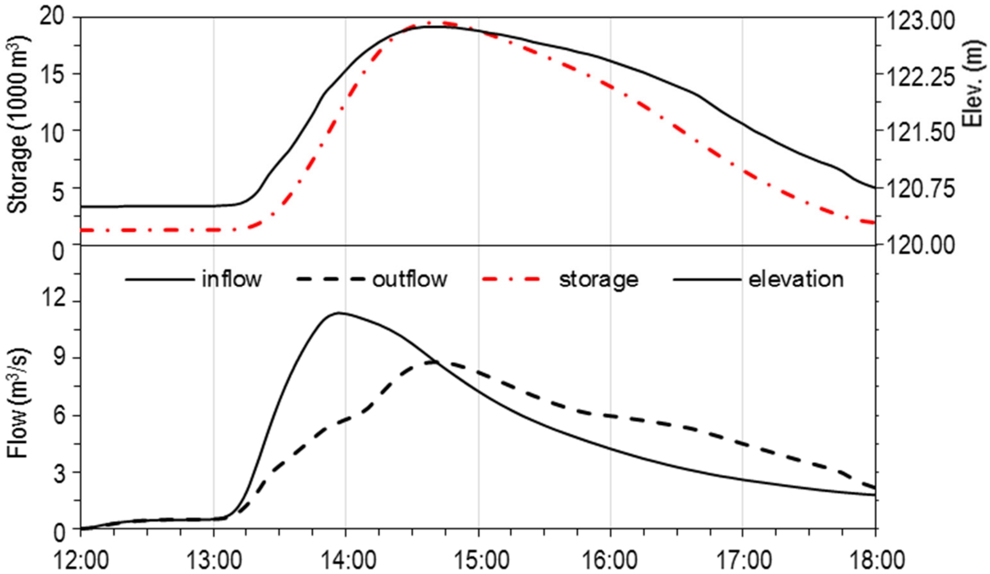

Figure 4. Flood routing through series of ponds for 5 year return period

3.2 Reducing stormwater runoff

Increasing ponds storage is not possible due to limited area, reducing surface runoff can be carried out by increasing stormwater infiltration in the Belik catchment. Number of techniques for reducing storm runoff/increasing stormwater infiltration could be applied by implementing zero runoff approach in which stromwater for a certain depth (say for 2 years return period) should be retained in the rainfall area. The approach includes recharge well and rain garden as shown in Figure 5. In the study area, recharge well is promising approach for reducing surface runoff because soil type of the area is mostly sandy soil. The infiltration rate of this soil is very high. Rain garden can be effective for storing rainfall water by increasing levee height about 10cm above the soil surface. It means that rainfall with 2 year period can be retained in the rain garden without overflow.

Figure 5. Recharge well and rain garden

3.3 Other functions

The Belik river restoration that is called “wisdom park” has multiple functions such as for flood reduction, recharge area, raw water sources, recreation and sport as well as outdoor lectures. Those functions, for instance, are given in Figure 6. Academic and the community surrounding campus area can spend their time in the park for having sport and recreational activities and even doing academic lectures. (Universitas Gadjah Mada, 2014).

Figure 6. Multifunctions of Belik river area

4 CONCLUSIONS

Based on the study, it can be concluded that by constructing both retention and detention ponds of Belik River inthe UGM campus area, flooding still occurs at the downstream area of the campus, which is mainly due to limited storage of the pond and carrying capacity of the river is too small. Eventhough flood peak reduction is less than 30%, Belik river restoration project has other advantages including for raw water sources for dringking water entirely campus, sport and recreation as well as for academic activities. Flood peak reduction could be improved by applying zero runoff approach in catchment area.

ACKNOWLEDGEMENTS

The authors thank the Department of Civil and Environmental Engineering, Faculty of Engineering and Directorate of Planning and Development, Universitas Gadjah Mada for supporting the research.

.

REFERENCES

CEED UGM. (2017). *Remote Monitoring* Hydraulics Laboratory Civil and Environmental Engineering Department Universitas Gadjah Mada – INDONESIA BO/CO (UGM-Sipil) http://data.hydraulic.lab.cee-ugm.ac.id/ugm-cee/ [accessed, February 27, 2017].

Chow, V.T., Maidment, M.R. & Mays, L.W. (1988). *Applied Hydrology*, McGraw-Hill, New York.

Directorate of Planning and Development UGM. (2006). *Survei Drainasi Lingkungan Kampus UGM*. Research Report, UGM.

Ford, D., Pingel, N., J.J. DeVries & J.J. (2008). *Hydrologic Modeling System*, HEC-HMS: Application Guide, US Army Corps of Engineers, Hydrologic Engineering Center, Davis, California.

Jung, S. & Moon, J. (2001). The Comparison of Existing Synthetic Unit Hydrograph Method in Korea. *Journal of Korea Water Resources Association*, 34(6), 659-672.

Japanriver (2013). *Protecting People from Flooding: Tsurumi River Multipurpose Retarding Basin*, http://www.japanriver.or.jp/EnglishDocument/DB/file/004%20Kanto%2023/02.htm (accessed, April 23, 2013).

Sujono, J. (2011). Evaluation of the SCS-CN Method Using Data of a Catchment in Yogyakarta Province, *Proceeding of the 4th ASEAN Civil Engineering Conference*, November 22-23, 2011, Yogyakarta.

Sujono, J. (2013). *Kajian kolam detensi Kali Belik lembah UGM untuk mitigasi banjir Kota Yogyakarta*, *Research Report.* Department of Civil and Environmental Engineering, Faculty of Engineering, Universitas Gadjah Mada, Yogyakarta.

PREPAREDNESS FOR DISASTER RISK MANAGEMENT (DRM), CASE STUDIES: KELANTAN FLOOD 2014

MOHD SAYUTI HASSAN[(1)], NOR AZAZI ZAKARIA[(2)], KAMARULAZIZI IBRAHIM[(3)], MURSHIDAH ABDUL JAFFAR[(4)], SHAHAD KHALDOON ABDULAMEER[(5)]

[(1,3,4)]Center for Global Sustainability Studies (CGSS), Universiti Sains Malaysia, Main Campus
sayuti@usm.my; kamarul@usm.my; murshidah291@outlook.com
[(2)] River Engineering and Urban Drainage Research Centre (REDAC), Universiti Sains Malaysia, Engineering Campus, Nibong Tebal, Penang, Malaysia
redac01@usm.my
[(5)]School of Industrial Technology, Universiti Sains Malaysia, Main Campus
shahadkhaldoon@gmail.com.

ABSTRACT

In accordance to the massive flash floods that hit Eastern part of Malaysia, which is mostly Kelantan state, a conference was held to explore ideas and sustainable solutions for the disaster. This paper describes one output of the five pillars of disaster management cycle that is “Preparedness” in Disaster Risk Management for Sustainable Development (DRM-SD) model, which was developed by Centre for Global Sustainability Studies (CGSS) Universiti Sains Malaysia (USM). The purpose is to come out with possible solutions and steps to be taken to mitigate the flood disaster while preparing for any possibilities. The method used for the conference is The Town Hall-World Café concept. Over 225 possible solutions are produced in two days in which the conference is conducted. Included in this paper are the recommendations that were found and the organizations which are responsible for the act.

Keywords: Preparedness; sustainable development; flood disaster; World Café; sustainable solution.

1 INTRODUCTION

Flood happens nearly every year during monsoon season from late November till March. Since then, it has been a worrying issue for the Malaysians. It has become the most common disaster in Malaysia. Flooding in Malaysia is most probably due to the cyclical monsoon during wet season that happens in Malaysia due to our geographical location (Ibrahim, K. K., 2013).

Flood disaster that happened in 2014 in Kelantan created collaboration between USM, UMK, Federal Development Department of Kelantan (JPPK) and the States Secretary Office of Kelantan (SUK) to organize a stakeholder meeting that was called Kelantan Flood Disaster Management Conference 2015.

The main issues presented and discussed at the conference related to the flooding that happened and the various ways to solve the problem. The conference topics were based on Disaster Risk Management for Sustainable Development (DRMSD) model. In this model there are five main disaster risk management pillars namely prevention, preparedness, response, recovery and governance. DRMSD model is developed by the Centre for Global Sustainability Studies (CGSS), USM (Ibrahim et al., 2013).

2 METHODOLOGY

Universiti Sains Malaysia had organized a post-flood disaster recovery conference USM/CGSS in Kelantan (14-16 Feb 2015) on disaster risk reduction and Centre’s on-going focus on disaster risk management for sustainable development (DRM-SD). It is true that all vulnerable communities are at risk when faced with hazards and it is this risk that gets realized as disaster eventually; the flood disaster in Kelantan being no different. A number of win-win and no-regret early interventions can reduce risk to an acceptable level with correspondingly reduced disaster impacts making recovery faster and losses bearable. This would involve the vulnerable communities as active participants in the risk reduction process than remain as passive victims. Such disaster risk reduction depends on well-coordinated governance mechanisms across sectors and at all levels.

A meeting was held to assemble 500 members from Government Ministries, offices, private area, Institute of Higher Learning, government offices, media columnists and non-administrative associations (NGOs) in which it gave a chance to them to contribute thoughts on deluge debacle management. The Town Hall-World Café idea was utilized for the exchange. The Town Hall World Cafe method means that there would be exactly five tables each regarded as World Cafes. Members were partitioned into five gatherings and they would move starting with one World Café then onto the next as each of the cafes were allotted to talk about on only one specific component contained in the Disaster Risk Management for Sustainable Development (DRM-SD) model, be it prevention, preparedness, response, recovery or governance. Every one of the members would have the chance to contribute their thoughts in every component as they move between the cafes. Every cafe would be taken care of by a facilitator who is a specialist for the component of the cafe appointed to them. The facilitator was capable to ensure the members centered their thoughts to the separate component at the World Café.

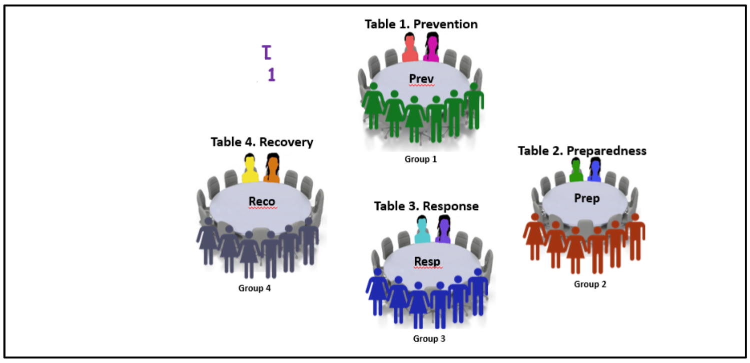

Figure 1. World Café Discussion Method Round1.

The World Café method is designed to create a safe, friendly environment in which to intentionally connect multiple ideas and perspectives on a topic by engaging participants in several rounds of small-group conversation. The use of this method was mainly to explore participants to multiple perspectives of Risk Management for Sustainable Development (DRM-SD) model. Since DRM-SD model content four_elements, therefore, four groupsre we formed. Each of the four groups was distributed to café (table with the specific topic) as in Figure 1. This figure also shows the first round of discussion will take 60 minutes, where, the first 20 minutes, the facilitator in charge on a café briefed the group members on their topic as well as explaining that there will be five rounds for each group with 30 minutes of discussion.

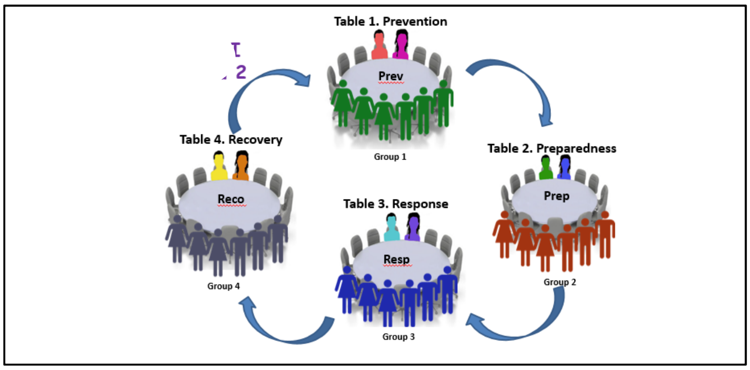

Figure 2. World Café Discussion Method Round 2

Each group had to move to another café after the first round of discussion. Figure 2 shows the second round, which took 40 minutes, the first 10 minutes were divided between groups movement to their second café, like group one moved from café prevention to café preparedness , group two moved to café Response, while group three moved to café Recovery and finally group four moved to café Prevention, coupled with briefing about the new café topic by their new facilitator. As for the discussion took only 30 minutes.

3 BACKGROUND

Beryl, M. (2014) stated that the flood management governance structures vary with geography, population size, infrastructure type, historical district legislation, and public policy. Khalid and Shafiai (2011) highlighted that the disaster management in Malaysia has three levels and every committee in every level has its own responsibility - Level I - the committee ensures coordinated actions, with sufficient asset and human resources, in relation to the media, Level II, must provide to the District assistance such as financial aid, assets and human resources, and Level III, the committee must determine the national disaster management policy, finance, assets and human resources. Activation of the specific executing committee will depend on the characteristics and scale of event as well as coverage of impacted areas (Abdul Wahab, 2011). In Malaysia, disaster management is almost entirely based on a top-down approach. At the very top is the National Disaster Management Risk Centre (NDMRC) running a National Crisis and Disaster Management Mechanism (NCDMM) (Chan 2015). According to Chia (2004), this machinery was established with the objective of co-coordinating relief operations at the federal, state and district levels so that assistance can be provided to flood victims in an orderly and effective manner. The flooding that occurred in late December 2014 was an unprecedented act of nature that displaced hundreds of thousands of Malaysians not just in the flood-prone northern states of the peninsular but also in the south and as far as Sarawak. Chan (1995) stated that it has been estimated that 70% of the kampungs (villages) in Kelantan, or nearly half of the state's population, were affected. Currently, in the end of December 2014, Eastern Malaysia state, especially Kelantan experience serious flooding which had a negative impact on several states especially on the economy and society in general. Azlee (2015) stated that the National Security Council (NSC) confirmed the massive flood that hit Kelantan was the worst in the history of the state and its secretary Datuk Mohamed Thajudeen Abdul Wahab said water levels of the recent floods superseded the floods of 1967.

The focus of preparedness phase has been generally on moves that states can take on activities by government organizations along with non-governmental organizations (NGOs), neighborhood groups, families, and people. The presumption is that negative impacts of disasters can be diminished through preparation (Hansson et al., 2006). Much exertion has gone into getting individuals to be well prepared and informed about the places that are prone to flooding so that they could take measures to withstand the effects afterwards. Folks are always said to have a special attachment of feelings for places, this is called "place attachment" (Low, 1992). This kind of attachment might disturb the act of preparedness along with evacuation process. It is best for not developing this kind of feelings towards places. That act of preparedness would be on the people themselves. Now, moving on to the Kelantan Flood Disaster Management Conference 2015, there were a plenty of other steps recommended and discussed during the conference in order to have better preparation for the flood that might happen anytime.

Cambodia, Lao PDR, Thailand and Viet Nam, had implemented Flood Management and Mitigation program to reduce the impact of flooding caused by Mekong River (Perwaiz, 2008). Flood preparedness programme core element of the FMMP resulted in positive relation, remarkably in encouraging sustainability and ownership of the program and in initiating mainstreaming of Flood Risk Reduction (FRR). It emphasised on capacity building, knowledge sharing and public awareness campaigns at provincial, district and community levels, by encompassing five main components: 1) establishment of the regional Centre, 2) structural measurement and flood proofing, 3) mediation of transboundary flood issues, 4) flood emergency management strengthening, 5) land management. In Central Europe (Germany, Austria, the Czech Republic and Slovakia), severe flooding happened in August 2002(Thieken et al., 2007). The household preparedness was lower than 30% who took no precautionary measures before the flood event, while only 26% of all households knew how to react to the flooding event (Kreibich, H., 2011). Implementing the Flood Risk Management helped to reduce unprepared householders to 10% only during 2006 flooding, by focusing on three features: (a) flood regression, with the aim to avoid peak flows, (b) flood control, aimed at preventing inundation by means of structural measures, e.g. embankments or detention areas; and (c) flood alleviation with the goal of reducing flood impacts by non-structural measures (Parker, 2000). The last can be classified into precautionary and preparative measures. Precaution and preparation help to limit and manage the adverse effects of a catastrophe, and to build up coping capacities by flood-resilient design and construction, development of early warning systems, insurance, awareness campaigns, education, training, putting rescue units on stand-by, which help to reduce unpreparedness among the householders (Thieken et al., 2007). But also this method had its limitation as it only implements for the householder not including the businesses (Kreibich, H., 2011).

4 FINDING

One of the most important findings from that discussion is all stakeholders and the National Security Council are urged to provide latest databases about flood information to the staff who works under them that are responsible for it. This is to make sure all staff carryout surveillances on the weather and monsoon changes. Latest technology is definitely more than possible in today's rapidly developing world. Therefore, a little upgrade on technology is always in favor for us. Remote Sensing is one of the technologies mentioned. It is a very effective way in providing synoptic coverage over a wider area and very cost effective. In the upgraded version of this technology exist a tool of monitoring the change or reconstruct progress of past flood (Sanyal et al., 2004).

Ministry of Communications and Multimedia Malaysia along with Telecommunication companies should join forces in times like this to upgrade the networking for the sake of improved communication. The step that they could take is by expanding the Government Integrated Radio Networking (GIRN) coverage. Expanding radio networking is a wise step to do since communication is very important in the course of natural hazards (Ibrahim et al., 2013). Better communication reduces effects. Ministry of Finance should come up with budget allocation for implementation of these measures especially for areas that are prone to floods.

After expanding the coverage, these companies should now build electrical substations in appropriate area. The substations should only be developed in that particular area after analyzing the area carefully (Sanyal et al., 2004). This is to ensure that electrical substations are not built in rural area without any residents residing. Living has become so much easier due to the developing technology (Jeyaseelan, 2002). We now can even charge our phone without the need to search for direct current supply. In times of disaster, power banks stock supply should be provided for mobile phone in terms of communication purposes. For this, the availability of power banks should be ensured by the company and Federal Government. Power banks should be provided to the workers at the evacuation centres to exchange information from headquarters and also the evacuation centre. The public should also be provided with one but the workers or the volunteers should be prioritized. Other relevant equipment should also be enhanced and revised their specifications and capacities to suit the flooding disaster. Another crucial step that needs to be taken by Tenaga Nasional Berhad is to provide every district prone to flooding with a stand-alone electrical generator. The generator capacities should just be enough to dispense adequate power to meet the necessity.

During flooding season, people still have to eat and continue their lives. Therefore, adequate food supplies are needed. In order to prepare for flooding season, food supply is one of the main worrying factors. There are babies and kids who need to be fed on time. Food supply should be collected and gathered at flood evacuation sites. Food allocation sites purposely should be built on higher grounds to prevent water to reach the evacuation sites and destroy them too. All stakeholders can come up with initiatives like generating a coupon system for food distribution together with basic needs distribution. This storage should be built at flood evacuation centres. People are vulnerable to starvation if they do not have enough supply of food (Blaikie, 2014). Water is equally important as food. Getting clean water for drinking and cooking is the major problem during flooding. Therefore, to avoid that kind of sticky and unappealing situation, local authorities and Department of Environment should work together in order to prepare extra water tanks to hold clean water as a preparation to face floods. The water is to meet the consumer or the flash flood victim demands. This is because at times like that, they will be in need of clean water that can be consumed. When there is clean water provided, safety measures should be practiced in a way that water is only used for crucial purposes and are not wasted arbitrarily. There should be a government officer who is assigned to monitor this action to preserve clean water during flooding season. The first action that should be taken after adverse weather conjecture is shipping the bottled water stocks to the evacuation centres (Ibrahim et al., 2013). This should be done right after the weather forecast by the Meteorological Department. District and Land Office who are responsible for this matter should always monitor weather forecasts.

Monitoring water quality is very important in food preparation. Water sample should always be monitored and warning system should be developed at the permanent sampling sites. Water sampling process is to supervise the quality of water from time to time. Hydrologists found difficulty in coping with water quality problems. This is indeed because there are not many studies and surveys regarding this area carried out by earlier scientists and hydrologists. Then, the joint of UNESCO/WHO publication Water Quality Surveys (1978) intended to synthesize the assessments of the hydrological regime and quality changes brought about by nature (flood) and man (Keith, 2008).

Since water quality drops during flooding season and consuming it could be harmful to human, therefore this act is very vital. Other than that, river should be taken care too. River improvement is also needed since flooding is mostly caused by overflow of river water. As for Natural River, there is always room for improvement. The same goes for man-made river that can be improved in order to let the flood water flow through them. Monsoon season which is also known as wet season causes heavy rain almost every day. When rain water flows through mountains, most probably landslide will occur. As a preparation measure, warning system for landslides should be provided to avoid any unforeseen circumstances (Keith, 2008). It is always better to expect the unexpected. These actions should be best taken into responsibilities of the Department of Irrigation and Drainage, Department of Environment, and also Malaysian Public Works Department. As for the non-waterproof property, it is best to move them to a higher ground. In that way, they will not be damaged. The non-waterproof property include books, wood furniture, electronic devices like mobile phone, laptop and few other important and valuable electronic products, and clothing. If there is a warning for flash flood, the masses should start to prepare all of these things before it is too late.

Because of flood water, many areas and roads might be affected and damaged to certain point, therefore, the responsible parties should install road block and opened other alternative roads for the people to use in case of emergency. Operator who is in charge should assist them whenever they need it. Malaysian Road Transport Department along with Police Department should join forces to make it happen. This is also a way of preparing to face the flood that could happen anytime especially at the disaster prone area (Ibrahim et al., 2013).

As for the safe areas that will not be affected by the floods, Defense Department and Ministry of Defense will have to provide every day basic facilities. These basic necessities are needed for the victims and also people living in those area to use it in times of the monsoon season. Just like non-waterproof properties, valuable assets will also need to be transferred to higher grounds. The transferred assets should be also secured to avoid unexpected situations to happen.

In order to prepare for the upcoming flood, the people should be briefed about the health and safety measures. This is significant because the victims should know what steps they should take and also the prohibitions that exist. This briefing session can also be executed at the respective evacuation centers in the midst of the disaster. All evacuation centres need to be identified by the Department of Social Welfare to ensure the food, water and other basic necessities are sent over there.

We also did a study regarding the preparedness when the flood happened. The scope of the study was limited to get information about their knowledge, practice, flood preparedness, and flood response. The area of the study consisted of six villages including Kampung Kemerok, Pantai Sabak, Pengkalan Chepa; Kampung Wakaf Aik, Bachok; Kampung Pulau Gajah, Bachok; Kampung Pulau Pisang, Kedai Buluh; Kampung Pulau Pak Amat, Pantai Cahaya Bulan; and Kampung Padang Jambu, Pantai Cahaya Bulan. Fifty respondents from each village were selected for the study, making a total of 300 respondents.

This study used two methodologies, namely the qualitative method and the quantitative method. The qualitative research focused on meanings, traits, and characteristics of events, people, interactions, settings or cultures, and experiences. According to Richard (2009), a leading proponent of qualitative method, aspects of quality are issues related to the what, how, when, and where of a thing; including its essence and ambience. Qualitative research thus refers to the "meanings, concepts, definitions, characteristics, metaphors, symbols, and descriptions of things" (Berg, 2007). From each village, 10 stakeholders were interviewed, making altogether 60 stakeholders from six villages.

Figure 3 shows that most of the communities (47.3%) live in the coastal areas because they have stayed there for many generations. Then, 23.7% of the respondents lived there because they stayed on their own personal land. Another 18.7% said that they stayed there because the location is very strategic. Finally, 6.3% of the respondents said they moved to that area. Clearly, 81.3% of these communities living in the coastal areas due to place attachment syndrome, while 18.7 % were affected by life requirement. Figure 4 shows that 42.7% of the sample received information regarding flood from electronic media, 11.30% from JKKK, 9.30% from police, 8.3% from printed media, and 6.7% from the Department of Irrigation and Drainage. After all, only 49 % of the residence had been notified by governmental departments while the rest 51% depend on the different types of media.

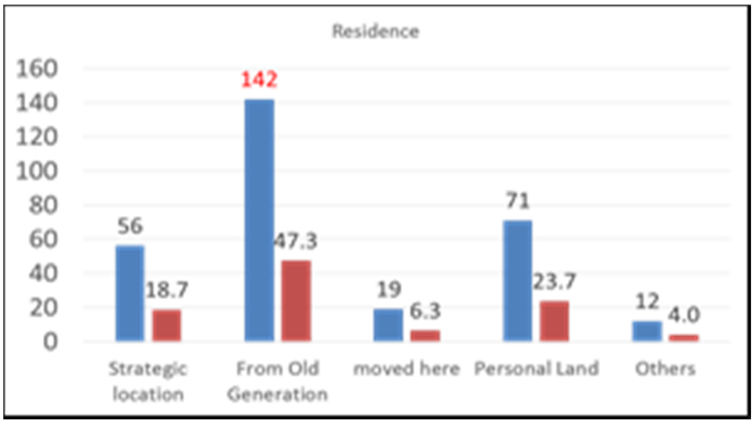

Figure 3. Communities living in coastal areas

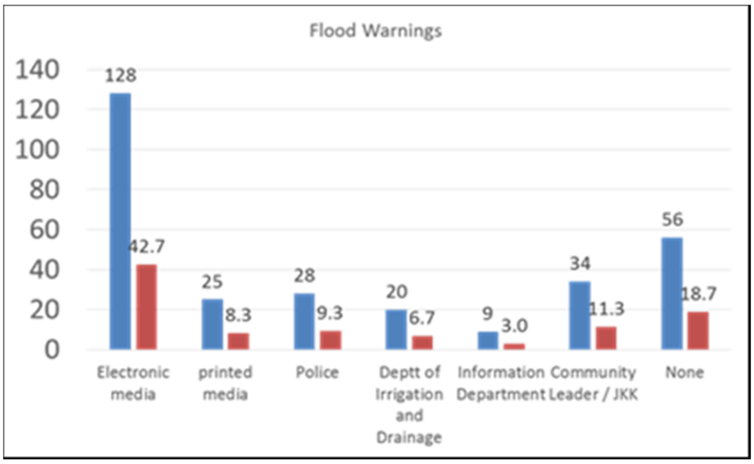

Figure 4. Flood information

Figure 5 shows that 44.67% of the respondents knew about flooding. A flood is an annual event for them, but the 2014 flood was none like previous floods. Furthermore, 29.67% of respondents answered they were not sure with their knowledge on the flood, 9.67% said they have a good knowledge, 9.00% had few knowledge and the remaining 6.67% had no knowledge about the flood. It seems, only 54.34% of the residences had awareness about the safety procedures. while 45.66% of the residents where lack of knowledge related to safety procedures.

Figure 6 shows the result of the questionnaire on the residents' agreement to the statement "Possess knowledge on the importance of cooperating with each other to solve flood issue." On this response, 48.7% of them said they agree with the statement, 28.0% respondents were not sure, 11.30% did not agree, 9.7% strongly agreed and the remaining 2.3% strongly disagreed. In another word, 58.4% of the residents' positive knowledge of the importance of the cooperation in solving flooding issue, whereas, 28% and 13.6 % were uncertain and reject the importance of cooperation, respectively.

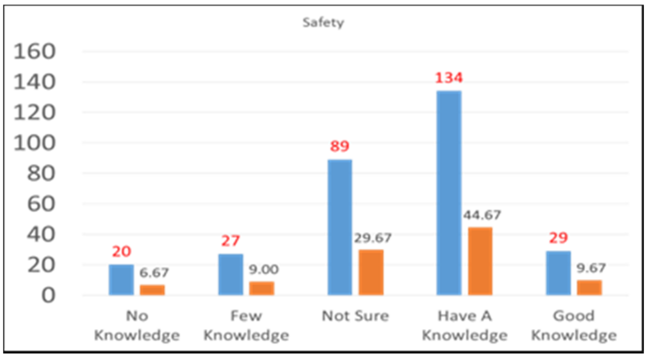

Figure 5. Safety knowledge

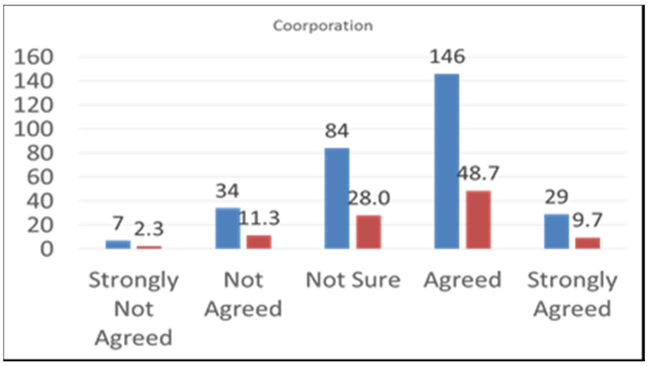

Figure 6. The importance of cooperating

Table 1 shows that 18.33% respondents stored enough food before flood occurred, 16.00% focused on keeping important documents at a secure place, 12.67% said they stayed cautious during heavy rainfall and 10.00% of them said they keep their belongings and vehicles at a safe place or location as a preparation to face flood.

Table 1. Preparation to Face Flood

Items	Frequency	%
Store enough food	55	18.33
Keep important documents in a secured place	48	16.00
Cautious during heavy rainfall	38	12.67
Keep belongings and vehicles at a safe place/location	30	10.00

Table 2. When Flood Occurs

Items	Frequency	%
Move to a safe place	76	25.33
Take care of the safety of family and own self	34	11.33
Listen and follow orders from the authority	26	8.67
Take care of the safety and health	24	8.00
Save family members	20	6.67

Table 2 shows that when flood occurs, 25.33% of the respondents said they would move to a safe place, 11.33% said they would ensure the safety of the family and their own self, 8.67% listened and followed orders from the authority, 8.00% took care of the safety and health, and lastly, 6.67% said they would save family members first.

5 CONCLUSION

The principle point of urban flood risk management is to minimize human misfortune and monetary harms. Flood dangers cannot be totally maintained from a strategic distance; in this manner they must be overseen. Hence, flood management does not endeavor to wipe out flood hazard but rather to mitigate them. Disaster risk management activities have concentrated on danger recognition and management, arranging or absence of in building in danger inclined territories, proper areas and development strategies if individuals choose to live in high-chance zones, evasion, deferral and moderation of impacts, building of protections and fortresses, safe houses and shelters, procurement of data, notices and requests, clearing potential outcomes, modes, arranges, and penetrates, and readiness for catastrophes(Lewis & Kelman, 2009). However, not everyone avoids high-risk areas. This may be due to things that are inevitable like finance problem or other circumstances. Therefore, preparedness efforts should be taken by various agencies to face flooding season. Disaster preparation is crucial especially to those states prone to natural disasters.

REFERENCES

Abdul Wahab, M.T. (2011). National Progress Report on the Implementation of the Hyogo Framework for Action (2009-2011), Malaysia.

Azlee, A. (2015). *Worst Floods In Kelantan*, Confirms NSC, Malaymail.

Berg, Bruce. (2007). *Qualitative Research Methods for the Social Sciences* (6th Ed). Boston: Pearson Education.

Beryl, M. (2014). *Yolo County Flood Governance Study*. University Of California, Davis.

Blaikie, P. C. (2014). *At Risk: Natural Hazards, People's Vulnerability And Disasters*. Routhledge.

Chan N.W. (1995). Flood Disaster Management in Malaysia: An Evaluation of the Effectiveness of Government Resettlement Schemes. *Disaster Prevention and Management*, 4(4), 22–29.

Chan, N. W. (2015). *Impacts of Disasters and Disaster Risk Management in Malaysia: The Case of Floods. In Resilience and Recovery in Asian Disasters.* Springer, Japan. 239-265 pp.

Chia, C. W. (2004). Managing Flood Problems in Malaysia. *Buletin Ingenieur*, 22, 38-43.

Hansson, K., Danielson, M. & Ekenberg, L. (2006). A Framework for Evaluation of Flood Management Strategies. *Journal of Environmental Management*, 86(3), 465–480.

Ibrahim, K., Koshy, K.C., Akib, N.A.M., Nor, R.M., Manaf, N.A., Azhar, S.N F.S. & Muslim, M. (2015). *Resolution Kelantan Flood Disaster Management Conference 2015*.

Ibrahim, K. K. (2013). *Development with a Difference: Neo-Disaster Risk Management for Sustainable Development.* In Geomatics, Natural Hazards and Risk. Taylor & Francis, London. 1-6 pp.

Jeyaseelan, A. (2002). *Droughts & Floods Assessment and Monitoring Using Remote Sensing and GIS: Satellite Remote Sensing and GIS Applications in Agricultural Meteorology*, Crop Inventory and Drought Assessment Division National Remote Sensing Agency Department of Space, Govt. of India, Hyderabad 291-313.

Keith, H. D. (2008). Disaster Management and Response: A Lifelines Study for the Queenstown Lakes District. *Master Thesis*, University of Canterbury.

Khalid, M. S. B. & Shafiai, S. B. (2015). Flood Disaster Management in Malaysia: An Evaluation of the Effectiveness Flood Delivery System. *International Journal of Social Science and Humanity*, 5(4), 398.

Kreibich, H., Seifert, I., Thieken, A. H., Lindquist, E., Wagner, K. & Merz, B. (2011): Recent Changes in Flood Preparedness of Private Households and Businesses in Germany. *Regional Environmental Change*, 11(1), 59-71.

Lewis, J. & Kelman, I. (2009). *Housing, Flooding and Risk-Ecology: Thames Estuary South-Shoreland and North Kent.* Journal of Architectural and Planning Research, 26(1), 14-29.

Low, S. A. (1992). *Place Attachment: A Conceptual Inquiry*. New York: Plenum Press.

Parker D.J. (2000a). "Introduction To Floods And Flood Management". In: Parker, D.J. (Ed.): Floods, Volume I, London & New York, 3-39.

Penning-Rowsell, E. C. & Green, C. (2000). New Insights into the Appraisal of Flood-Alleviation Benefits: (1) Flood Damage and Flood Loss Information. *Journal of Charted Institutions for Water Engineers*, 14, 347–353.

Perwaiz, A. (2008). *Flood Preparedness and Emergency Management People-Centred approach in Integrated Flood Risk Management*, Annual Flood Report 2008,MRCS.

Richard (2009), Understanding Why Qualitative Methods Are Superior For Criminology And Criminal Justice: Qualitative Versus Quantitative Methods. Journal of Theoretical and Philosophical Criminology, 1(1), 1-21

Sanyal, J. & Lu, X. (2004). Application of Remote Sensing In Flood Management with Special Reference to Monsoon Asia: A Review. *Natural Hazards*, 283-301.

Thieken, A.H.(2007). Coping With Floods: Preparedness, Response and Recovery of Flood-Affected Residents in Germany in 2002. *Hydrological Sciences Journal*, 52(5), 1016–1037.

ESTIMATION OF TSUNAMI FORCE REDUCTION AND THE BREAKING MODE OF COASTAL TREES APPLICABLE TO COASTAL FOREST MANAGEMENT AS A BIOSHIELD

NORIO TANAKA[1], HAJIME SATO[2], YUTA AKASAKI[3]& HIROYUKI TORITA[4]

[1,3]Graduate School of Science and Engineering, Saitama University, Saitama, Japan,
[1] International Institute for Resilient Society, Saitama University, Saitama, Japan,
tanaka01@mail.saitama-u.ac.jp
[2] Forestry Research Institute, Hokkaido Research Organization, Hokkaido, Japan
[4] Donan Branch, Forestry Research Institute, Hokkaido Research Organization, Hokkaido, Japan

ABSTRACT

The effectiveness of coastal forests to mitigate tsunami has received increased attention since the 1998 Papua New Guinea tsunami, the 2004 Indian Ocean tsunami, and the 2011 Great East Japan tsunami. When a large tsunami attacks the coastal forest, many of the trees were broken or overturned. For estimating the effectiveness, it is important to reproduce the forest breakage situation numerically. The objective of this study is to improve two-dimensional nonlinear long-wave equation model including the tree-breaking mode in detail considering the stand structure of trees, to demonstrate the energy reduction effect even when forest is broken, and to utilize the information to manage the coastal forest properly. In these regards, two locations of coastal forests in Shiranuka and Taiki Town, Hokkaido, Japan were selected. Numerical simulation demonstrates that a tree whose crown is high from ground tends to be broken at the tree trunk when root anchoring strength is high. Pine trees and broad-leaved tree (*Quercusdentata*) tend to be overturned and broken at the tree trunk, respectively, at the two study sites. In addition, even when the trees with dense crown are broken, they contribute to resist tsunami to some extent. The reduction of fluid force changes not only with the forest thickness but also with the tree species and the destruction mode. To maintain the fluid-force reduction and to reduce secondary damage by driftwood, large diameter trees at the landward side of forest can be planted to trap the driftwood produced.

Keywords: Ecosystem-based disaster risk reduction; coastal forest; fluid force; management of coastal forest; stand structure of trees

1 INTRODUCTION

The effectiveness of coastal forests on sand dunes or mangroves in reducing the fluid force of a tsunami has received increased attention since the 1998 Papua New Guinea tsunami, the 2004 Indian Ocean tsunami, and the 2011 Great East Japan tsunami even though the trees were broken (Thuy et al., 2012; Tanaka et al., 2013). Tanaka et al. (2014) investigated the effectiveness of coastal forest in the 2011 Japanese tsunami by post-tsunami surveys and by simulating the reduction of washout regions of houses with/without a coastal forest and a sea embankment. The study indicated that the effect of vegetation was small compared to that of the sea embankment, but it was not negligible as a mitigation countermeasure when a large tsunami arrived and overflowed the sea embankment.

When a large tsunami attacks the coastal forest, many of the forests are broken or overturned. To estimate the effectiveness, it is important to reproduce the forest breakage numerically. Previous study (Tanaka et al., 2015) indicates the importance to consider the tree stand structure including crown height, and two important breaking mode (Tanaka et al., 2013). Therefore, the objective of this study is to improve two-dimensional nonlinear long-wave equation model including the tree-breaking mode in detail considering the stand structure of trees (i.e. tree height, crown height, projected area of crown and trunk, and drag characteristics of leaves), to demonstrate the energy reduction effect even when forest is broken, and to utilize the information to manage the coastal forest properly. For that objective, two locations of coastal forests in Shiranuka and Taiki Town, Hokkaido, Japan were selected.

2 MATERIAL AND METHODS

2.1 Differential equations

To calculate the tsunami propagation, five regions with different grid sizes were selected (Figure 1). In this study, the grid sizes of Regions A, B, C, D, and E were set to 1350 m, 450 m, 150 m, 50 m, and 16.7 m,

  / ISSN 1562-6865 (Online) - ISSN 1063-7710 (Print)

respectively. The simulated values in a large region were applied as a boundary condition in the next smallest region (nesting method). The linear long-wave equations and non-linear long-wave equations were applied to Region A and Regions B–E, respectively. At the coast line, a perfect reflection boundary was applied in Regions A–D, and inundation was calculated for only Region E.

To clarify the mitigating effect of the combined system of a coastal forest and sea wall quantitatively, numerical simulations in Region E were conducted using the model of Thuy et al. (2009), which is formulated by two-dimensional nonlinear long-wave equations (continuity equation: Eq.(1), momentum equations: Eqs.(2)–(5)), and the sub-depth scale (SDS) turbulence model (Nadaoka and Yagi (1998), which was slightly modified by Thuy et al. (2009).

$$\frac{\partial \zeta}{\partial t}+\frac{\partial (hV_x)}{\partial x}+\frac{\partial (hV_y)}{\partial y}=0 \qquad [1]$$

$$\frac{\partial V_x}{\partial t}+f_A\left(V_x\frac{\partial V_x}{\partial x}+V_y\frac{\partial V_x}{\partial y}\right)+g\frac{\partial \zeta}{\partial x}+f_A\left(\frac{\tau_{bx}}{\rho h}\right)+f_D\left(\frac{F_x}{\rho h}-\frac{E_{Vx}}{h}\right)=0 \qquad [2]$$

$$\frac{\partial V_y}{\partial t}+f_A\left(V_x\frac{\partial V_y}{\partial x}+V_y\frac{\partial V_y}{\partial y}\right)+g\frac{\partial \zeta}{\partial y}+f_A\left(\frac{\tau_{by}}{\rho h}\right)+f_D\left(\frac{F_y}{\rho h}-\frac{E_{Vy}}{h}\right)=0 \qquad [3]$$

$$\left(\tau_{bx},\tau_{by}\right)=\frac{\rho g n^2}{h^{1/3}}\times\left(V_x\sqrt{V_x{}^2+V_y{}^2},\,V_y\sqrt{V_x{}^2+V_y{}^2}\right) \qquad [4]$$

$$\left(F_x,F_y\right)=\gamma\frac{1}{2}\rho C_D A\times\left(V_x\sqrt{V_x{}^2+V_y{}^2},V_y\sqrt{V_x{}^2+V_y{}^2}\right) \qquad [5]$$

where x and y are the horizontal coordinates; V_x and V_y are the depth-averaged velocity components in x and y directions, respectively; t is the time; h the total water depth ($h = h_0+\zeta$); h_0 the local still water depth (on land, the negative height of the ground surface); ζ the water surface elevation; g the gravitational acceleration; F_x and F_y are the drag forces by trees in x and y directions, respectively; γ the density of trees (number of trees/m^2); ɣ is the fluid density; A is the projected area of trees. E_{Vx} and E_{Vy} are the viscosity in x and y directions, respectively (for more details on the viscosity terms, see Thuy et al. (2009), n Manning roughness coefficient, C_D drag coefficient of which values for trees were different with respect to the tree species and after breaking or overturned explained in the next section.

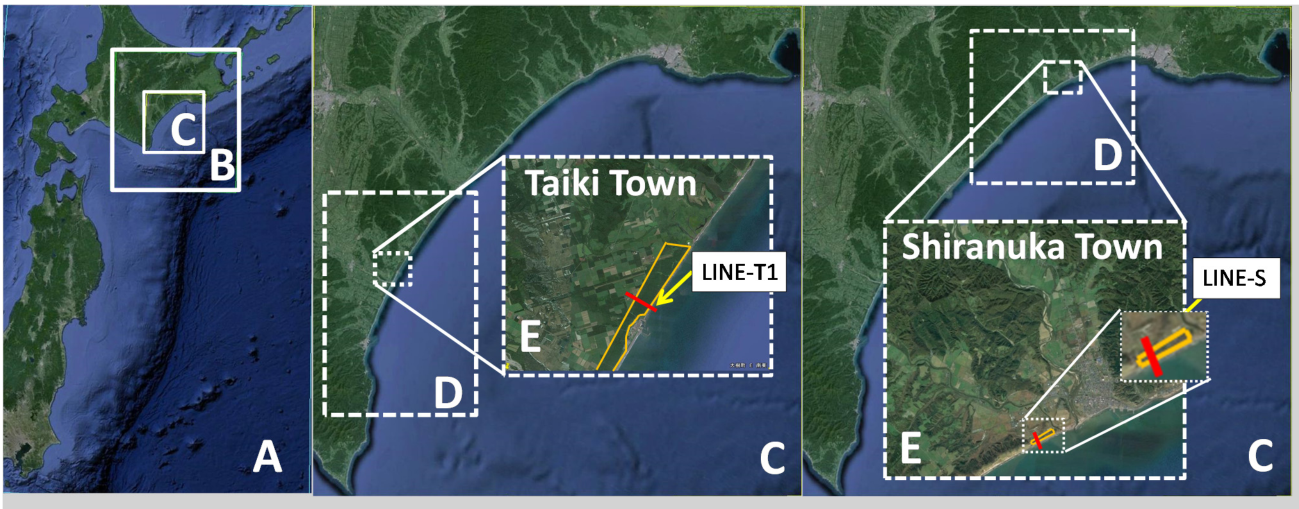

Figure 1. Definition of the grid system. A: linear long-wave equations are used, B-D: non-linear long-wave equations are used. E: non-linear long-wave equations with a turbulence model are used. Orange line shows the forest area, and red line shows the line analyzed in detail.

As already explained, suitable differential equations were applied according to the calculated region. Thus, different coefficients of f_A and f_D in Eqs.(2) and (3) were used, i.e., $f_A = f_D = 0$ for Region A (linear model), $f_A = 1$, $f_D = 0$ for Regions B–D (non-linear model without turbulence), and $f_A = f_D = 1$ for Region E (non-linear model with SDS turbulence). A set of the model equations were solved by the finite-difference method using a staggered leap-frog scheme, which is used widely in numerical simulations of tsunamis (Thuy et al., 2009). An upwind scheme was used for nonlinear convective terms in order to maintain numerical stability. Sea surface displacements calculated by the fault model of Mansinha and Smylie (1971) were given as initial conditions of the simulation. The fault parameters in Hokkaido in this district were applied (Tanaka et al., 2015). The tsunami run-up to inland was calculated by method of Iwasaki and Mano (1979). As a boundary condition, the non-reflective wave condition was applied.

2.2 Modeling the drag force and the destruction mode

In Region E, tree destruction model was included considering the moment by fluid force at each height of tree trunk for judging trunk breakage, and the moment at ground level for estimating the probability of tree overturning. Tree breakage was modeled as a function of critical tree diameter at breast height or critical resistant overturning moment examined at the sites. The change of drag force after the break was also modeled for each breaking mode and the destruction height.

$$C_D = C_{D-ref}\int_0^h \alpha(z)\beta(z)dz \qquad [6]$$

$$\alpha(z) = b_{bra}(z)/b_{ref} \qquad [7]$$

$$\beta(z) = \frac{A_{bra}C_{D-bra} + A_{lea}C_{D-lea}}{C_{D-ref}A_{bra}} \qquad [8]$$

Where, b_{ref}, $b_{bra}(z)$: total width of trunk and branches at breast height (=1.3 m from ground) and height z respectively, A_{bra} A_{lea}: area of branches area of leaves, respectively, C_{D-ref}: reference drag coefficient of tree trunk at breast height, C_{D-bra}, C_{D-lea}: drag coefficient of branches and leaves (=0.06, 0.015), respectively (for more details, see Tanaka et al. (2015).

For the fluid force and moment acting on a tree as shown in Figure 2 are as:

When $h<H_c$

$$M_X = -F_X H_{GX} \qquad [9]$$

$$F_X = 0.5C_{D\text{-}X}\rho b_{ref}(h-X)u^2 \qquad [10]$$

When $H_c<h<H_t$

$$M_X = -F_X H_{GX} - F_c(0.5(h - H_c) + H_c - X) \qquad [11]$$

$$F_X = 0.5C_{D-X}\rho b_{ref}(H_c - X)u^2 \qquad [12]$$

$$F_C = 0.5C_{D-C}\rho b_{ref}(h - H_c)u^2 \qquad [13]$$

When $H_t<h$

$$M_X = -F_X H_{GX} - F_c(H_c - X + 0.5L) \qquad [14]$$

$$F_X = 0.5C_{D\text{-}X}\rho b_{ref}(H_C - X)u^2 \qquad [15]$$

$$F_C = 0.5C_{D\text{-}C}\rho b_{ref}Lu^2 \qquad [16]$$

Where, h: water depth, H_t: tree height before breaking, H_C: crown height, M_x: moment acting on the tree trunk at height X, F_X, F_C: drag force acting on tree trunk and crown at height X, respectively, H_{GX}: metacenter of the projected area of crown, dX: trunk width at X, dh: trunk width at h, u: velocity, L:crown length, $C_{D\text{-}X}$,$C_{D\text{-}C}$ are the drag coefficient calculated by Eqs.6-8 by integrating from 0 to X, and from Hc to min(h, Ht), respectively.

For each parameter of the tree species are given by the allometry equation measured at the sites bellow are used.

$$y = kx^c \qquad [17]$$

Where, k, c: dimensional constant.

For x, D^2H were selected and model parameters (y) for expressing the tree stand structures were analyzed by field investigation data at the sites. Table 1 and Table 2 show the coefficient.

2.3 Critical condition of tree-trunk breakage and overturning

This study considers that tree-trunk breakage or overturning occurs when M_x exceeds the critical values of the two phenomena.

In order to analyze the critical breaking movement of tree trunk at X (M_{criX} MNm), below equation was applied.

$$M_{criX} = \sigma_{MAX} \times \pi \frac{d_X{}^3}{32} \qquad [18]$$

Where, σ_{MAX}: critical breaking strength of the species (pine= 29.0MPa, *Quercusdentata*=29.5MPa), dX: tree trunk diameter at X.

In order to analyze the critical overturning movement of a tree (M_{criOT} MNm), below equation was applied.

$$M_{criOT} = k_O b_{ref}{}^2 H_t + k_C \qquad [19]$$

Where, k_O, k_C: species specific coefficient examined by field test (Tanaka et al., 2015). This study applies (k_O, k_C) = (26000, 3100) and (86400, 0) for pine and *Quercusdentata* in Shiranuka, and (k_O, k_C) = (57300, 0) and (93900, 0) for pine and *Quercusdentata* in Taiki, respectively.

After the tree trunk breakage, projected area was changed as shown in Figure 2. After overturn, drag coefficient was changed with the same method used by Thuy et al. (2012) assuming that the inclination from ground was 30 degree.

Table 1. Coefficient of allometry equations (Siranuka)

	⇧	⇦	*k*	⇈	*correlation coefficient R*
Pine	Tree height H	D	5.7057	0.2203	0.50
	A_{bra}	D^2H	31.2019	0.6667	0.98
	A_{lea}	D^2H	110.6033	0.6667	0.76
Quercus dentata	Tree height H	D	10.411	0.2803	0.56
	A_{bra}	D^2H	8.9254	0.6667	0.94
	A_{lea}	D^2H	71.8659	0.6667	0.97

Table 2. Coefficient of allometry equations (Taiki)

	⇧	⇦	*k*	⇈	*correlation coefficient R*
Pine	Tree height H	D	38.45	0.7655	0.77
	A_{bra}	D^2H	10.53	0.667	1
	A_{lea}	D^2H	37.712	1	1
Quercus dentata	Tree height H	D	36.077	0.6921	0.75
	A_{bra}	D^2H	8.226	0.667	1
	A_{lea}	D^2H	305.98	1	1.00

Table 3. Tree characteristics change with the change of distance from the shoreline (Siranuka)

Line No.	Distance from the shoreline (m)	Pine				*Quercus dentata*			
		Tree density (trees/m^2)	Diameter at breast height (m)	Tree height (m)	Crown height (m)	Tree density (trees/m^2)	Diameter at breast height (m)	Tree height (m)	Crown height (m)
1	50.0-66.6	0.066	0.086	3.32	1.53	0.252	0.065	4.81	2.92
2	66.7-83.3	0.080	0.118	3.63	1.35	0.090	0.076	5.06	2.88
3	83.4-99.9	0.076	0.091	3.37	1.01	0.180	0.078	5.12	3.85
4	100.0-116.6	0.064	0.077	3.22	1.05	0.249	0.074	5.03	4.15
5	116.7-133.3	0.150	0.110	3.56	1.69	0.075	0.084	5.24	2.41
6	133.4-149.9	0.031	0.074	3.18	1.35	0.197	0.087	5.32	3.38

Table 4. Tree characteristics change with the change of distance from the shoreline (Taiki)

Line No.	Distance from the shoreline (m)	Pine				*Quercus dentata*			
		Tree density (trees/m^2)	Diameter at breast height (m)	Tree height (m)	Crown height (m)	Tree density (trees/m^2)	Diameter at breast height (m)	Tree height (m)	Crown height (m)
1	70.9	0.220	0.103	6.76	4.28	0.096	0.060	5.15	1.79
2	141.7	0.328	0.105	6.83	5.08	0.100	0.119	8.27	5.27
3	212.6					0.088	0.205	12.06	6.69
4	283.4					0.128	0.186	11.27	6.74
5	330.6					0.064	0.238	13.37	6.88
6	401.5					0.100	0.184	11.18	6.42
7	472.3					0.120	0.159	10.11	4.93
8	543.2	0.028	0.241	12.95	7.31	0.060	0.171	10.65	5.33
9	614.1	0.076	0.230	12.48	7.07				
10	684.9	0.084	0.224	12.24	7.29				
11	755.8	0.028	0.246	13.16	6.47	0.008	0.139	9.18	6.85

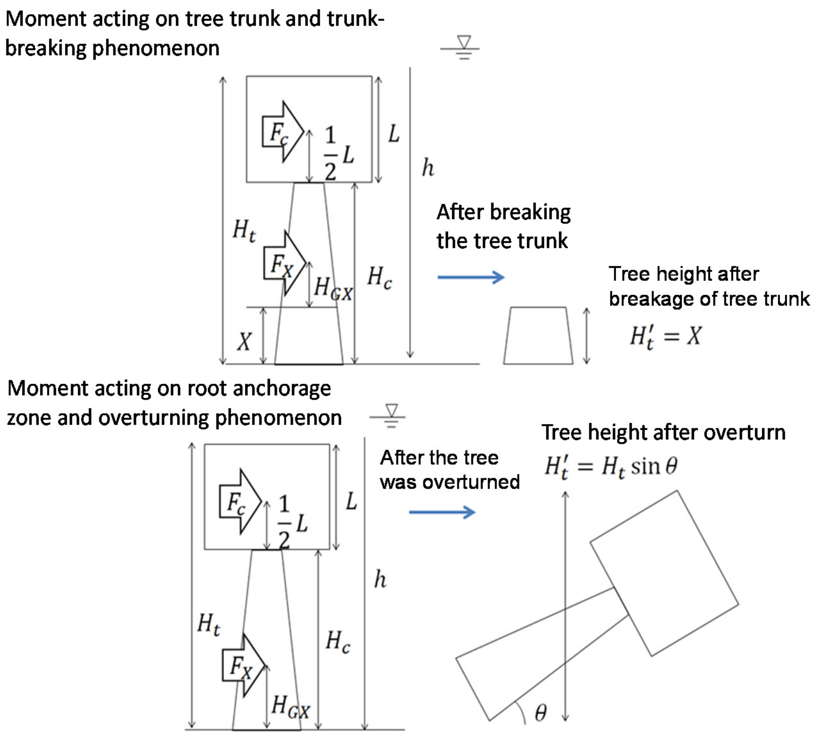

Figure 2. Schematic of the modelling the two typical tree breaking mode

3 RESULTS AND DISCUSSION

3.1 Differences of the simulated breaking situation of the two species at two sites

Figure 3 shows the simulated breaking situation of the two species. In Siranuka (Figure 3a, b), dominant breaking mode of pine and *Quercusdentata* were 'overturn' and 'trunk breakage', respectively. All the trees in the forest were damaged in case of Shiranuka (forest width is around 100 m, land elevation is low as compared to Taiki). However, in Taiki (Figure 4) where forest width is around 700 m, landward trees were not damaged except for the area where forest width is thin. The difference of the breaking mode is mainly caused by the difference of the standing structure of the trees (i.e. crown height, amount of branches and leaves) and the tree trunk diameter at breast height as shown in Table 1-4.

When the tree trunk breakage occurs and the upper part of a tree is washed out, only the remaining part of the tree trunk can provide resistance to tsunami. The resistance by trees is greatly reduced and the forest also produces driftwood. At the landward side, there is a possibility to add to the secondary damage due to the driftwood. On the contrary, when 'overturn' occurs, it can provide a drag by the inclined tree even though the resistance is decreased. It can also trap small debris by the remained part of the tree. Even when 'overturn' occurs, even a whole tree has a possibility to become driftwood. However, the production of driftwood of a whole tree was restricted to the scoured region behind an embankment or a step at the 2011 Japanese tsunami (Tanaka et al., 2013).

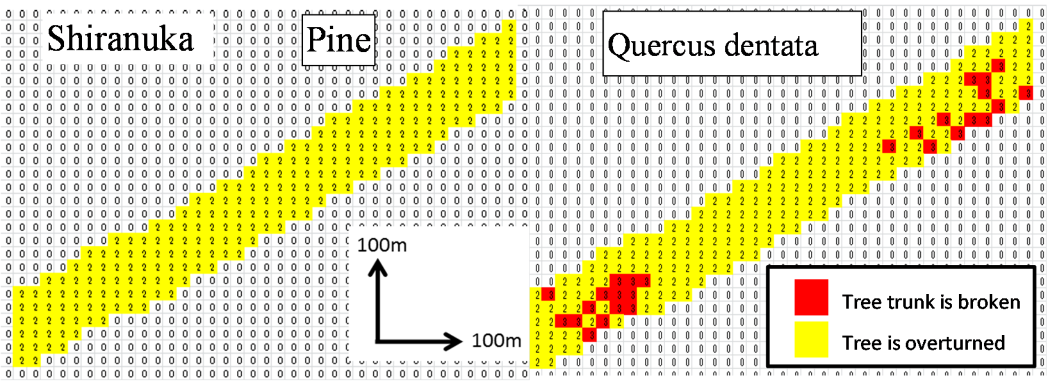

(a) (b)

Figure 3. Breaking mode of different tree species at Shiranuka. (a) Pine tree, (b) *Quercusdentata*

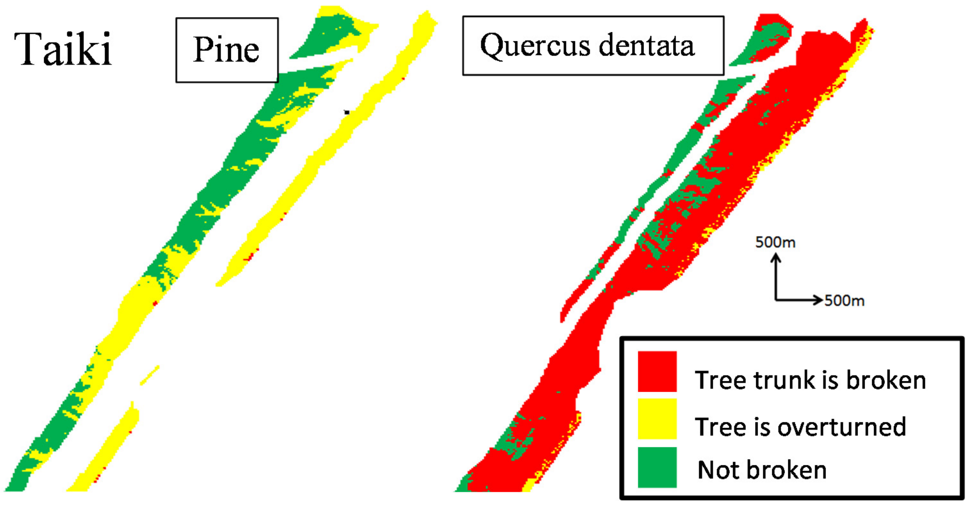

(a) (b)

Figure 4. Breaking mode of different tree species at Taiki. (a) Pine tree, (b) *Quercusdentata*

3.2 Fluid force reduction at two sites

Figure 5 shows the time series of fluid force index (u^2h, where u is a velocity, h is a water depth) with/without coastal forest and tree-breaking model just behind coastal forest in the two study sites. At Shiranuka (Figure 5a), tsunami fluid force is much larger than the threshold values of tree breakage. So the trees were damaged at initial stage of the tsunami. Howeverl they can still act as a resistance because most of the pine trees were overturned and can maintain the resistance to tsunami flow. At Taiki (Figure 5b), tsunami fluid force was relatively smaller than that at Shiranuka because land elevation is around 13-15 m at Taiki which is larger than that at Shiranuka (around 5 m). In addition, forest width is very large at Taiki (700 m). Therefore, tsunami arrival time was around 500 seconds delayed as compared to the situation at Shiranuka, and hence the landward trees can withstand the fluid force and survive (Figure 4). Without tree breakage, the bioshield can reduce the tsunami fluid force by 27 and 50 % for Siranuka and Taiki respectively, but it overestimates the mitigation effect. By our estimation including the tree destruction, it can reduce the tsunami by 22 and 20 % for Shiranuka and Taiki, respectively. Although the forest width is far greater in Taiki, the reduction effect is not much increased. This is related to the crown height of the trees as the high crown height has a possibility to withstand tsunami, but its role on the reduction of tsunami fluid force decreases. This is discussed further in the next section.

3.3 Effects of tree crown height and tree trunk diameter of the breaking mode

Figure 6 shows the variation of maximum tsunami water depth to cross-shore direction together with the stand structure of trees. Table 5 and 6 show the tsunami characteristics at Line-S (Siranuka) and Line T1 (Taiki), respectively, when the breakage occurred. Pine trees at Shiranuka were mostly damaged when tsunami exceeded the low crown height as the velocity was high. However, *Quercusdentata* has dual destruction mode. When the crown height is small and velocity is large, the destruction mode becomes 'tree trunk breakage'. This corresponds to the seaside front line of the forest at Shiranuka. Similar situation was also observed in the 2011 Japanese tsunami (Tanaka et al., 2013).

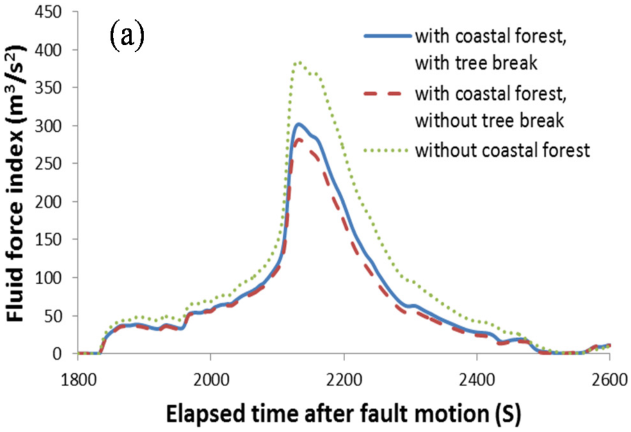

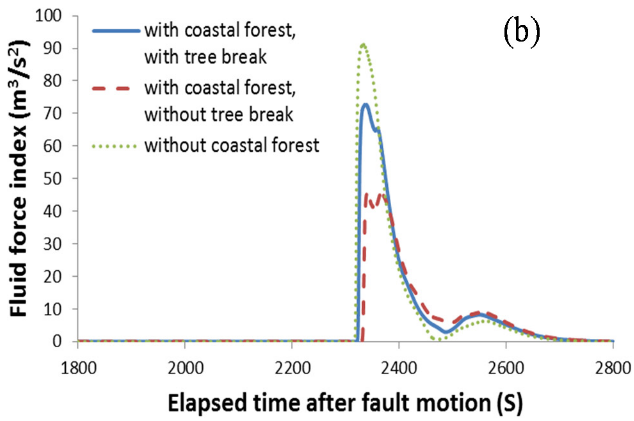

Figure 5. Reduction of fluid force index (u^2h, where u is a velocity, h is a water depth) with/without coastal forest and tree-breaking model just behind coastal forest in two study sites. (a) Shiranuka, (b) Taiki

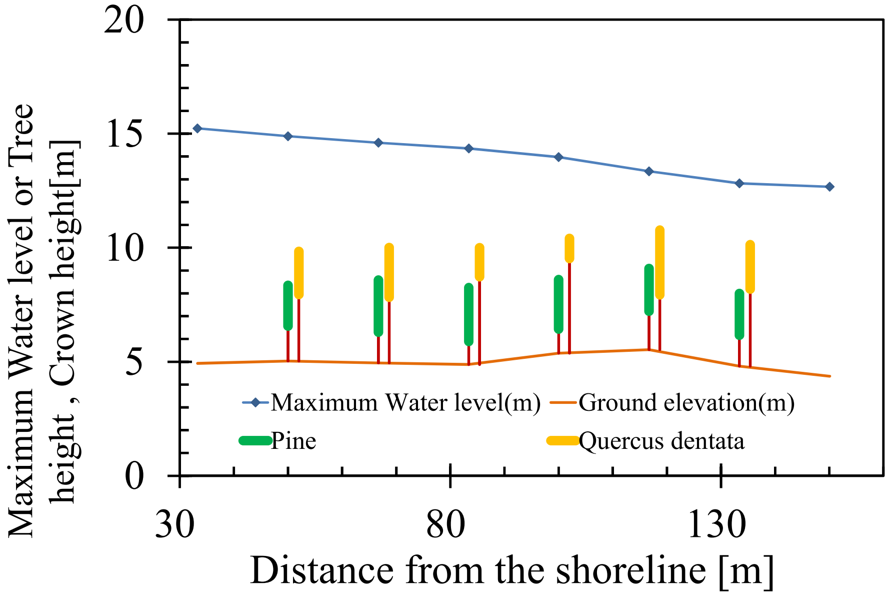

(a)

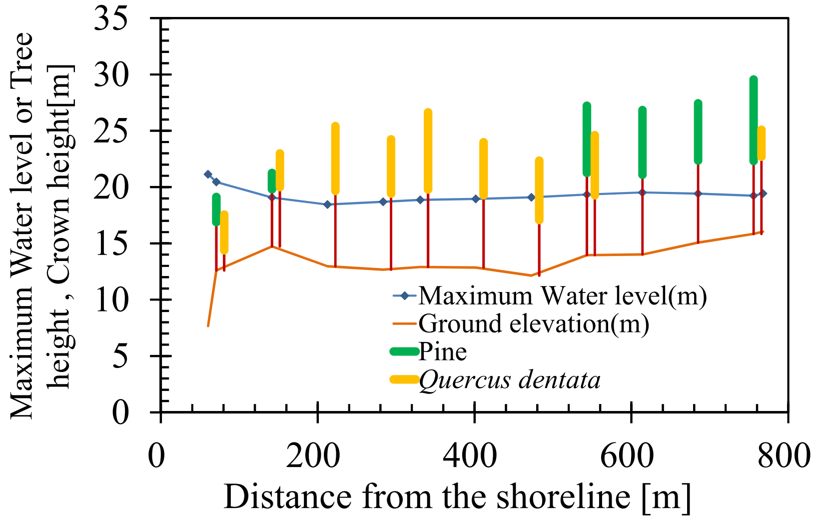

(b)

Figure 6. Variation of maximum tsunami water depth to cross-shore direction together with the stand structure of trees. (a) Siranuka, (b) Taiki

  / ISSN 1562-6865 (Online) - ISSN 1063-7710 (Print)

Table 5. Comparison the Tree break timing with the species and the location (Line-S: Shiranuka)

Line No.	Pine							
	Breaking mode	Height of tree trunk breakage (m)	Crown height (m)	Inundation depth when tree was broken (m)	Velocity when tree was broken (m/s)	Time when tree was broken (s)	Froude number when tree was broken	Fluid force when tree was broken (m^3/s^2)
1	OT	×	1.5	1.5	4.5	1817.8	1.2	31.2
2	OT	×	1.4	1.5	4.4	1822.4	1.2	28.7
3	OT	×	1.0	1.2	4.7	1822.4	1.4	25.7
4	OT	×	1.1	1.0	5.2	1826.4	1.7	26.4
5	OT	×	1.7	1.5	5.0	1848.0	1.3	38.7
6	OT	×	1.4	1.0	5.8	1843.4	1.8	34.5

Line No.	*Quercus dentata*							
	Breaking mode	Height of tree trunk breakage (m)	Crown height (m)	Inundation depth when tree was broken (m)	Velocity when tree was broken (m/s)	Time when tree was broken (s)	Froude number when tree was broken	Fluid force when tree was broken (m^3/s^2)
1	BR	0.2	2.9	2.8	3.9	1843.6	0.8	43.4
2	BR	0.2	2.9	2.9	3.7	1846.2	0.7	39.6
3	BR	1.4	3.9	3.9	2.7	1990.0	0.4	29.2
4	OT	×	4.1	4.1	3.6	2017.0	0.6	51.7
5	OT	×	2.4	2.6	3.4	1985.8	0.7	28.8
6	OT	×	3.4	3.4	3.0	1991.8	0.5	30.0

BR : Tree trunk is broken
OT : Tree is overturned

Table 6. Comparison the Tree break timing with the species and the location (Line-T1: Taiki)

Line No.	Pine							
	Breaking mode	Height of tree trunk breakage (m)	Crown height (m)	Inundation depth when tree was broken (m)	Velocity when tree was broken (m/s)	Time when tree was broken (s)	Froude number when tree was broken	Fluid force when tree was broken (m^3/s^2)
1	OT	×	4.3	3.1	4.3	2238.2	0.8	58.3
2	OT	×	5.1	1.6	8.6	2244.2	2.2	116.7
8	×	×	7.3	×	×	×	×	×
9	×	×	7.1	×	×	×	×	×
10	×	×	7.3	×	×	×	×	×
11	×	×	6.5	×	×	×	×	×

Line No.	*Quercus dentata*							
	Breaking mode	Height of tree trunk breakage (m)	Crown height (m)	Inundation depth when tree was broken (m)	Velocity when tree was broken (m/s)	Time when tree was broken (s)	Froude number when tree was broken	Fluid force when tree was broken (m^3/s^2)
1	BR	0.2	1.8	2.4	2.8	2237.6	0.6	19.5
2	BR	0.3	5.3	2.1	8.7	2244.6	1.9	156.2
3	BR	0.4	6.7	3.1	9.4	2255.4	1.7	271.7
4	BR	0.4	6.7	3.0	8.9	2259.0	1.7	234.3
5	×	×	6.9	×	×	×	×	×
6	×	×	6.4	×	×	×	×	×
7	×	×	4.9	×	×	×	×	×
8	×	×	5.3	×	×	×	×	×
11	×	×	6.9	×	×	×	×	×

BR : Tree trunk is broken
OT : Tree is overturned
× : not broken

From Table 5, it can be seen that the destruction does not always occur from the seaside but it depends on the crown height and breast height diameter. At Taiki, the tree trunks were broken when the tsunami was less than the crown height, as the crown height was large as compared to Shiranuka. The destruction mode wassimilar to Shiranuka, but 'tree trunk breakage' was easy to occur for *Quercusdentata*, although they (No.2,,3 and 4 at Taiki) can withstand very large fluid force compared with Shiranuka and the front line at Taiki (No.1) as shown in Table 6. The destruction mode means the production of driftwood. Therefore, when the crown height is high, some countermeasure to trap driftwood is required.

From the disaster prevention and mitigation point of view, pine trees can provide a large drag at the early stage of tsunami as well as after the breakage as most of its destruction mode is 'overturn'. In case of *Quercusdentata*, the effect is a little smaller as compared to the pine trees. In most cases, tree trunk breakage occurs as it has high crown height. It has a tendency to produce driftwood, but also to withstand high tsunami water depth and trap driftwood when the tree trunk becomes larger than the critical value. Considering the characteristics, the combination of the two species e.g. large resistance tree with low crown height (seaward) and high crown height tree with a large diameter (landward) is recommended. Optimum management should be discussed in due course.

4 CONCLUSIONS

This study developed tsunami inundation model that included the destruction mode of coastal trees related to the driftwood production in detail. Numerical simulation demonstrated that a tree whose crown was high from ground tended to be broken at the tree trunk when root anchoring strength was high. Pine trees and broad-leaved tree (*Quercusdentata*) tended to be overturned and broken at tree trunk, respectively, at two study sites. In addition, even when the trees with dense crown were broken, they contributed to resist tsunami to some extent. The reduction of fluid force was changed not only with the forest thickness but also with the tree species and the destruction mode. In order to maintain the reduction effects and reduce the secondary damage, overturning-type destruction and large diameter trees at the landward side of forest which can trap driftwood were` recommended.

ACKNOWLEDGEMENTS

This study was partly funded by a JSPS Grant-in-Aid for Scientific Research (No. 15H02987).

REFERENCES

Iwasaki, T. & Mano, A. (1979). Two-Dimensional Numerical Simulation of Tsunami Run-Ups in the Eulerian Description (In Japanese), *Proc. 26th Conf. Coastal Eng. JSCE, 70-72* (Japan Soc. Civil Engineers, Tokyo).

Mansinha, L. & Smylie, D.E. (1971). The Displacement Field of Inclined Faults. *Bulletin of the Seismological Society of America*, 61(5), 1433-1440.

Nadaoka, K. & Yagi, H. (1998). Shallow-Water Turbulence Modeling and Horizontal Large-Eddy Computation of River Flow. *Journal of Hydraulic Engineering*, 124(5), 493-500.

Tanaka N., Yagisawa J. & Yasuda S. (2013). Breaking Pattern and Critical Breaking Condition of Japanese Pine Trees on Coastal Sand Dunes in Huge Tsunami Caused by Great East Japan Earthquake, *Natural Hazards*, 65, 423–442.

Tanaka, N., Yasuda, S., Iimura, K. & Yagisawa, J. (2014). Combined Effects of Coastal Forest and Sea Embankment on Reducing the Washout Region of Houses in the Great East Japan Tsunami, *Journal of Hydro-Environment Research*, 8, 270-280.

Tanaka, N., Niwata, Y., Sato, S., Torita, H. & Noguchi, H. (2015). High-Precision Tsunami Simulation Method Considering the Difference in Breaking and Overtopping Phenomenon by Stand Structure of Coastal Trees Applicable to Coastal Forest Management (In Japanese With English Abstract), *Journal of Japan Society of Civil Engineers, Ser. B2 (Coastal Engineering)*, 71(2), 307-312.

Thuy, N.B., Tanimoto, K., Tanaka, N., Harada, K. & Iimura, K. (2009). Effect of Open Gap in Coastal Forest on Tsunami Run-Up - Investigations by Experiment and Numerical Simulation. *Ocean Engineering*, 36, 1258-1269.

Thuy, N.B., Tanaka, N. & Tanimoto, K. (2012). Tsunami Mitigation by Coastal Vegetation Considering the Effect of Tree Breaking, *Journal of Coastal Conservation*, 16(1), 111-121.

Proceedings of the 37th IAHR World Congress
August 13 – 18, 2017, Kuala Lumpur, Malaysia

RETARDING EFFECT EVALUATION OF PADDY FIELDS AND THEIR LAND-USE CHANGE

MUTO YASUNORI[1], MURATA YUKI[2] , MIYOSHI MANABU[3] & TAMURA TAKAO[4]

[1,4] Institute of Science and Technology, Tokushima University, Tokushima, Japan,
muto_yas@ce.tokushima-u.ac.jp
[2] Graduate School of Advanced Technology and Science, Tokushima University, Tokushima, Japan,
[3] NITA Consultant Co., Ltd, Tokushima, Japan

ABSTRACT

Retarding capacity of wetland paddy fields was evaluated using a commercial inundation simulation software, AFREL, based on 2-D shallow flow model for both surface and channel flows. Effects of several land-use change, such as housing land development, rice cropping abandonment and river improvement works, on the capacity were also examined. Sensitivity analysis for the roughness coefficient was carried out and the best set of the coefficients was validated with the inundation records in Typhoon 1511, July 2015. The simulation results successfully illustrated temporal variations of the inundated area and its depth distributions. When about 30% of the wetland are changed to develop houses, the maximum flooded volume reduces about 90% of the present situation, mainly due to raising land elevation for housing. When rice cropping abandonment arises alternatively, the maximum flooded volume does not change so much, probably due to slightly change of roughness coefficient from 0.06 to 0.05. When the river and irrigation channels are enlarged, reduction of the maximum flooded volume is about 89% of the present situation, similar to the housing development. Responses of the wetland against rainfalls with different return periods are also studied and the results show that the effect of land-use change is somewhat different under the rainfall with an extreme long return period like over 100 years from that in less precipitation magnitudes. The housing land development, nevertheless, is effective in retarding inundation area, mainly by raising land elevation for housing.

Keywords: Retarding effect; paddy fields; inundation simulation; land-use change; roughness coefficient.

1 INTRODUCTION

Recently, a terminology “Green Infrastructure” has been widely recognised and accepted. Green Infrastructure, however, is a relatively new idea and covers wide ranges of ideas and objectives, thus one universal definition has not yet been established. Green Infrastructure Association, Japan, defines it as “infrastructures and land use planning that contribute to sustainable society and economic development through wise use of nature with regard to its various functions” (2017). In the same reference, they listed up to 13 types of Green Infrastructure as follows: urban tree[7] plantation, parks and green spaces, gardens, city farmlands, green ways, rivers, roads, vacant lots, retarding ponds, forests, seashores, agricultural lands and villages.

This paper focuses on paddy fields. Paddy fields are well known to have many functions as Green Infrastructure, including flood risk reduction, water resources conservation, food production for both human and animal, landscape improvement, community maintenance through agricultural activities, etc. (Ministry of the Environment, Japan, 2016). As for flood risk reduction, although this has been pointed out qualitatively from early days, there can be found quite few papers evaluating quantitatively the flood retarding capacity of paddy fields. On the other hand, owing to recent advances of numerical simulation technique, inundation simulation models have been widely applied to urban flooding and are now proved to reproduce well inundation processes of interior runoff (Thang et al., 2004). Such models can also be applied to wetland, mainly covered by paddy fields, in order to evaluate their flood retarding capacity through inundated volume and its time variation (Miyazu et al., 2012).

An advanced commercial inundation simulation software, AFREL, was employed here for the aforementioned purposes (http://www.nita.co.jp/index.php/software/afrel). Since wetland paddy fields in Japan are pressurised by both urban development and decreasing birth-rate and aging of the population (Ichinose, 2007), several scenarios of land-use change are considered. In addition to evaluate flood retarding capacity of wetland paddy fields themselves, the effects of land-use changes on flood retarding process, presumably cutting down the retarding effect, were also of interest.

2 STUDIED AREA

The studied wetland is located in the southern part of Tokushima Prefecture, Japan (see Figure 1). It forms a basin-like geometry of 2.32km^2 in an inland area, and over 50% of the area is utilised as paddy fields.

Bathymetry of the studied area is shown in Figure 2 in terms of altitude distribution drawn from 5m mesh DEM data, and land-use classification in 25m mesh used in the simulation is shown in Figure 3. A small stream, the Otsuda River, with lots of irrigation channels spread over the wetland are connected eventually to a major river, the Kuwanogawa River, and build a network drainage system of the area. During floods in the Kuwanogawa River, floodgates at the confluence point of the rivers are closed and pumps of 2×5m^3/s are operated for the drainage.

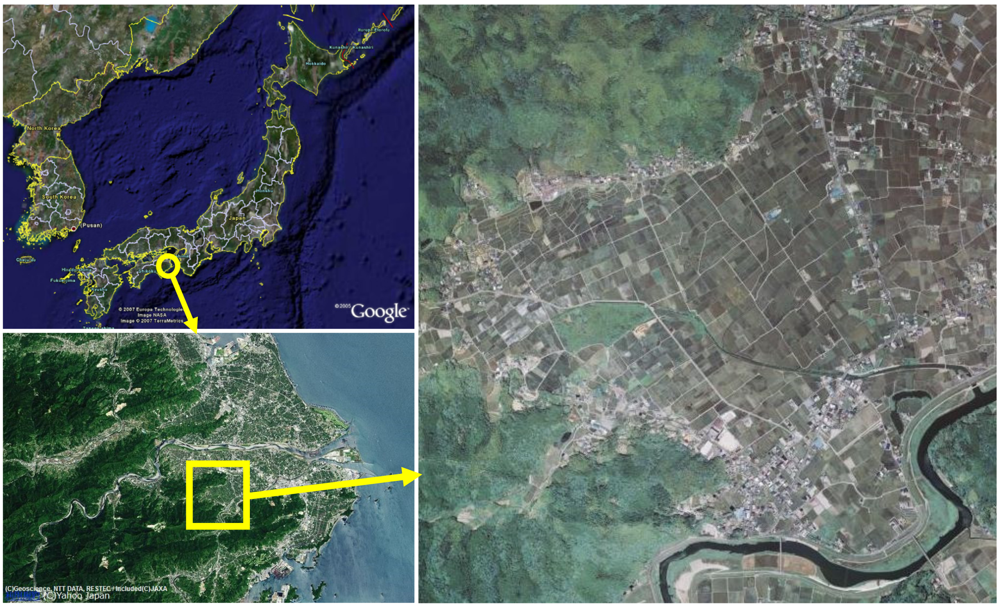

Figure 1. The studied area: the Otsuda River basin.

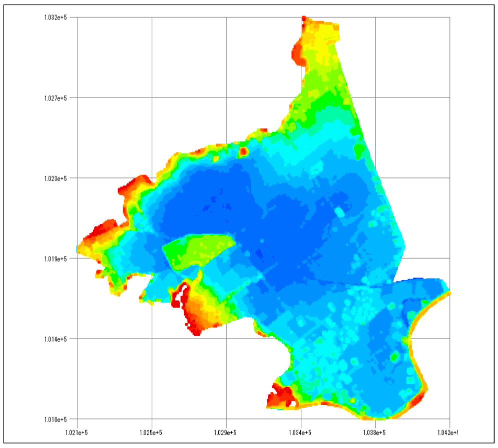

Figure 2. Bathymetry of the studied area.

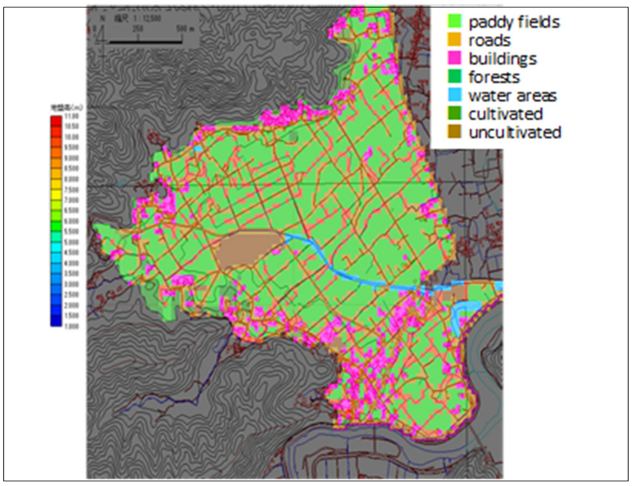

Figure 3. Land-use classification of the studied area.

3 INNUNDATION SIMULATION

A commercial inundation simulation software, AFREL, is employed in this study. As shown in Figure 4, AFREL can treat not only surface flow due to interior runoff, but channel and pipe flow networks overlapped on the surface. Moreover flow exchanges among these three forms can also be simulated. In the studied area a pipe sewerage network is not installed thus is omitted in the simulation.

Governing equations for the surface flow based on Iwasa and Inoue (1982) are as follows:

$$\frac{\partial h}{\partial t}+\frac{\partial M}{\partial x}+\frac{\partial N}{\partial y}=r(t)+q_{CH}+q_{SW} \quad [1]$$

$$\frac{\partial M}{\partial t}+\frac{\partial}{\partial x}uM+\frac{\partial}{\partial y}vM=-gh\frac{\partial H}{\partial x}-\frac{\tau_{bx}}{\rho} \quad [2]$$

$$\frac{\partial N}{\partial t}+\frac{\partial}{\partial x}uN+\frac{\partial}{\partial y}vN=-gh\frac{\partial H}{\partial y}-\frac{\tau_{by}}{\rho} \quad [3]$$

$$\frac{\tau_{bx}}{\rho}=\frac{gn^2M\sqrt{u^2+v^2}}{h^{4/3}},\quad \frac{\tau_{by}}{\rho}=\frac{gn^2N\sqrt{u^2+v^2}}{h^{4/3}} \quad [4]$$

Governing equations for the channel flow are basically the same as for the surface flow but omitting the advection terms in the momentum equations, as follows:

$$\frac{\partial h}{\partial t}+\frac{\partial q_x}{\partial x}+\frac{\partial q_y}{\partial y}=q_{GR}+q_{SW} \quad [5]$$

$$\frac{\partial q_x}{\partial t}=-gh\frac{\partial H}{\partial x}-\frac{\tau_x}{\rho} \quad [6]$$

$$\frac{\partial q_y}{\partial t}=-gh\frac{\partial H}{\partial y}-\frac{\tau_y}{\rho} \quad [7]$$

$$\frac{\tau_x}{\rho}=\frac{gn^2R_x^{\,1/3}|q_x|q_x}{h^2},\quad \frac{\tau_y}{\rho}=\frac{gn^2R_y^{\,1/3}|q_y|q_y}{h^2} \quad [8]$$

where, q_{CH}, q_{SW} and q_{GR}: interacting discharge with the channel, the sewerage and the ground surface respectively. q_x and q_y are defined at the same grid point as that for M, N and h.

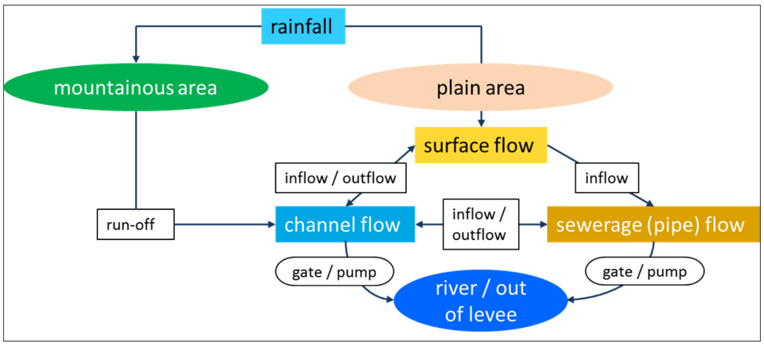

Figure 4. Structure of the inundation simulation model, AFREL.

These equations are numerically solved explicitly on the staggered grid in space, and by the leap-frog method in time. Runoff discharge from the surrounding mountainous areas of 2.68km^2 are estimated by the rational method and given at the upstream end of a channel connected to the relevant mountain stream. Table 1 shows roughness coefficients adopted here in accordance with the land-use classification.

In the simulation, 3 scenarios of land-use changes were demonstrated. In case of housing land development, an area along a prefectural highway crossing the studied area is assumed to be developed, raising land elevation 1.0m and changing the roughness coefficient from paddy fields, 0.06, to building areas, 0.05. The changed area reaches up to almost 30% of the whole studied area (see Figure 5 (a)). In case of rice cropping abandonment, 2 options are considered, one is the abandonment along the prefectural highway, the same area as the housing land development just mentioned above, the other is that near the mountainous area (see Figure 5 (b) and (c)). Here, the roughness coefficient is changed from paddy fields to uncultivated areas, 0.05, but the land elevation is maintained in the same level. Furthermore, one more scenario of river and channel improvement works was examined, where the Otsuda River and major irrigation channels are enlarged and deepened (see Figure 5 (d)).

Table 1. Standard roughness coefficients adopted in the simulation.

Land-use	Roughness Coefficient
Paddy Ffields	0.060
Roads	0.047
Buildings	0.050
Forests	0.060
Water Areas	0.030
Cultivated Areas	0.050
Uncultivated Areas	0.050
Irrigation Channels	0.015

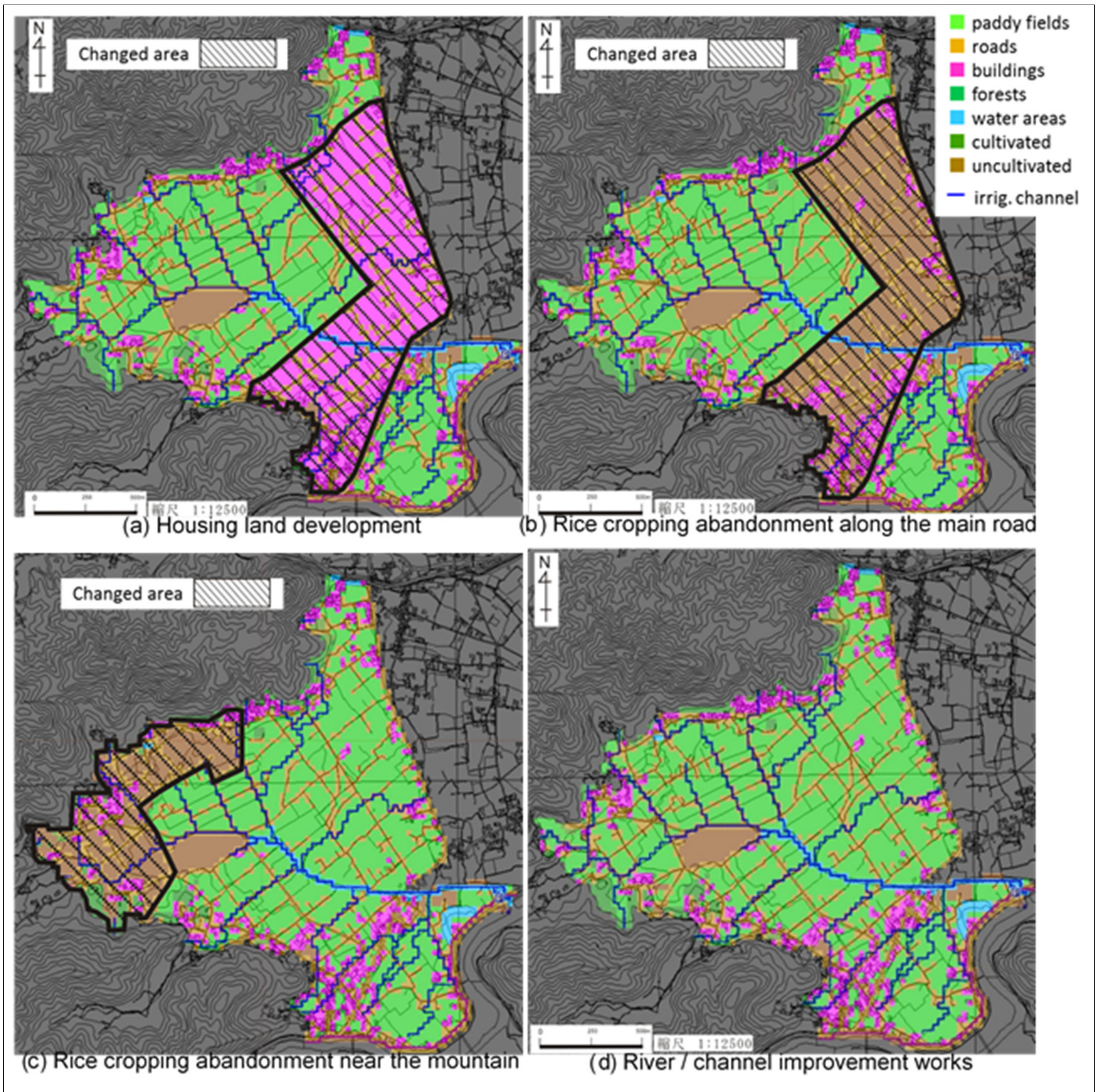

Figure 5. Studied land-use change scenarios.

4 RESULTS AND DISCUSSIONS

4.1 Model verification and sensitivity analysis

First of all, in order to check whether the model can reproduce well an actual inundation event, model verification was performed with the inundation records in Typhoon 1511, July 2015, in which the total rainfall was 297mm within 43 hours. Here at the same time, whether the selected set of roughness coefficients is appropriate or not was also checked, by varying the roughness coefficient for paddy fields from 0.02 to 0.10 in 0.02 pitch. The reason why only the parameter of paddy fields was varied is because paddy fields occupies the largest area in the studied area, over 50%, thus the results were expected to react most clearly. The given precipitation hyetograph is shown in Figure 6.

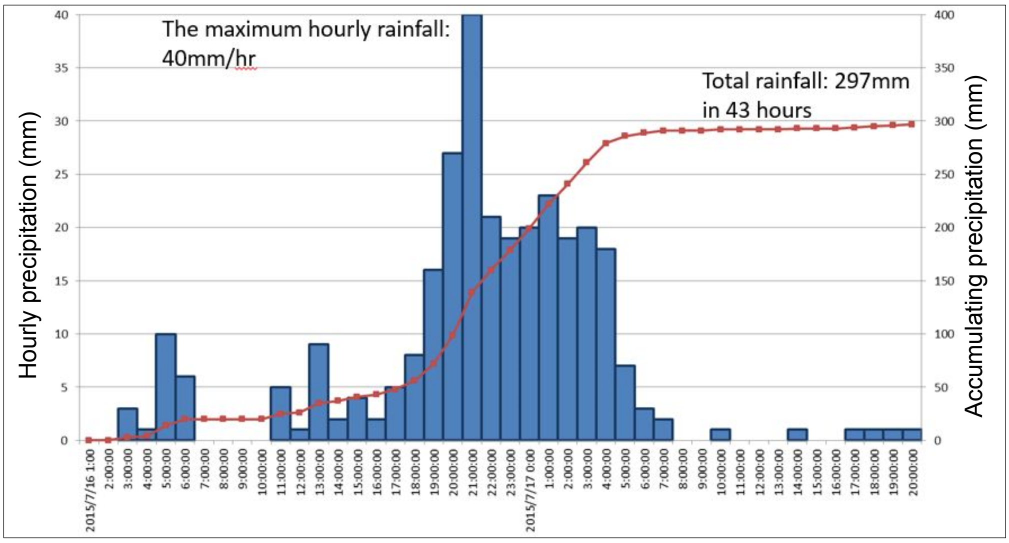

Figure 6. Precipitation hyetograph for model verification (Typhoon 1511).

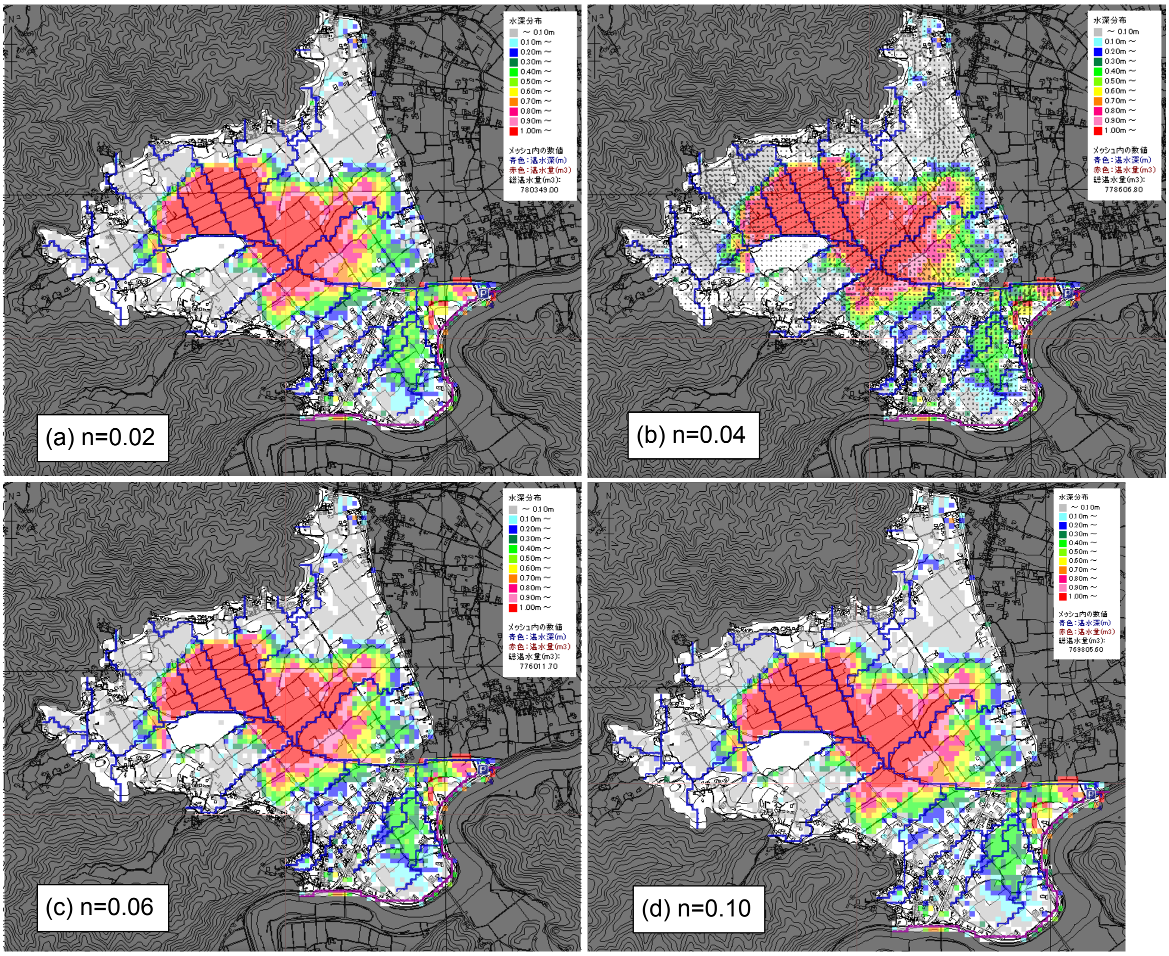

Figure 7. Sensitivity analysis of roughness coefficient n for paddy fields.

Figure 7 shows the simulation results. Here, the maximum depth recorded during the event at each grid is shown in a contour form. As shown in the figure, the effect of roughness coefficient variation is quite a few, almost negligible. In order to check the model verification as well as to select the best roughness coefficient value, water depths read from the flood marks at 10 points in the field were used. Table 2 shows the errors and their statistics. The table shows that the errors are mostly within 20cm, and the best roughness coefficient for paddy fields can be 0.06 or 0.08. In this study, 0.06 was used hereafter, following several foregoing studies (Kazama, 2008).

Table 2. Model verification: error analyses for the point depths.

Point No.	Errors at Each Depth Measured Point (meter)				
	Roughness Coefficient				
	0.020	**0.040**	**0.060**	**0.080**	**0.100**
1	-0.165	-0.165	-0.165	-0.165	-0.165
2	0.115	0.115	0.105	0.105	0.105
3	-0.035	-0.035	-0.035	-0.035	-0.045
4	0.097	0.097	0.097	0.097	0.087
5	-0.081	-0.081	-0.091	-0.091	-0.091
6	-0.022	-0.022	-0.022	-0.022	-0.022
7	0.207	0.207	0.207	0.207	0.207
8	-0.191	-0.191	-0.191	-0.191	-0.191
9	-0.114	-0.114	-0.114	-0.114	-0.124
10	0.084	0.084	0.084	0.084	0.084
Simple Mean	-0.0105	-0.0105	-0.0125	-0.0125	-0.0155
Magnitude Maen	0.1111	0.1111	0.1111	0.1111	0.1121
RMS	0.1255	0.1255	0.1253	0.1253	0.1259

4.2 Retarding capacity estimation and the effects of land-use change

Retarding capacity of the paddy fields was estimated with a model rainfall, based on the records by Typhoon 1412, August 2014, in which the total rainfall within 24 hours was 590mm, over 1/100 years return period in probability analysis. Here, the effect of land-use change on the retarding capacity was also examined. The model precipitation hyetograph is shown in Figure 8. Inundation depth distributions at the peak inundation volume are shown in Figure 9 for the present condition together with after 3 land-use change scenarios being applied to.

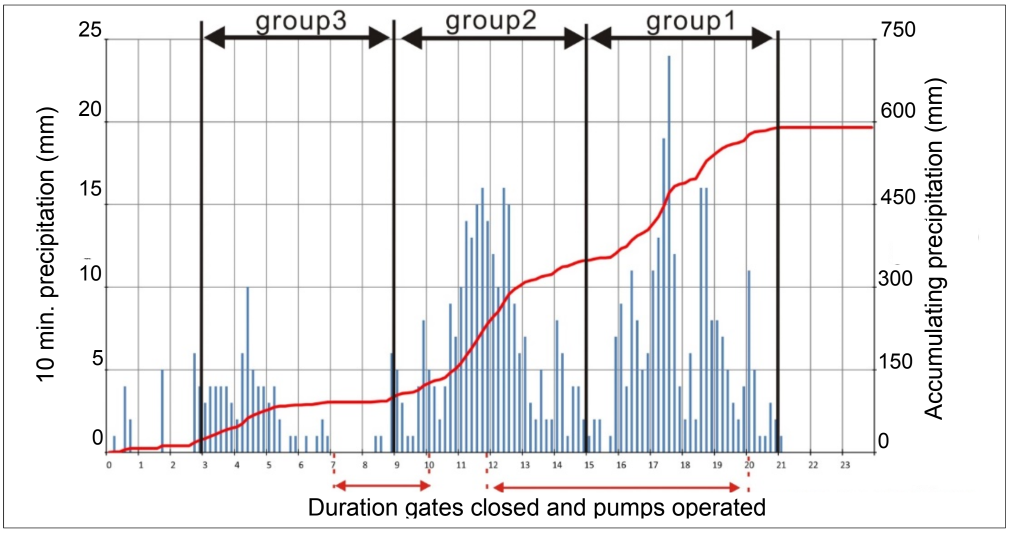

Figure 8. Precipitation hyetograph for retarding capacity estimation.

In the present condition, Figure 9 (a), an area over 2m water depth widely spreads in the central part of the studied area. Over 2m depth line well coincides with 3.0m altitude line, and the boundary between the inundated and non-inundated areas is around 5.0m in altitude (see Figure 2). The peak inundation volume reaches 2,368×10^{3}m^3.

When housing land is developed, Figure 9 (b), it is clear that inundation depths in the developed area decreases about 1.0m. This is presumably due to the land elevation rise for the house development. On the other hand, inundation depths in the unchanged area are not so much changed from the present condition. This means that the housing land development does not affect the drainage process in the unchanged area, but just reduces the inundation volume in the developed area. This can also be understood from the peak inundation volume, reduced to 2,125×10^{3}m^3 from the present condition, mainly by the inundation depth reduction in the developed area.

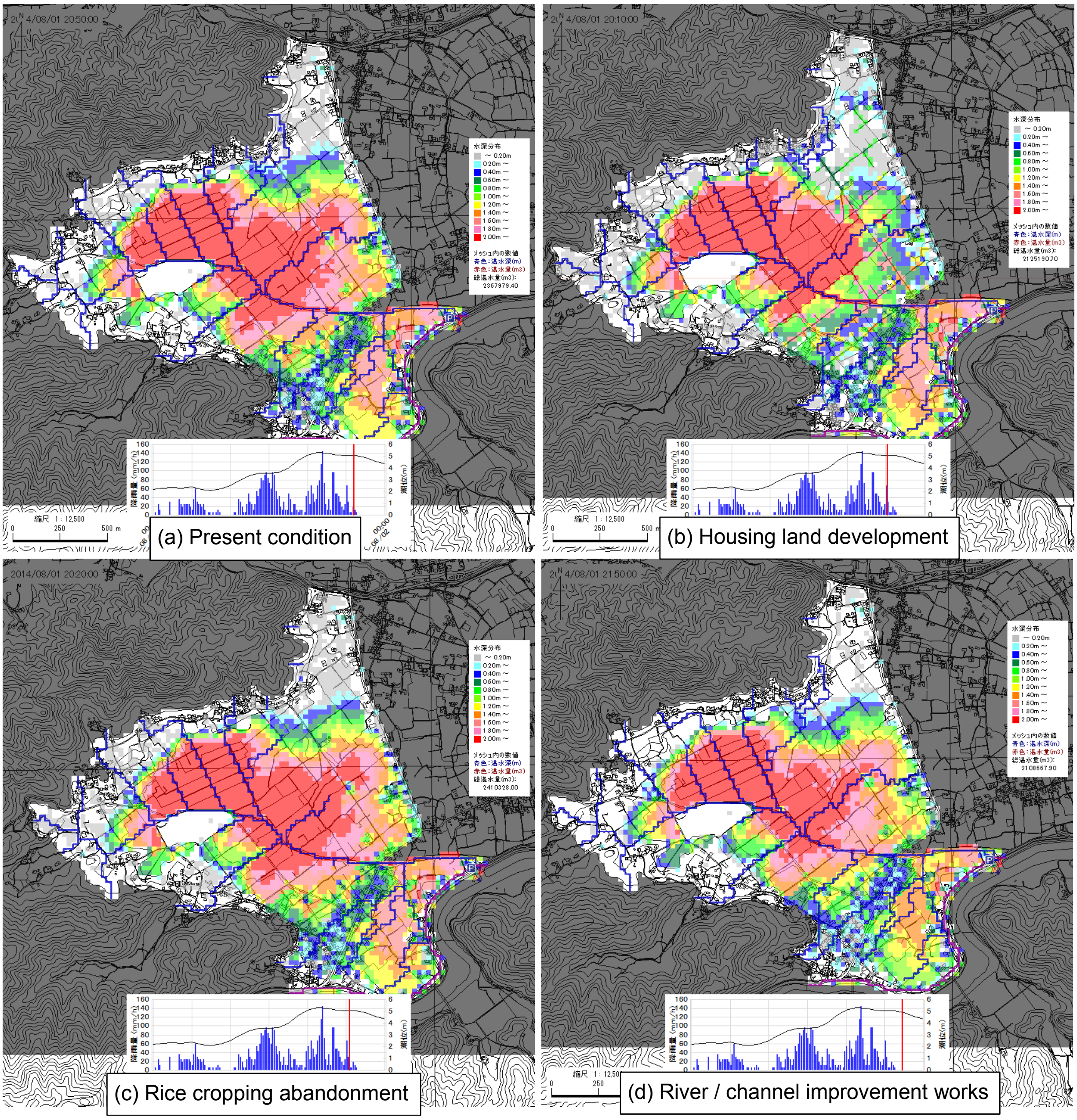

Figure 9. Inundation depth distributions at the peak inundation volume.

When rice cropping abandonment arises along the prefectural highway, Figure 9 (c), different from the first expectation, the peak inundation volume is not changed, rather slightly increases, from the present condition, 2,410×10^{3}m^3. In the inundating process, before reaching its peak, instant inundation volumes are always smaller than the present condition when comparing at the same time, probably due to a smaller roughness coefficient value in the uncultivated area than in the paddy fields. However, as approaching the peak, the inundation volume for the case gradually catches up that for the present condition. This indicates that, considering that the given precipitation is rather large as mentioned above, the effect of land-use change itself, only by adjusting the roughness coefficient, is not so significant under such a rare event. Here, the result for rice cropping abandonment near the mountainous area is not shown, but is more or less similar to those mentioned in this paragraph.

When river / channel improvement works is applied, Figure 9 (d), the inundated area at the peak volume is similar to the present condition, but the inundation depths are slightly smaller. This is attributed to the drainage improvement by enlarging the river and channels. One can also notice that the effect of drainage improvement spreads equally over whole of the studied area, that is, the depth reduction can be seen everywhere, although the reduced value itself is not so noticeable. The peak inundation volume is reduced to

2,109×10^{3}m^3, the minimum among the tested cases, however the inundated area is not changed so much, indicating further necessity of river improvement works.

Table 3 summarises the peak inundation volumes for all the tested cases. Both the housing land development and the river / channel improvement works can reduce the peak inundation volume up to about 90% of the present condition among the tested cases. However, this vice versa means that flood retarding capacity is reduced in these scenarios, which implies further necessity of river improvement works in the downstream. It should also be mentioned that the peak occurrence time is different for each scenario, suggesting the inundation process is somewhat different according to the selected scenario.

Table 3. Peak inundation volume for different land-use scenario.

Land-use Scenario	Inundation Vlolume (10^3 cubic meter)	% to Present Condition	Peak Occurece Time
Present Condition	2,368	---	20:50
Housing Land Development	2,125	89.7	20:10
Rice Cropping Abandonment (along the main road)	2,410	101.8	20:20
Rice Cropping Abandonment (near the mountain)	2,424	102.4	20:20
River / Channel Improvement Works	2,109	89.1	21:50

4.3 Inundation response onto different precipitation magnitude

In the previous section, retarding capacity of paddy fields and its variation after land-use changes are evaluated only in terms of the peak inundation volume. However, when checking the inundation process shown in Figure 10 more closely, where temporal variations of inundation volume are shown, it was found that the summary in Table 3 is not always applicable to the whole inundating duration. That is, one can notice in the figure that relative differences among the tested cases are basically the same up to 19:30 hours in the simulation time, nevertheless they are suddenly changed at around that time and afterward. The peak inundation volume appear after that time for all the cases, thus it may only show one, rather prejudice, aspect of inundation. This is presumably attributed that the rainfall event modelled here is a rare and extraordinary case, over 100 years return period, as mentioned above. This at the same time indicates that response of the paddy fields against inundation can vary according to precipitation magnitude.

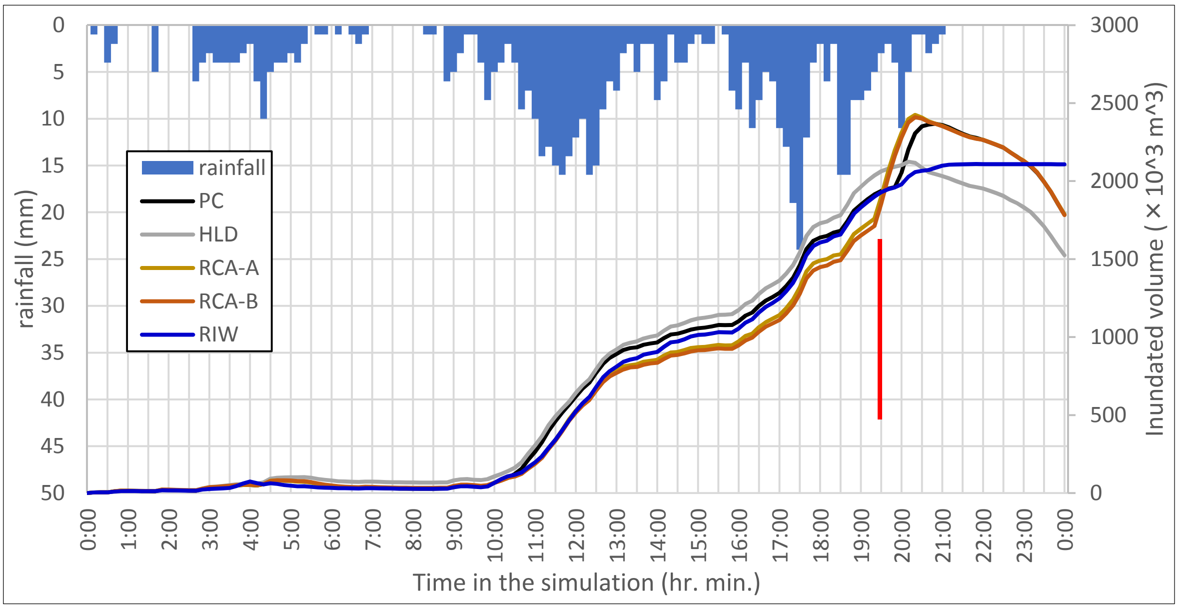

Figure 10. Temporal variations of inundation volume in the whole simulation time.

Instead of preparing and testing several different rainfall models, the adopted model precipitation distribution shown in Figure 8 was divided into 3 groups, and 2 new model rainfalls were defined. Model A is up to 8:00 hours in the simulation time, where the total rainfall is 91mm and is evaluated to be 1.25 years return period. Model B is up to 15:30 hours, where the total rainfall is 353mm and to be 20 years return period. Figures 11 and 12 show temporal variations of inundation volume in first and second 8 hours in the simulation time respectively.

Figure 11 shows that for a rainfall event occurred almost every year, the river / channel improvement works is most effective in drainage. The rice cropping abandonment does not change the situation so much, that is the case for the peak volume, too. Only the housing land development increases the inundation volume than the present condition for this rainfall amount, probably due to blockage of drainage in some parts affected by the land elevation rise.

For a large rainfall event such as 20 years return period, Figure 12, the river / channel improvement works gradually loses its effectiveness. This is quite reasonable since the river / channel enlargement adopted in this study is basically designed against floods of 10 years return period. In contrast, decreasing the inundation volume by the rice cropping abandonment gradually becomes noticeable, suggesting that roughness value change due to the land-use change is effective in some limited ranges such as considered here. The housing land development is drawn over the present condition throughout, opposite to the estimation for the peak volume, indicating the blockage effect is more predominant than the inundation relief effect by land elevation rising for this amount of rainfall.

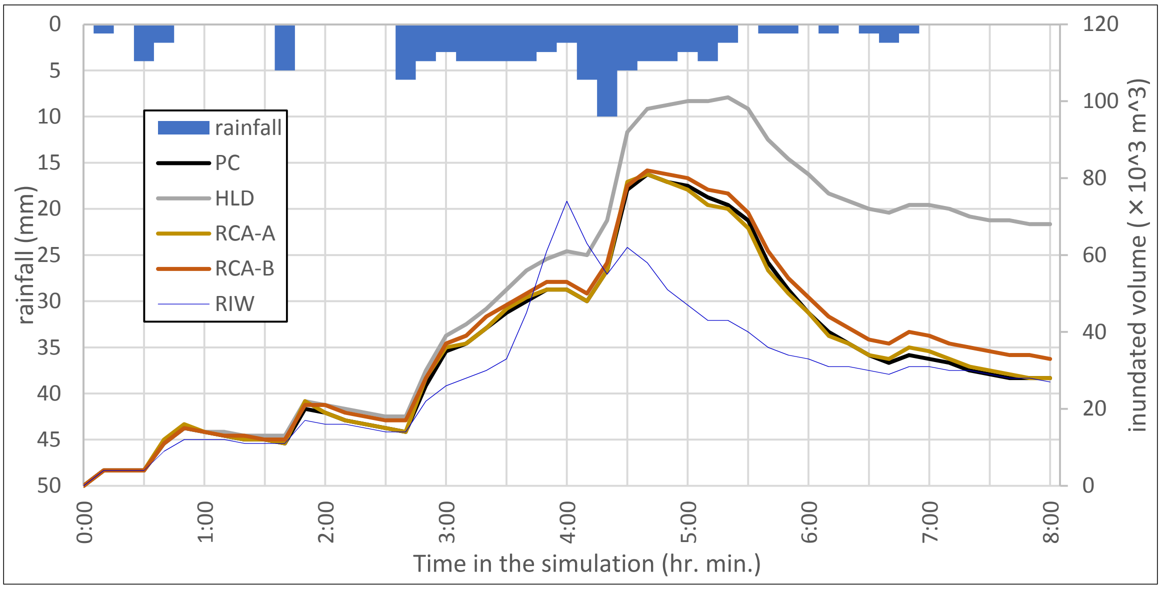

Figure 11. Temporal variations of inundation volume in the first 8 hours.

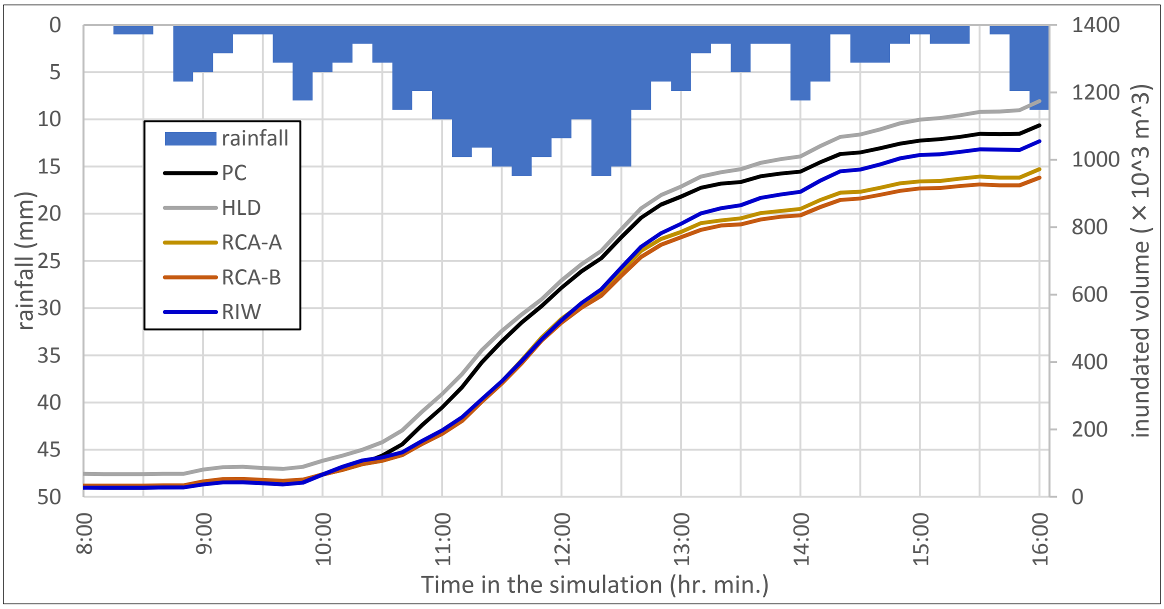

Figure 12. Temporal variations of inundation volume in the second 8 hours.

5 CONCLUDING REMARKS

Summary of the paper can be given as follows:

- Retarding capacity of wetland paddy fields was evaluated using a commercial inundation simulation software, AFREL. The simulation results successfully illustrate temporal variations of the inundated area and its depth distributions, giving errors in the depth within 20cm everywhere in the studied area;

- Sensitivity analysis for the roughness coefficient in the simulation model was carried out. It was found out that the simulation results do not so sensitively respond to the change of roughness coefficient, especially that of less than 0.02. From the error analyses, the best solution is shown to be 0.06 as the roughness coefficient for paddy fields;
- Comparing the peak inundation volume under quite large rainfall over 100 years return period, the housing land development and the river / channel improvement works can reduce the peak inundation volume up to about 90% of the present condition;
- Effects of land-use change on the retarding capacity vary in accordance with precipitation magnitude. As long as a rainfall event is under the designed level, river / channel improvement works can drain the inundating volume most promptly and effectively, but it vice versa means reducing retarding capacity of the wetland, and additional improvement works in the downstream river may be necessary. When an event exceeding the design level occurs, the drainage effectiveness of rice cropping abandonment gradually becomes noticeable. However, this too indicates reducing the retarding capacity of the wetland;
- Cost / benefit analyses, comparing between maintaining the paddy fields as retarding ponds and river improvement works following to drainage acceleration by land-use changes like studied here, will be necessary in the future study;

ACKNOWLEDGEMENTS

We acknowledge the funding support by the Environment Research and Technology Development Fund (4-1504, the principle investigator: Prof F. Nakamura, Hokkaido University) of the Ministry of the Environment, Japan.

We also acknowledge Prof M. Kamada, Tokushima University, for his valuable comments from the viewpoint of ecology and Eco-DRR, and Mr. K. Shimada, formerly an undergraduate student of Tokushima University, for his computation works.

REFERENCES

Green Infrastructure Association (2017). *Green Infrastructure: A Definitive Edition*. Nikkei BP, Japan, 392 (in Japanese).

Ichinose, T. (2007). Wetland Environment and Its Conservation and Restoration in Agricultural Area under a Pressure of Deterioration due to Cropping Abandonment. *Chikyu Kankyo, Association of International Research Initiatives for Environmental Studies*, 12, 37-47, (in Japanese).

Iwasa, Y. & Inoue, K. (1982). Mathematical Simulation of Channel and Overland Flood Flows in View of Flood Disaster Engineering. *Journal of Natural Disaster Science*, 4(1), 1-30.

Kazama, S. (2008). Research on Evaluation and Adaptation toward AR5. *Symposium on Promotion of Utilising Information on Future Climate Change in Hydrology Area*, http://hydro.iis.u-tokyo.ac.jp/cc2008ws/. (in Japanese).

Ministry of the Environment (2016). *Ecosystem-Based Disaster Risk Reduction in Japan, A Handbook for Practitioners*. Japan, 24.

Miyazu, S., Yoshikawa, N., Abe, S., Misawa, S. & Yasuda, H. (2012). Development of Application of Evaluation Model for Interior Flood Damage Mitigation Effect of a Paddy Field Dam. *Transactions of The Japanese Society of Irrigation, Drainage and Rural Engineering*, 80(6), 479-488, (in Japanese).

NITA Consultant Co., Ltd. (undefined). Introduction to AFREL. http://www.nita.co.jp/index.php/software/afrel. (in Japanese).

Thang, N.T., Inoue, K., Toda, K. & Kawaike, K. (2004). A Model for Flood Inundation Analysis in Urban Area: Verification and Application. *Annuals of Disas. Prev. Res. Inst., Kyoto Univ. B*, 47, 303-316.

Proceedings of the 37th IAHR World Congress
August 13 – 18, 2017, Kuala Lumpur, Malaysia

A METHOD TO ASSESS GREEN INFRASTRUCTRE COSTS AND BENEFITS FOR URBAN HEAT ISLAND REDUCTION

KYEON J. WOO[1], SANG R. KIM[2], JIN Y. SHIN[3], JAE S. PARK[4],
WOO B. BAE[5], YUN M. PARK[6] & YONG G. KIM[7]

[1,2,3,4,5,6,7] Korea Conformity Laboratories, Seoul, South Korea,
ykkim@kcl.re.kr

ABSTRACT

This study presents a method to quantitatively assess a performance of green infrastructure for urban heat island reduction based on “A Guide to Assessing Green Infra-structure Cost and Benefits for Flood Reduction,” which is published by National Oceanic and Atmospheric Administration (NOAA) in the US. The study proposes a method to assess GI performance by utilizing a climate chamber which can generate artificial climate conditions such as rainfall, solar radiation, temperature, and relative humidity. The experiments to evaluate drought resistance of GI at solar radiation strength (800W/m^2, 1200W/m^2), freezing resistance of GI at low-temperature (-40°C), and water permeability and moisture absorption capability of GI at rainfall intensity (24mm/hr, 75mm/hr) are carried out by using this climatic chamber. The performance factors derived from these experiments will be used as quantitative factors for the establishment of GI strategy on targeted evaluation area in the city, and it is expected to be used for the future GI costs and benefits for UHI reduction.

Keywords: Urban heat island; green infrastructure; climatic chamber; hydrological cycle management; costs and benefits.

1 INTRODUCTION

In summer 2016, the Korean peninsula, which is located under monsoon climate, had suffered from numerous disasters. The Korean government had the death toll at 16, which was caused by urban heat island (UHI) and heat wave in the same year. In October, Typhoon Chaba caused 7 deaths, 3 missing, and 10 injuries in southern regions of the Korean peninsula. From 2003 to 2013, the heat waves caused a total of 293 deaths, while flood with typhoons and heavy snow caused total 280 deaths. These facts mean that the death caused by a heat wave and tropical night is not numerically less than any other disasters happened during the recent years of rapid climate change. An increase of impermeable urban regions causes drought, flood, and heat wave. In 2010, the impermeability of Seoul City increased up to 6.1 times much higher than the year in 1962. According to climate data of Korea Meteorological Administration from 2001 to 2011, 60% more of heavy rainfall, 6 times more of tropical nights, and 3 times more of heat wave would likely occur in 2050. However, the damage caused by flood, drought, and UHI can be reduced by hydrological cycle management based on green infrastructure strategy.

The green infrastructure strategy is an alternative option to manage the hydrological cycle considered with Korean regional and seasonal elements; therefore, the cost-benefit and performance of green infrastructure’s UHI reduction need to be quantified. In searching for that case, US National Oceanic and Atmospheric Administration (NOAA)’s “A Guide to Assessing Green Infra-Structure Costs and Benefits for Flood Reduction” is provided to suggest a process that communities can use to assess the costs and benefits of green infrastructure for flood reduction. Unlike NOAA’s complete guide, it is still inadequate to quantify green infrastructure’s mitigating effect on reducing UHI. In addition, the study of assessing green infrastructure is required to advance the Korea’s ongoing policy relate to the hydrological cycle management to reduce flooding, drought, heat wave, and UHI.

Therefore, this study proposes a methodology for evaluating net benefit of GI through performance evaluation for UHI reduction. It focuses on the empirical experimental stage, which is among the six methods, to assess GI costs and benefits by UHI reduction. The 5 steps of total 6 steps are based on NOAA’s method. The fourth step, which is based on the empirical evaluation, is added as a new step in the method. The specific GI elements that used commonly in the cities are selected to test this new step in the method. The deduction of performance evaluation factors of GI elements using the climatic chamber are as follows:

1) Freezing resistance of GI at cold with dry winter climate, or polar climate;
2) Stormwater permeability and water absorption performance of GI at rainy climate;
3) Drought resistance at desert climate.

In conclusion, this study proposes a method to assess GI costs and benefits for UHI reduction by using a quantitative evaluation method.

2 A NEW METHOD TO ASSESS GI COSTS AND BENEFITS FOR URBAN HEAT ISLAND REDUCTION

NOAA's method of assessing green infrastructure costs and benefits for flood reduction outlines a six-step process with specific tasks associated with each step:

1) Identify the scope of comprehensive problems in the evaluation of city area;
2) Modeling the current and future flood situation in the evaluation of city area to derive flood damage cost;
3) Establish GI strategy by selecting GIs that can achieve stormwater runoff management targets for flood mitigation;
4) Quantify flood damage by remodeling based on selected GI strategies for current and future flood situations;
5) Calculate the cost of the GI strategy and the installation cost of the GI, and calculate the regional common interest through the GI strategy, and converting convert them to the annual GI cost and net benefit.

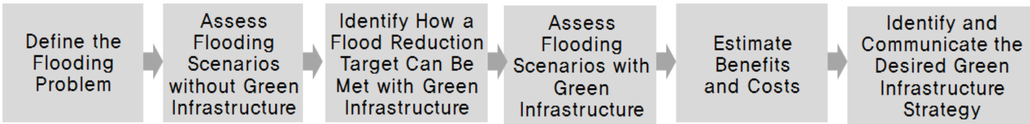

Figure 1. A process to assess GI costs and benefits for flood reduction, NOAA, 2015.

NOAA's systematic method uses the simulation program, such as SWMM 5.0, to calculate the flood reduction value, the common interest of the target area, and the cost to install the GI when the strategically selected GI element is installed in the evaluation area, and convert net benefit to an annual rate. This method is already in progress to evaluate the United States' regional cities through a variety of cases. This method is a quantitative way to see how much of the current GI technology can be used for flood mitigation. However, although it is a good methodology to evaluate flood reduction of targeted cities, the result of this current method cannot be accurate because it does not consist of real evaluated factors of GI in the targeted cities for simulation. GI factors such as permeability, impermeability, moisture content capacity, evapotranspiration, and many other factors are not tested with testing equipment. Therefore, a new testing step to accurately derive the GI factors is required to evaluate GI elements, and ultimately evaluate the targeted area with GI elements.

Based on the stepwise method that assess costs and benefits of GI for flood reduction, this study proposes a method to assess GI performance for UHI reduction in the following orders:

1) Identify the cause of the urban heat island and the damage factors in the targeted area where the urban heat island occurs;
2) The modeling of the urban heat island situation in the evaluation area will quantify the damage caused by urban heat island occurrence in the absence of GI as cost;
3) Establish a preliminary GI strategy that can achieve setting target of urban heat island reduction by installing GI elements in targeted area;
4) Establish final GI strategy after evaluating each GI unit's reduction performance of urban heat island using climatic chamber;
5) Quantify the damage of targeted evaluation area where the urban heat island occurs by remodeling current and future urban heat island reduction scenarios based on selected GI strategy;
6) The cost of both GI strategy and GI installation are compared with the common interest of the targeted evaluation area of city through GI strategy, and convert GI cost and net benefit into annual rate.

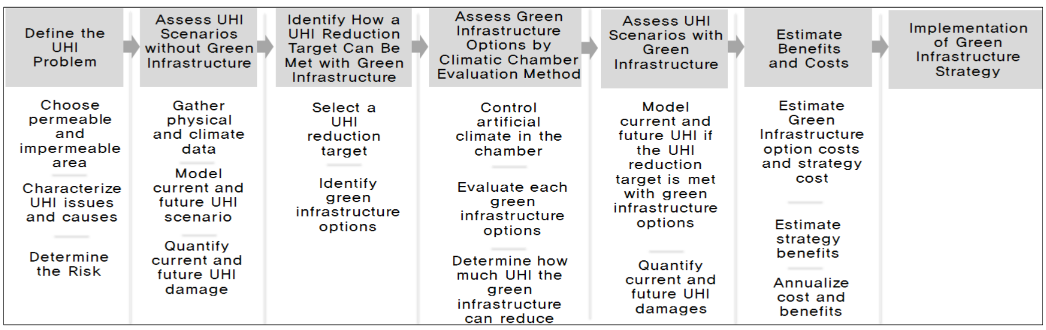

Figure 2. A new process to assess GI costs and benefits for urban heat island reduction.

NOAA's method of assessing green infrastructure costs and benefits for flood reduction is limited to the modeling method of the target area using the simulation program so that the quantitative performance of each

GI unit is not certain. In order to secure this, a climatic chamber is used to simulate the actual climatic conditions, which are generated to derive a step of quantitatively evaluating the performance of each GI unit. Thus, this new step of evaluating each GI unit's performance of UHI reduction using climatic chamber is added to complete the methodology of evaluating UHI reduction of targeted area based on NOAA's method.

3 GI PERFORMANCE EVALUATION METHOD USING CLIMATIC CHAMBER

3.1 Selection of green infrastructure elements

There are various types of GI, and they can be classified as reservoir type, filtration type, and sediment type. The reservoir type is intended to protect rivers and banks due to floods by preventing stormwater runoff. It has a function of the reduction of non-point pollutant sources such as sedimentation by plants in the reservoir and decomposition of absorbed microorganisms. The filtration type reduces non-point pollutant sources by using vegetation adsorption, biochemical reaction, and permeability of coloring soil, and it also reduces stormwater runoff through the rubbles in the lower layer of GI. The sediment type reduces non-point pollutant sources by filtration and moisture adsorption effect through soil infiltration and penetrates rainfall to prevent stormwater runoff and fills underground water. All of the reservoir type, filtration type, and sediment type have the function of stormwater runoff reduction, and it leads to the reduction of non-point pollutant sources, flood, and urban heat island. Among them, the most common and frequently used permeable and filtration type of GI elements in the present city are selected and their performance is evaluated. We have selected GI elements, permeable high-density polyethylene (HDPE) tree pit cover plate, polyvinyl chloride (PVC) tree pit frame, and high-density polyethylene (HDPE) permeable pipe, which forms a filter box for roadside trees. Tree pit frame supports tree pit cover plate and connects it to the support framework of the filter box. HDPE permeable pipe installs into the soil of ground, around the tree roots, and penetrates the rainwater to the drainage layer of the tree, and the air flows into the inside of the pipe, thereby allowing the root to breathe in the air. The performance of these GI elements is evaluated in the range of dry winter, or polar climate, rainy climate, and desert climate.

1) Performance evaluation targets: permeable HDPE tree pit cover plate, PVC tree pit cover frame, permeable HDPE pipe
2) Performance evaluation factors : capability of moisture absorption, capability of infiltration, and freeze resistance
3) Climatic conditions : dry winter climate, or polar climate, rainy climate, and desert climate

3.2 Introduction of climatic chamber

As part of the project to establish a distributed shared infrastructure of the Ministry of Land, Infrastructure and Transport, the Korea Conformity Laboratories constructed a multi-environmental test facility for response to climate change. A large climatic chamber (20mx25mx25m (H)), which is part of the experimental facility, has a temperature of -10 ~ 60°C, humidity of 10 ~ 90% RH, solar radiation of 800 ~ 1200W/m^2, rainfall 25 ~ 150mm/hr, and snowfall 50mm/h. It can simulate most of the climatic conditions abroad.

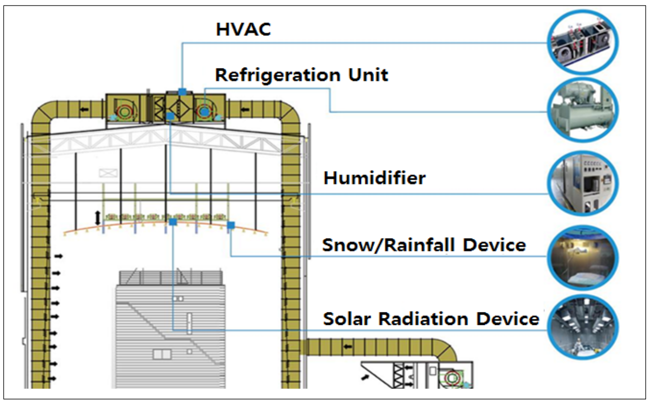

Figure 3. Drawing of climatic chamber with equipment.

3.3 Establishment of mock-up

In order to evaluate the performance factors of GI elements such as permeable HDPE tree pit cover plate, PVC tree pit cover frame, permeable HDPE pipe, the mock-up in which these elements can be installed for the experiment were designed by considering the factors such as follows:

1) The amount of water penetrated into the soil should be measured quantitatively;
2) After the water is supplied to the soil from the outside, water should be drained by gravity and the amount of water should be measured in the state where there is almost no movement of water at the lower layer;

3) The outflow of water (runoff) that cannot penetrate the soil should be measured;
4) The weight of the specimen should be measurable excluding the weight of the mock-up.

The mock-up was designed to satisfy following specification to measure the above factors:

1) Dimensions: dimension (1m x 1m) that enable to fit into rainfall area and solar radiation area of the climatic chamber;
2) Height: The height(1.5m) that can measure the precipitation particle size by measuring device (2m high) in between the distance of rainfall device and specimen(1.5m) installed on the top of mock-up;
3) GI installation space: maximum space for installing soil, erosion-proof gravel, non-woven fabric, drainage material, permeable block, etc.;
4) Water Collecting space: space for collecting water poured into the soil;
5) Drain valve: a device capable of measuring the amount of water which drained by collected water in the catchment space;
6) Capable of moving mock-up: installation of wheels for movement into the chamber;
7) Weighing: A load cell to measure the weight of installed GI, infiltrated water and moisture content of soil.

3.4 Installation of green infrastructure elements on mock-up

GI elements like permeable HDPE tree pit cover plate, PVC tree pit frame, permeable HDPE pipe were selected to evaluate their capability of infiltration of water into the soil, the capability of moisture absorption, and freezing resistance. The specification of each GI element is as follows:

Table 1. GI elements specification.

	Cover Plate	Cover Frame	Pipe	Soil
Material	Hgih Strength HDPE	PVC	Hgih Strength HDPE	Standard Soil (KSL51000)
Dimension (LWH, mm)	211 x 308 x 80	90x80x80	148 diameter x 300	N/A
Number	12 each	8 each	4 each	30 bags

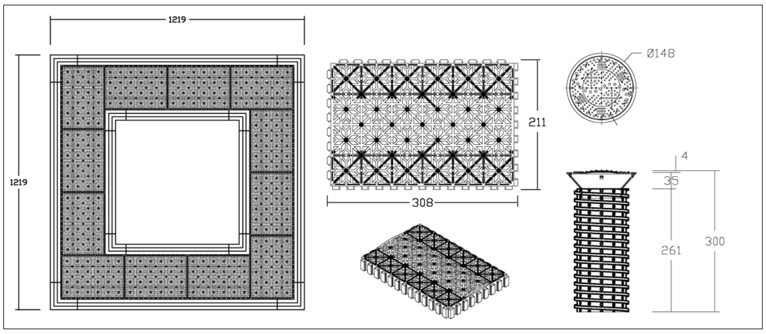

Figure 4. Green infrastructure elements installed on a mock-up.

3.5 Setting climate conditions

A variety of climatic conditions is needed to quantitatively evaluate the performance of GI elements for UHI reduction. Therefore, the purpose of this experiment is to demonstrate the quantitative evaluation of performance such as capability of moisture absorption, capability of stormwater infiltration, and freezing resistance of GI elements in representative climates, and the preparation of experimental procedures to set up a new process to assess GI costs and benefits for urban heat island reduction.

Table 2. A variety of climate conditions for evaluating performance factors of GI elements.

	Winter Climate	Polar Climate	Rainy Climate	Desert Climate
Temperature	-40~5±0.5℃	-40~5±0.5℃	N/A	46~56℃
Humidity	16~55%±0.5% RH	16~55%±0.5% RH	N/A	2% RH
Solar Radiation	N/A	N/A	N/A	800,1200W/m^2
Rainfall	N/A	N/A	25,75mm/hr	N/A

3.6 Evaluation of freezing resistance at low temperature (-40°C) in dry winter, or polar climate

In the case of low-temperature experiments in the cold climate, experiments were conducted in order to evaluate the durability of the GI elements and to evaluate the feasibility of establishing the climate environment of the climatic chamber. Simulation of the climate and environment in the cold zone was conducted at -40°C in about 2 hours and 30 minutes. The temperature of climatic chamber decreased from -5°C to -35°C after approximately 72 minutes, and it took approximately 16 minutes to drop the temperature from -35°C to -40°C. The temperature dropped at the rate of 0.5°C/min from -5°C to -35°C which shows a favorable climate control conditions. The temperature decreased at the rate of 0.07 °C/min from -35°C to -

40°C. This climate condition control indicates that a maximum of 136 minutes is required to maintain the temperature at -40°C.

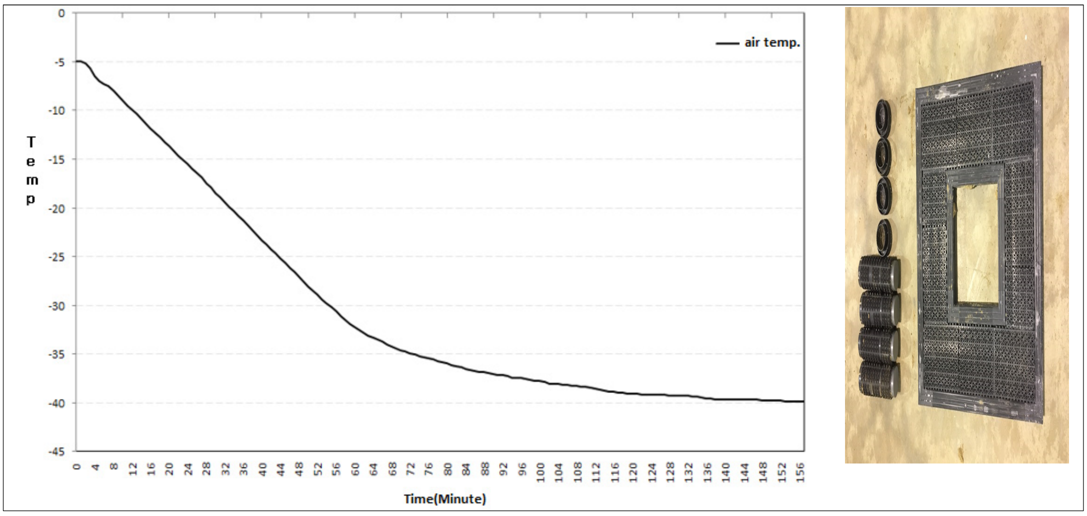

Figure 5. The graph of temperature decrease in a climatic chamber and tested GI elements.

Under these climatic chamber conditions, the GI elements and the mock-up are visually confirmed for their respective damage. The results of the damage of GI are as follows:

Table 2. The results of freeze resistance performance evaluation of GI at various climate.

Conditions	Permeable HDPE Pipe	HDPE Tree Pit Cover Plate	PVC Tree Pit Cover Frame	Mock-up
Blockage	Clogged air holes due to water condensation	Clogged air holes due to water condensation	No condensation	No Condensation
Crack	N/A	N/A	N/A	N/a

Experimental results show that permeable HDPE pipe and HDPE tree pit cover plate have some problems. The air/water holes are clogged through the water condensation and show that air penetration and water infiltration might not occur from sudden climate change. No other cracks were observed due to the freezing. This experiment can be regarded as an experimental attempt on evaluating freezing resistance due to the climate change rather than quantitative performance factors for urban heat island reduction.

In conclusion, this experiment evaluates the feasibility of operating climatic chamber, whether the cold climate condition is maintained or not. It is also done to evaluate the freezing resistance of the GI elements and to understand the procedural conditions of the demonstration phase at the stage of performance evaluation for the urban heat island reduction.

3.7 Evaluation of permeability and moisture absorption capability at rainy climate

Moisture infiltration amount and soil moisture content were measured according to the rainfall intensity (25mm/hr, 75mm/hr) in a rainy climate; therefore, permeability and moisture absorption were evaluated. The evaluation of both infiltration and moisture absorption performance of the GI elements and the evaluation of the feasibility of the climate environment of the climatic chamber are tested in this experiment. The climate condition of the rainy climate was emphasized by simulating the rainfall environment through the correction of the rainfall intensity and the distribution of rainfall, excluding the temperature and humidity conditions. Within the area of 2.5m x 2.5m, both rainfall intensity of 25mm/hr and 75mm /hr need to narrow the uncertain range by controlling them within ±10%.

Table 3. The rainfall intensities at 4 location points of mock-up.

Location(X,Y)	Point 1(0, 0)		Point 2(0,5)		Point 3(-5,0)		Point 4(-5,5)	
Condition	**25MM/HR**	**75MM/HR**	**25MM/HR**	**75MM/HR**	**25MM/HR**	**75MM/HR**	**25MM/HR**	**75MM/HR**
Rainfall Intensity	24mm/hr	69 mm/hr	27 mm/hr	72 mm/hr	24 mm/hr	69 mm/hr	24 mm/hr	69 mm/hr
Diff.	-4%	-8%	+8%	-4%	-4%	-8%	-4%	-3%

The following soil moisture content measurement sensors were installed to evaluate the soil moisture content and to evaluate the moisture absorption performance. The FDR type of sensor were installed at both 15cm and 30cm height from the bottom of the mock-up and they were installed 10cm away from the position of HDPE pipe to evaluate its permeability.

Table 4. The moisture content measurement sensors that installed in soil.

Sensor	FDR Type	Note
Installation Height	15cm, 30cm	Height from the Base

As the result of the experiment, the initial soil moisture content increased rapidly as the rainfall intensity increases (75mm/hr) at a height of 30cm from the base of mock-up when the lower soil moisture level (15cm) was saturated. It can be seen that the soil moisture content, which was left in the soil after infiltration of water, increases more than the infiltration of water amount.

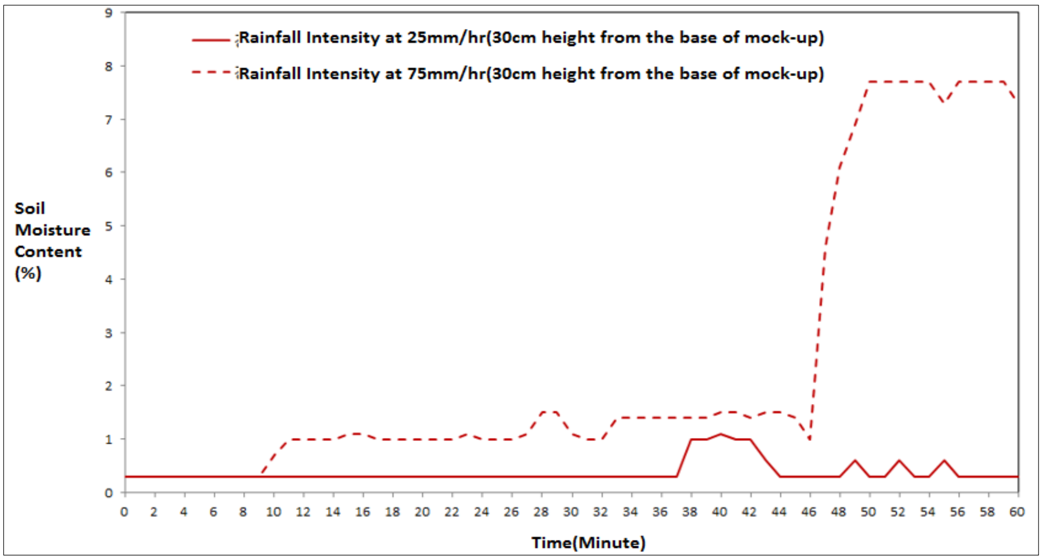

Figure 6. The graph of soil moisture content at 30cm height from the base of mock-up.

At the point of 15cm height from the bottom of mock-up, the initial soil moisture content increased rapidly with increasing rainfall intensity (75mm/hr), and tended to remain constant when the moisture content reaches 18% after 30 minutes. This is the maximum moisture content of the lower layer of soil that has infiltrated into the soil. In the case of low rainfall intensity (25mm/hr), it took a long time for water to infiltrate and the initial moisture content of the soil is small, but after 54 minutes, the soil moisture content increased suddenly that it increases at the rate of 5% per second.

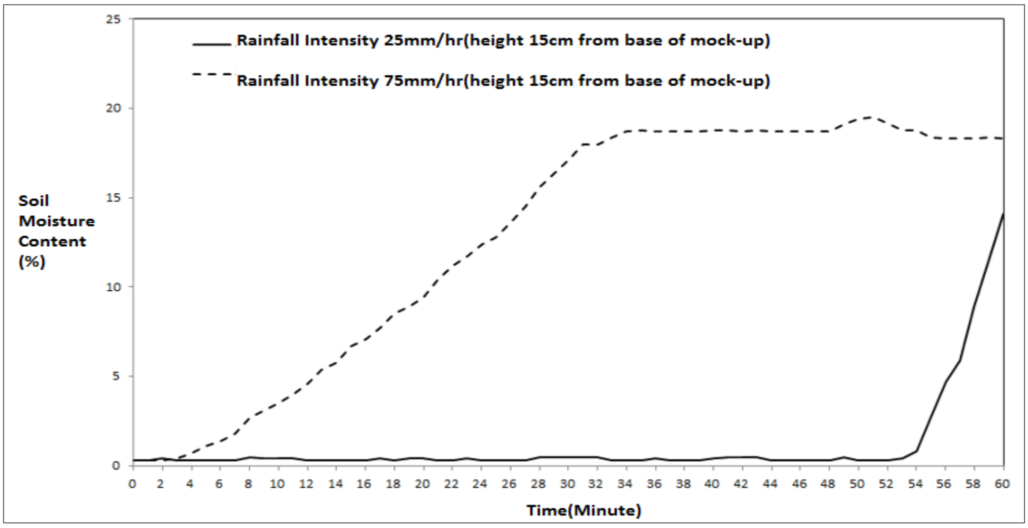

Figure 7. The graph of soil moisture content at 15cm height from the base of mock-up.

As a result, the GI elements show that when the infiltration of 75mm/hr rainfall is maintained for 50 minutes, the amount of water stored in the upper part (30cm) and that in the lower part (15cm) are saturated, and infiltration of water keep continued. However, the assessment of the amount of rainfall is based on a total area of 6.25m^2 at a rainfall of 75mm for one hour, resulting in 468.75 liters of water drop for one hour. Mock-up that installed GI elements in the area of 0.5m^3 infiltrates total 27.43L of water by permeability and flows out approximately 9.48L of water. As a result, it can be seen that about 37.5% infiltration effect can occur by 1m^2

size of GI element in an impervious area of 6.25m^2. However, if the moisture content of soil is included, the infiltration water amount will increase. It seems that the method of calculating the weight of moisture content of soil should be devised more in the future. In the future, it is expected that this method will be able to evaluate the performance for stormwater runoff reduction by measuring the infiltration water amount(permeability) and the moisture content amount (moisture absorption) of GI element.

Table 5. The measurement of different GI factors at two rainfall intensities.

Rainfall Condition	Rainfall Area	GI Area	Amount of Rainfall(60min)	Moisture Content of Soil(60min)	Infiltration Water Amount (60min)	Water Runoff Amount (60min)
25mm/hr	2.5mx2.5m	1m x 1m	156.25L	0.5%(Height 30cm) 1%(Height 15cm)	1.64L	14.26L
75mm/hr	2.5mx2.5m	1m x 1m	468.7575L	7.5%(Height 30cm) 20%(Height 15cm)	27.63L	9.48L

The amount of water infiltration at 25mm/hr rainfall intensity was very small, because the soil was saturated with water by the first rainfall experimental attempt at 75mm/hr rainfall intensity. This tells that the soil must be dried first to have 0% of moisture content to test and evaluate permeability of GI element.

In the end, this experiment was carried out to derive the procedures and criteria of the experiment to evaluate the permeability of the GI elements using rainfall devices. The amount of evapotranspiration, which is the key point of the urban heat island reduction, would be calculated based on quantitative evaluation of the outflow water amount and infiltration water amount of the GI elements in the future.

3.8 Evaluation of drought resistance at desert climate

In case of desert climate, the drought resistance is evaluated by measuring the surface temperature and soil moisture content at the solar radiation intensity (800W/m^2, 1200W/m^2). The drought resistance evaluation was performed by controlling the internal temperature of the climatic chamber at 50°C±2°C and generating solar radiation intensity at the upper part of the mock-up, and measuring the change of 18% soil moisture content that already absorbed from rainfall intensity in previous experiment. It is possible to generate the solar radiation intensity from 800W/m^2 to 1200W/m^2 by using metal halide lamps. However, in order to confirm the experimental procedure, the above two strengths were selected to test for 1 hour.

Table 6. The solar radiation conditions at low and high intensity.

Condition	Solar Radiation	Solar Radiation Area
Low Intensity	800W/m^2	4m x 4m
High Intensity	1200W/m^2	4m x 4m

Sensors for measuring the solar radiation intensity were installed at the vertices of the top of the mock-up. The air temperature was measured by installing the temperature sensor at 5cm above the top of the mock-up. Soil moisture content was measured by FDR type of soil moisture content sensor.

Table 7. The location of sensors to measure soil moisture content at different heights.

Sensor	FDR Type	Air Temperature Sensor	Surface Temperature Sensor	Pyranometer
Installation Location	Height 30cm (from base of mock-up)	Height 5cm (from top of mock-up)	HDPE Tree Pit Cover Plate	Vertex of mock-up

As a result, the soil moisture content was reduced from 10% to 7% as the solar radiation intensity of 800W/m^2 applied to both the mock-up and GI elements for 60 minutes, under a 50°C indoor temperature of the climatic chamber. The soil moisture content was reduced from 10% to 5% as the solar radiation intensity of 1200W/m^2 applied to both the mock-up and GI elements for 60 minutes, under a 50°C indoor temperature of the climatic chamber.

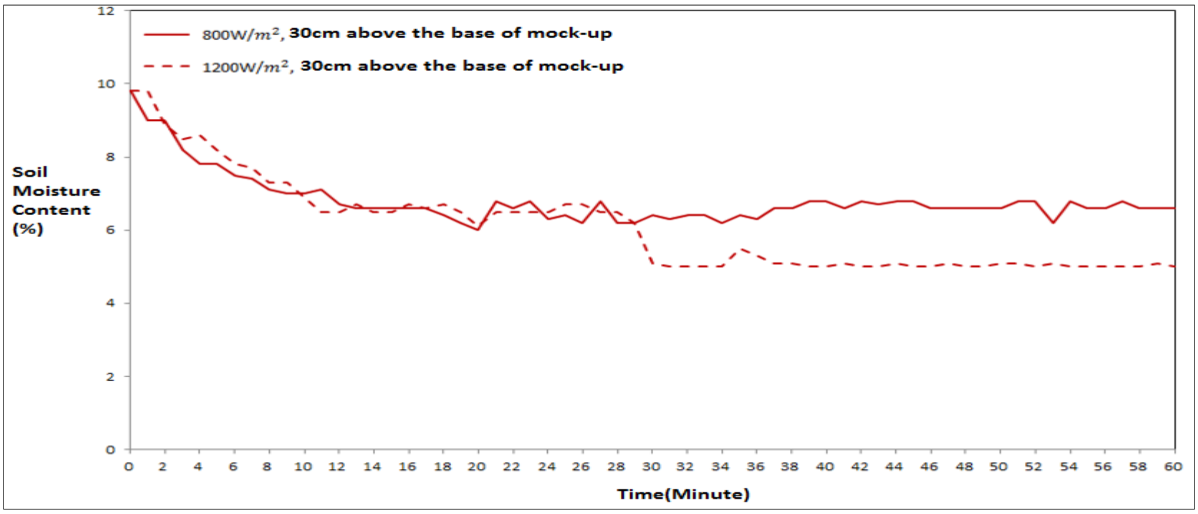

Figure 8. The graph of soil moisture content at 30cm above the base of mock-up under solar radiation

.

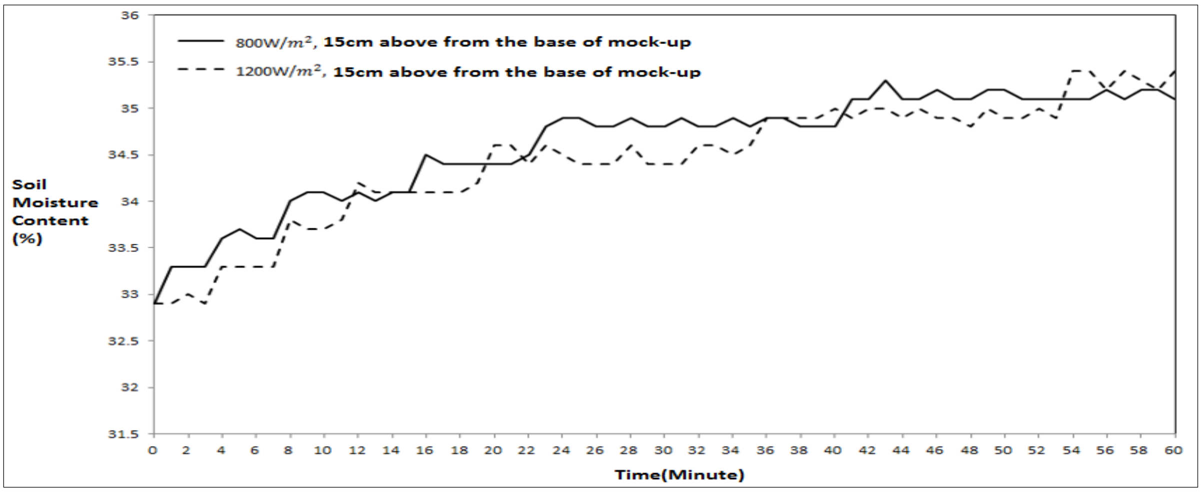

Figure 9. The graph of soil moisture content at 30cm above the base of mock-up under solar radiation.

15cm above the base of mock-up did not seem to be influenced by the solar radiation intensity, but the moisture content of the soil decreased at 30cm above the base of mock-up as the solar radiation intensity increased. This seems to have been caused by the evapotranspiration effect that the soil moisture content is evaporated by the solar radiation. The air temperature increased from 48°C to 56°C according to the intensity of 800W/m^2 for 1 hour. The surface temperature of HDPE tree pit cover plate increased from 32°C to 77°C because of solar radiation. Humidity was maintained at 1% to 3% RH with increasing temperature. If the humidity is experimented in an airtight location without any air circulation by the HVAC, the humidity will be increased by evapotranspiration effect.

Ultimately, this experiment was conducted to derive experimental procedures to facilitate evaporation of the GI elements through the use of solar radiation devices. In order to evaluate the performance for UHI reduction, it was aimed to measure the evapotranspiration of the GI elements by promoting the evaporation of the water that absorbed through the GI elements using the solar radiation device and calculating the evapotranspiration quantitatively with data collected through evapotranspiration measurement procedure.

4 METHODOLOGY FOR EVALUATING EVAPOTRANSPIRATION FOR URBAN HEAT ISLAND REDUCTION

In order to analyze UHI phenomenon of GI, it is necessary to analyze the temperature change, wind speed, and thermal environment after formation of the hydrological cycle system. Simulation of the fluid, temperature, and humidity distribution around the city is required, and a non-fluid model capable of analyzing urban environment indicators such as vegetation and atmospheric interactions is also needed. For this simulation, empirical values should be applied to the modeling through empirical method such as measurement of the air temperature change caused by the evapotranspiration.

The evaluation of how much evapotranspiration occur through GI elements can be possible by using the climatic chamber. It is possible by implementing rainfall into the GI elements by sealing the chamber as shown in Fig 10. The temperature, humidity, and enthalpy data will then be collected to evaluate the quantified performance of GI elements for UHI reduction. In addition, heat absorption rate, reflectance, surface temperature, emissivity, and etc. can be measured by evaluation of thermal characteristics of each GI element, and it will be possible to evaluate the performance of the GI elements for UHI reduction based on the quantitative measurement of performance factors of GI elements.

The procedure for evaluation of the evapotranspiration follows these orders:

1) The mock-up (2.5m×2.5m×1.5m) with GI elements are installed in the climatic chamber (5m×5m×3.5m);
2) It uses a rainfall facility to generate stormwater at a certain rainfall intensity(25mm) for one hour;
3) Eliminate the stormwater runoff that flows out from GI elements installed on mock-up (according to permeability and moisture absorption capability of GI elements);
4) Generate Temperature (25℃), Relative Humidity (50%);
5) Turn off the Heating, Ventilation and Air Conditioning (HVAC) system;
6) In order to minimize the HVAC system and disturbance, the damper is used to block the supply duct and return duct, and it will airtight the chamber;
7) Supply a certain amount of solar radiation (615W/m^2) to simulate the external environment;
8) Measure amount of evaporation, air temperature, surface temperature, relative humidity, and discomfort index at 1 minute interval for 24 hours;
9) Quantify and evaluate the performance of the GI elements for UHI reduction by comparing the experimented data of the GI elements and other impermeable products such as concrete blocks.

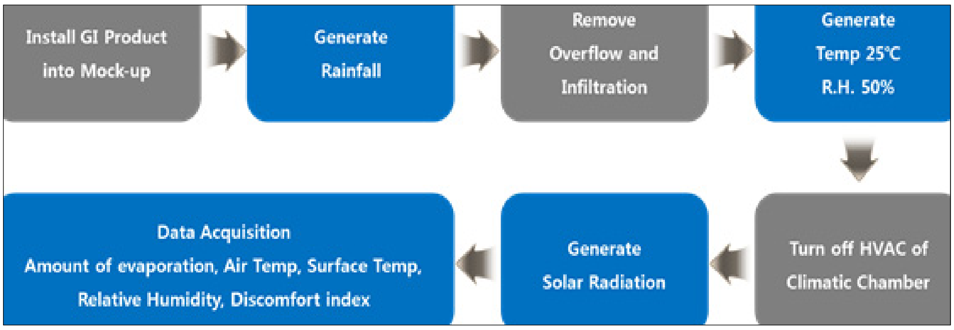

Figure 10. The procedure for evaluating the amount of evapotranspiration by using a climatic chamber.

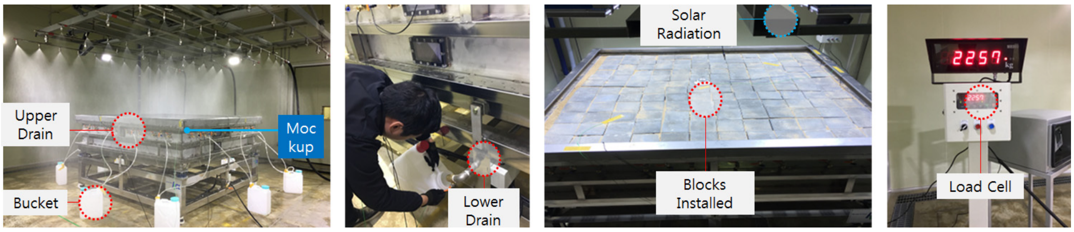

Figure 11. A climatic chamber and mock-up to evaluate evapotranspiration by experiment.

Figure 11 shows the mock-up that was used to measure evapotranspiration. After the blocks, or any other GI elements, were installed in the mock-up, the amount of rainfall can be measured through the upper drain, the amount of permeation can be measured through the lower drain, and the amount of rainfall and soil moisture can be measured through the load cell for weight measurement. The amount of rainfall was calculated by subtracting the weight of mock-up before the rainfall and immediately after the rainfall using the load cell. The runoff was calculated by measuring the weight of the water in the bucket connected to the upper drain after the rainfall test is completed. The amount of infiltration was calculated by measuring the weight of the water in the bucket connected to the lower drain after the rainfall test has been completed and when it has been determined that it has been sufficiently infiltrated (about 1 hour). Soil moisture content was calculated as the difference between the weights of the mock-up after solar radiation was generated and the weight of the mock-up before rainfall was generated using the load cell. The amount of evaporation was calculated by subtracting the amount of runoff, the amount of infiltration, and the moisture content of the soil, as shown in Equation 1. Fig. 9 also shows the procedure for evaluation of evapotranspiration using a climatic chamber. From left, rainfall and runoff measurement, infiltration measurement, solar radiation experiment and evaporation measurement are shown. However, vegetation could not be installed in this case, it needs to be done in the future, and it is only done to review the experimental procedure.

Equation 1. [Evapotranspiration = Rainfall – Runoff – Infiltration – Soil Moisture Content]

In order to evaluate the performance of the GI elements for UHI reduction to a specific area, the measured values of the GI elements need to be applied to the modeling of the hydrological cycle management simulation program. Weather data such as precipitation, wind speed, and cloudiness, and permeable/impermeable surface conditions such as buildings, roads, and vegetation need to be applied to the targeted area by using weather observation data, GIS, and hydrological cycle simulation program such as SWMM 5.0-Lid Module. The method would compare and analyze the performance of GI elements for UHI reduction by applying the measured values of the GI elements to the modeling of the simulation program. Based on the results of a comparative analysis, it will be possible to evaluate the performance of GI elements for UHI reduction by comparing before and after application of each GI element. The measured values of the quantitatively evaluated GI elements that are applied to the modeling of the city for simulation of UHI and comparison of the occurrence of UHI before and after the installation of each selected GI element are required to establish the final GI strategy in the methodology for evaluating net benefit. The costs and benefits of the GI elements are estimated by summing up the social expenditure due to the UHI damage, the installation cost of the GI elements, and the benefit of the UHI reduction through the installation of the GI elements. With this method, a very quantitative performance evaluation would become possible.

5 METHODOLOGY FOR ASSESS GI COST AND BENEFIT FOR THE PERFORMANCE OF UHI REDUCTION

This study introduced an experimental step to evaluate GI factors that work for UHI reduction using a climatic chamber. Amount of water infiltration and evapotranspiration are mainly evaluated to be applied to the modeling of the hydrological cycle management simulation program. Current NOAA's method cannot accurately derive the GI benefits because calculating GI benefits is hard to be assed quantitatively even with existing simulation program. Adding an experimental step using a climatic chamber to evaluate GI elements to derive GI factors would upgrade the result of method of evaluating cost-benefit of GI, based on NOAA's method. The calculation of cost-benefit of GI simply expressed by following equation:

Equation 2. [GI Cost – GI Benefit + GI Co-benefits] + [Annualize Costs - Annualized Benefits] = Annualized Net Benefits

In this formula, GI cost can be estimated by summing the total cost of all GI elements that need to provide enough amount of evapotranspiration to meet the UHI reduction target. GI benefit is sum of all benefits, such as damages avoided from reduced UHI and co-benefits such as the ecosystem services provide by natural features of GI elements. It is important to remember that nature features and ecosystem services provided by GI have value to community and should be included as benefits. The primary benefits are simply the difference between damages estimated in Step 2 and damages in Step 5 in Figure 2. Co-benefit is hard to express and identify because habitat, open space, aesthetics, increased property values, improved environment, need to be estimated. However, the primary benefits can be quantitatively assessed, by evaluation of the capacity of GI elements using a climate chamber and mock-up, and apply GI factors that reduce UHI, such as evapotranspiration, permeability, moisture absorption capability, and prevention capability of stormwater runoff, into the modeling program that runs hydrological cycle simulation of targeted area where GI elements are installed. After that, the reduced damage cost such as costs of treatment of diseases caused by UHI, cost of incidents and treatment of health damage caused by increasing discomfort index, the treatment cost of air (because UHI means that the pollution degree in the air is increased), building electricity consumption cost due to temperature increase, and any other damage cost by UHI in the targeted area need to be estimated. Then the damage cost of targeted area before GI installation and the damage cost of targeted area after GI elements installation need to be compared to find out the real benefits of GI elements. In order to make a fair comparison of costs (which are paid in the early years of a project) and benefits (which are realized year by year over a number of decades), the money values have to be converted to “present value” terms through “discounting.” Since the money invested today could yield far more than the money in, say, 10 or 20 years, an interest rate is used to discount future money to a present value, which shows what future benefits and costs are worth today. Distribute the present value across the years of analysis. This will produce the average benefit or cost in each year, referred to as an annualized benefit or annualized cost. At the end of this analysis, annualized net benefits can be determined by subtracting annualized costs from annualized benefits. Since the majority of GI costs occur in the early years of the project, it is important to take a long-term perspective (*e.g.*, 20 to 50 years) in decision-making. The value of GI benefits adds up over time. In that the benefits can exceed the costs after around 40 years. It is important to note that, even when an investment is a great idea over the long term, it can take years to recoup the initial cost. Shortsighted planning can lead to missed opportunities to put a community in a better, safer position for years to come.

6 CONCLUSIONS

Based on the flood mitigation assessment method, published by NOAA, we devised a method to evaluate the costs and benefits of the GI elements for UHI reduction based on actual quantitative figures. The evaluation of the GI elements using real-scale climatic chamber is designed to provide a procedural methodology for quantitative assessment of permeability, moisture absorption capability, and prevention capability of stormwater runoff. However, in the case of the evapotranspiration, there is no practical experiment in addition to the theoretical method. Therefore, we will quantitatively derive the evapotranspiration through the empirical experiment in the future with various types of vegetation by using the theoretical procedure for evaluation of the performance of GI elements in the climatic chamber. In addition, we will use the hydrological cycle management simulation program such as SWMM 5.0-Lid Module to simulate the UHI for a specific targeted area after applying experimented evaluation result from the procedural methodology for quantitative assessment. As a result, it is expected that evaluation of the net benefit of GI elements for UHI reduction based on actual quantitative figures would become possible.

ACKNOWLEDGEMENTS

The research is supported by Korea Ministry of Environment (MoE) as “Public Technology Program based on Environmental Policy.

REFERENCES

Eastern Research Group Inc. (2015). *A Guide to Assessing Green Infrastructure Costs and Benefits for Flood Reduction*, National Oceanic and Atmospheric Administration Office for Coastal Management.

Korea Environment Corporation (2013). *Low Impact Development Technological Elements Guideline*, Ministry of Environment.

Proceedings of the 37th IAHR World Congress
August 13 – 18, 2017, Kuala Lumpur, Malaysia

GREEN INFRA FOR NATURAL DISASTER RISK REDUCTION REVIVED FROM OLD WISDOM OF TRADITIONAL ECOLOGICAL PRACTICES IN KOREA – FOCUSED ON RESTORATION OF ECOLOGICAL FUNCTIONS OF RIVER

HYOSEOP WOO[(1)], JIN CHUL JOO[(2)], HONG-GU YEO[(3)] & JONG-MIN OH[(4)]

[(1)]School of Environmental Engineering, Gwangju Institute of Science and Technology (GIST),
hswoo@gist.ac.kr
[(2)]Department of Civil and Environmental Engineering, Hanbat National University,
jincjoo@hanbat.ac.kr
[(3)]Department of Water Resources and River Research, Korea Institute of Civil Engineering and Building Technology (KICT),
yeo914@kict.re.kr
[(4)]Department of Environmental Science and Engineering, Kyung Hee University,
jmoh@khu.ac.kr

ABSTRACT

This study focuses on the implementation of the Dutch concept of "Room for the River" in Korea by realizing one old wisdom of the traditional ecological green infra practices for natural disaster risk reduction, Baesanimsoo, which means a village locating on a hill slope with paddy field in front and a hill back to protect villagers from the cold northwesterly winter wind and from the summer stream flood. This study focuses especially on the possibility of the restoration of the ecological functions of the river including flood regulation and habitat by simply reconnecting the abandoned old channels to the main river corridors or setting levee back behind the old channel area. A demonstration project of the set-back levee was performed, and has been evaluated in terms of flood-risk reduction of the river and restoration of the old channel corridor. Then, a special attention is put on the specific geometrical configuration of agricultural lands, mostly paddy fields, located between the river embankment and the front-range of hill slope running parallel to the embankment. Additionally, this study introduces a case of the special geometric configuration of a stream flowing inside of the narrow floodplain surrounded in parallel with the front-range of hill-slopes on both sides. Through this study, it is expected that a complete removal of levee and/or setting back of levee, depending on the geometric configurations of the river channel and surrounding uplands and socioeconomic considerations, could be feasible ways to implement the concept of 'room-for-the-river' and thus to restore the ecological functions of the river including flood-risk reduction and habitat restoration.

Keywords: Green infra; disaster risk reduction; ecological function; flood-risk reduction; restoration of old channel.

1 INTRODUCTION

The concept of green infrastructure (GI), originated in USA in mid-1980s for best management practices of storm-water management as source control, has been extended by USEPA to application to the management of stormwater runoff at the local level through the use of natural systems, or engineered systems that mimic natural systems. In EU, the term "green-blue infrastructure" is used in order to represent the holistic approach to solve urban and climatic challenges by building with nature such as climate adaptation and increased quality of life as well as storm-water management especially in urban areas; and in addition the ecological framework of vegetation areas and waterways networks on land. In Japan and probably other parts of the world, the concept of GI is now extended to one of the sustainable approaches to the natural disaster risk reduction (DRR) from extreme weather events (i.e., violent droughts, storms, floods, coastal surges etc.).

Utilization of green, or green-blue, infra is based mostly on the ecological functions of the regulation, production, information and habitat (Martin et al., 2010), and green infra as the natural DRR is also an extension of the regulation function of the ecosystem. In this logic, this study tries to revive the old wisdom of the traditional ecological practices as a measure of the natural DRR, which have been mostly forgotten and replaced by the engineering infrastructure systems utilizing the modern built environment and supporting technologies.

This study introduces old but still functioning, in part, measures of the natural DRR in Korea based on the ecological regulation function, which can be found in other parts of the Asian region. Natural DRR in Korea are riparian forestation (tree belt) along the embankment to reduce the stream flood risk, costal forestation along the beach to reduce the risk of the storm surge and coastal sand arrestation, and village construction located on a hill slope with paddy field in front and on hill back to protect from the cold northwesterly winter wind and from the summer stream flood. The last example is called "Baesanimsoo (背山臨水)" in Korean, which has

  / ISSN 1562-6865 (Online) - ISSN 1063-7710 (Print)

been proven scientifically in the aspects of climatology, topology, and ecology.

In this study, the implementation of the concept of the Baesanimsoo in a newly-born modern type, i.e., set-back levee and/or removal of levee to accommodate flood water within the agricultural paddy lands was investigated. Thus, set-back levees constructed at a distance from the river channel in order to allow the river to occupy a portion of its floodplain was evaluated in terms of the restoration of ecological functions including the regulation function (flood regulation), habitat function, and informational function (aesthetics) of the river.

2 TRADITIONAL MEASURES OF DISASTER RISK REDUCTION IN KOREA

Local traditional cultures have interacted with their environments, and have developed the traditional ecological practices to mitigate the natural disaster risk reduction (DRR). Such traditional ecological practices can provide insight into present persistent environment issues in more sustainable ways in many cases. Considering that ecological strategies using local traditional cultures have been improved over thousands of years, traditional ecological practices have become of increasing interest as an extraordinary source of knowledge to meet present and future natural DRR with changing environment (Menzies and Butler, 2006; Armstrong et al., 2007).

Since the main objective of ecological engineering is the integration of human societies with their environment for the benefit of both (Mitsch and Jørgensen, 2004), this integration can be accomplished through the creation of eco-technologies operating at the interface of nature and culture. For example, the riparian forestation (tree belt) along the embankment to reduce the stream flood risk, costal forestation along the beach to reduce the risk of the storm surge and coastal sand arrestation can be installed in a site-specific manner. And, the village on a hill slope with paddy field in front and hill on back can be built to protect from the cold winter wind and from the summer stream flood. This traditional ecological practices were called as "backing hills and facing streams". Here, the wisdom of facing streams is that villagers cultivate paddy lands located near from their villages and at lower places along the streams or in the floodplain of large rivers. During floods, villagers are safe because their villages locate on higher places, while flood waters are retained in paddy lands that were mostly not protected with any artificial levees!

Current structural approaches such as dams and levees to reduce hazard damages may not be, in many cases, so effective due to their threats to environmental sustainability. Thus, an environmentally sustainable approach as hazard mitigation policy is required. According to the traditional ecological practices, this hazard mitigation policy employs traditional land use planning and management with non-structural approaches to reduce natural hazard damages. For example, various types of earthen structures were built to harvest monsoon rainwater, irrigate fields, and recharge groundwater in the past. By being aware of the philosophy and limitations of the traditional ecological practices, it is possible to concurrently provide benefits to local cultures and greater human society, and to contribute to sustainable ecological designs and environmental management.

2.1 Use of abandoned river corridor as wash land

2.1.1 Reconnection of abandoned river corridor for river restoration

During the rapid industrialization and urbanization in Korea from the 1960s to 1980s, parts of the river corridors have been continuously abandoned, i.e., excluded from the main river corridor during the river improvement works targeted to the efficiency of land use and flood defense. Floodplains have been encroached by the expansions of cities, industrial complexes, and agricultural lands (mostly paddy lands). Many floodplains were incorporated into agricultural lands and straightened river courses. Designated by the river management authority, the river corridor excluded from the so called "river zones" bounded usually by the artificial levees is named "abandoned river-channel area". Those lands were usually transferred to the lands for different purposes (i.e., agricultural lands, wet lands, or even lands for public facilities). However, the River Act was revised in 2004, and was specifically designated only for flood control and river-environment improvement. Based on the data compiled for the class of "National Rivers" by the Ministry of Construction and Transportation in 2005, the numbers of sites and areas of the abandoned channel areas by the major river watersheds in Korea are displayed in Fig. 1. Also, the present usage of the abandoned channels at each watershed is shown in Fig. 2, and summarized in Table 1. As shown in Fig. 2, most of the abandoned channel areas are farmlands and grasslands.

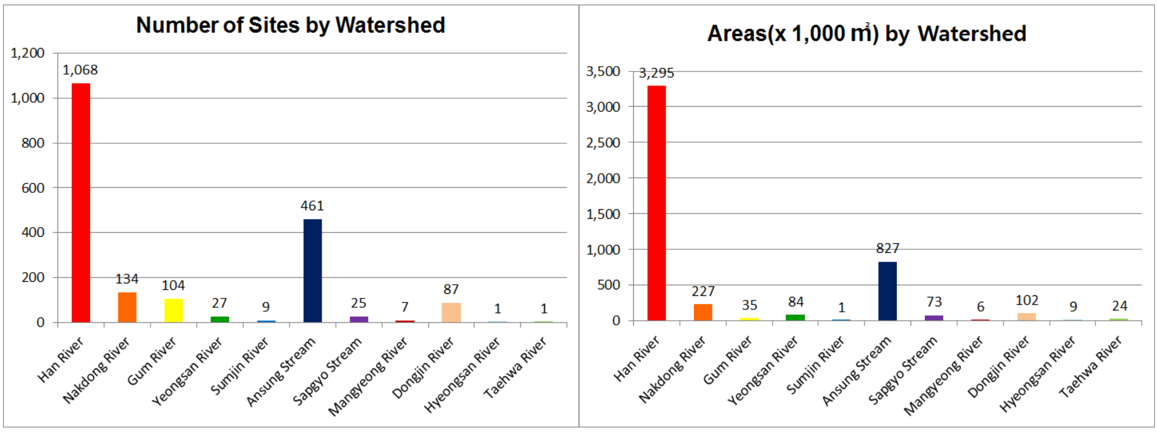

a) Number of Sites by Watershed b) Areas by Watershed

Fig. 1 Statistics of abandoned channel in the National Rivers in Korea

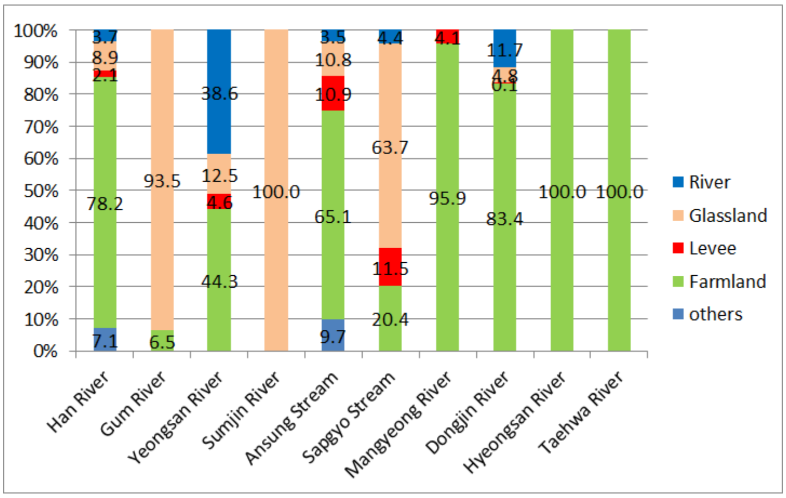

Fig. 2 Land uses of abandoned channel area

Table 1. Classification for land usage of the abandoned channels

Classification	Detailed Contents
River	stream, canal, waterway, fish farm, boat-race course
Grassland	miscellaneous land, grassland, abandoned land, woodland, forest land
Levee	levee, road
Farmland	rice paddy, farm, cultivated field, orchard, vinyl greenhouse
Others	dwelling, factory, parking lot, building, aggregate storage yard, stadium

Another survey was conducted on the abandoned channels in the class of “Local Rivers” of the major four (4) river basins in Korea by the Ministry of Environment in 2016 (see Fig. 3). The survey was made mainly by simply comparing the old topography map and the current map. The old topographic maps (1/50,000) surveyed and made in 1918 was used for this comparison. As a result, 472 river channels were identified to have been modified, indicating that 80% from the 591 river channels was changed. Among the total number of 1,682 abandoned channels, 1, 314 places, or 78% are being used for other purposes beside agricultural purposes, while 368 places, or 22% are left wetland (Korea National Spatial Data Infrastructure Portal, 2011).

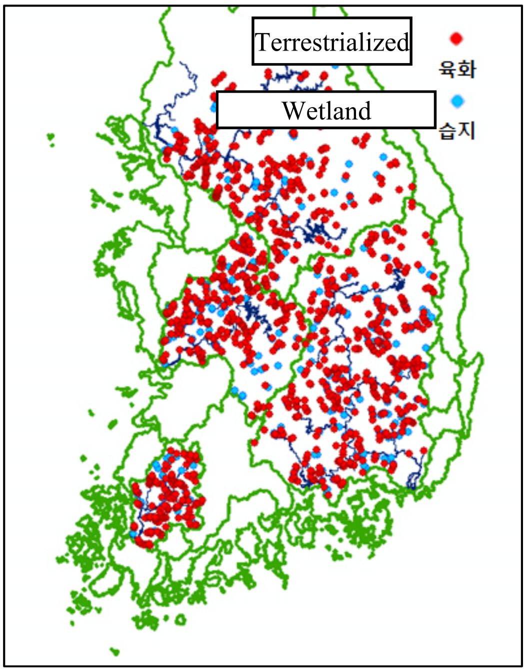

Figure 3. Location of abandoned channels in the local rivers in the four major river watersheds

In order to reconnect the abandoned channels to be used for wash land of river-flood water as well as river restoration, it is very ideal to remove the levee that separates the abandoned channel from the main river corridor (i.e., channel and floodplain) and construct a new levee behind the abandoned channel areas. In most cases, however, set-back levees usually costs a lot of expense, and construction of an inlet upstream and an outlet downstream for the passage of main channel water through the newly adopted abandoned channel corridor could be more feasible in many cases.Restoration projects of the abandoned river corridors were performed at Hampyeong-cheon (stream), Cheongmi-cheon, and others. In this study, the restoration projects of Cheongmi-cheon, where the levee was set back and the old river corridor was reestablished to restore the regulation functions of the river, was introduced.

3 CASE STUDY OF THE CHEONGMI-CHEON (PUNGGYE-JIGU)

This project was initiated by the National Research &Development project called Ecoriver 21, continued from 2006 until 2011, as a pioneer and demonstrative project of old channel restoration. The objectives of this project are as follows: 1) improvement of flood-conveying capacity of the river (regulation function), 2) restoration of old channel and ecosystem (habitat function), and 3) provision of recreational opportunity (information function) to local residents. Detailed design of the project was prepared by an engineering company in 2008, and the implementation work was finished in 2015. Main area of the old channel of 154,000 m^2 had been used for agricultural purposes.

For this project, privatized land of 17,595 m^2 was purchased from the land owner. The old levee which was constructed during the river improvement work in the 1970s and 80s was removed, and a new levee was constructed as a set-back levee in order to accommodate the restored old waterway within the river corridor and to protect the agricultural land behind. A walkway was made to allow citizens to enjoy the re-naturalized river view in the areas. Through this project, it is expected that the design flood stage could be lowered by 0.06-0.28 m and the design maximum velocity in the river could be reduced by 0.67 m/s.

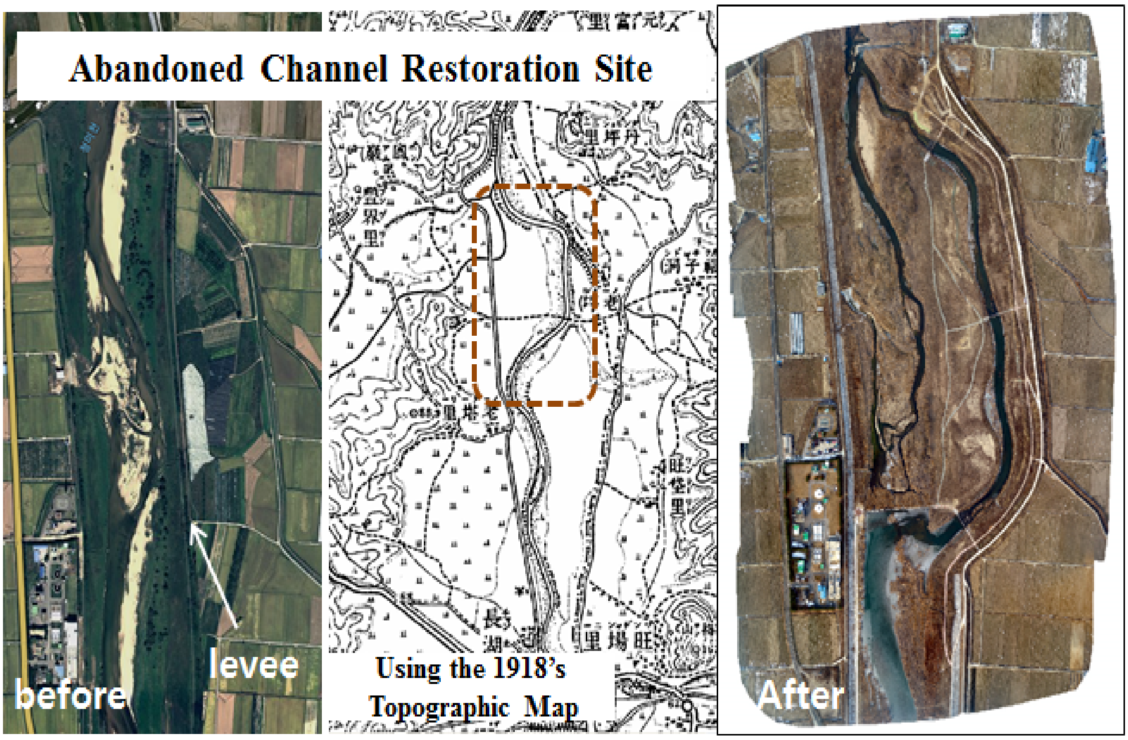

Figure 4. Cheongmi-cheon stream restoration project (from left to right; before the project, topographic map of 1918, and after the project)

Figure 5. The old-channel restoration project (left: removing levee at upstream inlet, 2014; right: restoring the old channel, 2015)

4 LEVEE REMOVAL

In some specific geometrical configurations, physical removal of levee could be considered without any new construction of set-back levee. It could be justified where the economic value from the lands protected by the levee is not large enough or even less than the countable and uncountable values of the regulating (including flood regulation), informational and habitat functions of the ecosystem restored by levee removal. Those cases could be found from a narrow and long agricultural (paddy) field located between the river embankment (levee) and the front-range of hill slope running parallel to the embankment or from a relatively small agricultural area surrounded by a hill slope and a levee.

As shown in Fig. 6, a sample site of the levee removal located at Deokchi-meon, the Seomjin-gang River is displayed. The agricultural area of about 950 ha is surrounded by the hill-slope front range and protected by a straight-lined levee, which was constructed many years ago. When the river improvement was performed, constructions of levees were progressed nationwide without much consideration of the conservation of riparian habitat. In Fig. 6, the yellow line is the existing levee protecting the left-side arc-shaped agricultural lands and buildings, which were originally a part of the floodplains of the river

  / ISSN 1562-6865 (Online) - ISSN 1063-7710 (Print)

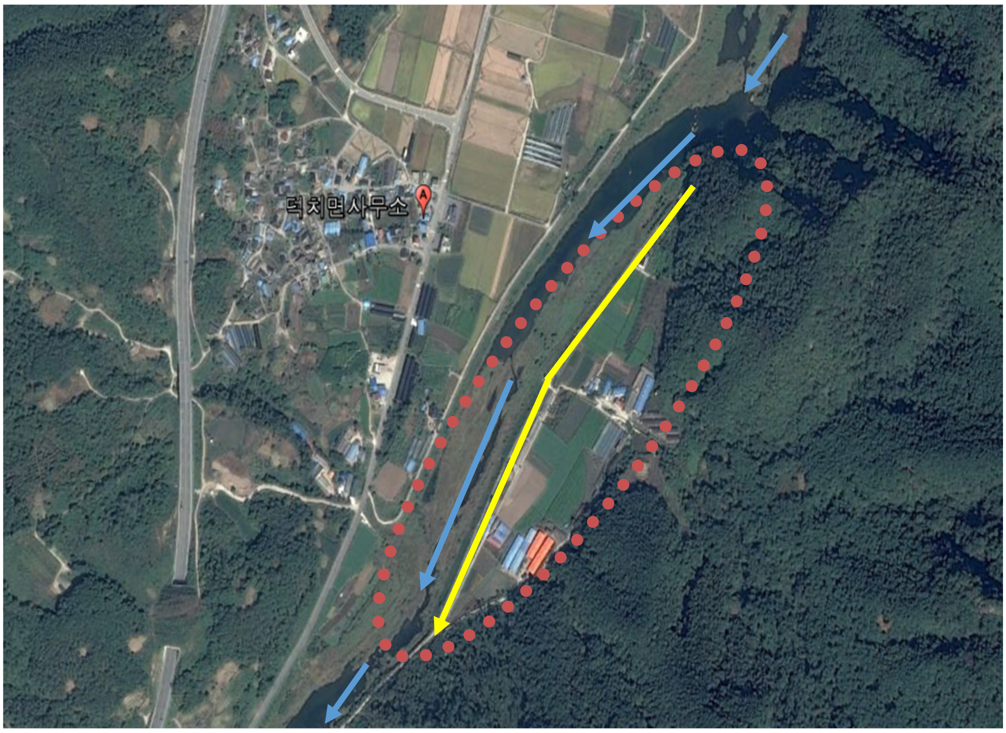

Figure 6. A sample site for the Case 1 for levee removal for increase in flood conveyance and floodplain restoration

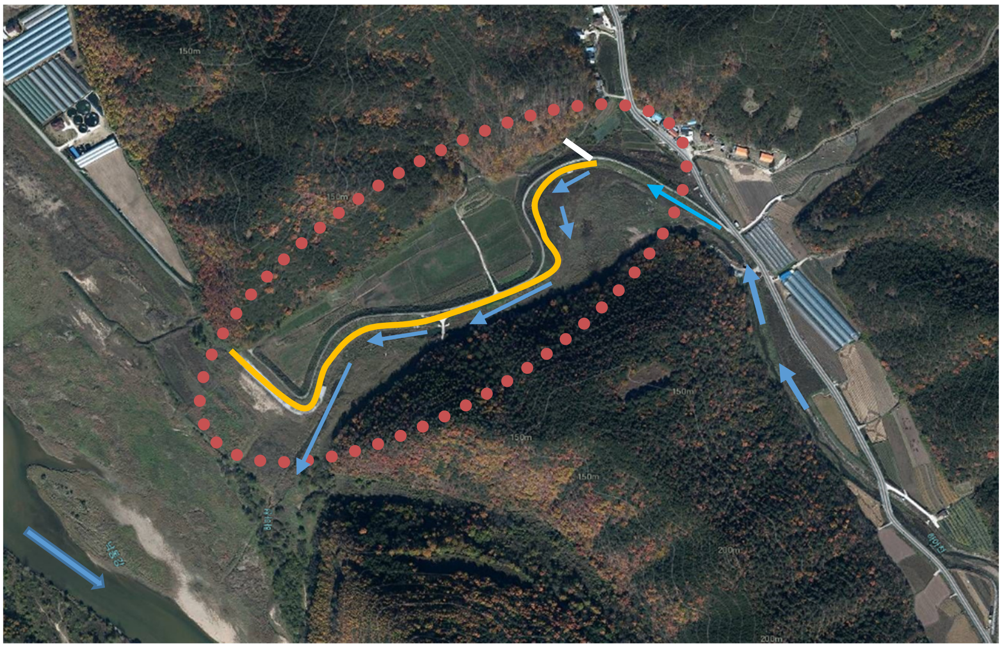

Figure 7. A sample site for the Case 2 for levee removal for increase in flood conveyance and floodplain restoration

As displayed in Fig. 7, a sample site of the the levee removal located at Haya-cheon, a small tributary of the Nakdong-gang River. A levee was constructed on the right side of the small stream in order to protect the right side small agricultural area surrounded by a hill-slope front range. The stream flows from the lower-right corner toward the upper-left and then turns left at about 90 degree angle and then meander before the stream merges the left floodplain of the Nakdong-gang River on its left side.

By this excessively-looking levee, only 40 ha of land is protected. In Fig. 7, the white narrow line indicates the walkway on the top of the levee. The white short line means a new levee to be constructed to protect a small village and highway on the right side, while the long yellow line means the portion of levee to be removed. The blue arrows indicate flow directions in the stream.

5 CONCLUSIONS

In Korea, we have an old wisdom of the traditional ecological practices, Baesanimsoo, indicating village locating on a hill slope with paddy field below in front and hill on back to protect villagers from the cold northwesterly winter wind and from the summer stream flood. This is equivalent basically to the Dutch concept of "Room for the River" in the sense that the former implies the conservation of the regulation function of the river ecosystem, while the latter implies the restoration of that function.

In this study, feasibilities of the revival of the old Korean wisdom of Baesanimsoo in terms of the modern concept of the room-for-the-river were investigated by identifying possible ways of its realization and implementation. First consideration was put on the restoration of the old channel corridor and reconnection to the main channel in order to use the old channel area as washland for flood regulation and to restore the ecosystem of the old channel. Two ways of management of the existing levee are proposed; installation of the inlet and outlet in the levee to pass the main channel water into the newly restored channel, and setback of levee behind the old channel areas. A case study of the setback of levee was introduced in this study. Second consideration was put on the specific geometrical configuration of agricultural lands, mostly paddy fields, located between the river embankment and the front-range of hill slope running parallel to the embankment. Sample cases were introduced for clarification of the concept.

Through this study, it is expected that old-channel reconnection by setback levee and floodplain restoration by levee removal could be a feasible way to implement the concept of "room-for-the-river" and thus to restore the ecological functions of the river including flood-risk reduction and habitat restoration.

REFERENCES

Armstrong, M., Kimmerer, R.W. & Vergun, J. (2007). Education and Research Opportunities For Traditional Ecological Knowledge. *Frontiers in Ecology and the Environment*, 5(4), 12–14.

Martin, J.F., Roy, E. D., Diemont, S.A.W. & Ferguson, B.G. (2010). Traditional Ecological Knowledge (TEK). *Ideas, Inspiration, and Designs for Ecological Engineering*, 36, 839-849.

Menzies, C.R. & Butler, C. (2006). *Understanding ecological knowledge.* In: Menzies, C. (Ed.), Traditional Ecological Knowledge and Natural Resource Management. University of Nebraska Press, Lincoln, NE, 1–20 pp.

Mitsch, W. J. & Jørgensen, S. E. (2004). Ecological Engineering and Ecosystem Restoration, John Wiley & Sons, 411 pp.

GREEN INFRASTRUCTRUE IN CONSTRUCTION OF SPONGE CITY- A CASE STUDY IN XIAMEN, CHINA

CHENYAO XIANG(1), JIAHONG LIU(2), WEIWEI SHAO(3), JINJUN ZHOU(4), CHAO MEI(5) & LIN XIA(6)

(1,2,3,4,5,6) State Key Laboratory of Simulation and Regulation of Water Cycle in River Basin, China Institute of Water Resources and Hydropower Research, Beijing 100038, China.
xiangchenyao@foxmail.com; liujh@iwhr.com; shaoww@iwhr.com; cyzzjjfq@126.com; hydromei@126.com; xialinxls@126.com
(2) Engineering and Technology Research Center for Water resources and Hydroecology of the Ministry of Water Resources, Beijing 100038, China.

ABSTRACT

Rapid urbanization and climate change have resulted in increasing risks of urban flooding, and promoting green infrastructures (GI) in urban areas is one of the main methods to minimize negative urbanization effects on water systems. Chinese government have launched the project of Sponge City Construction in 2015 and since then China has rapidly implemented comprehensive networks of GIs on city scale in approximately 30 demonstration cities. More than simply installing GIs, sponge city design integrated different GIs vertically, to achieve a stairway absorption, further reducing urban flood risk. This paper conducted a scenario study based on a residential area (6.2 ha) in Xiamen, which is currently equipped with green roofs of 1401 m^2 , bio-retention of 5325 m^2, vegetative swales of 1880 m^2, and rain barrels of 15 m^3 in total. The result shows that the GI system has obvious sliced surface runoff and peak flow in small rains, but the effect tends to weaken in larger rains. However, the combination of several different GIs showed notable superiority in not only controlling runoff volume and peak flow, but also in the resilience to variation of precipitation.

Keywords: Green Infrastructures (GIs); Sponge City; Urbanization; Flood Mitigation; Xiamen City.

1 INTRODUCTION

Extension of impervious surface and diminution of bare soil that accompany urbanization, has contributed to increasing of urban flood risks. Among many solutions, green infrastructure (GI) has been considered an effective way with multiple benefits and applied in many cities with different climates around the world (Versini et al., 2016; Maniquiz-Redillas et al., 2016; Liu et al., 2016; Norton et al., 2015; Pellegrino et al., 2014; Andersson et al., 2014; Rouse & Bunster-Ossa, 2013).

Chinese government and academia together proposed the approach of sponge city to tackle the urban water issue. China launched the Sponge City Construction program in 2015, and 30 demonstration cities has been selected so far. The measures included in sponge city design cover a wide range, which consist of both green and grey infrastructures. An urban region following sponge city design is supposed to hold about 70% of annual precipitation whether through retention or reuse, so the number and size of the GI system installed there should be able to retain the same percentage of a specific rainwater depth, which in the case of Xiamen is 26.8 mm.

More than simply installing the GIs, sponge city design integrated different GIs vertically to achieve a stairway absorption. Green roof, bio-retention unit, pervious pavement, vegetative swales and other GIs are arranged in order for rainfall to pass through GIs of different functions and be retained layer by layer. Although many demonstration regions have completed construction, performance of the whole GI system in different rain volumes and pattern has not been illustrated, and the effectiveness of combining GIs with different functions also has not been studied yet. This two puzzles drew forth this study.

Also, individual GI's performance under the effects of rain patterns or rain volumes has been demonstrated in some excellent studies (Hakimdavar et al, 2016; Zellner et al., 2016; Lewellyn et al., 2015; Wang Y et al., 2015; Liu W et al., 2014; Stovin et al., 2012; Basinger et al., 2010; Alfredo, Montalto & Golstein, 2009; Hathaway et al., 2008; Lee & Heaney, 2003), so it is not included in this study. In this study, we tried to focus on the performance and effectiveness of a systematically arranged GI configuration.

2 MATERIALS AND METHODS

2.1 Study site

This study chose a small urban residence region (Yangtang Neighborhood, YN) with an area of 6 ha, located in the south of Xiangan District, Xiamen city (Figure 1).

Xiamen is among the first group of 16 demonstration sponge cities in China's Sponge City Construction program. It is a coastal city in southern China, with a subtropical monsoon climate and an urban population of over 4 million. Xiamen's average annual precipitation between 1985 and 2014 is 1388 mm. YN is in the north of Xiamen. The primary soil types are clay and red loam (Mulan Zhu et al., 2013), which have quite low hydraulic conductivities, especially the clay. Therefore, in the construction of LID infrastructures in YN, the soil were replaced with gravel and sandy soil to enhance infiltration and ground storage. Based on observations and literature, the natural soil conductivity was defined as 5.87 mm/h, while that of the replacement was 29.93 mm/h.

Figure 1. Aerial view of Yangtang Neighborhood

YN is a typical residence region developed under sponge city philosophy, consisting of pervious pavement, LID measures (green roof, vegetative swale, rainwater tank and bioretention), high-rise buildings and lower blocks, impervious pavement and ordinary lawns. The land cover and elevations (varying from 27 m to 36 m) within the watershed were identified initially by construction plan maps, compared with satellite images from Google Earth (downloaded in 2016), and verified by field investigation. Information on drainage system was collected from local construction units. Underground drainers run to two ends: one leads to a landscape dry creek in a small wetland park lying aside, and the other is connected to downward drainers which ends over downstream, which is a natural water body.

2.2 Hydrological model

SWMM 5.1 by United States Environmental Protection Agency was chosen as the platform for simulations, because its efficiency for urban area modelling had been proved (Rossman, 2010) and it provides multiple GI simulation modules with remarkable flexibility (Elliot & Trowsdale, 2007).

Subdivision of subcatchments was particularly in detail. Every roof was depicted and assigned with parameters different from the ground. The ground was divided into ordinary lawns, impervious surface and roads. Every bio-retention unit was delineated and connected to proper drainage junctions consistent with practice (Figure 2). There are totally 123 subcatchments and 154 drainage conduits were depicted, and 47 road segments were identified.

Horton's equation was chosen to estimate infiltration, and routing model was dynamic wave. Soil parameters for all the LID measures were determined following guidance of the SWMM Users' Manual (https://www.epa.gov/water-research/storm-water-management-model-swmm#downloads). The simulation duration was set as 36 h for 24-hour rain events, in other words, simulations lasted 12 h more after rain stopped. This is to complete the outflow process and control the water quantity balance error below 5%. Dynamic routing was selected for simulations, with 30-second time step. Both flow routing continuity and runoff quantity continuity appeared quite good.

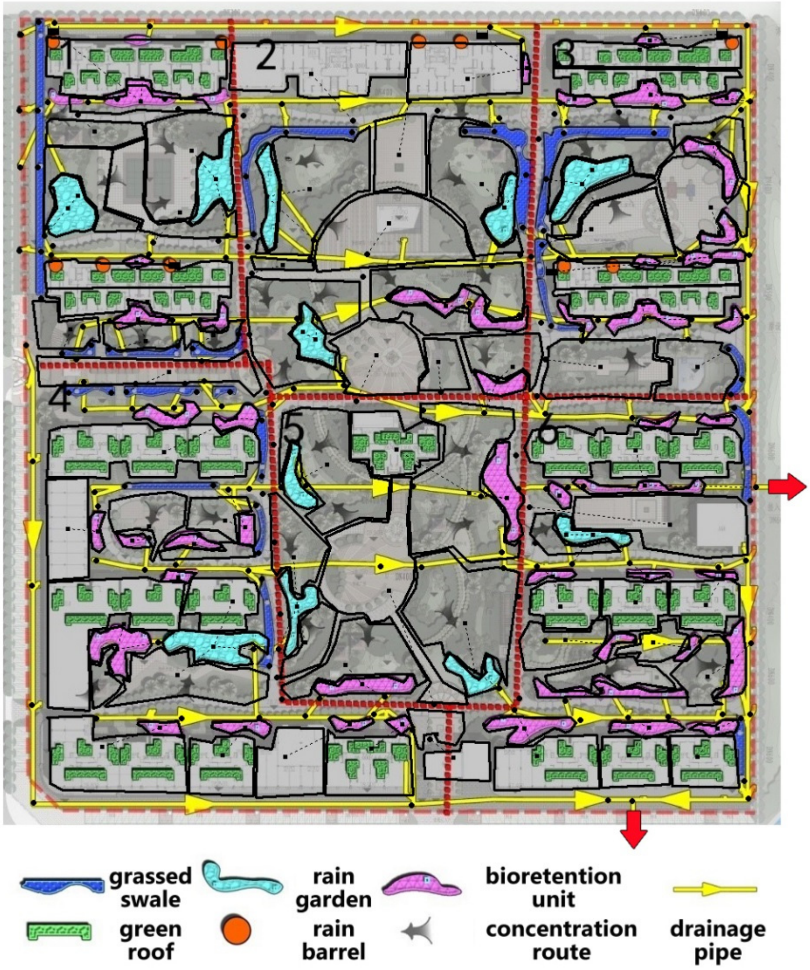

Figure 2. Division of subcatchments

2.3 Scenarios

Two scenarios were included: conventional development (CD) and sponge-city development (SC). In the SC scenario, green roofs, bio-retention and vegetative swales were implemented. The numbers, sizes and soil characteristics in the model are designed strictly according to the actual implementation. Green roofs cover 1401 m^2 in total and are installed on lower buildings (2~3 floors) only, with a 150 mm storage layer and a 20 mm drainage mat. The underdrains are connected to the rain barrels beside buildings. Instead of using LID modules in SWMM, bio-retention units were modeled as subcatchments with special roughness, infiltration and storage parameters defined by individual planting structure and soil type. This method was also used in modeling vegetative swales, except that those are set as open channels. There are two typical routes of rainwater in this scenario: 1) rainfall landing on the roof would first enter green roofs, then down the pipes to rain barrels and bio-retention units, and finally into drainage system through overflow entrance; 2) rainfall landing on the road would partly enter the drainage system through lower vegetative swales, and partly remain on the road and flow along until collected by a manhole. Bio-retention units cover a total area of 5325 m^2, and vegetative swales add up to 1880m2. There are also 10 rain barrels with storage volume of 15 m3.

On the other hand, the CD scenario was modeled following traditional development practice, meaning that green lands were higher than the road, rainfall on the roof was directly led into drainage system through pipes, and no LID measures were taken.

Since rainfall volumes and intensity have prominent effects on the performance of GIs, 4 rainfall events of frequencies of 20%, 10%, 5% and 2% were simulated for each scenario. Based on rainfall records between 1985 and 2014 supplied by local monitor stations, those precipitations were identified as 194.3 mm/d, 237.7 mm/d, 280.1 mm/d and 335.3 mm/d, respectively, and a 24-hour rain process with 5-minute time intervals was determined (Figure 3).

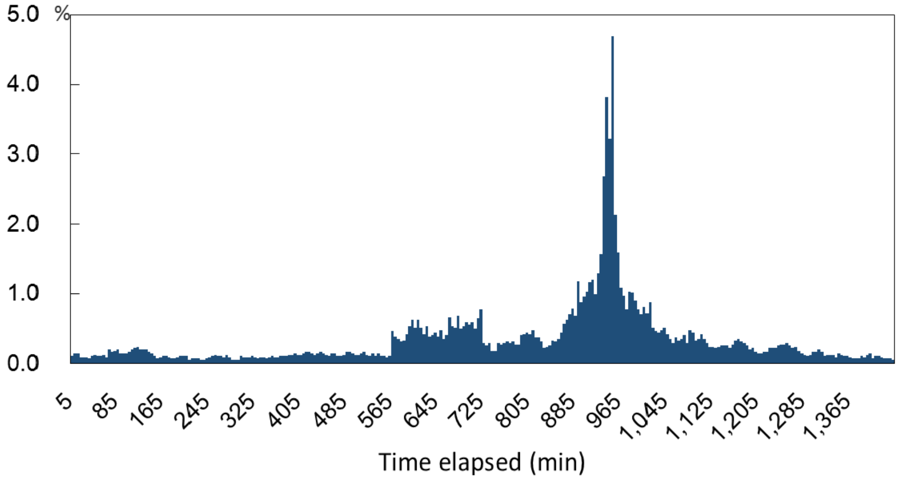

Figure 3. Design rainfall pattern of a 24-hour event

Sponge city design of YN combined different GIs in a vertical way that makes rainfall to be sliced layer by layer. Three combinations in SC scenario were selected together with their matches in CD scenario. Those segments were chosen rather than other combinations with the same routes for the similarity in area and in the proportion of LID units' area to roof area. The flow routes are shown in Table 1.

Table 1. Flow routes of GI combinations

Combination	Route	Components
V1	rain → roof with green roofs → bio-retention unit → grassed swale → drainage system	3 subcatchments, 2 conduits, 3 junctions
V2	rain → roof with green roofs → bio-retention unit → drainage system	2 subcatchments , 1 junction
V3	rain → ordinary roof → bio-retention unit → drainage system	2 subcatchments, 1 junction
N1/N2/N3	rain → ordinary roof + parterre (respectively) → drainage system	same with matching SC combinations

The effectiveness of combinations is represented by the change in the outflow processes and two variables, namely the reduction of the total runoff volume and that of the peak outflow. Specifically, these variables were calculated as following:

$$R_P = \frac{P_{CD} - P_{SC}}{P_{CD}} * 100\% \qquad [1]$$

where, R_P is the reduction rate of the peak outflow, P_{SC} is the peak outflow (for either the entire site or any one combination) in the sponge city scenario, and P_{DC} is the counterpart peak outflow in the conventional development scenario.

$$R_T = \frac{T_{CD} - T_{SC}}{T_{CD}} * 100\% \qquad [2]$$

where, R_T is the reduction rate of the total runoff, T_{SC} is the total runoff volume (for either the entire site or any one combination) in the sponge city scenario, and T_{DC} is the counterpart runoff volume in the conventional development scenario.

3. RESULTS

3.1 Influences of rain volume on the performance of a GI system

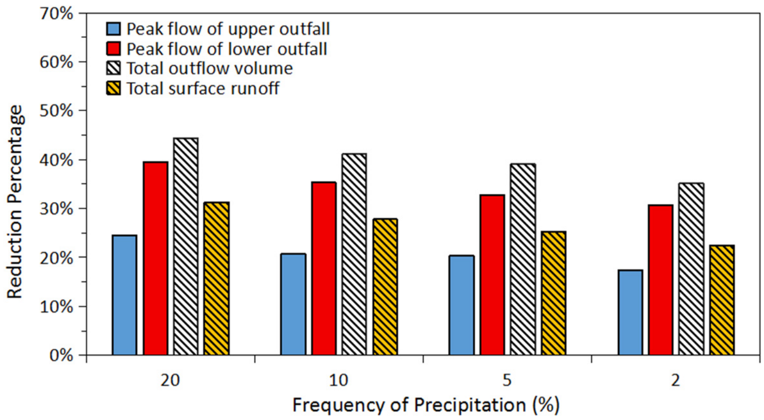

Figure 4. Reduction of peak flows, total outflow volume and total runoff volume by GI system

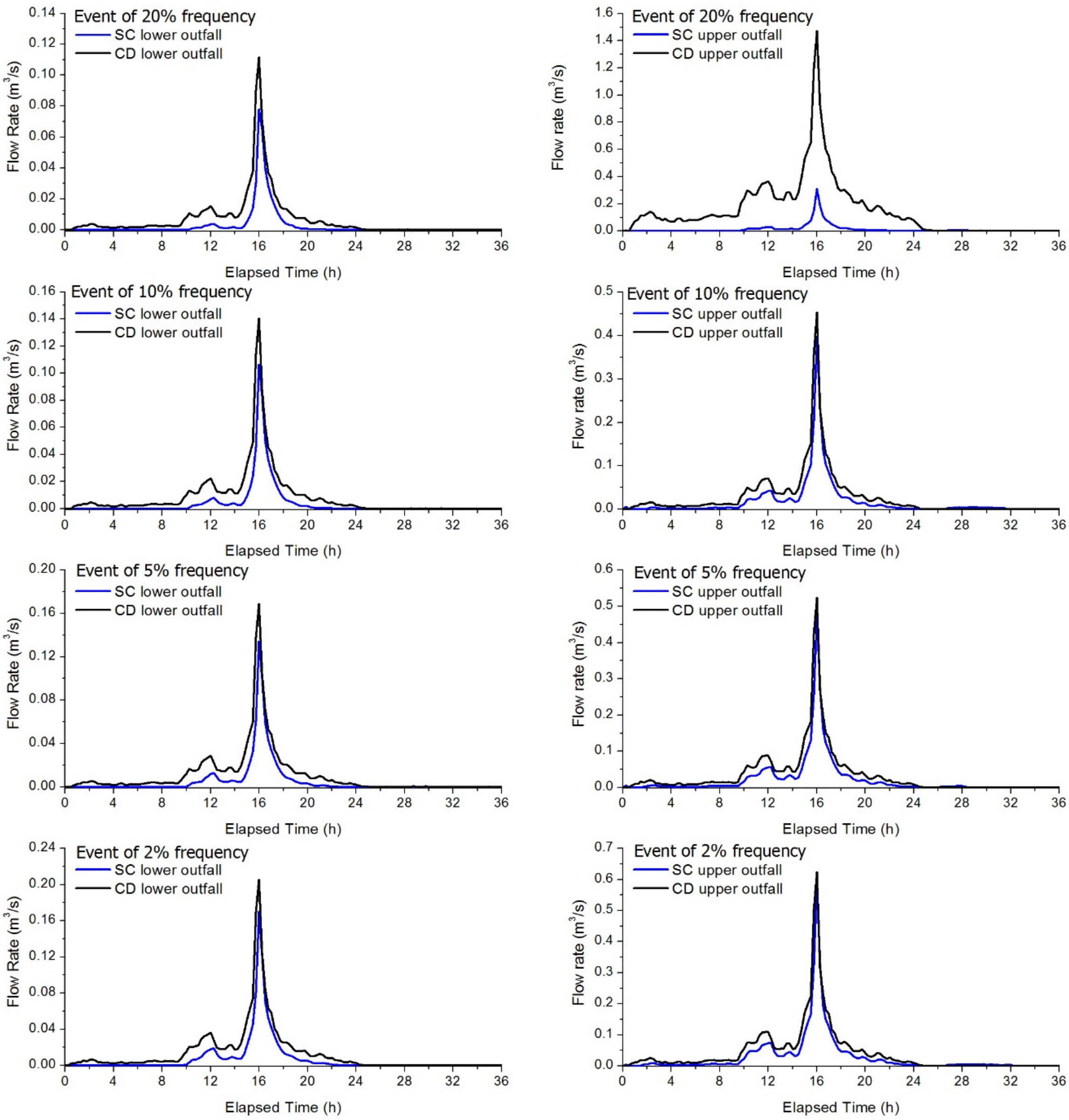

Figure 5. Outflow processes of two scenarios (SC stands for sponge city scenario and CD stands for conventional development scenario)

The GI system in marked study area reduces peak flows and total outflow volumes in every event (Figure 4). Specifically, the total outflow volume declined from 3,700, 4,730, 5,730 and 7,050 m3 to 2,090, 2,780, 3,490 and 4,570 m3 in 20%, 10%, 5%, and 2% rainfall event, respectively; the depth of runoff declined from 142.69, 182.61, 221.96, 273.75 mm to 98.09, 131.88, 165.76, 212.22 mm in those events, respectively; the peak flow of upper outfall declined from 0.13,0.17, 0.21, 0.25 m3/s to 0.08, 0.11, 0.14, 0.17 m3/s in 20%, 10%, 5%, and 2% event, respectively; and for the lower outfall the figures are 0.41, 0.50, 0.61, 0.71 m3/s to 0.31, 0.40, 0.48, 0.59 m3/s respectively. The control rates of all four variables mentioned above declined when the precipitation increased (Figure 4).

Similarly, the GI system smoothens outflow processes of the catchment notably under 20% precipitation, especially for the upper outfall (Figure 5). However, the effect weakens as the rainfall volume increases.

It implied that even systematic installation does not turn over the situation of urban flooding, and GI capacity is limited when it comes to extreme storm events. The GI system has remarkable control over small rain, but not the heavy one.

3.2 Evaluation of the vertical design of GI

Figure 6 shows the reduction of peak flow in the conduit that is directly connected to the GI systems (namely V1, V2 and V3). The peak flow after the treatment of V1 reduces significantly and remains at the same level as precipitation increases, while the other two combinations had negative effects. This result may be contrary to general perception that GI should reserve rainwater and reduce peak flow. In fact, both peak flow and volume of the outflows of the entire study site have declined, and the peaks in the conduits connected to GIs are delayed as shown in Figure 7 (the figure only shows flow processes in the five-year event because the situation in other three events show no considerable difference). This means that by gathering rainwater from surroundings, the GI system lightens other drainers' pressure at the price of burdening the drainers that are directly connected to it, as more water is directed towards those drainers. It is possible that in heavy rains, the green infrastructures like green roof or rain garden to have reached their capacity from previous rainwater long before the rain stops. Therefore, rainwater that is gathered and retained cannot infiltrate or be drained instantly and accumulates inside the infrastructure. Thereby, the conduits connected to GIs may produce higher peak flows and their stability can be threatened in heavy rain.

The difference between V1, V2 and V3 is probably due to the grassed swale in V1. By connecting a bio-retention unit to a grassed swale, ponded water could flow through a highly pervious channel, allowing more time and space for soil storage. Also, because rainwater would spread as a flow in the swale, high water head over the drainer can be avoided, benefiting the drainer's stability. The negative effect is less evident for V2, but tends to strengthen as precipitation increases, and the gap between V2 and V3 is decreasing. This implies that green roofs have certain power in peak flow control, but do not help with the negative effect of bio-retention on peak flow.

However, this kind of result is probably highly dependent on precipitation characteristics. In a rainfall event of a similar frequency but a smoother process, the results can be distinct: the great benefit showed by a grassed swale may vanish, or in a smaller rain the same configuration as V2 or V3 may have positive effect on peak flow.

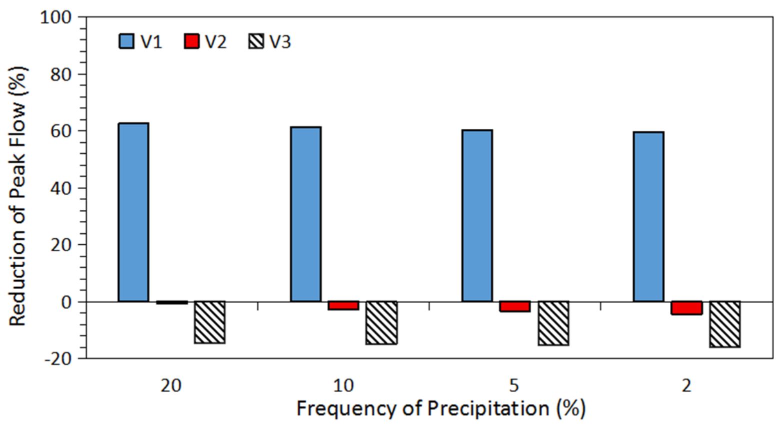

Figure 6. Reduction rates of peak flows in conduits connected to different GI systems

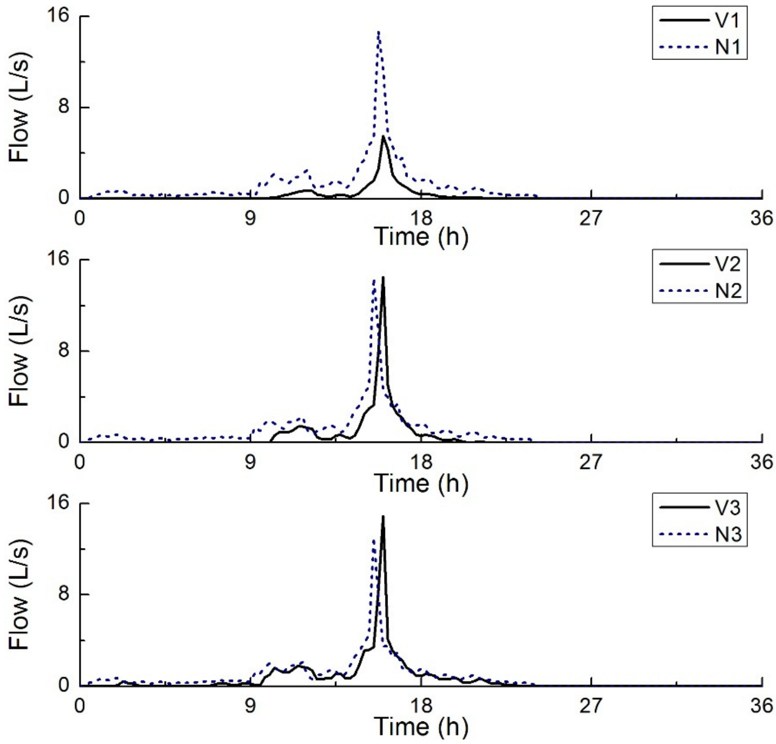

Figure 7. Changes in the flow process in conduits connected to different GI systems in the 20% rainfall event

On the other hand, when precipitation increases, reduction of total runoff by all three combinations show upward trends, but with different variations (5% for V1, 13% for V2 and 11% for V3) (Figure 8). The result implies that combining different GIs may have a positive influence on the sensitivity of GI performance to rainfall volume. Taking into account the relatively small storage volume of grassed swale compared to bio-retention units (Table.2), the superiority of V1 is not due to the added storage capacity, but more likely because the conveyance function of vegetative swale is well supplementary for storage/infiltration infrastructures. Although the reduction rate is significantly higher for the combination that applies more GIs, the gap between V2 and V3 is diminishing. Considering the minimum variation of the storage of green roofs in four events (Table.2), this result is probably due to the limited capability of green roof in the face of larger rainfall.

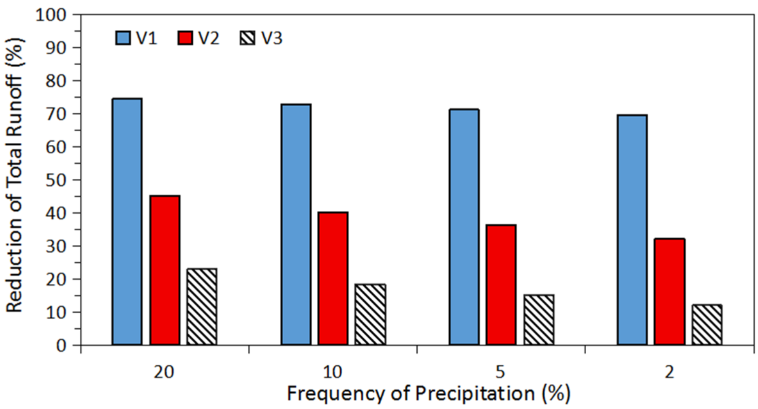

Figure 8. Reduction rates of total runoff volumes by different combinations of GIs

Table 2. Soil / tank storage of GIs in different events

Frequency of event	Green roof (m^3)	Bio-retention (m^3)	Grassed swales (m^3)
20%	436.11	2420.36	106
10%	436.96	2688.72	157
5%	437.54	2895.58	161
2%	438.16	3206.55	199

Overall, the combination of a unit with sizable storage like bio-retention ponds and a unit with conveyance function like vegetative swales appeared to be an excellent package in peak flow reduction as well as surface runoff control.

4 CONCLUSIONS

The GI system installed in study site was estimated to reduce 44% of the total outflow volume and 31% of the total runoff volume in a 20% rainfall event, while the figures in a 2% rainfall event was 35% and 22%, respectively. The storage of green roofs in four events of different frequencies is almost the same while those of bio-retention units and grassed swales increased notably along with the frequency of the event. Rain barrels reaches the maximum capacity, namely 15 m^3, in each event, so they hardly made any difference to the system and were not included in analyses.

The system smoothens outflow process quite fine in small rain, but the effect tends to weaken when rain volume increases. These results showed that the GI system remained the feature of a single GI in terms of the limited capacity in the face of low-frequency storms.

On the other hand, a vertically designed combination of GIs showed notable advantages. The combination of green roofs, bio-retention units and grassed swales not only had better performance in reducing peak flow and total runoff volume, but also showed superior resilience to variation of rainfall volume. In other words, this combination did not put as much pressure on connected drainers as the other combinations or a single bio-retention unit did.

Nevertheless, this study aimed at evaluation of the effectiveness of the GI system in a single rain event, so all the parameters were set to simulate a situation with no recently previous events. If previous rain events were taken into accounts, the reduction rates might decrease and there is a chance that the benefits of a combination might shrink.

ACKNOWLEDGEMENTS

The authors would like to extend their thanks to the Chinese National Natural Science Foundation (No. 51522907, No. 51279208) and National Key Research and Development Program of China (2016YFC0401401). The study was also supported by the Research Fund of the State Key Laboratory of Simulation and Regulation of Water Cycle in River Basin, China Institute of Water Resources and Hydropower Research (No. 2016ZY02).

REFERENCES

Alfredo, K., Montalto, F. & Goldstein, A. (2010). Observed and Modeled Performances of Prototype Green Roof Test Plots Subjected to Simulated Low and High-Intensity Precipitations in a Laboratory Experiment. *Journal of Hydrologic Engineering*, 15(6), 444-457.

Andersson, E., Barthel, S., Borgström, S., Colding, J., Elmqvist, T. & Folke, C. et al. (2014). Reconnecting Cities to The Biosphere: Stewardship of Green Infrastructure and Urban Ecosystem Services. *Ambio*, 43(4), 445-453.

Basinger, M. (2010). A Rainwater Harvesting System Reliability Model Based on Nonparametric Stochastic Rainfall Generator. *Journal of Hydrology*, 392(3–4), 105-118.

Hakimdavar, R., Culligan, P.J., Guido, A. & Mcgillis, W.R. (2016). The Soil Water Apportioning Method (Swam): An Approach for Long-Term, Low-Cost Monitoring of Green Roof Hydrologic Performance. *Ecological Engineering*, 93, 207-220.

Hathaway, A.M. (2008). Field Study of Green Roof Hydrologic and Water Quality Performance. *Transactions of the Asabe*, 51(1), 37-44.

Lee, J.G. & Heaney, J.P. (2003). Estimation of Urban Imperviousness and Its Impacts on Storm Water Systems. *Journal of Water Resources Planning & Management*, 129(5), 419-426.

Lewellyn, C., Lyons, C.E., Traver, R.G., & Wadzuk, B.M. (2015). Evaluation of Seasonal and Large Storm Runoff Volume Capture of an Infiltration Green Infrastructure System. *Journal of Hydrologic Engineering*, 21(1), 04015047.

Liu, J., Xiang, C., Shao, W. & Luan, Y. (2016). Sponge City Construction in Xiamen, China. *Hydrolink*, (4), 103-105.

Liu, W., Chen, W. & Peng, C. (2014). Assessing the Effectiveness of Green Infrastructures on Urban Flooding Reduction: A Community Scale Study. *Ecological Modelling*, 291(1), 6-14.

Maniquizredillas, M C. & Kim, L.H. (2016). Evaluation of the Capability of Low-Impact Development Practices For The Removal of Heavy Metal From Urban Stormwater Runoff. *Environmental Technology*, (18), 1-22.

Norton, B.A., Coutts, A.M., Livesley, S.J., Harris, R.J., Hunter, A.M. & Williams, N.S.G. (2015). Planning for Cooler Cities: A Framework to Prioritise Green Infrastructure to Mitigate High Temperatures in Urban Landscapes. *Landscape & Urban Planning*, 134, 127–138.

Pellegrino, P., Ahern, J. & Becker, N. (2014). Green Infrastructure: Performance, Appearance, Economy, and Working Method. In *Revising Green Infrastructure: Concepts between Nature and Design*. CRC Press, 385-404.

Rossman, L.A. (2010). *Storm Water Management Model User's Manual, Version 5.0*. National Risk Management Research Laboratory, Office of Research and Development, US Environmental Protection Agency, 1-298.

Rouse, D.C. & Bunsier-Ossa, I.F. (2013). Green infrastructure: a landscape approach. *Apa Planning Advisory Service Reports,* 571, 1-164.

Stovin, V., Vesuviano, G. & Kasmin, H. (2012). The Hydrological Performance of a Green Roof Test Bed under UK Climatic Conditions. *Journal of Hydrology*, 414(2), 148-161.

Versini, P.A., Jouve, P., Ramier, D., Berthier, E. & Gouvello, B.D. (2015). Use of Green Roofs to Solve Storm Water Issues at the Basin Scale – Study in the Hauts-De-Seine County (France). *Urban Water Journal*, 13(4), 1-10.

Wang, W., Li, J., Wang, E. et al. (2015). Introduction of Sponge City construction (chinese). *Construction Science and Technology*, 1, 19-21.

Wang, Y., Bakker, F., Groot, R.D., Wörtche, H. & Leemans, R. (2015). Effects of Urban Green Infrastructure (Ugi) on Local Outdoor Microclimate during the Growing Season. *Environmental Monitoring & Assessment*, 187(12), 732.

Zellner, M., Massey, D., Minor, E. & Gonzalez-Meler, M. (2016). Exploring the Effects of Green Infrastructure Placement on Neighborhood-Level Flooding Via Spatially Explicit Simulations. *Computers Environment & Urban Systems*, 59, 116-128.

Zhu, M., Liao, J., Chen, G., Wang, J. & She, N. (2013). Soil Permeability Improvement for Lid-Type Road Greenbelt. *Water Resources Protection.*

Proceedings of the 37th IAHR World Congress
August 13 – 18, 2017, Kuala Lumpur, Malaysia

PADDY FIELDS AS GREEN INFRASTRUCTRE

MAHITO KAMADA [1], YASUNORI MUTO [2] & YOTA IMAI [3]

[1,2] Graduate School of Technology, Industrial and Social Sciences, Tokushima University, Tokushima 770-8506, Japan
kamada@ce.tokushima-u.ac.jp; muto_yas@ce.tokushima-u.ac.jp
[3] Graduate School of Advanced Technology and Science, Tokushima University, Tokushima 770-8506, Japan
c501101059@gmail.com

ABSTRACT

It is estimated that rainfall would be heavier from year to year and hence risk of flooding would be raised in Japan due to global warming. However, social condition of Japan has led to not allow constructing new infrastructure such as banks and dams, because of decrease of tax income due to rapid population decrease. In addition, cost for renewal and repairing of existing infrastructures will become double than that of the present by 2030. In the situation, it is necessary to set ecosystems as infrastructures for reducing disaster risk and are used for flood control. Difficulty in realizing the idea has come mostly from floodplain/wetland as the ecosystems for flood control have been replaced by paddy fields and owned by famers. Therefore, consensus building with farmers as well as the society is necessary. In order to support consensus building, I have established a research project composed of two kinds of studies. One is evaluation of retarding effect of paddy fields, which can visualize the value of paddy fields on reduction of flooding risk and give a scientific base to regal regulation of land use. Another is for giving farmers incentive to keep cropping without land use change through setting hooded crane as symbols of biodiversity and safe cropping. The hooded crane (*Grus monacha*) is rare bird species with large body size and hence it must be easy for consumers to imagine healthy paddy fields and to buy rice with high price. An example of ecosystem-based flood disaster risk reduction at Yolo County in USA is introduced as a prior case, at where flood control, rice cropping and biodiversity conservation are all achieved.

Keywords: Climate change adaptation (CCA); ecosystem-based disaster risk reduction (Eco-DRR); flood control; hooded crane (*Grus monacha*); regulating service.

1 INTRODUCTION

It is anticipated that climate change impacts will exacerbate disaster risks. IPCC noted that several categories of hazards, such as heat waves, changes in precipitation patterns, droughts, tropical cyclone activity and sea level rise, would increase in intensity and/or frequency in the future as a consequence of climate change (IPCC 2007).

The impacts would vary from region to region (IPCC 2012), and Climate Change Adaptation Group (2013) estimated that average maximum rainfall (Fig. 1a) and frequency of flooding (Fig. 1b) would increase extremely in Japan. It is necessary to make policy and measures to adapt to climate change.

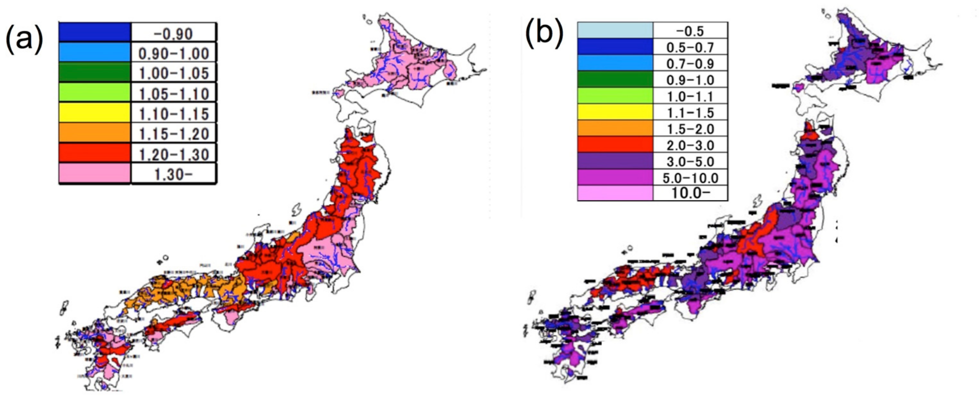

Figure 1. Estimated impacts from global warming in Japan. Amplified ratio in two periods, from [1979-2002] to [2075-2099], (a) averaged maximum rainfall, (b) frequency of occurrence of flooding. (After Climate Change Adaptation Group 2013)

Social condition of Japan, however, becomes to not allow constructing new “grey infrastructure” such as bank and dam. Population of Japan, which reached to peak at 127,840,000 in 2004, is now rapidly decreasing. The population will decrease to 95,150,000 in 2050, then to 47,710,000 in 2100, according to estimation by

Ministry of Land, Infrastructure, Transport and Tourism (http://www.mlit.go.jp/common/000134593.pdf, p.4). Population structure is also drastically changing; increase of older generation and decrease of younger generation. The change that represents tax income and budget for constructing grey infrastructures will decrease. In addition, cost for renewal and maintenance for existing grey infrastructures will increase from year to year; it was estimated that even if newly-built works were stopped after 2011, costs for renewal and maintenance would increase and become double in 2015 (Fig. 2).

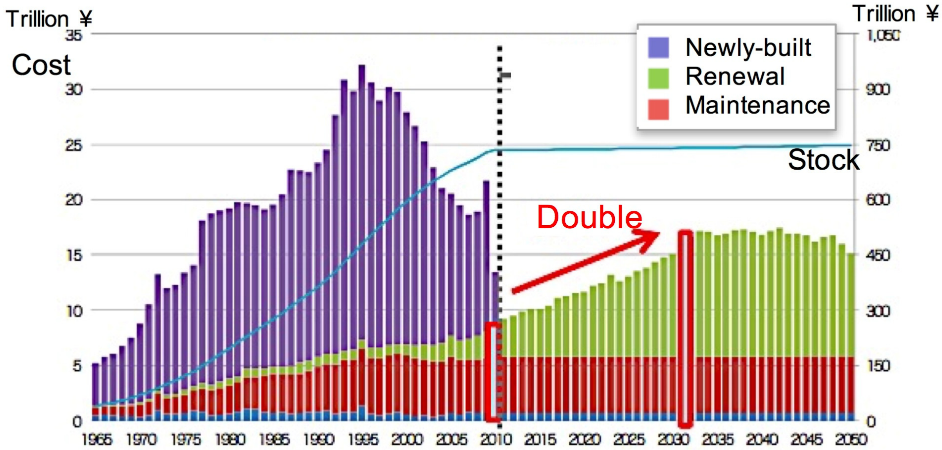

Figure 2. Increase of cost for existing infrastructure (After Ministry of Land, Infrastructure, Transport and Tourism 2013; p.48, http://www.mlit.go.jp/common/000134593.pdf)

In a situation, concept of ecosystem-based disaster risk reduction (Eco-DRR) and climate change adaptation (CCA) must be realized. Eco-DRR/CCA is defined as "the sustainable management, conservation, and restoration of ecosystems to reduce disaster risk and adapt to the consequences of climate change, with aim of achieving sustainable and resilient development" (Renaud et al. 2016). In the context, ecosystem is defined as "green infrastructure".

Wetland is the ecosystem usable to reduce a disaster risk from flooding (Estrella & Saalismaa, 2013). The European Union's Flood Directive spawned a number of country-level programs, which have an integrated approach to water risk management and aim to balance the ecological requirements of river flows; namely "Making Space for Water" in the UK, "Room for the River" in the Netherlands, "Living Rivers" in the UK and France (Renaud et al., 2013).

In Japan as well as other Monsoon Asian countries, wetlands have been altered to paddy fields (Fig. 3). Although the paddy fields are not natural ecosystem, they have provided several ecosystem services to our society, not only provisioning service as rice production. One of the important function of the paddy field is to reserve and infiltrate flooding water. Some local governments in Japan, such as Tokushima Prefecture, have established municipal regulation for flood control, which clearly expresses to use regulating service of paddy fields for CCA (http://www.pref. tokushima.jp/docs/2016122000055/files/jyourei_honbun.pdf). Another function is as habitat of various species and paddy field keeps biodiversity.

Figure 3. Paddy fields have appeared on flood plain of entire Japan, and functioned as alternative wetlands along with rice production.

In order to realize the concept, which is use of paddy field for flood control, there are some challenges to be solved. The biggest challenge is that the paddy fields are private property, which are owned and managed by famers. It is essential to build consensus with farmers and public as the consumer of harvested crops.

The paper aims to introduce an outline of our research project: i) propose a framework to realize the use of paddy fields as green infrastructure of flood control is proposed with use of concept of green infrastructure, ii) show research design to assist consensus building, and iii) show an example of ecosystem-based flood disaster risk reduction from Yolo County in USA and is introduced as a prior case, at where flood control, rice cropping and biodiversity conservation are all achieved.

2 CONCEPTUAL FRAMEWORK

In order to get involvement with farmers and the public and to realize the idea, two conceptual ways were designed and proposed by Kamada (Fig. 4).

Essential problem such as risk raise against flooding hazard is caused by land use change. Paddy fields, which have been developed on floodplain, have been altered to building lot in wide region of Japan, and it will cause increase of opportunity in facing the flood hazard. It is considered that drivers of the land use change are cheap price of the land for buyer, and high labor cost and cheap price of rice for famers. A social framework for keeping paddy field, inhibition of land use change, is necessary to reduce risk exposing to flood.

One way for inhibiting land use change might be achieved by regal and/or economical regulation through visualization of flooding risk and of usability of paddy fields for risk avoidance. When the public recognize flooding risk, interest for loaning the buyer might be set high by financial institutions and/or insurance for houses with high disaster risk might be set high by insurance company. When the public recognize the usability of paddy fields for risk reduction, it might become easy for government to regulate by law.

Another way is to give an incentive to farmers to keep cropping rice. Biodiversity, large sized rare bird in particular, is a key to add value. At Toyooka city, it has successfully added the value to rice by making stork (Ciconia boyciana) as icon of "good environment" and "safe food" (Yabe et al 2014). The iconic story is as follows: stork with the size over 1.5m is top-predator at the ecosystem of composed of paddy field, streams and rivers, and therefore the paddy field raising the stork contains huge amount of food animals such as fishes, frogs, snakes etc. Farmers reduce or stop using pesticide to keep food resources for the storks, and hence the rice harvested from the paddy field is safe. "Stork-raising rice" has being sold at a price of 1.5-2 times as usual rice. Concerning the Tokushima Prefecture, where is target region of our research project, hooded cranes (Gus monacha) have begun to fly into paddy field for spending winter, and it has a chance to make a new icon for additive value.

The scenario mentioned above represents a conceptual process of setting paddy fields as green infrastructure (GI). GI is defined as "an interconnected network of natural areas and other open spaces that conserves natural ecosystem values and functions (Benedict & McMahon, 2006)", which is also defined as "a strategically planned network of natural and semi-natural areas with other environmental features designed and managed to deliver a wide range of ecosystem services (European Commission 2013)". European Commission (2013) also stated that "ecosystem-based approaches are strategies and measures that harness the adaptive forces of nature, which are among the most widely applicable, economically viable and effective tools to combat the impacts of climate change, when appropriately used, such as approaches that use GI solutions". The theme involved in the GI concept is making use of natural processes and ecosystem services for functional purpose (van Wesenbeeck et al., 2016).

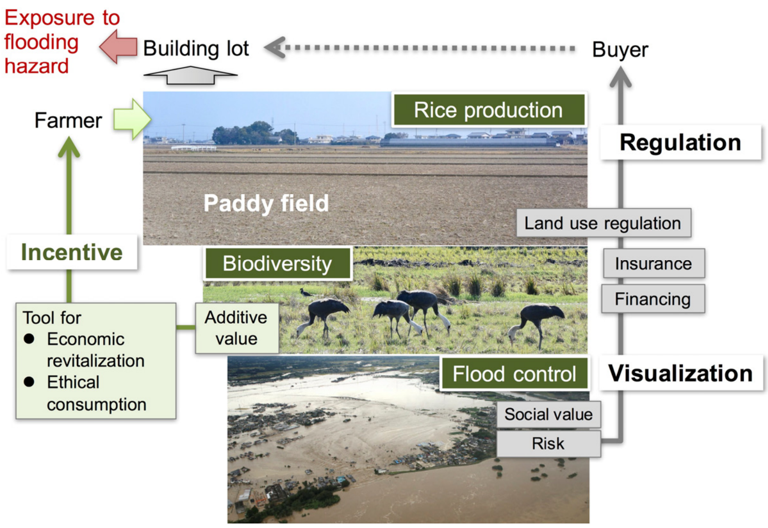

Figure 4. Conceptual ways to set paddy fields as a green infrastructure for Eco-DRR/CCA.

3 RESEARCH PROGRAMS

3.1 Design

In order to support consensus building, research program has been designed to i) indicate area of paddy fields available to hooded crane for wintering from the ecological aspect, ii) clarify flood retarding capacity of paddy fields from the hydraulics and/or hydrological aspect, and then iii) surface multifunctional vale of paddy fields by synthesizing the results (Fig. 5). Target region is Tokushima Prefecture, Shikoku, Japan.

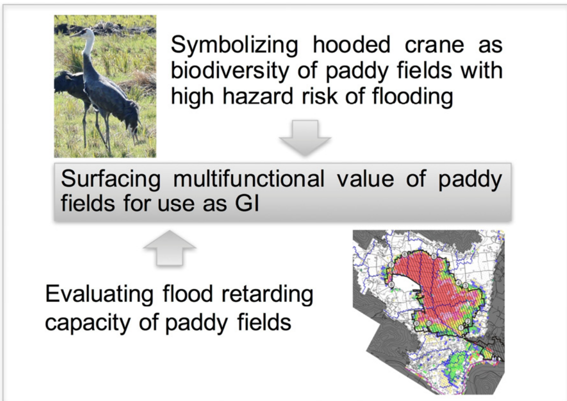

Figure 5. Design of the research program for supporting public involvement

3.2 Estimating potential area of hooded crane wintering

Hooded crane, which is rare bird species with large sized body, is expected to be an icon of “good environment” and “safe food”. The crane is a migratory bird, which breeds at a basin of Amur River of Russia and come to Japan for wintering. Since the bird uses flood plain as a habitat, it is considered that they use paddy fields cultivated on flood plains in Japan. In other words, hooded crane can be used as an indicator of paddy fields with high risk of flooding in addition to the icon of biodiversity.

Potential habitat for wintering was estimated for Tokushima Prefecture, Shikoku, Japan, as the research of Imai (unpublished). Through an interview with the chairperson of the Tokushima Branch of Wild Bird Society of Japan, it was revealed that the hooded crane flying to Tokushima used two different habitat types for wintering. One was for resting in rivers, and another was for foraging at paddy fields. After harvesting, rice can sprout and bear seeds again in late autumn in Tokushima as well as southern warm region of Japan, and the crane has eaten the second seeds for food at dried up fields. All sites recorded from 2008 to 2016 were clarified and stored into GIS. Then, averaged values of elevation and slope, and areas of paddy fields, mountainous vegetation and residential lot were calculated for all grids of 100m x 100m covering entire area of Tokushima; data from Digital National land information were used for getting elevation and slope, and Natural environmental information GIS for the areas of paddy fields, residential lots and mountainous vegetation. By using those values as variables, spatial model for explaining foraging area was constructed by the use of maximum entropy modelling (Maxent: Phillips et al., 2006, Arakida et al., 2011), and potential habitat map was produced (Fig. 6_left). Maxent is an automated learning method, to estimate the most uniform distribution (maximum entropy) across the study area given the constraint that the expected value of each environmental predictor variable under this estimated distribution matched its empirical average.

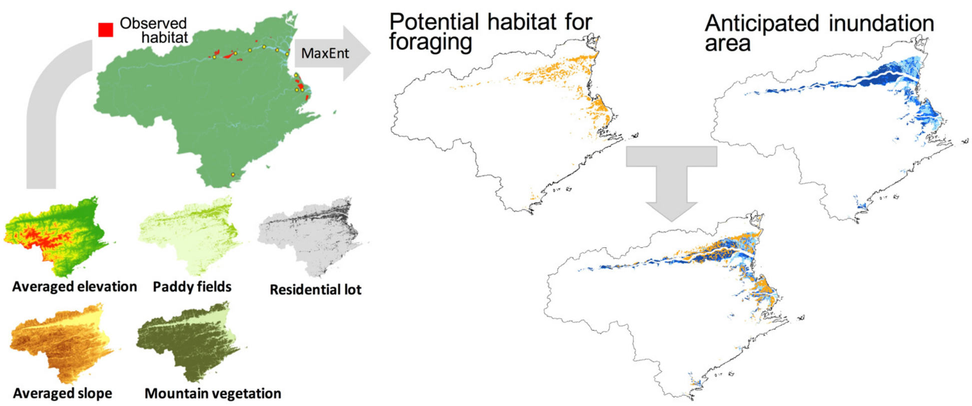

Figure 6. Potential habitat for wintering and anticipated inundation area. Area of darker blue in anticipated inundation area map is estimated to have deeper water-depth when flooding hazard occur.

The potential habitat map was overlaid with "anticipated inundation area map", which have been distributed by governments as GIS data. The result indicates that almost all area of the potential habitats for wintering/foraging were involved in anticipated inundation area (Fig. 6_right), and supported the hypothesis of that the hooded crane use paddy fields with high risk of flooding.

3.3 Evaluation of flood retarding capacity of paddy field

As the first step for evaluation of flood retarding capacity of paddy field, an availability of Application of Flood Risk Evaluation (AFREL, Fig. 7) was examined, and it was confirmed that the AFREL would be useful and practical as inundation simulation model as the work of Muto.

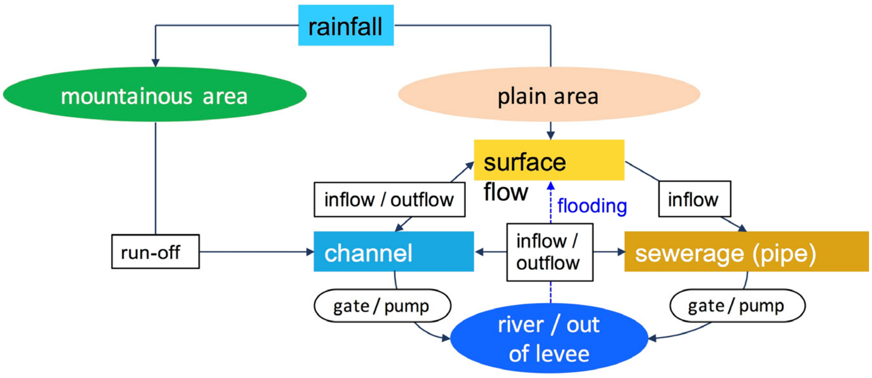

Figure 7. Inundation simulation model, AFREL; Application of Flood Risk Evaluation (Muto et al. 2017).

Muto et al. (2017) evaluated an effect of land use change, from paddy field to building lot by using AFREL, at an area where the potential was estimated high for wintering site of hooded crane. In this case, it is assumed that part of the paddy field area was mounded by soil and land elevation was raised for 1m. Influence of land use change on flood retarding capacity was different with an amount of precipitation. In a case of an extremely large flooding with 1/100 years of occurrence probability, flood retarding capacity is largely reduced compared to the case without land use change. It is estimated that reduced amount of water-storage at paddy field would increase discharge flowing into the river. And thus, a burden of rivers in flood control would be increased (Fig. 8).

For further and/or realistic analysis, simulation model for predicting land use change is now being established by a help of a researcher of regional plan.

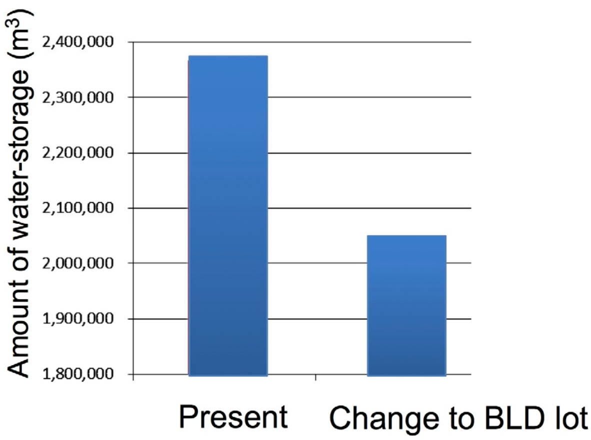

Figure 8. Change of water-storage ability of paddy field area in relation to land use change, in case of that part of paddy changes to building lot (Muto et al. 2017).

4 AN EXAMPLE OF SUCCESSFUL USE OF PADDY FIELDS FOR GI IN USA

Field trip was conducted in December 2015, and information was collected by interviewing with members of Yolo Basin Foundation (NGO), a staff of the California Department of Fish and Wildlife Natural Resources Agency, and a staff of Yolo County Resource Conservation District and farmers.

At Yolo County in USA, national government bought land and established the Yolo Bypass to receive overflowing water from Sacrament River during huge floods (Fig. 9). Local government has set Wildlife Area (WA), particularly for water birds, inside the Yolo Bypass and manage there with NGO. Part of the area of WA has been rent to farmers in cheap fee and the farmers grow rice there. Rice cropping is beneficial for government and NGO managing the Yolo Bypass and WA, because it inhibits vegetation succession and thus help to keep the land available for temporal reservoir and water bird habitat (Fig. 10).

The case is applicable to Japan; keeping rice-farming is functioned as vegetation management to keep alternative wetland on flood plain, and it is beneficial for flood retarding as well as for wildlife habitat. Thus, the paddy fields can supply multi-functions as GI in cropping, flood control and sustaining biodiversity.

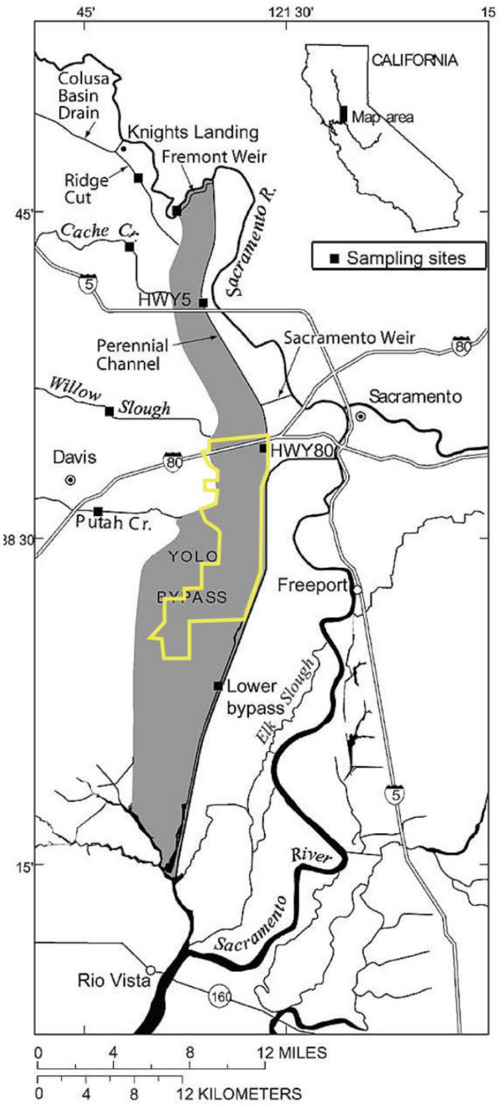

Figure 9. Yolo Bypass (grey colored area) and Wildlife Area (inside the yellow line). (After Yolo Bypass Wildlife Area, Land Management Plan 2008; https://nrm.dfg.ca.gov/FileHandler.ashx?DocumentID=84924 &inline)

Figure 10. Rice cropping in summer helps to provide habitat for wintering water birds.

5 CONCLUDING REMARKS

GI, which has been successfully implemented as a tool of Eco-DRR/CCA in USA, has been introduced into Japan just recently, and now efforts for implementation have begun by researchers and administrators. The same situation can be seen in the Republic of Korea, where population is going to decrease (Lee, 2008) and it is considered that tax income and budget for constructing infrastructure will decrease, which the same happening in Japan. Thus, GI for disaster risk reduction will also become an essential tool in the Republic of Korea.

Although the social background and land use pattern are different from those of the USA, the idea of that using paddy fields as GI for Eco-DRR/CCA must be useful and available to Japan, Korea and probably other Monsoon Asian countries. It is important to share and exchange ideas for implementing the GI into Asian societies where the paddy field is dominant in the landscape.

ACKNOWLEDGEMENTS

The study was supported by the Environment Research and Technology Development Fund (4-1504) of the Ministry of the Environment, Japan.

REFERENCES

Arakida, H., Mitsuhashi, H., Kamada, M. & Koyama, K. (2011). Mapping the Potential Distribution of Shorebirds in Japan: The Importance of Landscape-Level Coastal Geomorphology. *Aquatic Conservation: Marine and Freshwater Ecosystems*, 21, 553–563.

Benedict, M.A. & McMahon, E.T. (2006). *Green Infrastructure, Linking Landscapes and Communities*. Island Press, Washington. 299.

Climate Change Adaptation Group, National Institute for Land and Infrastructure Management (2013). Interim Report on Climate Change Adaptation Studies. *Technical Note of National Institute for Land and Infrastructure Management*, no.749.

Estrella, M. & Saalismaa, N. (2013). Ecosystem-Based Disaster Risk Reduction (Eco-DRR): An Overview. *The Role of Ecosystems in Disaster Risk Reduction*, Ed. G. Fabrice et al., United Nation University Press, Tokyo, 26-54.

European Commission (2013). Green Infrastructure (GI) –Enhancing Europe's Natural Capital. *COM,* 249.

IPCC (2007). *Climate change 2007: Impacts, Adaptation and Vulnerability. Contribution of Working Group II to the fourth assessment report of the intergovernmental panel on climate change*. Cambridge University Press, Cambridge.

IPCC (2012). *Managing the Risks of Extreme Events and Disasters to Advance Climate Change Adaptation. A Special Report of Working Group I and II of the Intergovernmental Panel on Climate Change*. Cambridge University Press, Cambridge and New York.

Lee, B.S. (2008). Trend of Population Change and Deindustrialization of Provincial Cities. *Tochi Sogo Kenkyu*, 16(3), 37-43. (in Japanese).

Muto, Y., Murata, Y., Miyoshi, M. & Tamura, T. (2017). Retarding Effect Evaluation of Paddy Fields and Their Land-use Change. *E-proceedings of the 37th IAHR World Congress. (in press).*

Phillips, S.J., Anderson, R.P. & Schapire, R.E. (2006). Maximum Entropy Modeling of Species Geographic Distributions. *Ecological Modelling*, 190, 231–259.

Renaud, F.G., Sudmeier-Rieux, K. & Estrella, M. (2013). The Relevance of Ecosystems for Disaster Risk Reduction. *The Role of Ecosystems in Disaster Risk Reduction*, Ed. G. Fabrice et al., United Nation University Press, Tokyo, 3-25.

Renaud, F.G., Nehren, U., Sudmeier-Rieux, K. & Estrella, M. (2016). Development and Opportunities for Ecosystem-Based Risk Reduction and Climate Change Adaptation. *Ecosystem-Based Disaster Risk Reduction and Adaptation in Practice*, Ed. F.G. Renaud et al., Springer, Switzerland, 1-20.

van Wesenbeeck, B.K., van der Meulen, M.D., Pesch, C., de Vriend, H. & de Vries, M.B. (2016). Nature-Based Approach in Coastal Flood Risk Management: Physical Restrictions and Engineering Challenges. *Ecosystem-Based Disaster Risk Reduction and Adaptation in Practice*, Ed. F.G. Renaud et al., Springer, Switzerland, 181-198.

Yabe, M., Hayashi, T., Nishimura, B. & Sun, B. (2014). Conservation of Biodiversity and Its Value in Agricultural Products. *Journal of Resources and Ecology*, 5(4), 291-300.

THE CONCEPT OF DIRECTLY CONNECTED IMPERVIOUS AREAS AND ITS IMPLICATION ON MITIGATION OF PEAK FLOWS IN URBAN CATCHMENTS

YONGWON SEO[(1)], JUNSHIK HWANG[(2)] & YOUJEONG KWON[(3)]

[(1,2, 3)] Department of Civil Engineering, Yeungnam University, Gyeongsan, South Korea,
yseo@ynu.ac.kr; jshwang@ynu.ac.kr; my218@ynu.ac.kr

ABSTRACT

The concept of directly connected impervious area (DCIA) or efficient impervious area (EIA) refers to a subgroup of impervious cover, which is directly connected to a drainage system or a water body via continuous impervious surfaces. The concept of DCIA is important in that it is a better predictor of stream ecosystem health than total impervious area. DCIA is a key concept for a better assessment of green infrastructure that is drawing more attention recently since DCIA has a direct relation with green infrastructures in urban environments. In this study, we evaluated several methods to calculate the DCIA based on a precise GIS database and showed the importance of the accurate measurement of DCIA in terms of resulting hydrographs. We also combined the width function-based instantaneous hydrograph with the concept of DCIA to evaluate the potential green infrastructures that can be introduced in the test catchment in South Korea. The results showed that the changes of DCIA, by green infrastructures, directly affect the shape of hydrographs and decreases peak flows. These results imply that we can introduce well-planned green infrastructure to urban catchments for flood risk managements and quantitative assessment of spatial distribution of DCIA is crucial for this.

Keywords: Directly connected impervious area; width function; green infrastructure; drainage network; hydrograph.

1 INTRODUCTION

DCIA is considered the subset of the total impervious areas (IA) with a direct hydraulic connection to a waterbody via continuous paved surfaces, gutters, drain pipes, or other conventional conveyance and detention structures that do not reduce runoff volume (EPA, 2014). As stormwater runoff flows across parking lots, roadways, and paved areas, the oils, sediments, metals, and other pollutants are collected and concentrated. If this runoff is collected by a drainage structure and carried directly along impervious gutters or in sealed underground pipes, it has no opportunity for filtering by plant material or infiltration into the soil. It also increases in speed and volume, which may cause higher peak flows downstream, and may require larger capacity storm drain systems, increasing flood and erosion potential (BASMAA, 1999). Best Management Practice (BMP) or green infrastructures contribute to the disconnection of IA and, thus, decreases DCIA. Therefore, DCIA is a key concept to evaluate green infrastructures introduced to urban spaces.

2 METHODS AND THE STUDY AREA

We selected the Shinweol catchment in Seoul as a test catchment for the application. The catchment suffered from continuous flood damages in 2010 and 2011.

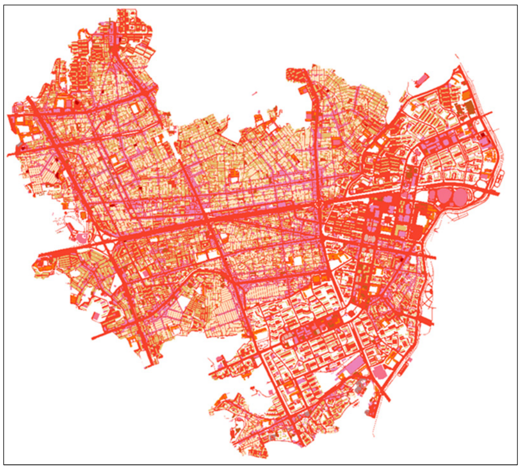

Figure 1. Total impervious map constructed from satellite images and orthophotograph of the Shinweol catchment in Seoul, South Korea.

In this study, we employed the width function based IUH (WFIUH) (Seo et al., 2012) and the detailed SWMM model for the comparison between the models.

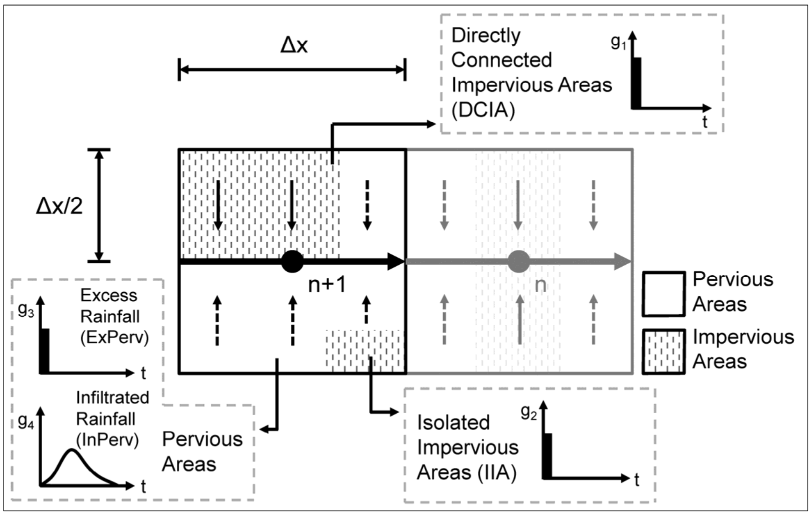

Figure 2. Response functions from excess rainfall and infiltrated rainfall contributing to runoff hydrographs (Seo et al., 2013).

We used a methodology that conceptualizes the contributing portion of an urban catchment (Seo et al., 2013; Seo and Schimdt, 2014) from the DCIAs that are directly connected to the main drainage network, isolated impervious areas (IIAs) that need to travel through pervious areas to get to the main water body or drainage network, and pervious areas. The contribution of the pervious areas can be further divided into excess rainfall amount (ExPerv) and infiltrated rainfall amount (InPerv). Traditionally, no design is considered for the urban drainage media (Yen and Akan, 1999). In contrast, this study includes the contribution from infiltrated rainfall (InPerv). In order to include the contribution from different parts of an urban catchment, this study introduces a hydrological response function at the outlet of a drainage network based on the WFIUH (Seo et al., 2013).

The original approach of WFIUH was suggested by van de Nes (1972) and applied to natural watersheds so far (Naden, 1992; Franchini and O'Connel, 1996; Da Ros and Borga, 1997). In order to account for the different flow paths from pervious and impervious areas following equations for the instantaneous unit hydrograph can be used (Seo et al., 2013):

$$h_i(t) = \sum_{j=1}^{n_w}\big(W_i(j\Delta x)\cdot f(j\Delta x, t) * g_i(t)\big)\Delta x \qquad [1]$$

where W is the width function, Δx is the grid size, i=1 for contribution from excess rainfall in DCIA, 2 for excess rainfall in IIA, 3 for excess rainfall in pervious areas (ExPerv), and 4 for infiltrated rainfall in pervious areas (InPerv). W_1 and W_2 are the same width functions obtained from impervious area and W_3 and W_4 are the same from pervious area, respectively. n_w is the maximum distance of the width function. f is a response function of the main drainage network and g is a response function defined in a cell (Figure 2). f and g both are assumed to have a form of inverse Gaussian function.

$$f(i\Delta x, t) = \frac{i\Delta x}{\sqrt{4\pi D_1 t^3}}\exp\left[-\frac{(i\Delta x - ct)^2}{4D_1 t}\right] \qquad [2]$$

where c_1 and D_1 are celerity and diffusion coefficient for the main drainage network. The response function in a cell, g_i from excess rainfall in DCIA, IIA as well as in previous areas (ExPerv) is given as

$$g_i(t=0) = 1, \text{otherwise } 0; \text{for } i = 1, 2, 3 \qquad [3]$$

The response function g_4 is from the infiltrated rainfalls in pervious areas (InPerv) by Assumption 1. Mejia and Moglen (2010) assumed a two-parameter inverse Gaussian travel time distribution for both hillslopes and channels to derive a geomorphologic unit hydrograph for a natural watershed. In this study, g_4 is assumed to have the same form with Equation 6.21 which is a solution of an advection-diffusion equation.

$$g_i(t) = \frac{\Delta x}{\sqrt{16\pi D_2 t^3}}\exp\left[-\frac{(\Delta x - 2c_2 t)^2}{16 D_2 t}\right]; \text{ for } i = 4 \qquad [4]$$

where c_2 and D_2 are celerity and diffusion coefficient of the flow path, through which the infiltrated rainfall in pervious areas contributes to the main drainage network. Given the length of f and g as M_f and M_k, respectively, the convolution for discrete time steps can be obtained as

$$(f * g)[k] \stackrel{\text{def}}{=} \sum_{m=0}^{max(M_f,M_k)-1} f[m]\, g[k-m], 0 < k < M_f + M_k - 2 \qquad [5]$$

The response at the outlet can be obtained as the sum of the convolution of the response function from each area and the corresponding precipitation.

$$Q(t) = \sum_{i=1}^{n_c} h_i * I_i \qquad [6]$$

where i=1 for DCIA, 2 for IIA, 3 for ExPerv, and 4 for InPerv, respectively. Excess rainfall and infiltrated rainfall for corresponding pervious and impervious areas are defined in Table 1 where I_{imperv} denotes the excess rainfall amount considering depression storage only in impervious areas, I_{ExPerv} denotes the excess rainfall considering depression storage as well as infiltration. I_{InPerv} is infiltrated amount of rainfall. In Table 1, r_i is impervious ratio of the watershed and r_c is the area of IIA divided by total impervious area. r_b is contributing ratio of infiltrated water to runoff.

Table 1. Precipitation separately assigned for four contributions in urban catchments.

Contribution	Soil condition	
	Unsaturated	**Saturated**
DCIA	$I_1 = (1 - r_c)I_{imperv}$	$I_1 = (1 - r_c)I_{imperv}$
IIA	$I_2 = 0$	$I_2 = r_c I_{imperv}$
ExPerv	$I_3 = 0$	$I_3 = I_{ExPerv}$
InPerv	$I_4 = \left(1 + \frac{r_i r_c}{1 - r_i}\right) r_b I_{InPerv}$	$I_4 = r_b I_{InPerv}$

3 RESULTS AND DISCUSSIONS

3.1 Obtaining the DCIA ratio from the impervious map

This study used high-resolution land cover data developed by the Ministry of Environment between 2013 and 2014 in Korea. This was built from various sources from satellites and air-photographs with a spatial resolution of 1 m. The data sets were divided into three levels: low-level, mid-level, and high-level land cover data. Table 2 shows each land cover level and its characteristics. High-level land cover data describe the land use with 41 land use classifications to identify the impervious areas (Table 2). The high-level land cover data for the entire Shinweol Basin where impervious areas can be obtained from this data as was shown in Figure 1. We estimated the DCIA for the study catchment considering followings:

- Isolated impervious areas surrounded by pervious cover were removed;
- Isolated impervious areas partly connected to other impervious areas but their downstream flow paths were blocked by pervious cover were removed;
- Schools and gardens were removed, which typically includes pervious areas not identified by land user cover;
- Apartments with pervious pavement, raingardens, playgrounds, and green alleys were removed from the total impervious areas.

3.2 Verification of the WFIUH modeling

Figure 3 show the simulation results for direct runoff hydrographs of the Shinweol catchment from the period of July 2012 and July 2013, which belong to the rainy season in Korea. We used the observed data produced by the Seoul Metropolitan Government and compared the results from both the SWMM (the red dash) and WFIUH modeling (the blue solid). The results indicate both models successfully reproduced the observed hydrographs (black dots).

Table 2. Land cover classification (Ministry of Environment, South Korea).

Low-level land cover data	Mid-level land cover data	High-level land cover data
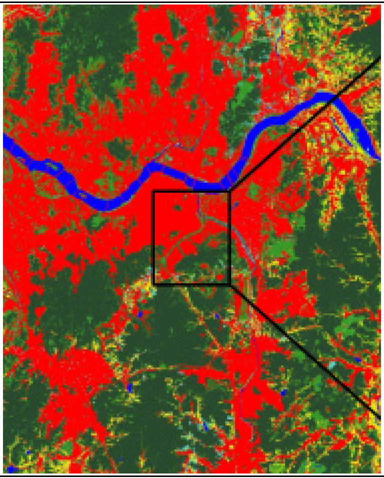		
·Spatial resolution: 30m ·Classification: 7 items ·Map scale: 1:50,000 ·Data: Landsat TM satellite image	·Spatial resolution: 5m ·Classification: 22 items ·Map scale: 1:25,000 ·Data: Landsat TM + IRS 1C, SPOT5, Arirang 2 satellite image	·Spatial resolution: 1m ·Classification: 41 items ·Map scale: 1:5,000 ·Data: Arirang 2, IKONOS satellite image, Air-Photographs

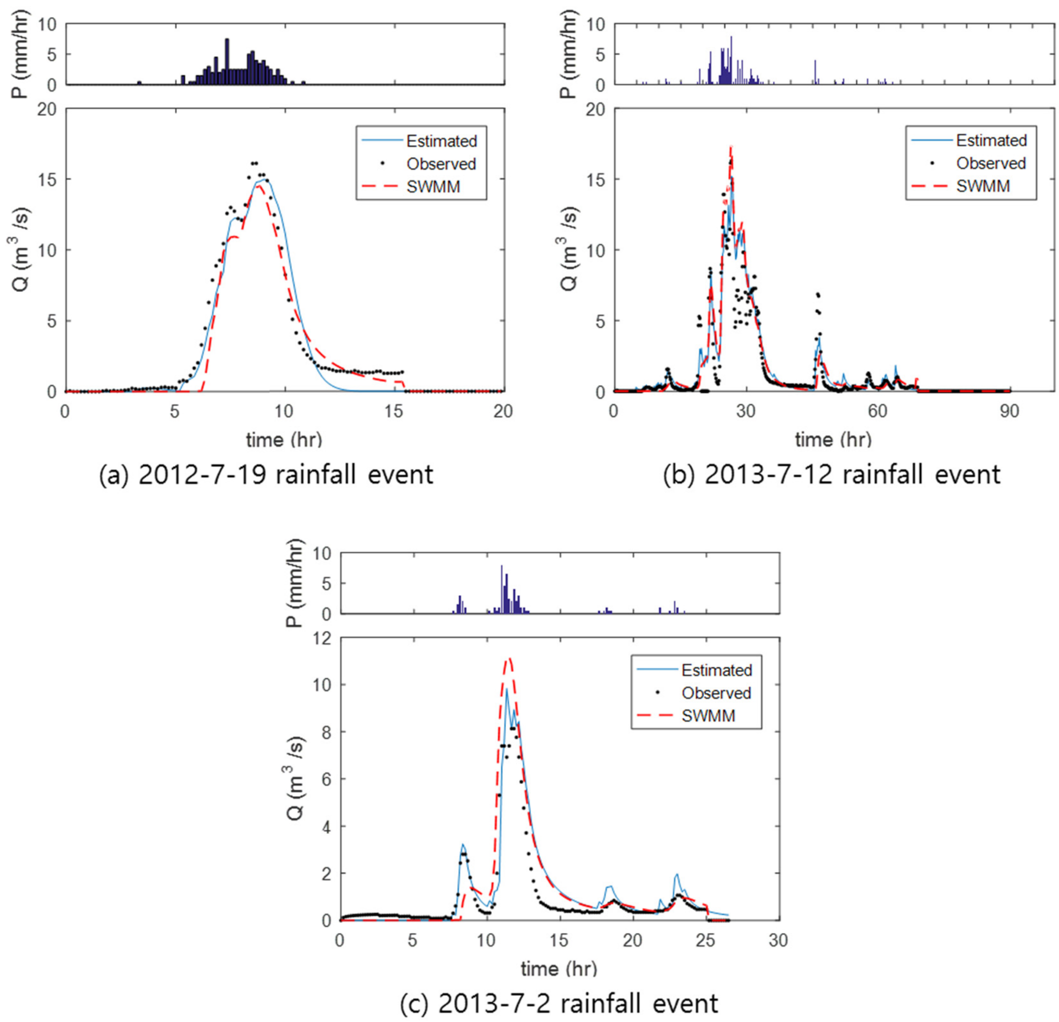

Figure 3. Direct runoff hydrographs estimated by the WFIUH compared with the observed flow and the highly detailed SWMM.

3.3 Changes of DCIA by green infrastructures

Table 3 shows the results of DCIA changes by green infrastructures. Scenario 1 converts existing impervious surfaces, such as individual residential and apartment parking lots, which were identified as the DCIA, to permeable pavement. Scenario 2 includes the redirection of rooftop runoff to infiltration areas; whereas, Scenario 3 includes the implementation of both Scenario 1 and 2. We applied the disconnection ratio suggested by the US EPA (2011) (Table 4). Basically, the green infrastructure disconnects the impervious areas, which makes less and less impervious areas get connected and decreases the ratio of DCIA from the total impervious areas depending on its types.

Table 3. DCIA calculated for the study area.

Scenario	Description	DCIA (%) Present	DCIA (%) Application
Scenario 1	CONVERT ROADS, INDIVIDUAL RESIDENTIAL AND APARTMENT PARKING LOTS TO PERMEABLE PAVEMENT	82.95	63.76
Scenario 2	REDIRECTION OF ROOFTOP RUNOFF TO INFILTRATION AREAS		74.94
Scenario 3	SCENARIO 1 + SCENARIO 2		62.69

Table 4. Determining DCIA based on Interim Default BMP Disconnection Multipliers or EPA's Infiltration Curves (US EPA, 2011).

BMP Description	% Runoff Volume Reduction1	BMP Disconnection Multiplier2
Removal of pavement; restoration of infiltration capacity	100%	0
Redirection of rooftop runoff to infiltration areas, rain gardens or dry wells	85%	0.15
Permeable pavement, bioretention practices, dry/vegetated water quality swales	75%	0.25
Disconnection to qualified pervious area3	50%	0.50
Infiltration trenches	15-100%	0.85-0
Infiltration basins	13-100%	0.87-0
Non-runoff reduction practices (*i.e.*, detention ponds, wetlands, sand filters, hydrodynamic separators, etc)	0%	1.0

3.4 Peak flow reduction by the changes in DCIA

Table 5 lists the resulting peak flow reduction by green infrastructures for the entire basin for implementation scenarios 1, 2, and 3, respectively. The results show that the peak flow was reduced mostly by 12 % for Scenario 3 compared to the current state. Scenario 2 shows a 2 % decrease in peak flows due to little changes in the DCIA. Scenario 1 shows a 1 % decrease in flow peaks by permeable pavements. These results show the peak flow reduction obtained by the implementation of green infrastructures. Moreover, the modeling feature implies the spatial planning of green infrastructure is of great importance in term of flood mitigation.

Table 5. Peak flow reduction by green infrastructures.

Application areas	Peak flows (m3/s) for the storm event on July 12, 2013			
	Current state	Scenario 1	Scenario 2	Scenario 3
Entire catchment	36.96	32.98 (-11 %)	36.39 (-2 %)	32.48 (-12 %)

4 CONCLUSIONS

Recent studies found that DCIA is a more accurate factor for evaluating the changes in ecological and hydrological regimes compared to the TIA. This study assessed the impact of BMP or green infrastructure in urban catchments focusing on their impacts on decreasing DCIA by disconnecting impervious areas. To accomplish this, three implementation scenarios of green infrastructure for the test catchment were introduced focusing on the effect of spatial implementation planning. Coupled with the WFIUH, which is able to consider the spatial distribution of the impervious areas considering DCIA, the results showed that changes in the DCIA immediately affects the shape of the direct runoff hydrograph and decreases peak flows. Especially, this study shows the spatial implementation of the green infrastructures affects the resulting direct runoff hydrographs depending on scenarios. The results imply that a modeling results should be verified using an appropriate hydrological model that is able to assess the effect of the DCIA on a catchment scale. The quantitative assessment of the spatial distribution of the impervious areas and the changes in the DCIA suggest that effective and strategic planning of green infrastructure can be introduced in urban environments for flood risk management.

ACKNOWLEDGEMENTS

The authors would like to acknowledge that Basic Science Research Program through the National Research Foundation of Korea (NRF) from the Ministry of Education (NRF-2016R1D1A1B03930893) supported this study.

REFERENCES

Da Ros, D. & Borga, M. (1997). Use of Digital Elevation Model Data for the Derivation of the Geomorphological Instantaneous Unit Hydrograph. *Hydrological Process*, 11(1), 13-33.

Franchini, M. & OConnell, P.E. (1996). An Analysis of the Dynamic Component of the Geomorphologic Instantaneous Unit Hydrograph. *Journal of Hydrology*, 175(4), 407-428.

Mejia, A. I., and Moglen, G. E. (2010). Impact of the Spatial Distribution of Imperviousness on the Hydrologic Response of an Urbanizing Basin. *Hydrological Process*, 24(23), 3359-3373.

Richman, T. (1999). *Start at the Source: Design Guidance Manual for Stormwater Quality Protection.* Bay Area Stormwater Management Agencies Association, CA.

Seo, Y., Choi, N.J. & Schmidt, A.R. (2013). Contribution of Directly Connected and Isolated Impervious Areas to Urban Drainage Network Hydrographs. *Hydrology and Earth System Sciences*, 17(9), 3473-3483.

Seo, Y. & Schmidt, A.R. (2014). Application of Gibbs' Model to Urban Drainage Networks: A Case Study in Southwestern Chicago, USA. *Hydrological Processes*, 28(3), 1148-1158.

USEPA (2014). *Estimating Change in Impervious Area (IA) and Directly Connected Impervious Area for Massachusetts Small MS4 Permit*, United States Environmental Protection Agency, Washington D.C.

Van de Nes, T.J. (1973). *Linear Analysis of a Physically Based Model of a Distributed Surface Runoff System*. Centre for Agricultural Publishing and Documentation, Wageningen.

Yen, B.C. & Akan, A.O. (1999). Hydraulic Design of Urban Drainage Systems. *Hydraulic Design Handbook*, Mays, L.W. (ed)., McGraw-Hill, New York.

Proceedings of the 37th IAHR World Congress
August 13 – 18, 2017, Kuala Lumpur, Malaysia

ADVANCED RESEARCH ON KOREA GREEN INFRASTRUCTURE AND LOW IMPACT DEVELOPMENT CENTER

HYUN-SUK, SHIN[1], JONGBIN, PARK[2], JAEHYUK, LEE[3], JAEHUN, AHN[4] & SOONCHUL, KWON[5]

[1,4,5] Department of Civil Engineering, Pusan National University, Busan, South Korea
hsshin@pusan.ac.kr; jahn@pusan.ac.kr; sckwon@pusan.ac.kr
[2,3] Green Land & Water Management Institute, Pusan National University, Busan, South Korea,
bbin63@pusan.ac.kr; rasmania@ pusan.ac.kr

ABSTRACT

Rapid decrease in pervious coverage in urban area and change in rainfall pattern and intensity make urban area more venerable for water disaster. As such, GI & LID (Green Infrastructure and Low Impact Development) is widely accepted as a design concept and management practice tool in urban areas over the world. In Korea, there is the GI & LID research center constructed under support of MOLIT (Ministry of Land, Infrastructure and Transport) that possess extensive real scale testbeds and laboratory test facilities. Among other goals, this research center aims at developing inclusive experimental program and certification process of hydraulic/hydrologic, environmental and structural performance of GI and LID facilities based on its testbed and laboratory facilities. The real scale testbeds are outdoor facilities where the plant and pavement based LID facilities can be instrumented with state of the art measurement systems and mobile rainfall simulators. The performance of prototype facilities can be well investigated under natural and artificial rainfall. This center is also well equipped with laboratory facilities, not only hydraulic/hydrologic and environmental performances but also structural performance of, for example, LID permeable pavements can be evaluated, assessing all-round aspects of GI and LID facilities. Korean GI and LID research center will make positive impacts in development of GI & LID, promoting it as disaster risk reduction measures in Korea and over the world.

Keywords: Green Infrastructure; Low Impact development; Verification; Certification; Integrated management system.

1 INTRODUCTION

Urbanization and climate change cause increased stormwater runoff and peak flow rates that led to flash floods and degradation of in-stream ecosystem health. Controlling flood runoff events and solving serious problems such as inundation is becoming increasingly difficult, especially for highly urbanized areas due to expanded impervious areas arising from the extension of urban areas and the consequent difficulties in hydrological processes and water environmental systems. In 2010 and 2011, Seoul, South Korea experienced shocking flooding damages due to heavy rainfall. These events led to increased interest in stormwater management in urban area (Lee, 2013). And Low impact development (LID) technologies and practices have been developed and applied to traditionally developed sites to overcome these problems. LID as defined by Washington State University's Puget Sound Action Team, "is a stormwater management strategy that emphasizes conservation and the use of existing natural site features integrated with distributed, small-scale stormwater controls to more closely mimic natural hydrologic patterns in residential, commercial and industrial settings." LID practices are measures to mitigate the impacts of development and urbanization. LID techniques focus mainly on site-specific hydrology since every aspect of site development affects the hydrologic response of the site. Thus, the primary goal of LID methods is to mimic the undeveloped site hydrology using site-design techniques that store, infiltrate, evaporate, and detain runoff.

Ministries in South Korea have prepared and implemented new stormwater management plans and strategies using Low Impact Development method. Now that the national initiative is realigned to meet the goals, and the policies of ministries are pursuing those goals as well, we should examine how the roles and responsibilities of participants are defined to ensure the effective implementation. Ministry of Land, Infrastructure and Transport Affairs (MOLIT) has established objectives (flood control and secure of water resource etc.) and strategies for application of LID. The ministry has pushed for stormwater runoff reduction and strategies for the climate change adaptation and energy independence while promoting green transportation and green jobs for creating green growth dynamics.

Ministry of Environment (ME) aims to create green wealth prosperity through environmental innovation, and to promote strategies to reduce pollution in stormwater runoff, develop new environmental technologies and industries, create new jobs and human resources, and promote environment-friendly lifestyle. The government of South Korea suggested LID approach as a national environmental policy to implement these policies (Park et al., 2008). The necessity of LID measures is increasing due to waterside urban development by the special act and guideline on the development of waterfront area.

Based on these objectives and strategies, In South Korea, new city development projects or retrofit projects of old towns are underway. But application without verification or certification system of GI & LID technologies was resulted in decrease of hydraulic cycle efficiency in spite of development of GI & LID technologies and efforts of government to execute a GI & LID project. Therefore, it is necessary to develop verification and certification systems and facilities. So, in this research, a center for certification and verification of GI and LID technology was established and an integrated operation management system to manage it was developed.

2 CHANGE OF STORMWATER MANAGEMENT POLICY IN SOUTH KOREA

Many water management laws in South Korea have been enacted for last half-century. Basic laws for water management were established from 1960 to 1970 such as Water supply and waterworks installation Act, Sewerage Act and Environmental protection Law. The 1980s is the times of development of stable water resources. Groundwater act and law for the preservation of water quality are established in 1990s, when it is the times of occurrence of water pollution accident. In the 2000s, many laws to flood protection, social amenity and environmental protection were enacted for balance of development and environment. Obligation of rainwater harvesting system in large-scale buildings was included in “Water supply and waterworks installation act” enacted by the Ministry of Environment in September 2001 year. Ministry of Public Safety and Security (MPSS) had a law entitled “Countermeasures against natural disasters acts”, which was enacted in July 2004 year, and is working on the projects for rainwater storage and infiltration. After 2008 year, many laws are enacted to develop the water cycle city in South Korea (UNESCAP, 2012). The ministry of Land, Infrastructure and Transport Affairs enacted “Special act on the utilization of waterfronts” in December 2010 year. Thereafter, a law to promote and support water reuse, which also promotes rainwater management for supplying alternative water resources, was enacted in 2010 and now is enforcing. And the ministry of Public Safety and Security amended the “Countermeasures against natural disasters act” as installation of runoff reduction facilities to prevent flood, drought, etc. Table 1 shows the status of major systems by each government department.

Table 1. Laws on water cycle management for resilience to climate change in Korea

LAW	DETAILS
SPECIAL ACT ON THE UTILIZATION OF WATERFRONTS (MOLIT)	[Guidelines] Require of application of low impact development in land use plan
COUNTERMEASURES AGAINST NATURAL DISASTERS ACT (MPSS)	Article 19-7 (Standards for Runoff Reduction Facilities) (1) Runoff reduction facilities shall have the function of reducing instantaneous rainwater runoff for mitigating damage caused by wind, flood, and drought.
ENFORCEMENT RULES ON DECISION, STRUCTURE & INSTALLATION CRUTERIA OF CITY & COUNTY PLANNING FACILITIES (MOLIT)	Article 8-3 Decision of city & county planning facilities to recover a water cycle of natural situation as minimum stormwater runoff happened from impervious area
ENFORCEMENT REGULAION ON WATER QUALITY & ECOSYSTEM CONSERVATION ACT (ME)	Article 73 Report of non-point pollutant reduction plan with LID method to minimize stormwater runoff happened from impervious area in order to urban development project
PROMOTION OF AND SUPPORT FOR WATER REUSE ACT (ME)	Article 8 Parties intending to construct sports complexes, gymnasiums, and government office buildings prescribed by Presidential Decree shall install and operate a rainwater harvesting facility

3 KOREA GREEN INFRASTRUCTURE & LOW IMPACT DEVELOPMNET CENTER

3.1 Introduction

Korea GI & LID Center that is opened in June, 2016 with the support of Ministry of Land, Infrastructure and Transport, Korea Government is located at a branch of Pusan National University in Yangsan City. This center is the world first research facility designed and constructed to focus on testing and evaluating various GI and LID systems to address water quality and runoff volume reductions from urban and rural runoff to not only be used in South Korea but anywhere in the world. The LID systems include:

- Multiple types of green roofs on the roof of the center,
- LID Building Planter systems,
- LID Street Planter systems,
- Rainwater Harvesting (Rain Barrels) system,
- Permeable Asphalt Pavement,

  / ISSN 1562-6865 (Online) - ISSN 1063-7710 (Print)

· Porous Concrete Pavement,
· Stone pavers with gravel joints,
· Rain garden,
· Sand filter system
· Wet Pond,
· Dry Pond,
· Grass Swale,
· Proprietary brick pavers with plastic spaces and open joints,
· Pavers with open PVC grids at corners for infiltration,
· Permeable pavers (water infiltrates through the paver surface),
· Propriety Rainwater Harvesting systems

The design is based on the lake in the middle of New York City's Central Park as well as the many water features found in the historic Royal Palace in Seoul. The open-water component is part of a fully functional LID stormwater management system consisting of bioswale, constructed wetland, sand filter, permeable pavement system for the exterior walkway, rainwater harvesting and reuse system as well as bioretention facilities. There are objectively three areas: LID testing and experiment space, LID education and research center, LID outside test-bed site. Especially, LID outside test-bed site is made of five zones which are architectural LID zone, road permeable pavement LID zone, Parking lot LID zone, industrial testing LID zone, and bioretention LID zone. The zones are completely useful for testing a diversity of LID factors including ecological wetland learning area, green-roof, ecological student rest spaces, convergence rain garden area, and environmental friendly plant area. All of the exterior LID systems are fully monitored to evaluate water quality and volume reduction. All of the monitoring results are available for viewing in real time in a dedicated room on the second floor of the center. Monitoring will occur during all rainfall events and can also be done when researchers use the rainfall simulator. The facility is designed so that the various components of LID systems can be monitored and evaluated. As an example, permeable pavement sections are made up of various layers of sand/gravel and crushed stone as well as the wearing surface itself and the monitoring results will allow researchers to see the water quality benefits which occur within each of the individual layers of the system. This research will lead to optimum design standards for these types of system. And this center conducts not only verification and certification test of GI & LID technologies but also GI & LID education, research & development and industrial cooperation (Table 2).

Figure 1. Bird's eye view(left) and photo(right) of Korea GI & LID center

Table 2. Business of Korea GI & LID center

CLASSIFICATION	BUSINESS INFORMATION
GI & LID TEST AND CERTIFICATION	· Verification/certification on performance of GI & LID technologies in hydraulic cyclem disaster prevention, soil, environment area - Architectural GI & LID zone, Road GI & LID zone, Parking lot GI & LID zone, Rain garden GI & LID zone, Bioretention GI & LID zone
GI & LID EDUCATION	· Professional education course · Student and citizen education · Support and consultant of goverment GI & LID policy
GI & LID RESEARCH AND DEVELOPMENT	· National R&D · Local government and business R&D · GI&LILD research service
GI & LID INDUSTRIAL COOPERATION	· Support of development of GI & LID technologies in business · Operation of technical seminar · Consultant on plan, design, construction and maintenance of GI & LID technologies

3.2 Outdoor facilities

The outdoor facility was designed to be pedestrian friendly with walkways throughout the site, which allows members of the public to view the various types of LID systems being evaluated. There is educational signage throughout the research facility which describes the LID systems as well as the monitoring systems. The outdoor facilities are consisted of a building type, a road type, a parking lot type, a rain garden type and a bioretention type. Indoor test facilities were ready for testing of GI & LID technologies using hydrology efficient analysis, pavement and soil analysis and water environment analysis method.

Table 3. Outdoor facilities for test of GI & LID technologies

LID ZONE	APPLIED LID TECHNOLOGIES	PHOTO
ARCHITECTURAL & BUILDING	Green roof (GR), rain distribution (RD), surface trench (ST), rain chain (RC), building planter box (BPB), rain barrel (RB), rainwater harvesting storage (RHS)	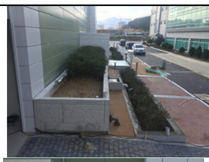
ROAD	Porous asphalt pavement (PAP), porous concrete pavement (PCP), street planter box(SPB), pervious block pavement (PB)	
PARKING LOT	Porous asphalt pavement (PAP), porous concrete pavement (PCP), pervious block pavement (PB), rainwater harvesting storage (RHS)	
RAIN GARDEN	Rain garden (RG), sand filter (SF), surface trench (ST), rainwater harvesting storage (RHS)	
BIORETENTION	Dry pond (DP), wet pond (WP), pervious block pavement (PB), rainwater harvesting storage(RHS), surface trench (ST)	

Architectural LID facility for test performances of LID technologies to manage stormwater runoff happened from building roof can be carried out performance evaluation of green roof, building planter box, rain barrel, rain chain, porous block pavement and rainwater harvesting storage. Performance evaluation is possible not only for the evaluation of each technology but also for the evaluation of a system in which several technologies are connected. Items of evaluation are effects of stormwater quantity management (volume of runoff, infiltration and

  ISSN 1562-6865 (Online) - ISSN 1063-7710 (Print)

reservation) storwmater quality (temperature, electrical conductivity, suspended solid, total phosphorus/nitrogen, heavy metal etc.). Also, connected with road LID facility, efficiency of stormwater management can be evaluated. And monitoring data of hydraulic characteristics and weather conditions (amount of rainfall, wind speed, wind direction and humidity) are transferred to integrated monitoring room in real time. Infiltration runoff is stored in stormwater tank in building after the measurement of water quality and water quality, and is used as indoor laboratory water.

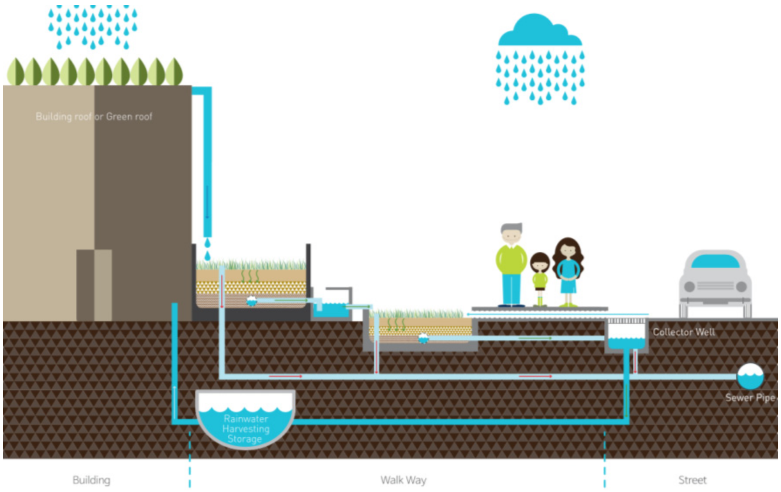

Figure 2. Cross section of architectural GI & LID facility

Parking lot GI & LID facility consists of asphalt pavement, concrete pavement, and block pavement zone. And the other one is rainwater harvesting system linked vegetative swale for the parking lot. Size of each pavement test section is 2.3m x 10.8m. Also, each section is made of concrete box type to prevent interference with other section. And, to measure quantity and quality of runoff from porous pavement, monitoring system with tipping bucket is constructed in the each section. We can measure quantity and quality of the overflow from surface of pavement and infiltration runoff by perorated pipe in sub-surface of pavement system.

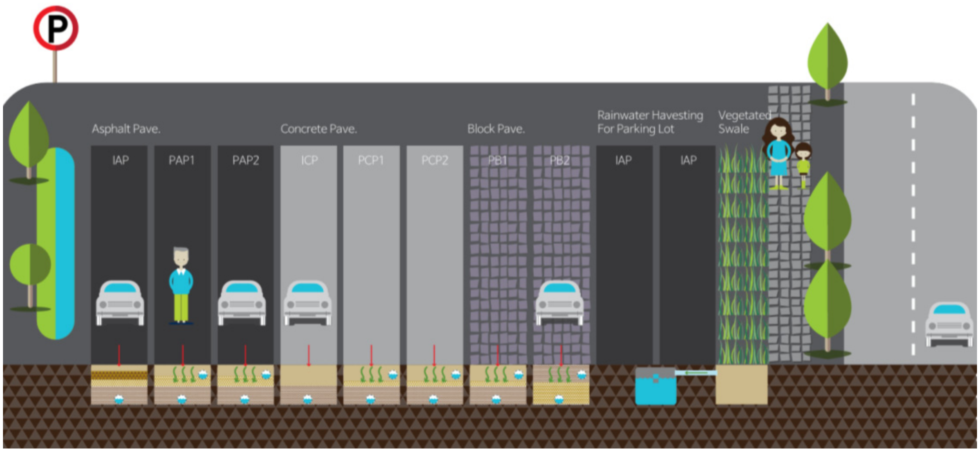

Figure 3. Image of parking lot GI&LID facility

3.3 Indoor facilities

There are LID-hydraulic test facilities, LID-Geotechnical test facilities and LID-water environmental test facilities in laboratory, Korea GI & LID center. Using these facilities, performance analysis of LID technologies can be carried out about field-scale as well as Lab-scale. Also, structure (soil and material) and disaster (like Inundation, landslide) efficiency tests of LID technology can be carried out. In case of LID-hydraulic efficiency tester, it is development a rainfall-runoff simulator could be possible to verify LID technology efficiency. Using this tester, the relation between allowable discharge range and RPM by nozzle types and verified the hydraulic cycle, such as the relation between infiltration rate, surface runoff and subsurface runoff at porous and impervious area was defined (Jang, 2014). And evaluation on hydraulic cycle efficiency of porous pavement is carrying out. LID-movable rainfall simulator has been developed to allow testing through artificial rainfall in times of no rain. This equipment is designed to allow free fall at a height of 2m, so that the actual rainfall is reproduced closely.

Table 4. Indoor facilities for test of GI & LID technologies

TITLE	DESCRIBUTION	PHOTO
LID-RUNOFF HYDRAULIC EFFICIENCY SIMULATOR	• Hydraulic efficiency and soil infiltration capacity experiment • Runoff Bed: 2,200 X 5,500 X 1,200mm • Slope: : 0~45	
LID-HYDRAULIC EFFICIENCY TESTER	• LID technologies verification experiment by artificial rain • Size : 3,000 X 3,000 X 5,000mm • Rainfall intensity : 0~200 mm/hr	
LID-SMALL MULTIPURPOSE SIMULATOR	• Small-Scale LID simulator that can experiment the character of variety samples at the same time • Runoff Plot: 300 X 500 X 50	
LID-CLOGGING TESTOR OF PAVEMENT-SOIL SYSTEM	• Evaluation of continuous permeability of porous material and product • specimen size: 40 X 40	
LID-MOVABLE RAINFALL SIMULATOR	• Self-assembly rainfall simulator • Movable rainfall simulator for Field test • Size: 2 X 2 X 12	

4 DEVELOPMENT OF INTEGRATED OPERATION MANAGEMENT SYSTEM

4.1 Development of LID Model (K-LIDM)

The existing LID modeling softwares (e.g, SWMM (Rossman, 2010), L-THIA-LID (Ahiblame et al., 2012b), SUSTAIN (Lee et al., 2012b)) are still having issues on reasonable LID simulations, such as infiltration under the unsaturated soil condition. This problem leads to deviations of simulated infiltration from the actual process (Herrada et al., 2014) and significant assumptions with regards to simulating infiltration in homogeneous soil with uniform initial moisture (Ali et al., 2016). Here, we developed a modeling software that was able to simulate and optimize bioretentions in a given watershed. The software consider three different hydrological conditions such as the followings: mitigating flood, restoring base flow, and making better hydrological properties. The Korea Low Impact Development Model (KLIDM) model is a decision-tool based on the World Wide Hydrology Model version 4 (WWHM4) (Beyerlein, 2011) and Hydrological Simulation Program – FRTRAN (HSPF) (Bicknel et al., 2001) for designing LID on a target watershed. The model can be used for a long-term simulation in order to derive practical strategies that can easily calculate the hydrologic processes of LID. KLIDM mostly consists of two parts: the watershed and LID modules. These modules calculate the hydrologic and hydraulic processes of the watershed and LID, respectively. The LID module of KLIDM can also consider water infiltration throughout the LID media under either the unsaturated or saturated soil conditions. The main goal of the KLIDM is to provide a practical solution in optimizing the LID performance in the watershed (Fig 4).

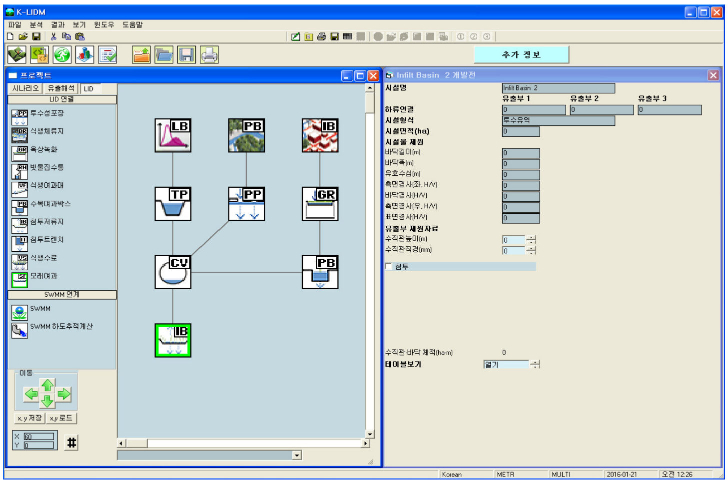

Figure 4. K-LIDM software

4.2 LID monitoring system

To control a various measured values in outdoor facilities, Korea GI & LID center, and proper monitoring system is operated by each facilities. Monitoring of water quality and water quality at each facility, groundwater level and pond water level and weather (temperature, precipitation, relative humidity and pressure) is underway. In addition, the measured monitoring is transmitted to the monitoring room in the center in real time. Therefore, not only the performance evaluation for each LID facility but also the water cycle analysis in the center complex can be performed. For example, in a parking lot LID facility, monitoring system using tipping bucket was installed to measure the flow rate of surface runoff and underground runoff, and a gauge was installed to measure the general water quality (water temperature, electrical conductivity, pH, DO). And quantity measurement of architectural LID facilities is monitored by using ultrasonic flowmeter, and water quality of infiltration runoff is measured by gauge.

Figure 5. Monitoring system for parking lot(left) and architectural (right)

4.3 LID information management system

The information management system provides an introduction to the LID technique, as well as materials on domestic and international papers, patents, and reports for LID. Also, it is configured to be able to observe real time monitoring analysis results.

Figure 6. LID information management system (information of LID model(left) and monitoring information(right))

5 CONCLUSIONS

In this study, a center equipped with indoor and outdoor verification test system to evaluate performance for LID technology and education system was developed for the first time in the world. And monitoring system, information management system and analytical model for efficient management of the center were developed and operated. Verification studies of standardized test methods for various fields such as hydrological, environmental and structural stability of LID technology are underway. Through these studies, it is expected that it will be possible to suggest the application direction of more effective LID method by inducing the selection of appropriate technology when applying the LID technique, which will contribute to the promotion of LID business in the future. It is also expected that an evaluation system, which can be used internationally, can be prepared through mutual discussion on verification method and procedures of LID technology with related foreign organizations.

ACKNOWLEDGEMENTS

This work is supported by the Korea Agency for Infrastructure Technology Advancement (KAIA) grant funded by the Ministry of Land, Infrastructure and Transport (Grant 1615009165)

REFERENCES

Ali, S., Islam, A., Mishra, P. K. & Sikka, A. K. (2016). Green-Ampt Approximations: A Comprehensive Analysis. *Journal of Hydrology*, 535, 340-355.

Ahiablame, L. M., Engel, B. A. & Chaubey, I. (2012). Representation and Evaluation of Low Impact Development Practices with L-THIA-LID: An Example for Site Planning. *Environment and Pollution*, 1(2), 1.

Beyerlein, D. (2011). Low Impact Development Computations—WWHM. *Proceedings of the World Environmental and Water Resources Congress,* 558-576.

Jang, young Su, Kim, Mi Eun, Baek, Jong Seok & Shin, Hyun Suk (2014). The Study on Development and Verification of Rainfall-Runoff Simulator for LID Technology Verification. J*. Korea Water Resourced Association*, 47(6), 513-522

Jung-min Lee, Kyung-hak, Hyun & Jong-Soo Choi. (2013). Analysis of the Impact of Low Impact Development on Runoff from A New District in Korea*. Water Science & Technology*, 68(6), 1315-1321

Lee, J. G., Selvakumar, A., Alvi, K., Riverson, J., Zhen, J. X., Shoemaker, L. & Lai, F. H. (2012). A Watershed-Scale Design Optimization Model for Stormwater Best Management Practices. *Environmental Modelling & Software*, 37, 6-18.

Herrada, M. A., Gutiérrez-Martin, A. & Montanero, J. M. (2014). Modeling Infiltration Rates in a Saturated/Unsaturated Soil Under the Free Draining Condition. *Journal of Hydrology*, 515, 10-15.

Steve Trinkaus. (2014) Research Team Leads LID Deployment in South Korea. *Stormwater Management*, 2(1), 23-25

UNESCAP. (2012). Low Carbon Green Growth Roadmap for Asia and the Pacific. *Urban Transport: policy recommendations for the development of eco-efficient infrastructures*, 16-37.

DISASTER REDUCTION CHARACTERISTICS BY A LAGOON AT THE GREAT EAST JAPAN TSUNAMI

YUTA AKASAKI[1], YOSHIYA IGARASHI[2] & NORIO TANAKA[3]

[1,2] Graduate School of Science and Engineering, Saitama University, Saitama, Japan,
[3] International Institute for Resilient Society, Saitama University, Saitama, Japan,
tanaka01@mail.saitama-u.ac.jp

ABSTRACT

Eco-system based Disaster Risk Reduction concept recommends taking advantage of the natural elements including sand dune, coastal forest, and tidal flats area like a lagoon for mitigating disasters. This study aims to clarify the tsunami mitigation effect of a lagoon on the surrounding area and the study site is selected around the Torinoumi Lagoon, which is the damaged area by the 2011 Japanese tsunami located on the southern side of the Abukumagawa River. In order to clarify the mitigation effects of the lagoon, the inundation depths around the lagoon were reproduced by numerical simulation using a two-dimensional (2D) depth averaged long-wave model, where the reduction of velocity and fluid force were analyzed. To clarify the lagoon effect on mitigating tsunami fluid force, the lagoon volume which can store the tsunami is considered an important parameter. The lagoon volume is changed by changing the land elevation height assuming with/without the lagoon. Furthermore, using a fragility curve for the house damaged by the fluid force index u^2h (u: velocity, h: water depth), the reduction of house damage probability is analyzed. The reduction of the percentage of washed out houses was more than 4 % in cross-stream direction due to the existence of lagoon in the 2011 tsunami. The tsunami fluid force index decreases around 20-40 (m^3/s^2) at maximum due to the existence of lagoon especially in the cross-shore direction, where the tsunami current from lagoon is not strong because of it getting mixed with the inundated current from seaside. Fluid force index in this area shows larger value for the same house damage probability compared to in another district. This means that the energy reduction by hydraulic jump that actually occurred behind the sand dune near the lagoon mouth is not reproduced well in the traditional 2D depth averaged equations.

Keywords: Ecosystem-based disaster reduction; energy dissipation; Hydraulic jump; fluid force; fragility curve.

1 INTRODUCTION

In response to the post-tsunami surveys on disasters such as the 2004 Indian Ocean tsunami and the 2011 Great East Japan tsunami, it has been re-recognized that natural terrain (mangrove, dunes and vegetation) can play a vital role in reducing tsunami force. After the 2004 tsunami, the elements of natural terrain, which contributes to mitigate disaster is defined as bio-shield, and the research in that field has been activated. Especially after the 2011 tsunami, United Nations (2013) proposed a concept ‘Eco-system based Disaster Risk Reduction (Eco-DRR)’, for reducing the potential risk factors. The concept has attracted attention because it addresses the mitigation through the management of environmental resources. In Japan, the concept of ‘disaster prevention and mitigation based on the natural ecosystem’ similar to Eco-DRR was also proposed by the Ministry of the Environment (Ministry of the Environment, 2015). The concept recommends taking advantage of the natural elements including not only sand dune and coastal forest but also, for example, tidal flats area aggressively (such as conservation and reproduction). Among these natural elements, there are a number of studies about the coastal forest (e.g. Dengler & Preuss, 2003; Danielsen et al., 2005; Tanaka et al., 2007; Tanaka, 2009; Thuy et al., 2009). A large lagoon, as a representative of natural structure in coastal area, is expected to mitigate disaster but little is known about its effectiveness on the tsunami-damage mitigation.

Therefore, this study aims to clarify the tsunami mitigation effect of a lagoon on the surrounding area. As for the study site, the damaged area by the 2011 Japanese tsunami around the Torinoumi Lagoon located on the southern side of the Abukumagawa River mouth in Miyagi Prefecture was selected. In order to clarify the mitigation effects of the lagoon, the inundation depth around the lagoon was reproduced by numerical simulation, and the maximum tsunami traits were compared with the 2011 situation. After the validation of the model, the reduction of velocity and fluid force were analyzed by comparing the fluid force with/without the coastal lagoon. Furthermore, using a fragility curve for house damage by the fluid force index (Onai & Tanaka, 2015), the reduction of house damage probability was analyzed.

2 MATERIALS AND METHODS

2.1 Damage situation of the study site revealed from the post-tsunami survey of the 2011 Great East Japan Tsunami

The Torinoumi Lagoon (herein after simply T-lagoon) is located on the southern side of the river mouth of the Abukumagawa River in Miyagi Prefecture, where there is an old estuary trace of the Abukumagawa River. Figure 1 shows the trace depth of the tsunami inundation of T-lagoon together with the aerial photographs before and after the Great East Japan tsunami. Tanaka et al. (2012) have reported the complex tsunami inundation pattern in the region. The tsunami made a major damage around the T-lagoon by overtopping from sand dune and embankment and entering into the mouth of the T-lagoon. In Figure 1, the houses at the right hand side of the river were washed away or destroyed. However, many houses at the northern side of the T-lagoon were not washed out but completely or partly broken; although they were around the same distance from the coastline as those on the right side. The T-lagoon has some possibility to reduce the fluid force of the tsunami toward houses. In order to clarify such situation in detail, 4 locations (Location A, B, C, and D) were selected in this study. In the Location A, there is a possibility to be directly hit by the tsunami. The Location B and D are set in the cross-stream direction where the tsunami current can be assumed to be weak. The Location C is set a little further away in the T-lagoon for comparison with the situation at Location B.

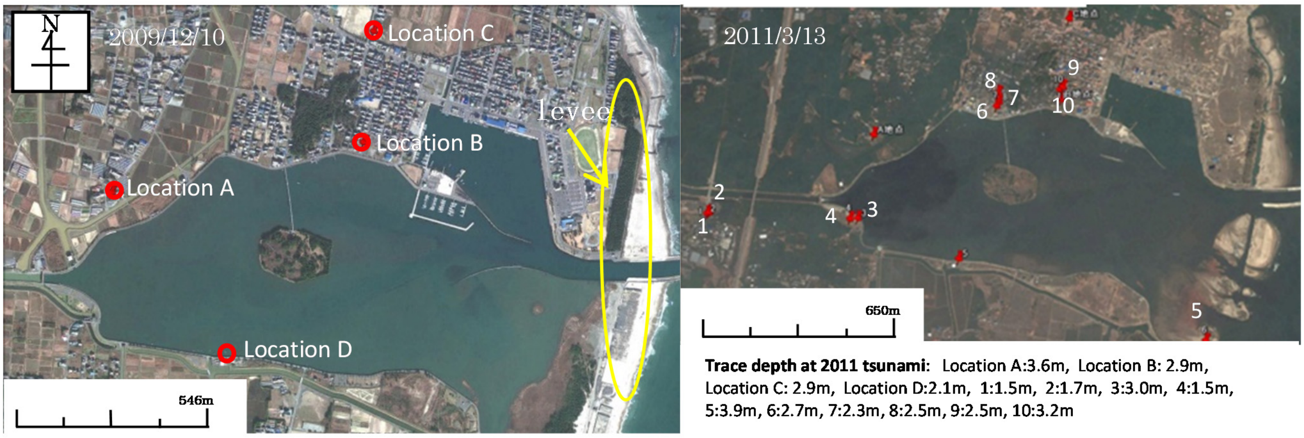

Figure 1. Aerial photos around the Torinoumi Lagoon before (left) and after (right) the 2011 tsunami (modified from Google earth).

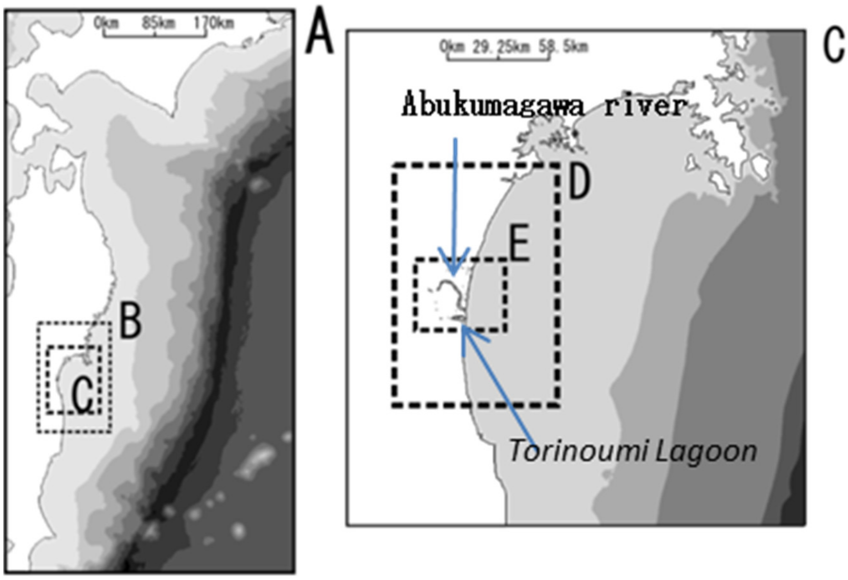

Figure 2. Definition of grid system. A: linear long-wave equations are used, B-D: non-linear long-wave equations are used. E: non-linear long-wave equations with an SDS turbulence model (Nadaoka and Yagi,1998; Thuy et al.,2009) are used.

2.2 Numerical simulation method

Numerical simulation of tsunami was conducted using the model developed by Tanaka and Sato (2015). To calculate the tsunami propagation, five regions (Figure 2) with different grid sizes were set. In this study, the grid sizes of regions A, B, C, D, and E were set to 1350 m, 450 m, 150 m, 50 m, and 16.7 m, respectively. The simulated values of a larger region were applied as a boundary condition to the next smallest region (nesting method). The linear and non-linear long-wave equations were applied to Region A and Regions B–E, respectively. At the coast line, a perfect reflection boundary was applied in Regions A–D, and inundation was calculated for only Region E.

The two-dimensional nonlinear long-wave equations (continuity equation: Eq.(1), momentum equations: Eqs.(2)–(4)) are:

$$\frac{\partial \zeta}{\partial t}+\frac{\partial (hV_x)}{\partial x}+\frac{\partial (hV_y)}{\partial y}=0 \quad [1]$$

$$\frac{\partial V_x}{\partial t}+f_A\left(V_x\frac{\partial V_x}{\partial x}+V_y\frac{\partial V_x}{\partial y}\right)+g\frac{\partial \zeta}{\partial x}+f_A\left(\frac{\tau_{bx}}{\rho h}\right)+f_E\left(\frac{\sum_{i=1}^{2}F_{x,i}}{\rho h}-\frac{E_{Vx}}{h}\right)=0 \quad [2]$$

$$\frac{\partial V_y}{\partial t}+f_A\left(V_x\frac{\partial V_y}{\partial x}+V_y\frac{\partial V_y}{\partial y}\right)+g\frac{\partial \zeta}{\partial y}+f_A\left(\frac{\tau_{by}}{\rho h}\right)+f_E\left(\frac{\sum_{i=1}^{2}F_{y,i}}{\rho h}-\frac{E_{Vy}}{h}\right)=0 \quad [3]$$

$$\left(F_{x,i},F_{y,i}\right)=\gamma_i\frac{1}{2}\rho C_{Di}A\times\left(V_x\sqrt{V_x{}^2+V_y{}^2},\,V_y\sqrt{V_x{}^2+V_y{}^2}\right) \quad [4]$$

Where, x and y are the horizontal coordinated in two direction. V_x and V_y are the depth-averaged velocity components in *x* and *y* directions, respectively. *t* is the time. *h* is the total water depth ($h = h_0 + \zeta$); h_0 is the local still water depth (on land, the negative height of the ground surface) and ζ is the water surface elevation. *g* the gravitational acceleration. $F_{x,i}$ and $F_{y,i}$ are the drag forces in *x* and *y* directions respectively and $C_{D\,i}$ is the drag coefficient (*i*= 1, 2, means obstacles, i.e. tree, house, respectively). ρ is the fluid density, *A* is the projected area of an obstacle in the water. E_{Vx} and E_{Vy} are the viscosity in *x* and *y* directions, respectively. τ_{bx} and τ_{by} are bottom face shear force in *x* and *y* directions. A manning roughness coefficient is *n*. Calculation methods of E_{Vx} and E_{Vy} are shown by Tanaka & Sato (2015). Fault displacement is given as the initial water level of the tsunami, and its displacement is given as the water level displacement of sea area on the vertical. Tanaka and Sato (2015) methods were used after adjusting the fault parameter of Fujii and Satake (2011) (the fault parameters between the Abukumagawa River and T-lagoon). As already explained, suitable differential equations were applied according to the calculated region. Thus, different coefficients of f_A and f_D in Eqs. (2) and (3) were used, i.e., $f_A = f_D = 0$ for Region A (linear model), $f_A = 1$, $f_D = 0$ for Regions B–D (non-linear model without turbulence), and $f_A = f_D = 1$ for Region E (non-linear model with SDS (the sub-depth scale) turbulence).

In order to clarify the lagoon effect on mitigating tsunami fluid force, the lagoon volume which can store the tsunami is considered an important parameter. Therefore, in this study the lagoon volume is changed by changing the land elevation height. The ground elevation of Torinoumi is set as follows: 1) Case1: 1 m (for comparison with the actual case (Case 2)) and 2) Case2: -2 m (actual). For Case 2, tsunami simulation model was validated for the 2011 Great East Japan tsunami and the model was applied to Case 1. In the present study, the initial water depth exists below ground elevation 0 m in the lagoon in Case 2.

3 RESULTS AND DISCUSSIONS

3.1 Validation of the reproduction of the 2011 Great East Japan tsunami

Trace water depths by post-tsunami survey simulated maximum inundation depths around T-lagoon as shown in Figure 3. The fault parameter (Fujii & Satake, 2011) was slightly modified and validated for the damage situation around the river mouth of the Abukumagawa River by Tanaka and Sato (2015). The study site was very close to that in our study, and hence the same parameters were used in this study. The simulated values are a little larger than the trace depths. This numerical analysis model does not include the changes of drag coefficient based on the destruction of houses. Thus, the simulated maximum inundation depth was evaluated larger of about ten percent. However, the simulation reproduced the situation of the 2011 Great East Japan tsunami quite well.

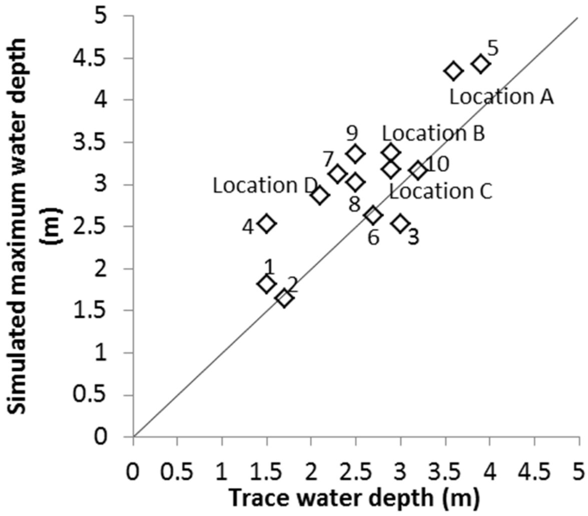

Figure 3. Comparison between trace depths by post-tsunami survey and simulated maximum inundation depths around T-lagoon

3.2 Differences of the effect of storage amount of the lagoon on tsunami mitigation at different locations

To compare the differences of the tsunami inundation situation in Case 1 and 2, the time series of calculated inundation depth at location A and B are shown in Fig.4 (a) and (b) respectively. Fig 4(a) shows that the first wave and second wave of tsunami arrived at Location A around 4,000 and 5,400 seconds after fault motion, respectively. In addition, the tsunami arrival time in Case 2 is faster than that in Case 1 because the resistance of ground surface is smaller due to the existence of water and high velocity in the T-lagoon in Case 2. At Location A, time series of inundation depth between Case 1 and Case 2 are not changed much. Fig 4(b) shows that the first wave and second wave of the tsunami arrived at Location B around 3,900 and 5,400 seconds after fault motion, respectively. In addition, arrival time of maximum inundation depth is 200 seconds slower in Case 2 than in Case 1 at Location B, although the arrival time of first wave in Case 1 and Case 2 at Location B are not changed much as Location A. This is because not all of the tsunami current passes through the lagoon at Location B where part of tsunami comes from the landward side and gets mixed there.

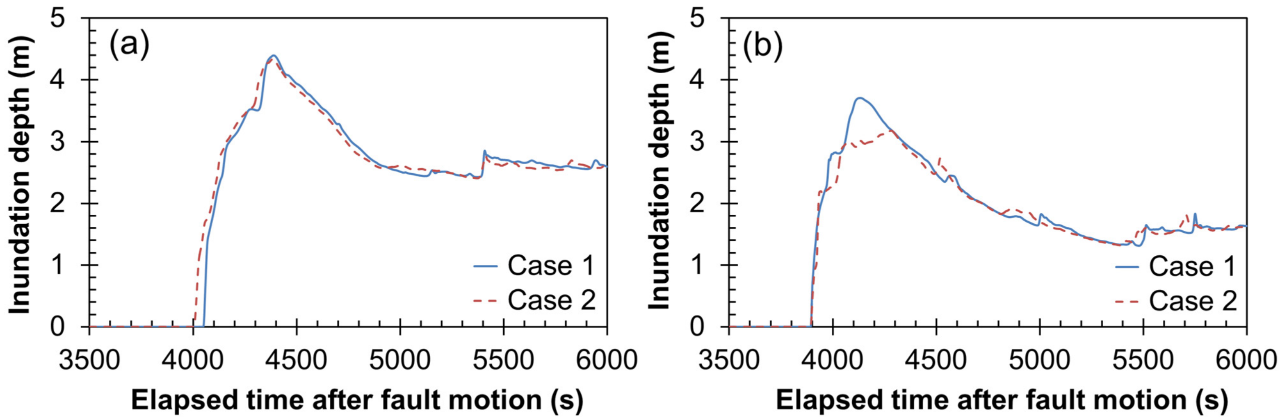

Figure 4. Time series of calculated inundation depth for Case 1 and Case 2 ((a): Location A, (b): Location B)

In order to further compare the difference of tsunami inundation situation between Case 1 and Case 2, the time series of calculated velocity at Location A and B are shown in Fig. 5(a) and (b), respectively. In Fig 5 (a), the maximum velocity at Location A in Case 2 is slower than that in Case 1, but the difference is small and similar to that in Fig 4(a). In addition, Fig. 5 (b) shows that the flow velocity at Location B at about 700 s after the first wave arrival has reduced considerably in Case 2 compared to the velocity in Case 1. There is a possibility that an effective zone may exist for the tsunami damping effect of the lagoon, depending on which side of the lagoon it is adjacent to, such as Location A and Location B.

  / ISSN 1562-6865 (Online) - ISSN 1063-7710 (Print)

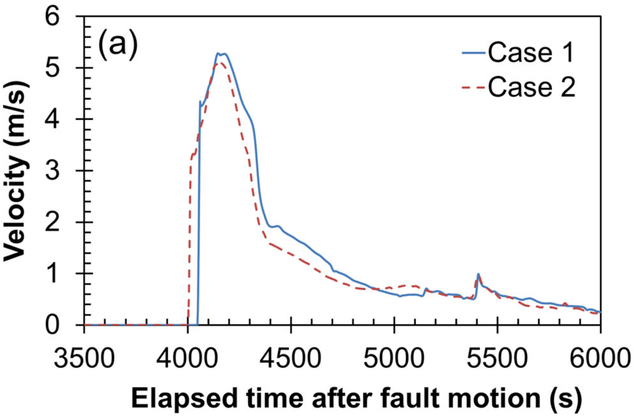

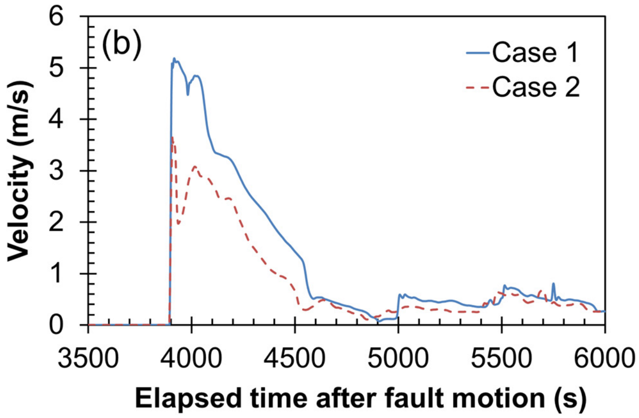

Figure 5. Time series of calculated velocity for Case 1 and Case 2 ((a): Location A, (b): Location B)

Table 1 shows maximum inundation depths, maximum flow velocities and maximum fluid forces at the Great East Japan tsunami for Case 1 and Case 2, where the storage volume of the lagoon was changed. At Location A and C, maximum inundation depths and maximum flow velocities are not changed much due to the storage amount of the lagoon. At Location B, maximum inundation depth in Case 2 is 0.6m lower than that in Case 1. Although the effect of the storage volume of the lagoon is not sufficient, maximum flow velocity in Case 2 is reduced to around 30% from Case 1 at Location B. Similarly, the velocity decreases at Location D. As a result, the fluid force index defined as u^2h decreases around 42 and 22 m^3/s^2 at Location B and Location D, respectively. Overflowing tsunami velocity from lagoons at Location B and Location D is low because it is in the lateral side of the tsunami direction. The tsunami current velocity was reduced by mixing the flow from the T-lagoon and from landside which had over-flown from sea embankment.

Table 1. Maximum inundation depths, maximum flow velocities and maximum fluid forces at Location A-D for Case1 and 2.

	Location A		Location B		Location C		Location D	
	Case 1	Case 2	Case 1	Case 2	Case 1	Case 2	Case 1	Case 2
maximum water depth (m)	4.40	4.34	3.71	3.18	3.47	3.37	2.98	2.86
maximum velocity (m/s)	5.28	5.09	5.19	3.65	6.88	6.87	4.59	3.33
maximum fluid force index(m^3/s^2)	84.2	78.2	66.3	24.6	99.3	99.2	44.3	21.6

For analyzing the house damage, it is necessary to determine the dominant parameter; the fluid force index (u^2h) or the moment index (u^2h^2) by fluid force which changes with Froude number (Tanaka et al., 2014). Table 2 shows the Froude number when the inundation depth, fluid force and the moment by Froude force were maximum. For most of the locations and cases, Froude numbers at the maximum condition exceeds the values, 0.8 (Tanaka et al., 2014) and 0.52 (Onai & Tanaka, 2015), where fluid force index can be applied. Therefore, this study selected the fluid force index for further analysis.

Table 2. Froude number and inundation depths at which tsunami characteristic values take the maximum for Location A-D and Case 1 and 2

		maximum inundation depth		maximum fluid force index		maximum moment index	
		inundation depth(m)	Froude number	inundation depth(m)	Froude number	inundation depth(m)	Froude number
A	Case1	4.40	0.30	3.04	0.96	3.06	0.95
	Case2	4.34	0.25	3.04	0.93	3.19	0.88
B	Case1	3.71	0.55	2.82	0.92	2.82	0.92
	Case2	3.18	0.29	2.97	0.53	3.00	0.53
C	Case1	3.47	0.71	3.00	1.06	3.07	1.03
	Case2	3.37	0.75	2.58	1.24	3.19	0.94
D	Case1	2.98	0.62	2.61	0.81	2.78	0.75
	Case2	2.86	0.47	2.80	0.53	2.82	0.53

3.3 Distribution of the probability of washed out houses

As tsunami mitigation affects appear in a wide area, the damaged probability of houses calculated by a fragility curve becomes a very useful tool for clarifying the effect (Tanaka & Onai, 2017). Figure 6 shows the distribution of differences of the probability of washed out houses from Case 1 to Case 2 for the Great East Japan tsunami. Fragility curve derived near this district (Onai & Tanaka, 2015) was used for calculating the probability for washing out houses. The differences of the probability for the washout at northern and southern side of the lagoon are larger than other locations. In particular, the difference in northern side is large because of the mixing of the tsunami current from lagoon (south direction) and seaward (east direction). This is because of the complex shape of the lagoon.

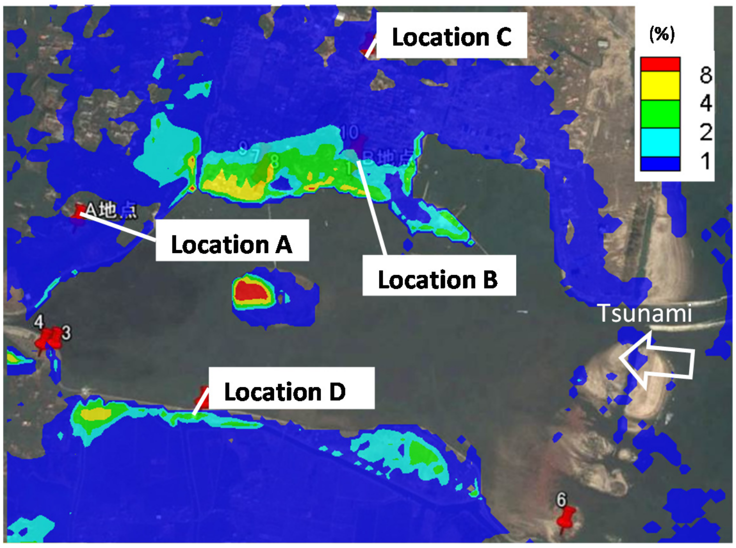

Figure 6. Distribution of difference of the probability from Case 1 to Case 2 for washing out houses at the Great East Japan tsunami (modified from Google earth)

3.4 Relationship between fluid force index and the probability for washing out houses in this area

Fig. 7(a) and 7(b) show the maximum fluid force index in the area of Case 1 and 2 respectively. In Case 2, the maximum fluid force index was 78.2, 24.6 and 99.2 (m^3/s^2) at around Location A, B and C respectively. In this case, the probability of washout houses is 100, 98.2 and 100 % by fragility curves of Koshimura et al. (2009) as shown in Fig 8. Using the Fragility curve of Onai & Tanaka (2015), damage probability of Location A, B and C are 99.8, 76.6 and 100%, respectively. However, the actual probability for washing out houses obtained by comparing the aerial photographs before and after the tsunami was 71, 0 and 40% at around Location A, B and C respectively. This study can show the energy loss differences among the locations mainly by the velocity difference from the T-lagoon and seaside. However, the actual energy loss can be expected to be large in the T-lagoon due to hydraulic jump and the tsunami colliding with bottom of lagoon because it has around 2-3m seaside dune near the lagoon mouth. Therefore, the maximum fluid force index around the T-lagoon can be actually decreased. However, two-dimensional numerical simulation cannot be reproduced by these effects. Further modelling is needed for fully discussing the lagoon effect quantitatively.

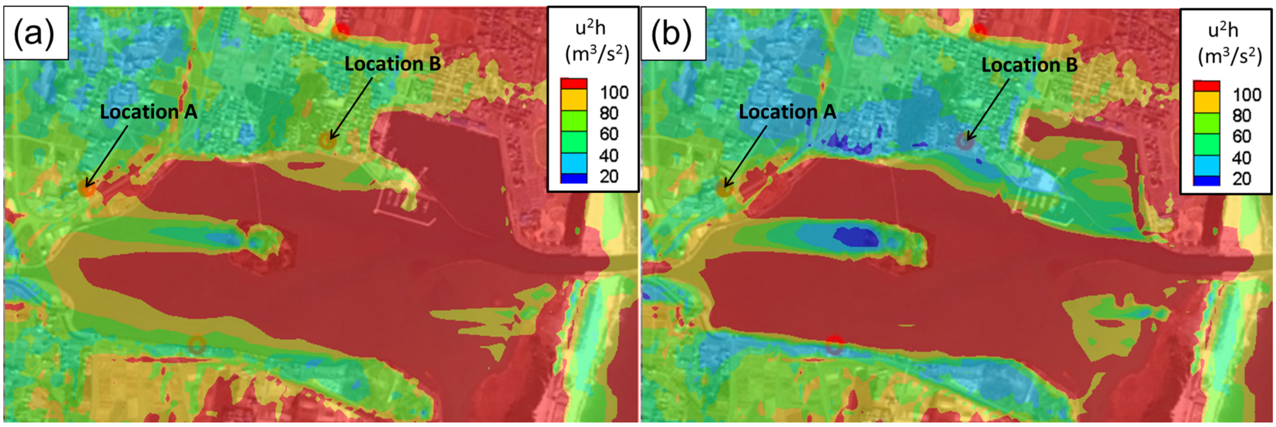

Figure 7. The maximum fluid force index (m^3/s^2) around the T-lagoon (modified from Google earth), (a): Case 1, (b): Case 2

  / ISSN 1562-6865 (Online) - ISSN 1063-7710 (Print)

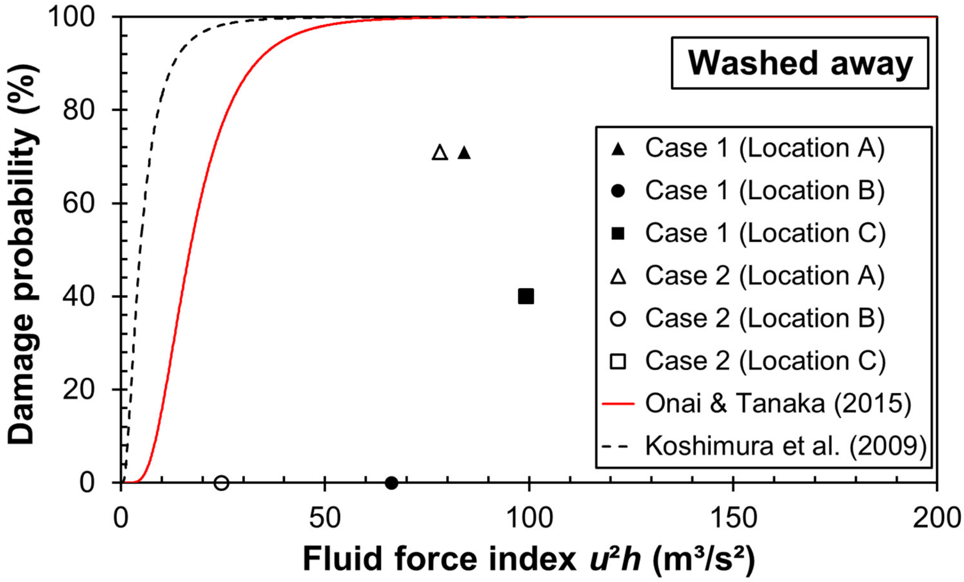

Figure 8. Distribution of difference of the probability from Case 1 to Case 2 for washing out houses at the Great East Japan tsunami in comparison with the previous studies in other district

4 CONCLUSIONS

1) The tsunami fluid force index u^2h decreases around 20-40 (m^3/s^2) in maximum due to the existence of the lagoon especially in the cross current direction, where the tsunami current from lagoon is not strong because of it getting mixed with the inundated current from seaside overflown from embankment.

2) Fluid force index calculated in this area by two-dimensional depth averaged equations show larger value for the same house damage probability than those in previous studies. This means the energy reduction by hydraulic jump actually occurred behind the sand dune near the lagoon mouth which is not reproduced well in traditional two-dimensional depth averaged equations.

ACKNOWLEDGEMENTS

This study was funded by a JSPS Grant-in-Aid for Scientific Research (No. 15H02987).

REFERENCES

Fujii, Y., & Satake, K. (2011). Tsunami Source of The Off Tohoku-Pacific Earthquake on March 11, 2011. *Web site: http://iisee. kenken. go. jp/staff/fujii/OffTohokuPacific2011/tsunami_inv. html*.

CNRD-PEDRR (2013). Disasters, Environment and Risk Reduction – Eco-DRR Master's Module, Instructor's Manual', Cologne and Geneva: Center for Natural Resources and Development, Partnership on Environment and Disaster Risk Reduction. http://www.unep.org/disastersandconflicts/portals/155/dnc/docs /drr_training/Eco-DRR%20InstructorManualApril2013.pdf

Danielsen, F., Sorensen, M.K., Olwig, M.F., Selvam, V., Parish, F., Burgess,N.D., Hiraishi, T., Karunagaran, V.M., Rasmussen, M.S., Hansen, L.B.,Quarto, A. & Suryadiputra. N. (2005). The Asian tsunami: A protective role for coastal vegetation, *Science*, 320(5748), 643.

Dengler, L. & Preuss, J. (2003). Mitigation lessons from the July 17, 1998 Papua New Guinea tsunami, *Pure ApplGeophys*, 160, 2001–2031.

Koshimura, S., Oie, T., Yanagisawa, H. & Imamura, F. (2009). Developing Fragility Functions for Tsunami Damage Estimation Using Numerical Model and Post-Tsunami Data from Banda Aceh, Indonesia, *Coastal Engineering Journal*, 51(3), 243–273.

Ministry of the Environment. (2015). Annual Report on the Environment, The Sound Material-Cycle Society and Biodiversity in Japan, http://www.env.go.jp/en/wpaper/

Nadaoka, K. & Yagi, H. (1998). Shallow-Water Turbulence Modeling and Horizontal Large-Eddy Computation of River Flow, *Journal of Hydraulic Engineering*, 124(5), 493-500.

Onai, A. & Tanaka, N. (2015). Numerical Analysis Considering the Effect of Trapping the Float Age by Coastal Forests and Fragility Curve by Houses (In Japanese With English Abstract), *Journal of Japan Society of Civil Engineers*, Ser. B1 (Hydraulic Engineering), 71(4), I_727-I_732.

Tanaka, N. (2009). Vegetation Bioshields For Tsunami Mitigation: Review of Effectiveness, Limitations, Construction, and Sustainable Management, *Landscape and Ecological Engineering*, 5(1), 71-79.

Tanaka, N. & Sato, M. (2015). Scoured Depth and Length of Pools and Ditches Generated by Overtopping Flow from Embankments During The 2011 Great East Japan Tsunami, *Ocean Engineering*, 109, 72-82.

Tanaka, N., & Onai, A. (2017). Mitigation of Destructive Fluid Force on Buildings Due to Trapping of Floating Debris by Coastal Forest During the Great East Japan Tsunami. *Landscape and Ecological Engineering*, 13(1), 131-144.

Tanaka, N., Sasaki, Y., Mowjood M.I.M. & Jinadasa, K.B.S.N. (2007). Coastal Vegetation Structures and Their Functions in Tsunami Protection: Experience of The Recent Indian Ocean Tsunami, *Landscape and Ecological Engineering*, 3, 33-45.

Tanaka, N., Yagisawa, J., & Yasuda, S. (2012). Characteristics of Damage Due to Tsunami Propagation in River Channels and Overflow of Their Embankments in Great East Japan Earthquake. *International journal of river basin management*, 10(3), 269-279.

Tanaka, N., Yasuda, S., Iimura, K. & Yagisawa, J. (2014). Comparison of The Effects of Coastal Forest and Those of Sea Embankment on Reducing the Washout Region of Houses in The Tsunami Caused by The Great East Japan Earthquake, *Journal of Hydro-environmental Research*,*8*, 270-280.

Thuy, N.B., Tanimoto, K., Tanaka, N., Harada, K. & Iimura, K. (2009). Effect of Open Gap in Coastal Forest on Tsunami Run-Up - Investigations by Experiment and Numerical Simulation, *Ocean Engineering*, 36, 1258-1269.

FLOOD CONTROL MANAGEMENT IN STEEP RIVERS USING DIKES

OMAR SELEEM[1], AKIHIRO KADOTA[2] & ITANI DALE NDWAMBI[3]

[1,2,3] Ehime University, Matsuyama, Japan,
omar_abdelwahab92@yahoo.com; akado@cee.ehime-u.ac.jp; itanidalendwambi@gmail.com

ABSTRACT

Shigenobu River is located at North West of Shikoku Island in Japan. Shikoku Island is the smallest island of the four main islands in Japan. The River passes through Matsuyama city, the city area with roughly 428.86 km^2 of area and the city population is about 516,459 capita in December 2014. Shigenobu River length is 36 km, the river watershed area is approximately 445 km^2. Shigenobu River is considered short and steep. Due to river properties, many floods have occurred in the past which caused several damages to public and private properties. In order to protect human life, public and private properties from river flooding, nine dikes have been constructed in the last 300 years. The main purpose of constructing these dikes is to reduce the flow discharge and decrease downstream water depth. Construction of concrete structure along the river is to control the flood from terribly affecting the river ecosystem. The aim of this study is to analysis the effect of existing dikes at Shigenobu River from the point of flood control and to recommend using green infrastructures in order to restore the river ecosystem. Dike is analyzed for the shape, length and transition of inundation areas by using field measurement data and result of flood inundation analysis in order to get the most proper shape and dimensions.

Keywords: Flood mitigation; Steep River; dikes; open levees.

1 INTRODUCTION

In recent years, due to the effect of global warming, Japan is being effected with the global warming by increase in temperature and occurrence of many massive typhoons and torrential rains as Japan consists of Islands. Also, due to the increase in population the land use map is changing, and river watershed is urbanized. So, the probability of occurrence of damage due to natural disaster such as flood, typhoon and tsunami is increasing.

Climate change affect the river ecosystem as it affects the animals and plants living in fresh water such as ponds, lakes and rivers, changing their properties and bring diseases as displacement of cold water species, formation of dead zones, effect on fish reproduction, stress on plants, and diseases from mixing flood water with sewer system.

Shigenobu River is located in Matsuyama city at north-west side of Shikoku Island in Japan. Shigenobu River characteristics are very steep and short in length. Therefore, the several disasters of floods have been occurred in the form of massive flooding. As a countermeasure for the flooding, nine dikes have been constructed in the last 300 years in order to control the flood by reducing the flood discharge and flow depth at the river downstream. The current study focuses on the effect of existing dikes on the Shigenobu River. Dike is analyzed for the shape, length and transition of inundation areas by using field measurement data and result of flood inundation analysis in order to get the most proper shape and dimensions.

The nine dikes constructed on Shigenobu River affect the river ecology. As the world now is going to green infrastructures in order to protect the environment and decrease the amount of CO2 in the atmosphere, this study support replacing the existing dikes with green walls like the one used to restore the Thames River ecology in London.

The studied dike is located at 8.3 km from the river moth which is named 'IDO GASUMI' as shown in Figure 1. The dike has been constructed by historical flood control system. The dike consists of discontinuous dual embankments and aperture, so that the dike has effects of delaying flow and retuning of flooding. Therefore, these effects protect flood inundation disaster at downstream side of the river.

However, the area around 'IDO GASUMI' dike has natural ground elevation lower than flood water level. So, in case of occurring flood humans, buildings, roads, and farmlands will suffer from flood. In recent years, the study is urbanized, so that the frequency of occurring of flood disaster is increasing.

So, in order to protect human lives, private and public property, it is necessary to have maintenance to the existing dike. Currently, the Ministry of Land, Infrastructure and Transport, Matsuyama River National Highway Office, has attracted attention and are planning to make maintenance work.

After executing the maintenance work, estimating the effect of the maintenance work can be done by developing flood simulation. Then, it is probable to construct effective dike in order to secure human life and control the flood plain. Therefore, the current study produces the flood discharge and flood plain at the peak water discharge by two-dimensional shallow flow analysis and analysis the flood plain after the maintenance work. The result will be effective for river management and planning in term of maintenance work. Furthermore, it is also helpful for creating hazard map of evacuation routes by using the results for time variation of flood plain areas.

Several previous studies have been done. As its pioneering research, Iwasa et al. (1980), studied two-dimensional flood analysis using a two-dimensional unsteady flow model for flood water in the protected inland. In addition, simulating the behavior of flood flow in case of the Uji River dike break, codified empirical analysis technique also performs calculations drainage and embankment is also taken into consideration. In addition, Iwasa et al. (1980), have set the roughness coefficient for the land use of the floodplain.

There are some advanced studies for the flood management. A typical study has been done by Kawanaka, et al. (2012). They performed flood analysis for flood for Typhoon No.13 at 1953.

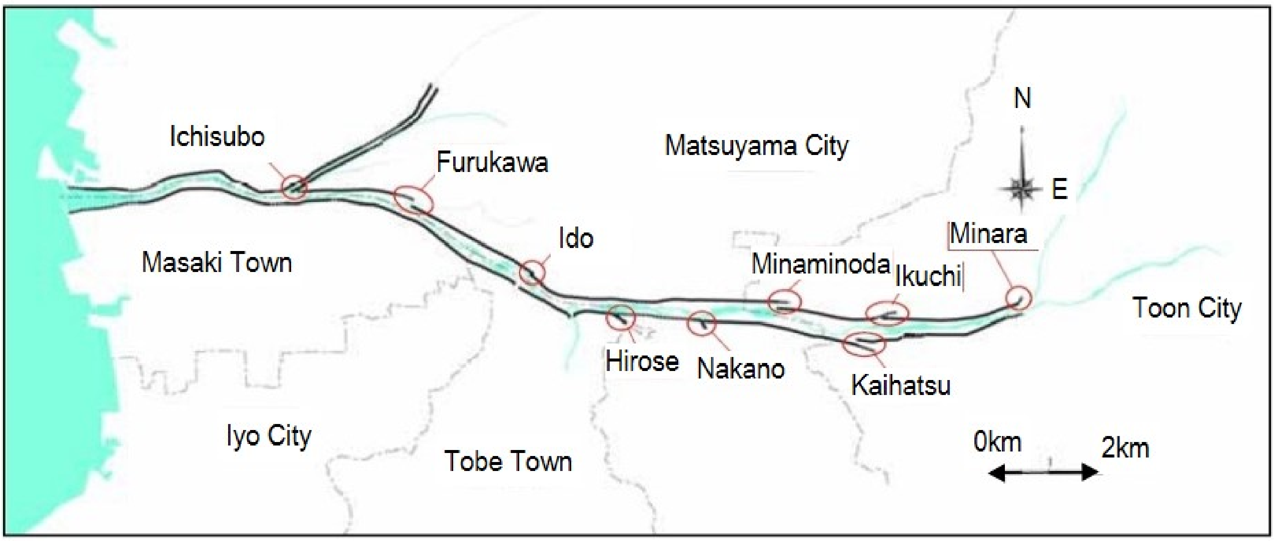

Figure 1. Location of The Nine Dikes Along The Shigenobu River.

The study area is located at Yura river basin in Fukuchiyama city of Kyoto Prefecture, Japan. An evacuation difficulty index is valued by using the unit width ratio force and examined the conventional hazard map to compare the hazard map that takes into account the evacuation start time unit width ratio force, more detail evacuation plan was publicized.

In addition, Uno et al. (2010) accomplished the flood analysis by two-dimensional plane flood simulation. The objective was to study typhoon No.9 that hit northwest area of the Hyogo Prefecture in the early morning of August 9, 2009. The flood characteristics was obtained by using results of field survey and numerical simulation. Kobayashi et al. (2012) accomplished simulation and represented the heavy rain disaster in Sayo river basin of Hyogo Prefecture, Japan and flooding phenomenon that occurred on August 9 to 10, 2009. Based on the estimated flood depth, they valued the economic damage of agricultural land and buildings. The assumption of damage amount, the damage rate corresponding to flood depth of farmland and buildings was used, assuming the amount of damage by the "area per building valuation × area × damage rate" for the building, "area to be estimated was the amount of damage each by crop yield × unit weight per crop price × area × damage rate " for farmland. Tanaka et al. (2011) developed river morphology based on the historical article in the rivers before the flood control project initiates. They developed a numerical simulation for the flood plain after the excavation of Toyohira new waterway, and also produce a comparison of the flooding area. Nays2D flood is used to make the simulation. In order to discuss result of the comparison, the effect of past flood control projects were evaluated. As described in the above studies, flood risk management is developing. However, reliability of the analysis results is necessary. In this study verification of reproducibility for analysis results on current bed profile, to get a flood analysis result of the assumed accurate construction.

2 OVERVIEW ON THE EXISTING DIKES

Along Shigenobu River, nine historical dikes have been assembled in the last 300 years to control the flood plain by reducing the flood peak discharge and reduce the downstream flood depth, as mentioned before. The dike consists of discontinuous dual embankments and aperture.

There are two main effects for the dike. The first effect is called “retarding effect”, which means by flowing into the basins to allow water to escape from main river channel, it is efficient to decrease the water discharge flowing in the river. So, in case of flood by embankment destroying, we are avoiding the occurrence of disastrous damage.

  / ISSN 1562-6865 (Online) - ISSN 1063-7710 (Print)

The second effect is called “flooding back effect”. When the embankment at upstream side is breached, the dike is effective to attract water flooded from city to levee opening. The location of the constructed nine open levees along Shigenobu River are shown in Figure 1.

As the natural ground elevation of Matsuyama plain is lower than the river bed level in middle and downstream sections of the Shigenobu River (i.e. around Ichitsubo, Furukawa, Ido, Hirose, Nakano). Therefore, when peak discharge occurs, flooding from the opening of the levee occurs, and the risk of occurrence of flood damage is high.

Among them, The Ido open levee is very important as it is located near Matsuyama Highway as shown in Figure 2. Area surrounding the dike is changing rapidly from farming fields to residential buildings. Based on field survey done by Matsuyama office of Land, Infrastructure and Transport, the Ido open levee is assumed extremely dangerous as the ground level is lower than the expected flood water level, so in cause of flood occurring at this area roads, houses and administrative buildings will be in flood risk. So flood analysis at this location is necessary as there is danger on human life, public and private property. The Ido open levee is planned to have renovation by extending the one embankment at downstream.

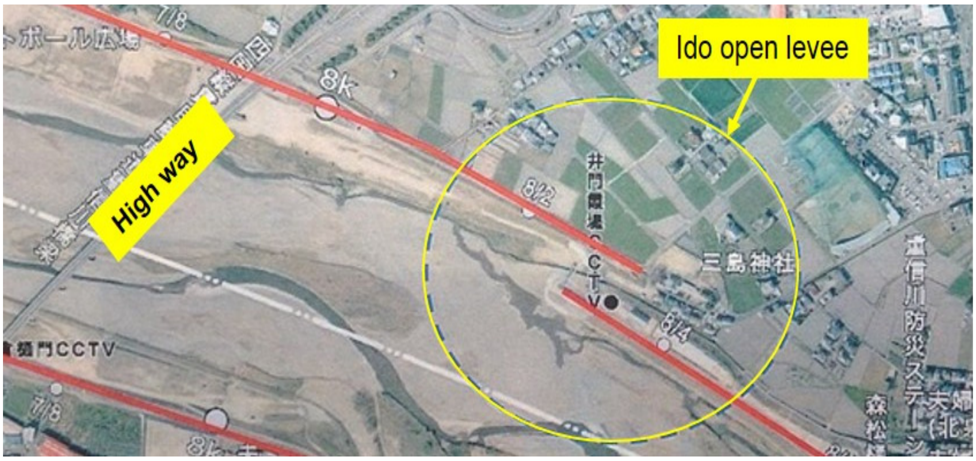

Figure 2. Area Around Ido Open Levees .

3 FLOOD ANALYSIS AROUND IDO DIKE

3.1 Overview About Flood Analysis

In the current study, by assuming occurrence of flood due to peak flow discharge in Shigenobu River, flood risk management based on shallow two-dimensional flow (iRIC Nays2D Flood) is accompanied around the opening of Ido open levee. Then, the result for time variation of flood was analyzed. Afterward, the area effected by flood and the flood water depth were varied by examining different length for the dike.

The results were analyzed and compared to be used in verification of reliable flood hazard map done by Matsuyama city office. This hazard map take into consideration the maintenance condition of Shigenobu River channel with the peak flood discharge in the river. In this analysis, existing river bed profile was used for integrity check of the analysis. When changing the dike length, modification of level height was adjusted on the extended open levee.

3.2 Arrangement of Morphological Data

In order to do flood analysis, firstly, the data should be obtained. Ground elevation data around the dike DEM (Digital Elevation Model) data (5 m cell size) which was obtained from “Geospatial Information Authority of Japan”. The Manning’s roughness coefficients were estimated at the areas of flood plain, main channel, vegetation area, landside and road independently. In addition, the length of examined dike was changed from 100 m to 300 m. Figure 3 shows the arranged bed profile applicable for the numerical simulation for flood analysis.

3.3 Flood Analysis Using Existing River Bed Profile

The numerical mesh around the Ido dike is shown in Figure 3. As shown in the figure, the upstream inflow and the downstream outflow were estimated. The computational mesh cell size is of 10m. The number of cells is 100 in stream-wise and span-wise directions, respectively. Computational time interval is 60 sec and flood discharge was calculated for time variation of rainfall in order to obtain peak discharge of 2600 m^3/sec. The rainfall data was reasonably obtained from Japan Meteorological Agency. In the current analysis, maximum rainfall in recent data was analyzed and data for two days from 30th to 31st August 2012 were chosen to calculate the discharge data. The discharge time series (hydrograph) is shown in Figure 4. Then, roughness coefficient was set on each grid. The results of the analysis were compared with the hazard map and was used to verify the integrity.

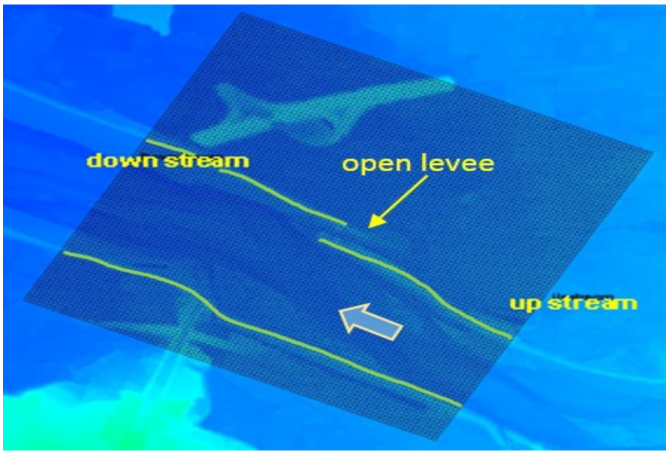

Figure 3. Mesh Around The Ido Dike for Flood Analysis.

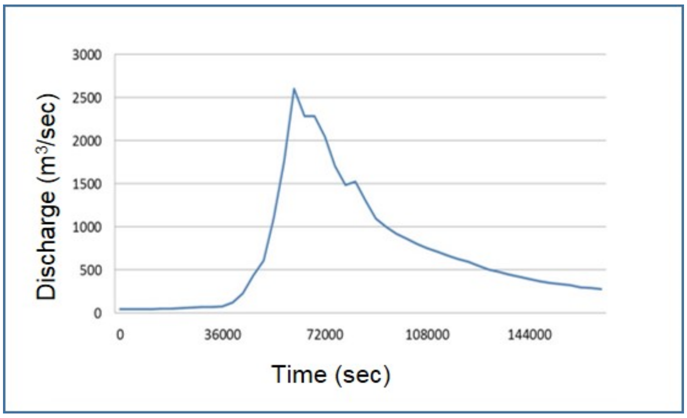

Figure 4. Flow Hydrograph.

3.4 Flood Simulation at Extended Dike

As countermeasure of flooding, extending dike is planned by Ministry of Land, Infrastructure and Transport. The current study analyzed the extension of the dike at downstream in order to get proper dike length. In addition, the ground roughness was also set as the same value as dike surface. The simulation was performed under dike length of 100 m, 200 m and 300 m, respectively.

3.5 Roughness Coefficient for River Channel and Surrounding Area

Roughness coefficients of the river channel and the surrounding urban area around the river were applied to the roughness coefficient which was received from Ministry of Land, Infrastructure and Transport. So, the roughness values were set to be 0.035 for the dry weather flow river channel, 0.05 for the flood plain, and 0.08 for the vegetation area. In addition, roughness at inland was determined from the roughness coefficient setting method proposed by the Ministry

The above-mentioned method for estimating the roughness coefficient was used to examine the area occupied by each land use in each mesh cell. The land use were categorized from A1 to A3. Buildings and farmland were considered as A1, roads and sidewalk were considered as A2 and others were A3, i.e. farmland means paddy, vineyards, orchards, etc. Wasteland, lawn, wetlands, etc. were considered as other land use. Ground roughness coefficient of non-building calculated from the below weighted average Equation (1).

$$n_o^2 = \frac{n_1^2 A_1 + n_2^2 A_2 + n_3^2 A_3}{A_1 + A_2 + A_3} \qquad [1]$$

where,

$$n^2 = n_0^2 + 0.020 \times \frac{\theta}{100-\theta} \times h^{4/3} \qquad [2]$$

By applying Equation (2) to estimate the roughness coefficient we get that n_1=0.060, n_2=0.047, n_3=0.050. Where, θ: building occupancy, h: water depth. In this flood management analysis, the bed level is higher than the land ground elevation, which make the flow is slightly effected by roughness difference between road and inland, so this study considers roughness coefficient, which is estimated, as same as building n_1 for inland and n_2 for road.

According to these procedure, estimated roughness coefficients are shown in Figure 5.

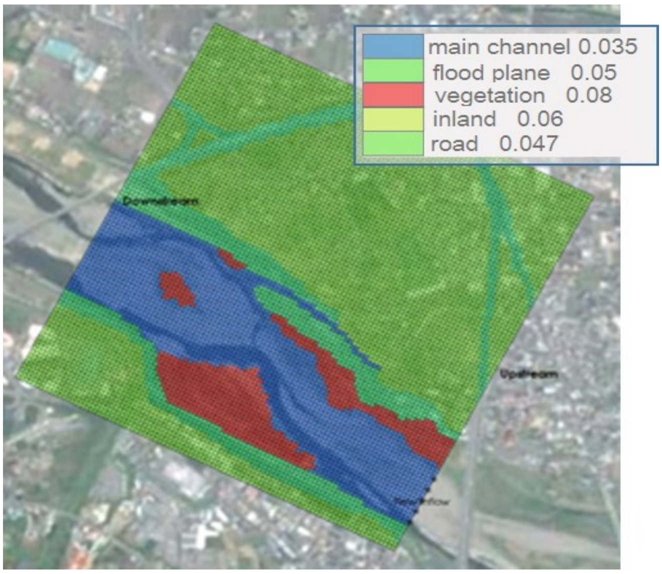

Figure 5. Distribution of Roughness Coefficient Around Ido Gasumi Dike.

4 RESULTS & DISCUSSIONS

4.1 Flood Plain with Time Variation

Inland Flood occurred at 15 hours 12 min (hydrograph in Figure 4) from the start of flooding. The flow discharge at this time was 1094 m^3/sec. Figure 6(a) shows the flood plain at this time. Water spread to the land from the open levee till the highway side embankment.

Water spread formed thin shape at 15 hour 55 min as shown in Figure 6(b) then the water spread headed to the north. After that, the water spread expanded till it stopped as shown in Figure 6(c) the maximum water spread was seen near cross point between open levee and Highway road. Figure 6(d) shows the final water spread after 25 hours.

Hazard map for the area surrounding the Ido Gasumi dike is shown in Figure 7. This hazard map was based on return period 150 years and reproduced by making simulation under the conditions of peak flow continues for a certain period of time. On the other hand, the flow discharge used in this simulation was based on the flow discharge at the time of flood occurrence in July 1943. This discharge was applied to adjust the permeability coefficient and ground water level. Therefore, the hazard map shown in Figure 7 was performed under discharge more than planned discharge in order to tell the difference between Figure 6.3 for areas under flood water depth of 0.5m. Furthermore, this study is not concerning with the northwest side of Highway, therefore this area was excluded from the analyzed study area. By applying these conditions, the area with flood water depth under 1.0 m to 2.0 m have the same profile of water spread where flood damage is significant. By comparing the two simulation results.in the area with flood water depth ranges from 2.0 m to 5.0 m, as this area has huge destruction according to the assumed hazard map. Similar results obtained from for the simulated flood area for the area with flood water depth higher than 2.0 m. So, the current analysis is based on the existing morphology is inferred as being with high accuracy. Therefore, by using the current analysis conditions, only geographic data are analyzed for flood after renovation by adjusting the stretching open levee.

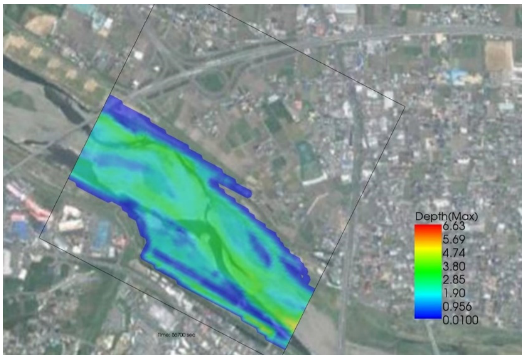

(a) Water Spread 15:12 (30th August, 2012)

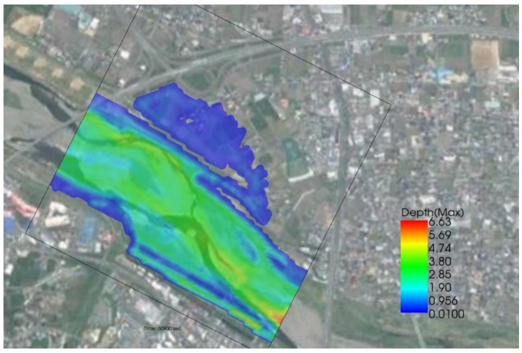

(b) Water Spread 15:55 (30th August, 2012)

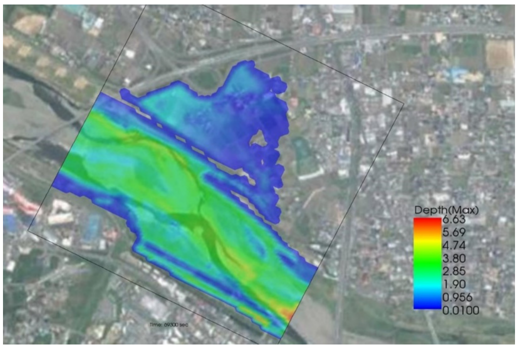

(c) Water Spread 17:50 (30th August, 2012)

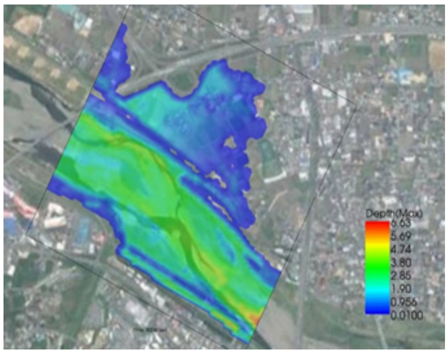

(d) Water Spread 17:00 (31th August, 2012)

Figure 6. Water Spread at Ido Gasumi Dike.

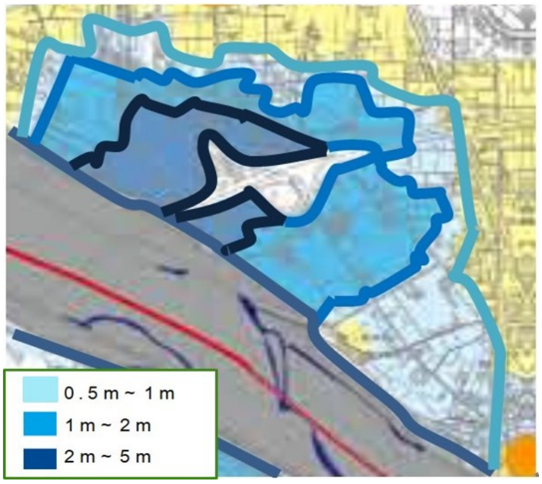

Figure 7. Hazard Map for the Area Surrounding Ido Gasumi Dike.

4.2 Flood Plain with Varying the Dike Dimensions

A result of flood analysis, in case of extending the dike 100 m, is shown in Figure 8(a). The profile is for the simulating area after 19 hours when the flood ended. The flood began after 40 min from the beginning of the simulation and it is noted that there is delaying in time compared to the current situation (i.e.no extended dike). Flood profiles along 2 m flood depth can be observed and flood plain area decreases compared to the current situation. However, the dike length is not effective for secure life and prevention of resident damage.

Figure 8(b) shows flood plain for the case of extending the dike length with 200 m. flood begin almost one hour later than the begin of the flood in the current situation. Flood plain area stop expansion after 19 hours and become in stable condition after 20 hours. It is obvious that the flood water depth is not exceeding 1m. However, flood plain area expands in large area and in case of occurrence of large typhoons and heavy rains, it will not be safe for human lives, private and public property.

Figure 8(c) shows flood plain for the case of extending the dike length with 300 m. Although there is no water spread by extending of dike, submerged flow still occurs. The returning effect didn't occur so the water depth increased as the flow discharge increased.

  / ISSN 1562-6865 (Online) - ISSN 1063-7710 (Print)

In order to keep water in the river channel only, the height of dike is modified and adjusted as submerged flow depth. Figure 8(d) shows the flood plain area after modifying the dike height. As a result, submerged flow and flood disappears and proper modification is obtained.

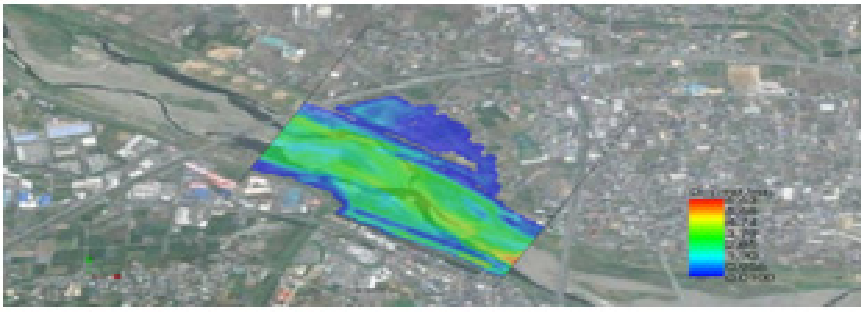

(a) Flood plain in case of extending the dike length 100m after 19 hours.

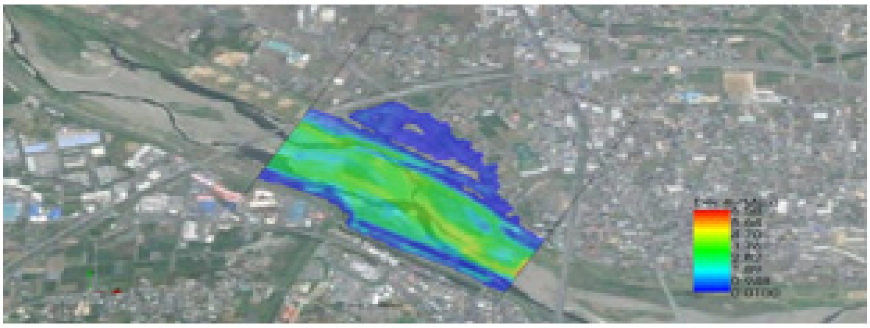

(b) Flood plain in case of extending the dike length 200m after 19 hours.

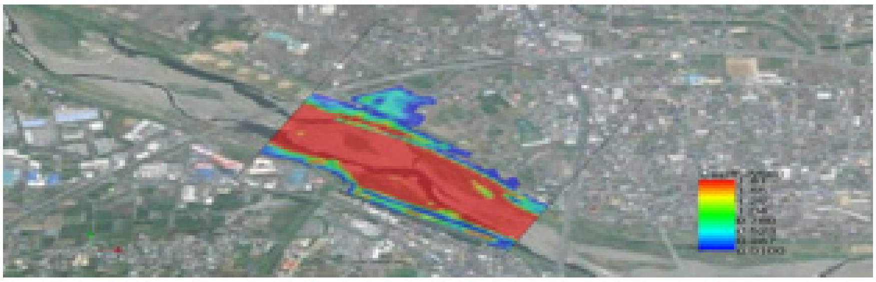

(c) Flood plain in case of extending the dike length 300m after 19 hours.

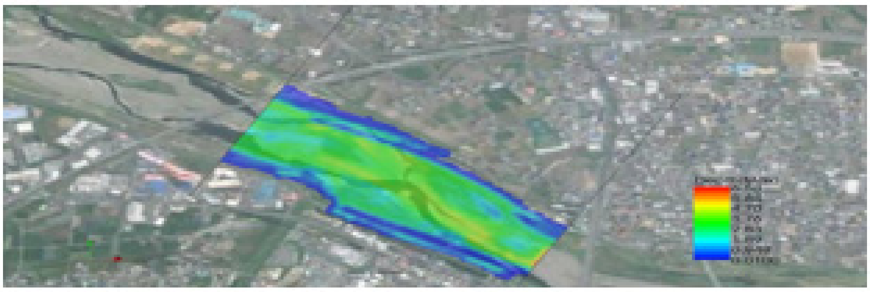

(d) Flood plain in case of extending the dike length with modification

Figure 8. Flood Plain With Different Sceneios

5 CONCLUSIONS

In the current study, flood risk analysis is done around the dike with assuming the peak discharge in Shigenobu River. Time variation of the flood plain area is analyzed based on two-dimensional shallow flow equation by extending the length and height of dike. If the expected peak discharge flow occurs, the flood disaster expands largely with water depth ranges from 2 m to 3 m which will be very hazardous. The flood analysis, in the current study, focuses on the flood from the river with open levee. However, the food inundation in the city area, because of the heavy rain and the typhoon, must be considered together. It is appeared that we should take the river ecosystem in consideration. It is better for future studies to concentrate on decreasing the runoff flow by using green infrastructures as green roofs, permeable pavement, grass channels and other green structures.

ACKNOWLEDGEMENTS

We appreciate the cooperation of Ministry of Land, Infrastructure and Transport, Matsuyama River National Highway Office for several data for river geophysical and flood discharge.

REFERENCES

Kawanaka, R. & Ishigaki, T. (2012). Flood Hazard Map Considered Timing and Criteria For Safe Evacuation, *Journal of JSCE*, B1 (Hydraulic Engineering), Vol.68, No.4, I_1081-I_1086.

Kobayashi, K., Takara, K. & Oku,Y. (2011), Development of an Integrated Model For Rainfall-Runoff / Flood Inundation Simulation And Economic Loss Estimation Focusing on Sayo town, Hyogo, Japan. *Journal of JSCE*, Vol. 55., pp.949-954.

Toshiyuki, T., Yasuyuki, S., Ichiro, K., & Toshiki, I. (2011), Historical transition of river training works and inundation characteristics in Sapporo, *Journal of JSCE*, Vol.67, No.4, I_8951-I_9002.

Uno, K., Nakano, S., Umeoka, H. & Watanabe, K. (2010), Preliminary report of heavy rainfall disaster caused by typhoon no.0909 a case study of Kuzaki district in Sayo town, *Journal of JSCE*, Vol. 54., 865-870.

Iwasa, Y., Inoue, K. & Mizutori, M. (1980). Hydraulic Analysis of Overland Flood Flows by Means of Numerical Method, *Buletin of the Disaster Prevention Research Institute*, Vol.B-2, No.23, 305-317.

RESEARCH ON THE HYDROLOGICAL PROCESSES OF LID-TYPE ROAD: THE CASE OF SHIYANG ROAD

YANFEN GENG (1), JIANDONG MAO (2) & ZHAOWEI WANG (3)

(1,2,3) Department of Harbor, Waterway and Coastal Engineering, School of Transportation, Southeast University, JiangSu,China
yfgeng@seu.edu.cn

ABSTRACT

With the rapid growth of impervious paving surfacing in the urban area, many cities are facing the inland flooding risk due to the global warming. To increase the resilience of cities under extreme storm weather, the design philosophy name Sponge City has been recently adopted by many China's cities during the upgrading of old areas or planning the land use of new districts. Thus, it is] of paramount important to evaluate the hydrological process from macro to micro scale. In this paper, a hydrodynamic model coupling ground runoff and water movement in drainage facilities is presented to simulate the hydrological process of the Shiyang road near Outer Qinhuai river in Nanjing. The results indicate that LID-type road could decrease the depth of surface runoff and narrow the ponding area due to the insufficient drainage capacities along the road, and the runoff coefficient of the zone is decreased about 10% by the implementation of permeable pavements, which means that LID-type road could be a sufficient method to mitigate water-logging and urban flood in urban road. It can be concluded that as an ongoing research, this paper demonstrates the capabilities of the coupled model in quantitatively evaluation of the LID-type road impact on hydrological process of small urban area with the improvement will be made for the investigation of large-scales.

Keywords: Hydrodynamic model; urban road; Low Impact Development (LID); coupled model.

1 INTRODUCTION

Many cities are suffering from urban floods more often than most due to extreme climate, reduction of natural surface retention capacity and inadequate design of drainage system, which caused tremendous loss of life and property every year around the world. The Indian city Chennai drenched with 1049 mm of rainfall due to the El Nino phenomenon, and more than 500 people had died of flood-related causes in November 2015. Beijing was hard hit by the worst rains in 61years on July 21, 2012, caused 10 billion yuan-worth of economic damage. Of 351 cities assessed by the Ministry of Housing and Urban-Rural Development of the People's Republic of China in 2010, about 62% of Chinese cities have suffered urban flood disasters. Therefore, it is urging to effectively control urban water-logging for reducing flood disaster risk and ensuring the safety and development of city.

The traditional idea of managing surface water runoff in an urban environment often referred to as conventional development (CD). The idea is to funnel that water away from cities as fast as possible to avoiding flood (CEI, 2003), which have focused on improving the city drainage network system and raising the drainage design standards. It is difficult for many Chinese cities to improve the poor drainage system in a short time as the economic cost and engineering amount are very huge. In contrast, known as "Sponge Cities," the new economy and environment friendly design aims to build up infrastructure to collect and reuse excess rainfall and integrate flood control in urban planning was proposed by scientists and politicians in China in recent years. A sponge city is one that can hold, clean, and drain water in a natural way using an ecological approach that a city can solve water problems instead of creating them. As a result, cities act like "sponges" will have the ability to use and control water resources far more effectively not only be able to deal with extra water, but also reuse rainwater to ease their thirst when there is not enough water. The similar concept is already established in many urban areas around the world on various scales through sustainable urban drainage systems (SUDS) in the UK (Scholz and Grabowiecki, 2007) and low impact development (LID) in Canada and the USA (Coffman, 2002).

In recent years, low impact development (LID), an innovative approach of land development and water management has gained popularity, a large number of studies have researched about LID. The principles of LID are as follows (PGCo, 1999; DoD, 2004):

- Take consideration of stormwater management in the stage of urban planning and design;
- Focus on prevention rather than mitigation and remediation;
- Develop environmentally sensitive design;
- Protect and develop natural water features and natural hydrologic functions;
- Reduce costs for the construction and maintenance of stormwater infrastructure;

Following LID principles, many studies have discussed on runoff reduction (peak and volume), infiltration increase and water quality enhancement (Hunt et al., 2010). The performance of LID practices is relatively well documented. Bioretention (or rain garden) systems are generally designed to collect the extra runoff and improve the water quality. Chapman and Horner (2010) evaluate the reduction of runoff volume and peak flow rate using bioretention systems by field investigation, which showed that the reduction is about 48 % to 74% of runoff volume. The reduction of metal in soil media and plant was also monitored in laboratory from simulated runoff events, about 88 % to 97 % reduction in soil media, and 0.5 % to 3.3 % in plant species (Sun and Davis, 2007). Permeable pavements include block pavers, plastic grid systems, porous asphalts, and porous concretes are designed to temporarily store surface runoff (Dietz, 2007). Hunt et al. (2002) demonstrated that about 75 % of rainfall were captured by the porous media, in a 2-year monitoring study of a permeable parking lot in North Carolina. Much literature discussed the performance of LID practices by field and laboratory monitoring, and simulation modeling also provides valuable insight to discover the clear information of LID practices. In recent years, a number of researchers have used a variety of modeling techniques to assess the effectiveness of LID practices in stormwater management. A two-dimensional variable saturated flow model was developed to simulate subsurface flow in bioretention facilities by He and Davis (2011). Model results indicate that the outflow volume via underdrain is less than the inflow; the flow peak is significantly reduced and delayed. A mathematical and statistical model based on a mass balance equation and an advection-dispersion transport for simulating contaminant removal from a surface sand filter is reported by Avellaneda et al. (2010).

This paper proposed a LID-type road in Nanjing Shiyang Road to mitigate urban water-logging. A hydrodynamic model coupling ground runoff and water movement in drainage facilities was presented to simulate the hydrological process of the study area in this study. It is significant to evaluate the effectiveness of LID-type road with the coupled model.

The depth of surface runoff and ponding area in different stages were simulated by coupled model, which show the performance of LID-type road clearly. The study also investigated the runoff coefficient of the study zone with permeable pavement, and then based on the investigated values to evaluate the proposed LID-type road to reduce storm water runoff. This study provided a new approach and important theoretical basis for relevant government departments to control urban water-logging in the future. This paper also demonstrated the potential application of the coupled approach in evaluation of the LID-type road impact on hydrological process of small urban area. It is expected that coupled model could be an important tool in the research of the performance of LID in the large-scales area.

2 LID PRACTICES

As an important functional part of urban area, the road lines connect the different area of urban and attract lots of people. The serious storm events always result in water-logging on the road surface cause a huge loss of property and life. With the rapid development of urbanization, the proportion of road area to urban area is about 15%-20% in China. The impervious urban roads change the natural hydrological cycling, which increase the flood disaster risk significantly. In this study, low elevation greenbelt and permeable pavement as the LID practices were applied in the Shiyang Road to reduce the negative influence of urban road on hydrological cycling.

The traditional road greenbelt as the permeable ground in urban road zone has little contribution on collecting extra road surface runoff. Most of road surface runoff is collected by sewer system through grate inlet on the side of the road. Road surface runoff cannot flow into greenbelt and infiltrate to groundwater easily because the traditional road greenbelt is usually higher than road surface. In this study the traditional greenbelt was replaced by low elevation greenbelt to collect and reuse the extra road surface runoff. In comparing to the traditional road greenbelt, the most important characteristic of the LID-type road greenbelt is its lower elevation and the opening curb which ensures surrounding rainwater could easily flow into the LID-type road greenbelt.

As the traditional road design, grate inlets provide a grate opening in the gutter or waterway, runoff on road surface have to be collected and drained away by sewer pipe system which are easily clogged by floating trash. In this study, the curb-opening inlets which can convey large quantities of water and debris were combined with low elevation greenbelt as a LID-type system to mitigate the water-logging on road.

Figure 1 shows the details of opening curb, the length of one curb is 1 m with height 0.15 m, the distance between curbs is about 0.3 m in this study.

Figure 2 shows a sketch of the proposed LID-type low elevation road greenbelt. The low elevation greenbelt's slope is set to not only slow down the velocity of runoff flowing into greenbelt to avoid destroying the plants in greenbelt, but also filter various trashes contained in stormwater. The overflowing well is set to avoid rainwater diffusing out of greenbelt when a storm exceeding design standard occurs. Rainwater will flow into the municipal drainage system automatically through overflow outlet once the level of rainwater in greenbelt exceeds the design impoundage level.

Figure 1. Details of opening curb

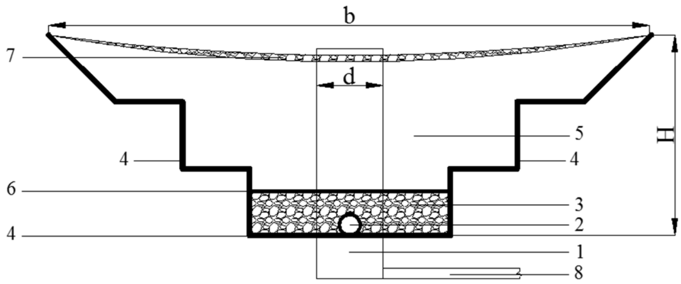

Figure 2. A sketch of low elevation greenbelt

1-overflowing well 2-collector pipe 3-gravel layer 4-waterproof geotextile
5-Improved soil layer 6-Permeable geotextile 7-Anti erosion layer
8-Transverse connecting pipe
b-width of bioretention ponds is 2m, H-height of bioretention ponds is 1.45m, d-diameter of overflowing well is 0.6m. The depth of greenbelt is about 15cm.

As a popular and efficient facility of LID technology, the permeable pavement was also applied in the bicycle lane of Shiyang Road project which could reduce runoff by allowing for retention and infiltration. Permeable pavements allow water to flow vertically through hard paved surfaces. It can be used as a substitute for impervious paving in areas such as parking lots and walkways, In addition to reducing runoff, this effectively traps suspended solids and filters pollutants from the water.

3 HYDRODYNAMIC MODEL

A two-dimensional hydrodynamic model coupling ground runoff and water movement in drainage facilities was presented to simulate the hydrological process of the zone.

The two-dimensional shallow water equations can be written in vector form as:

$$\frac{\partial \mathbf{U}}{\partial t}+\frac{\partial \mathbf{F}(\mathbf{U})}{\partial x}+\frac{\partial \mathbf{G}(\mathbf{U})}{\partial y}=\mathbf{B}(\mathbf{U}) \qquad [1]$$

Where x and y are the Cartesian coordinates; t is the time; $\mathbf{U}$ is the state vector; $\mathbf{F}$ and $\mathbf{G}$ are the x- and y-directional flux vector respectively; $\mathbf{B}$ is the source term vector. These vectors are defined as follows:

$$\mathbf{U}=(h,hu,hv)^T=(h,q_x,q_y)^T$$

$$\mathbf{F}=\left(hu,hu^2+\frac{1}{2}gh^2,huv\right)^T$$

$$\mathbf{G}=\left(hv,huv,hv^2+\frac{1}{2}gh^2\right)^T$$

$$\mathbf{B}=\left(0,gh\left(S_{0x}-S_{fx}\right),gh\left(S_{0y}-S_{fy}\right)\right)^T \qquad [2]$$

Where h is the water depth; u and v are x- and y- directional velocity components; $q_x=hu$ and $q_y=hv$ are the unit discharge in the x- and y- directions respectively; S_{0x} is the bottom slope and S_{fx} is the energy loss due to bottom friction along the x axis and similarly, S_{0y} and S_{fy} for the y axis. The friction slopes were evaluated using the Manning formula.

$$S_{fx}=\frac{ghm^2u\sqrt{u^2+v^2}}{h^{4/3}},S_{fy}=\frac{ghm^2v\sqrt{u^2+v^2}}{h^{4/3}}$$

$$S_{0x} = gh\frac{\partial z_b}{\partial x}, S_{0y} = gh\frac{\partial z_b}{\partial y} \quad [3]$$

The Eq.1 was solved using a finite volume method and Roe type approximate Riemann solver on unstructured meshes (Wang and Geng, 2013). A second order TVD scheme with the van Leer limiter was used in the space discretization and a two-step Runge-Kutta approach was used in the time discretization. The source terms of the bed slope were decomposed in the characteristic direction so that the numerical scheme can exactly satisfy the conservative property. This robust is shock capturing, and describes the hydraulic discontinuities accurately (e.g. shock waves over initially dry bed, and transition between subcritical and supercritical flows). Thus, it is particularly appropriate for simulating rainfall runoff on urban road.

The exchange flow rate between the ground and drainage facilities was calculated with weir formula

$$Q = mb\sqrt{2g}H_0^{3/2} \quad [4]$$

Where m is discharge coefficient, b is the width of weir, g is the acceleration of gravity, and H_0 is the water depth of the ground flow at the drainage facilities.

4 CASE STUDY

Shiyang Road in Nanjing was taken as a study case to evaluate the performance of coupled model. The length of Shiyang Road is 1604 m with width 45m near Outer Qinhuai River in Nanjing (Figure 3). The average rainfall of Nanjing is about 1034 mm per year, and the rainfall of June to August account for 45% of all-year rainfall. Nanjing often affected by heavy rain and unstable weather because of plum rain and typhoon. Low elevation greenbelt and permeable pavement are applied in Shiyang Road to ease the terrible situation of water-logging.

Figure 3. Location of Study area: Shiyang Road Nanjing China

The 2-year return period and 5-year return period rainfalls in Nanjing were selected as the rainfall input of the hydrodynamic model.The rainstorm intensity formula of Nanjing was calculated by Equation 5. :

$$i = \frac{A_1 + C \lg P}{(\mathrm{t} + b)^n} n A_1 \qquad [5]$$

Where: i ——rainstorm intensity, $mm/\min$;

t ——rainfall duration, min;

P ——return period, year;

n ——Rainstorm attenuation coefficient;

A_1、C、b ——region parameter

In Nanjing the rainstorm intensity formula is as follows:

$$i = \frac{17.92\left[1 + 0.57\ \lg\left(P - 0.09\right)\right]}{(\mathrm{t} + 13.45)^{0.79}} \qquad [6]$$

In this case, 2-year return rainfall and 5-year return rainfalls with 120 minutes duration's rainstorm intensity were calculated using Equation 6. The rainfall peak occurred at the start time, however it usually occurred at r=0.3~0.5t in the actual situation. Chicago Hydrograph Method as in Equation 7 was used to correct the hydrograph.

$$i_b = \frac{a[\frac{(1-n)t_b}{r} + \mathrm{b}]}{(\frac{t_b}{r} + b)^{n+1}}$$

$$i_a = \frac{a[\frac{(1-n)t_a}{1-r} + \mathrm{b}]}{(\frac{t_a}{1-r} + \mathrm{b})^{n+1}} \qquad [7]$$

Where: r is the rainfall peak time, i_b is the rainstorm intensity before peak time, i_a is the rainstorm intensity after peak time, t_a, t_b are the time intervals between peak time and rainfall duration. 2-year return rainfall and 5-year return rainfall with 120 minutes duration's rainstorm intensity calculated with Chicago Hydrograph Method is shown in Figure 4.

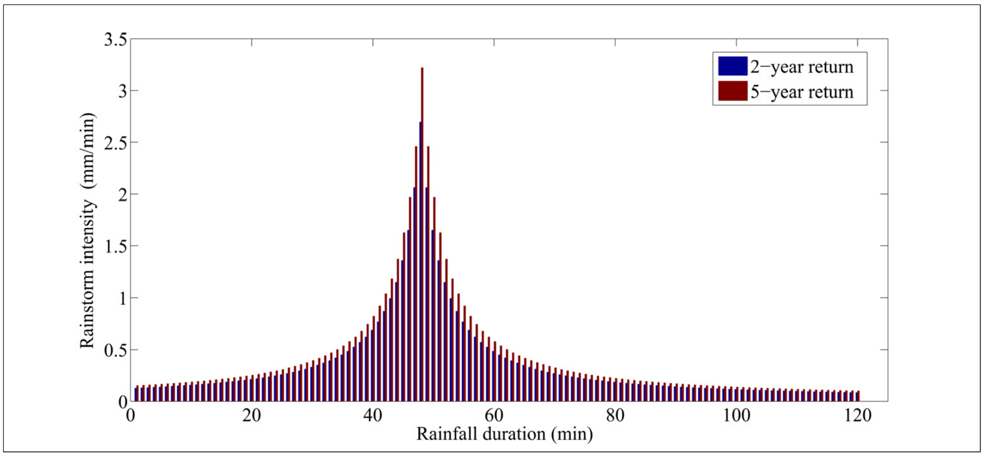

Figure 4. 2-year return period and 5-year return period rainfall with 120 minutes duration's rainstorm intensity calculated with Chicago Hydrograph Method

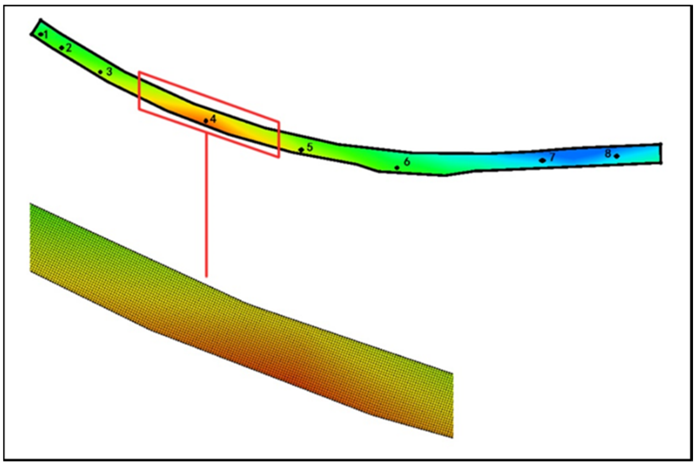

Figure 5. Details of study area and computational meshes

Construction of meshes is an essential and important step of mathematical simulation because hydrodynamics model is a disperse model, the mesh resolution has a significant impact on the quality of the simulation results. In this research, most domains are meshed in quadrilateral grid. Figure 5 shows details of study area and computational meshes.

In this study, 4 cases were taken to simulate the performance of different road designs and rainfall situations, as Table 1 shows.

Table 1. Details of 4 simulating cases

Case number	Road design and rainfall conditions
A	2-year return rainfall and traditional greenbelt with grate inlet
B	2-year return rainfall and low elevation greenbelt with curb-opening inlet
C	5-year return rainfall and traditional greenbelt with grate inlet
D	5-year return rainfall and low elevation greenbelt with curb-opening inlet

A series of simulations were carried out to evaluate the capabilities of the coupled approach in evaluation of the LID-type road impact on hydrological process of small urban area. After about 60 steps' calculation, the water level of complete hydrology process including incipient (about 20th min), peak(about 60th min) and recession stage (about 100th min) were presented.

The figures below show the 3 stages' flow field of road with LID-type greenbelt and normal greenbelt with 2-year return and 5-year return rainfall. As can be seen from Figure 6 and Figure 7, the LID-type greenbelt could reduce the water-logging area and depth significantly in every stage of hydrology process, which reduce the risk of flood disaster and traffic accident. The average water level of Case B and Case D with low elevation greenbelt and curb-opening inlet was about 0.005 m, about 90% reduction compared to the water level of Case A and Case C with traditional greenbelt and grate inlet. Most of the road surface runoff was collected by the low-elevation greenbelt, and has a close efficiency of reducing runoff of 2-year and 5-year return period rainfall. With the help of coupled model, the depth and area of water-logging could be simulated accurately and promptly, which could be applied to give much details of performance of LID practices.

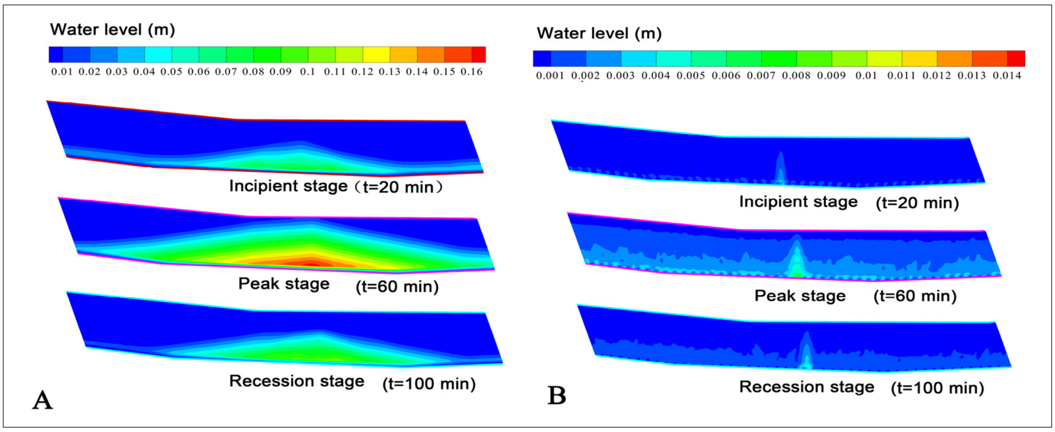

Figure 6. The flow field of Case A and Case B.

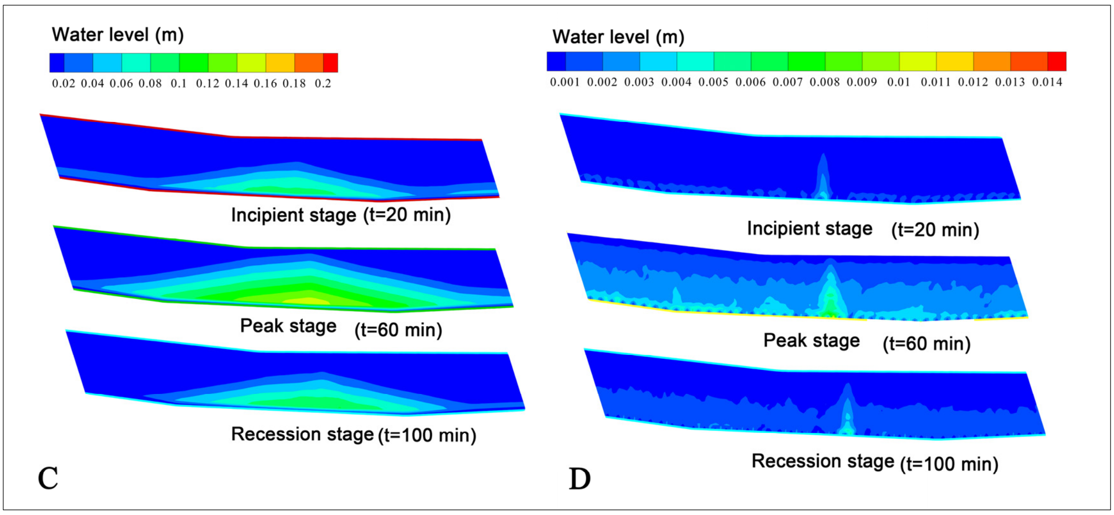

Figure 7. The flow field of Case C and Case D.

The simulation results of above 4 cases has showed that the coupled model could simulate the flow field of micro scale area such as road area very well. The coupled model could become a useful tool to assess the performance of LID facility.

The permeable pavement is applied widely to reduce runoff and mitigate water-logging efficiently. In this study, the performance of permeable pavement was evaluated with the analysis of runoff coefficient of the zone.

The comprehensive runoff coefficient was calculated as follows:

$$\varphi = \frac{\sum \varphi_n S_n}{\sum S_n}$$

Where: φ is comprehensive runoff coefficient; φ_n is the runoff coefficient of road component **n**; S_n is the area of road component **n**.

The runoff coefficient of normal road is as follows:

$$\varphi = \frac{\varphi_d F_d + \varphi_b F_b + \varphi_w F_w + \varphi_g F_g}{F_d + F_b + F_w + F_g} = 0.793 \qquad [8]$$

Where $\varphi_d = 0.95$ is the runoff coefficient of driveway; φ_b=0.95 is the runoff coefficient of bicycle lane; φ_w=0.6 is the runoff coefficient of walkway; $\varphi_g = 0.2$ is the runoff coefficient of Greenland. F_d=32769 m^2 is the area of driveway; F_b=9240 m^2 is the area of bicycle lane; F_w=9240 m^2 is the area of walkway; F_g=8151 m^2 is the area of green land.

The bicycle lane was replaced by the permeable pavement in this study, and the runoff coefficient of it is as follows. Where the φ_p=0.6 is the runoff coefficient of permeable pavement.

$$\varphi = \frac{\varphi_d F_d + \varphi_p F_b + \varphi_w F_w + \varphi_g F_g}{F_d + F_b + F_w + F_g} = 0.738 \qquad [9]$$

As can be seen from the above calculations, the application of permeable pavement could reduce the runoff coefficient about 10%, which could reduce the water-logging efficiently.

The results indicate that low elevation greenbelt with curb-opening inlet can achieve a high level of runoff reduction in 2-year return rainfall and 5-year return rainfall conditions. The runoff coefficient of study area was also assessed, which showed that the permeable pavement can reduce about 10% runoff coefficient.

5 CONCLUSIONS

In this study, a coupled model was presented to evaluate the performance of LID-type road in reducing urban flood. With the help of coupled model, the depth and area of water-logging were simulated, which could give technical support of planning and construction of LID-type road. The simulation results of LID-type road clearly showed that the LID-type road could narrow the depth and area of water-logging greatly. The performance of permeable pavements was also evaluated in this study which showed that the permeable pavements could reduce the runoff coefficient of road. The green infrastructure such as low-elevation greenbelt and permeable pavement could reduce the urban flood disaster risk efficiently. The capabilities of the coupled approach in evaluation of the LID-type road impact on hydrological process of small urban area was demonstrated in this paper, and the performance of coupled approach in large scales is also hopeful. There is a room for improvement of our coupled model to be applied in large scales area in the future.

REFERENCES

Avellaneda, P., Ballestro, T., Roseen, R. & Houle, J. (2010). Modeling Urban Storm-Water Quality Treatment: Model Development and Application to a Surface Sand Filter. *Journal of Environmental Engineering,* 136(1), 68–77.

Coffman, L. S. (2002). *Low-Impact Development: An Alternative Stormwater Management Technology. In R. L. France (Ed.), Handbook of Water Sensitive Planning and Design*. 2002, 97–124. Washington, D.C.: Lewis.

CEI (Comprehensive Environmental Inc.). (2003). *City Of Nashua, New Hampshire Alternative Stormwater Management Methods Planning And Guidance,* Final Report, Part 1, March.

Chapman, C. & Horner, R. R. (2010). Performance Assessment of a Street-Drainage Bioretention System. *Water Environment Research,* 82(2), 109–119.

Davis, A. P. & He, Z. (2011). Process Modeling Of Stormwater Flow in a Bioretention Cell. *Journal of Irrigation and Drainage Engineering,* 137(3), 121–131.

Dod (Department Of Defense). (2004). *The Low Impact Development Manual,* UFC-3-210-10.

Dietz, M. E. (2007). Low Impact Development Practices: A Review of Current Research and Recommendations for Future Directions. *Water, Air, And Soil Pollution,* 186, 351–363.

Hunt, W. F., Traver, R. G., Davis, A. P., Emerson, C. H., Collins, K. A. & Stagge, J. H. (2010). *Low Impact Development Practices: Designing To Infiltrate In Urban Environments. Effects of Urbanization on Groundwater.* Reston: ASCE, Environmental Water Resources Institute. 308–343 pp.

Hunt, W. F., Stephens, S. & Mayes, D. (2002). Permeable Pavement Effectiveness in Eastern North Carolina. *Proceedings of 9th International Conference on Urban Drainage*. ASCE. Portland, OR.

Pgco (Prince George’s County). (1999). *Low-Impact Development Hydrologic Analysis,* Maryland: Department Of Environmental Resources, Prince George’s County.

Scholz, M. & Grabowiecki, P. (2007). Review of Permeable Pavement Systems. *Building And Environment,* 42, 3830–3836.

Sun, X. L. & Davis, A. P. (2007). Heavy Metal Fates in Laboratory Bioretention Systems. *Chemosphere,* 66(9), 1601–1609.

Wang, Z. L. & Geng Y.F. (2013). Two-Dimensional Shallow Water Equations with Porosity and Their Numerical Scheme on Unstructured Grids. *Water Science & Engineering*, 6(1), 91-105.

HYDRAULIC PERFORMANCE OF SUBSURFACE DRAINAGE MODULE

MUHAMMAD MUJAHID MUHAMMAD(1), KHAMARUZAMAN WAN YUSOF(2),
MUHAMMAD RAZA UL MUSTAFA(3), NOR AZAZI ZAKARIA(4) & AMINUDDIN AB. GHANI(5)

(1,2,3)Department of Civil and Environmental Engineering,
Universiti Teknologi Petronas, Tronoh, Perak Darul Ridzuan, Malaysia
mujahidmuhammad8@gmail.com; akhamaruzaman.yusof@utp.edu.my, raza.mustafa@utp.edu.my
(4,5)River Engineering and Urban Drainage Research Centre (REDAC),
Universiti Sains Malaysia, Engineering Campus, Nibong Tebal, Pineng, Malaysia
redac01@usm.my; redac02@usm.my

ABSTRACT

This paper studies flow resistance through subsurface drainage modules, which can convey runoff and allow natural infiltration in waterways such as ecological swales. In this regard, experiments were performed using a new design of three (3) number single subsurface drainage modules arranged in parallel within a rectangular channel. The hydraulic performance of the subsurface module was determined in terms of the flow resistance and discharges of the upstream and downstream of the modules respectively. It was found that the upstream discharge was lowered in the range of 30.03% to 37.49%. This indicates the occurrence of flow attenuation especially when the bed slope was 1 in 500. Hence, the newly designed subsurface drainage module can be used in managing of stormwater runoff.

Keywords: Flow Resistance; Ecological Swales; Subsurface Drainage; Hydraulic Performance; Flow Attenuation.

1 INTRODUCTION

The knowledge of flow resistance through subsurface drainage module is of paramount importance. This is because inappropriate selection of Manning's n can cause module to be filled up quickly with less ability to infiltrate the peak runoff. This means flash flood may result in waterways with such module. Ecological subsurface drainage module is specially applied in pervious paving systems, drainage blanket for retaining structures and as an underground storage system for grass swale construction. In this study, more emphasis is given on its application in grassed swales, as currently practiced in Malaysia by River Engineering and Urban Drainage Center (REDAC), located at Universiti Sains Malaysia (USM), Engineering Campus, Pinang, Malaysia. In USM Engineering Campus, three types of ecological swales can be classified as Type A, Type B and Type C respectively, shown in Figures 1, 2 and 3, which depend on their sizes and capacities as well as the number of subsurface modules. The swale Type A consists of a single sub-surface module, swale Type B has two numbers of single sub-surface modules and swale Type C contains 3 numbers of single modules respectively (Zakaria et al., 2003). These ecological swales consists of grass-earthen channel, combined with subsurface modules enclosed within a permeable geotextile materials to manage both water quantity and quality control, which is known as best management practice (BMP).

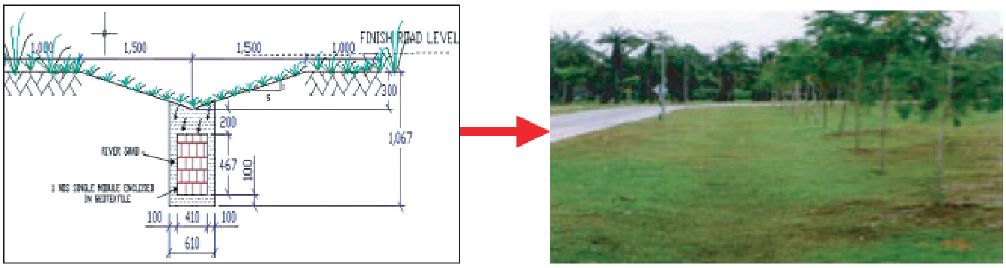

Figure 1. Typical cross section ecological swale Type A with example

Figure 2. Typical cross section ecological swale Type B with example

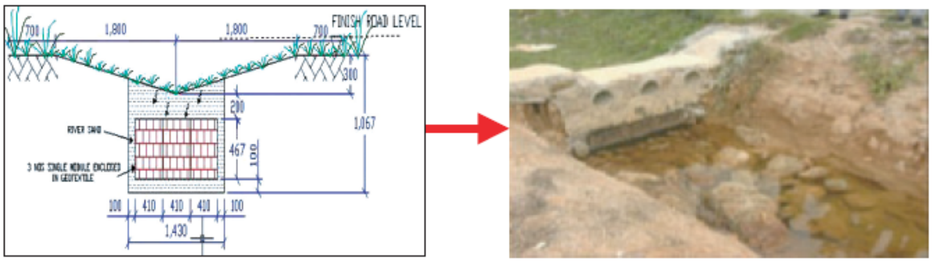

Figure 3. Typical cross section ecological swale Type C with example (outlet)

Field and Laboratory studies had been carried out to investigate the flow characteristics through the underground drains particularly for subsurface perforated pipe systems (Chiu and Shackelford, 2000; Barber et al., 2003; Ahmed et al., 1997; Abida et al., 2007). Among these, Barber et al. (2003) have developed an ecology ditch BMPs for stormwater using compost, sand and gravel build together with a perforated pipe drain, and they found out that for larger storms, the ecology ditch was able to achieve a peak reduction in the range of 10 to 50%. Also, Abida et al. (2007) performed some computer simulations for the hydraulic analysis of grassed swale and perforated pipe system. However, for the case of flow in modular channels or subsurface drainage modules, very few studies can be found in literature as its application is gradually being recognized as a conveyance system in stormwater management (Choo, 2011).

Table 1. Previous Studies on Subsurface Drainage Modules

Author (s)	Structure of Module	Remark
(Ab. Ghani et al., 2004, Sidek et al., 2002, Hin et al., 2010)		Pre-existing module at USM Engineering Campus ecological swales. Only preliminary results were reported by testing single module in the laboratory. However, Hin et al., 2010, examined the single module under field condition. It has dimension of 607 mm X 465 mm X 405 mm
(Lai et al., 2009, Kee et al., 2011)		Studied only parallel arrangement of single modules in the laboratory. It has dimension of 685 mm X 450 mm X 410 mm
Present Study		New design in internal structure, also three (3) single of such module were arranged in parallel and tested in the laboratory. It has dimension of 710 mm X 400 mm X 400 mm

 ©2017, IAHR. Used with permission / ISSN 1562-6865 (Online) - ISSN 1063-7710 (Print)

The only comprehensive analysis on modular channels were investigated by Sidek et al. (2002), Hin et al. (2010), and Kee et al. (2011), as illustrated in Table 1. Mohd Sidek et al. (2002) had investigated the flow profiles and hydraulic capacity of storage tank module applied in the bio-ecological drainage systems (BIOECODS) of USM; they found that the velocity distributions beside the modules are higher than the velocity profiles inside the modules. They concluded that the flow patterns in the module look like the flow distribution in between open channel and closed conduit, with more emphasis that the velocity distribution in the modules resembled that of a pipe flow. Similarly, Hin et al. (2010) carried out a case study on a small scale of Sustainable Urban Drainage System (SUDS), which consists of grassed swale with subsurface drainage module. The main objective of their study was to investigate the performance of subsurface drainage module in managing urban stormwater runoff in the catchment area. The results show that the subsurface drainage module is effective in reducing peak flow of surface runoff as well as in enhancing groundwater recharge in the study area. The subsurface drainage module was able to cater a percentage of surface runoff volume in the range of 15.2% to 20.5% for rainfall events of less than 6-month ARI. Additionally, Kee et al. (2011) modelled a subsurface modular channel in a laboratory. They deduced that the Manning's n was inversely proportional with the hydraulic parameters especially the velocity of flow.

However, with the above studies on modular channels, none of these researchers was able to study the hydraulic performance of flow through three (3) single modules which were newly designed. The previous researchers considered either single module or parallel arrangement of screen plates during their investigations. Thus, the aim of this study is to simultaneously examine the hydraulic characteristics in both upstream and downstream of the modular channel in order to evaluate its performance.

2 EXPERIMENTAL METHODS

The testing of the three (3) single modules was carried out in a rectangular re-circulating. Flume of dimensions 20 m length, 1.5 m width and 1 m deep, located in the new Hydraulics Laboratory of REDAC. The flume is composed of Perspex and metal materials on the side walls and bottom respectively. Hydraulic parameters, such as flow depth, flow velocity, and discharges were measured under uniform flow conditions. Water was pumped by using up to four (4) hydraulic pumps in order to vary the discharge. The flume was equipped with upstream screens to dampen the turbulence effect from the pump. The flume has a gate at the downstream for regulating of flow depths. The gate was adjusted using electric motor. Also, the bed slope of the flume was adjusted using an electric hydraulic press machine, which is located near the upstream end. Three slopes were fixed in this experiment that include 1/1000, 1/750 and 1/500 respectively. These slopes were chosen in order to replicate the existing slopes of the grassed swales in USM Engineering Campus, with particular attention on Type C grassed swale as it consists of three (3) single modules.

The rectangular re-circulating Flume was first tested without module to serve as a control, and to as well determine the length of uniform flow. Then, three (3) single modules were installed over the length of 5 m (between 10 m to 15m of the flume bed). Figures 4(a) & 4(b) show the structural design and coupling arrangements of the single modules used in this study respectively. Subsequently, the three (3) single modules consists of 21 number of single modules arranged in three (3) rows, with 7 single modules in each row arranged in parallel with each other. These modules were tied together using a rubber cable. Also, fly woods were used to support the modules from the uplift of water. Figure 4 (c) shows the modules within the flume, with an automatic flow meters installed at the upstream and downstream of the modules respectively.

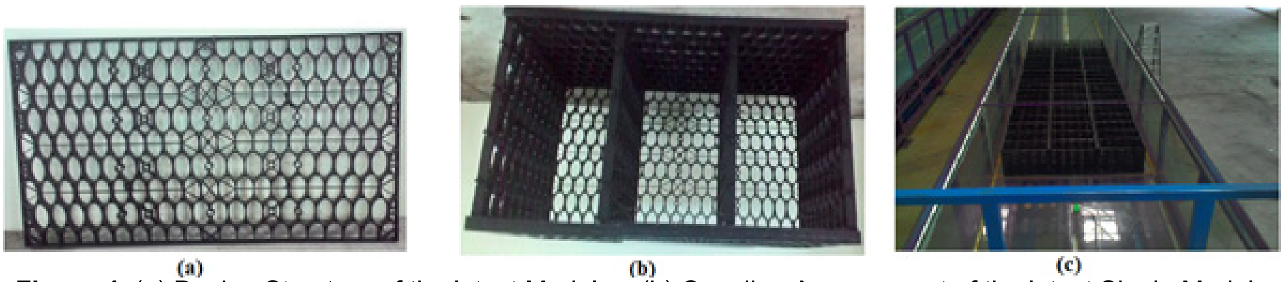

Figure 4. (a) Design Structure of the latest Modules, (b) Coupling Arrangement of the latest Single Module, and (c) Top View of the Modular Channel

Furthermore, experimental works begin when the flume gate was fully opened (GFO) and partially opened (GPO) respectively. In each case of GFO and GPO, the depth of flow was varied from 0.2 to 0.5 m, resulting in different discharges. Hydraulic data were collected in each experimental run, comprising of flow depth, flow velocity, and discharges using the Automatic Flow Meters located in the upstream and downstream of the test section. This process was repeated by changing the three (3) different slopes stated earlier. The performance of the subsurface drainage modules was determined in terms of flow attenuation. The flow attenuation was determined based on the percentage difference between the upstream and downstream discharges passing through three (3) single modules test section.

3 RESULTS AND DISCUSSIONS

1195 experimental data set of velocity, flow rate and flow depth were collected using the automatic flow meter for both flume without module (when the gate is fully opened - GFO, as well as gate partially opened - GPO) and modular channel (considering upstream and downstream of modules when the gate is fully opened (GFO), that is, under free flow condition only).

3.1 Data Collection

Table 2 shows the range of data collected in the laboratory, where n –values were calculated using Manning's equation (Chow, 1959). The hydraulic performance of the modular channel was determined by comparing the upstream and downstream discharges as given in Table 3, generally the slope 1 in 500 has the highest average percentage reduction of 37.49%, followed by that of 1 in 750 with 35.37% and lastly, 1 in 1000 with 30.03%.

Table 2. Range of Flow Parameters Collected in the Laboratory Experiments

	Flume without Module		*Modular Channel - Free Flow	
Flow Parameter	**Gate Fully Opened (GFO)**	**Gate Partially Opened (GPO)**	**Upstream**	**Downstream**
Flow Rate, Q (m3/s)	0.008 - 0.045	0.001 - 0.052	0.004 - 0.034	0.008 - 0.054
Velocity, V (m/s)	0.17 - 0.39	0.01 - 0.10	0.03 - 0.13	0.08 - 0.44
Flow Depth, Y (m)	0.02 - 0.08	0.01 - 0.39	0.07 - 0.18	0.01 - 0.08
Hydraulic Radius, R (m)	0.023 - 0.070	0.011 - 0.257	0.065 - 0.144	0.011 - 0.073
Channel Slope, S	0.001 - 0.002	0.001 - 0.002	0.001 - 0.002	0.001 - 0.002
Reynolds Number, Re	5401 – 27138	949 - 23154	3160 - 18676	3418 – 31951
Manning's Coefficient, n	0.011 - 0.026	0.017 - 0.201	0.067 - 0.206	0.011 - 0.068

***Free Flow refers to as when the gate was fully opened (GFO).**

Table 3. Comparison of Discharge for Upstream and Downstream in Modular Channel

	Slope		
Percentage Reduction of Q (%)	**1/1000**	**1/750**	**1/500**
Maximum	58.94	72.00	72.71
Minimum	2.52	6.60	6.89
Average	30.03	35.37	37.49

3.2 Upstream relationships of the modular channel

Figures 5 to 7 show the graphical relationships of rating curves and Manning's versus flow rates for the different slopes in the upstream position of the modules, which were compared with the flume free of modules under GFO and GPO respectively. For example, Figure 5 (a) demonstrate that when the gate is under GPO is similar to the effect of the module blockage, with Manning's values greater than modular channel and GFO as in Figure 5 (b), when the slope is 1 in 1000. The same trend was observed for the other slopes of 1 in 750 and 1in 500 respectively in Figures 6 and 7, except that the Manning's values are very high when the slope is 1 in 500 compared to rest of the slopes, this is also obvious in Figure 8 where all slopes were compared.

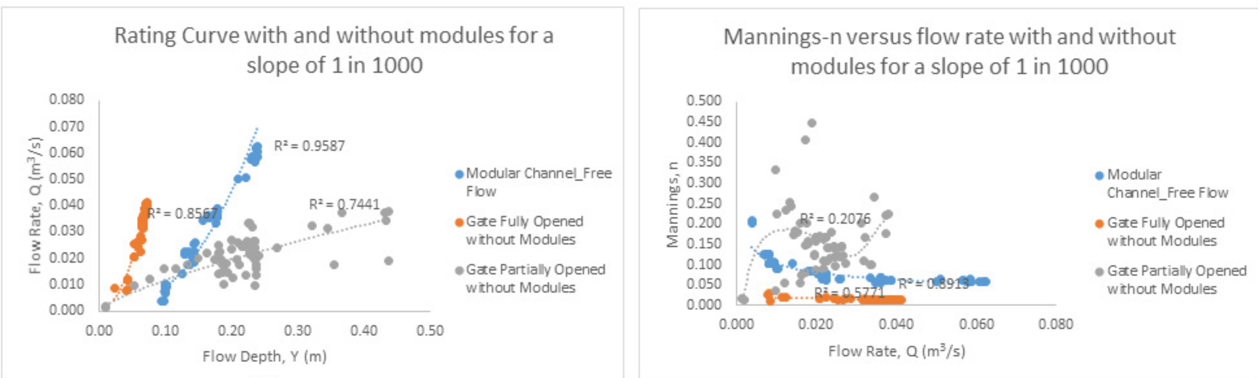

(a) (b)

Figure 5. (a) Rating curves (b) Manning's versus flow rate for 1 in 1000 slope

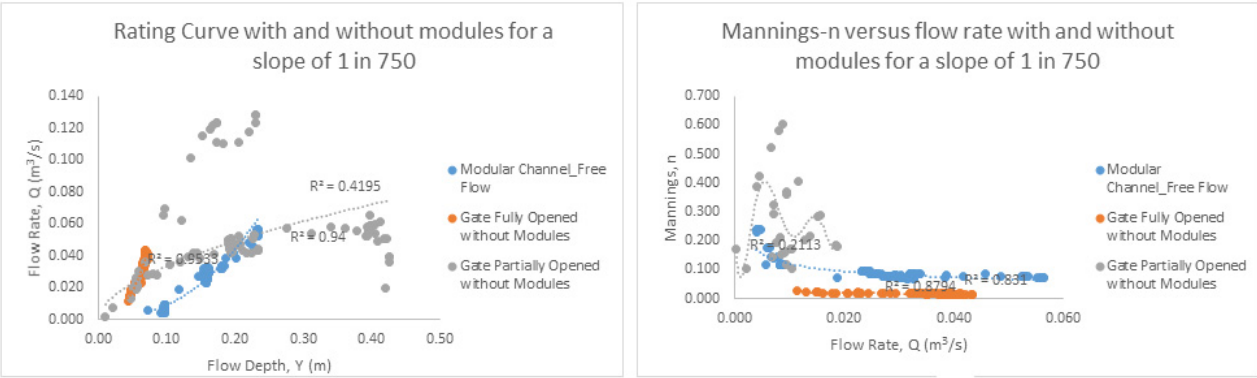

(a) (b)

Figure 6. (a) Rating curves (b) Manning's versus flow rate for 1 in 750 slope

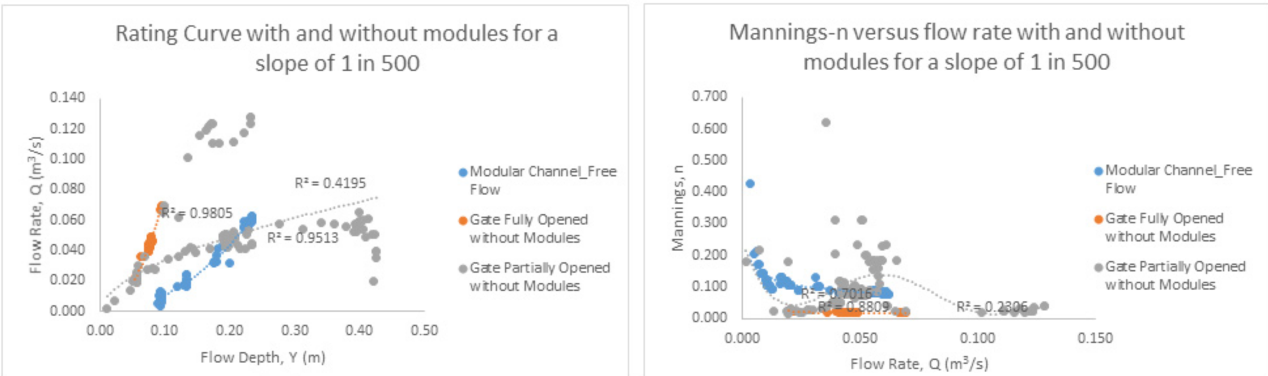

(a) (b)

Figure 7. (a) Rating curves (b) Manning's versus flow rate for 1 in 500 slope

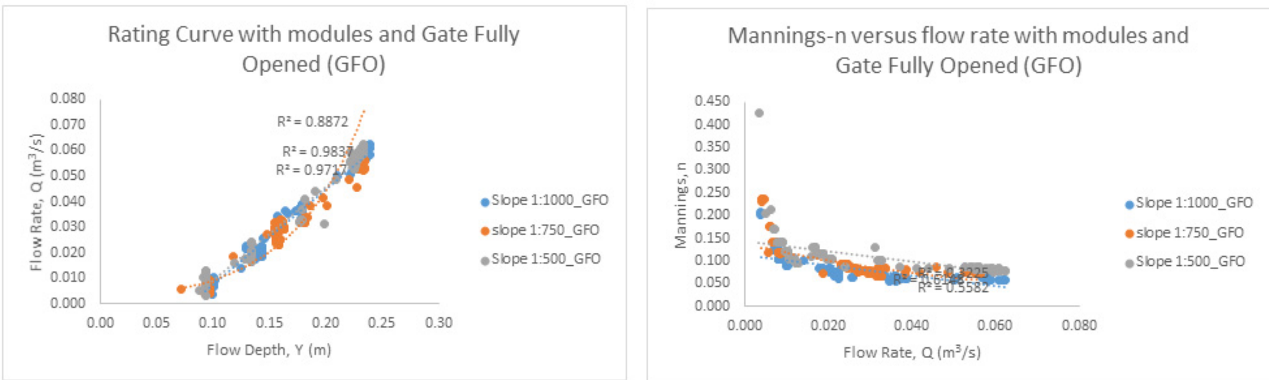

(a) (b)

Figure 8. Comparison of (a) Rating curves (b) Manning's versus flow rate for all the slopes

3.3 Downstream relationships of the modular channel

The same trends were observed in the downstream, as the case of the upstream relationships above, however, for the downstream relationships, both the rating curves and the variations of Manning's with flow rate do overlap especially with the curves of modular channel under free flow and that of GFO, only the curves of GPO deviated from the modular channel and GFO, as can be seen in Figures 9 to 12.

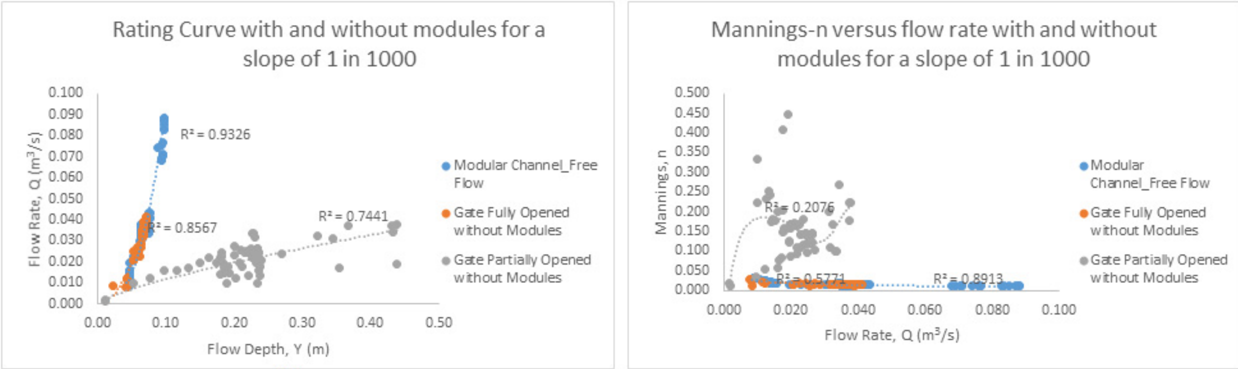

(a) **(b)**

Figure 9. (a) Rating curves (b) Manning's versus flow rate for 1 in 1000 slope

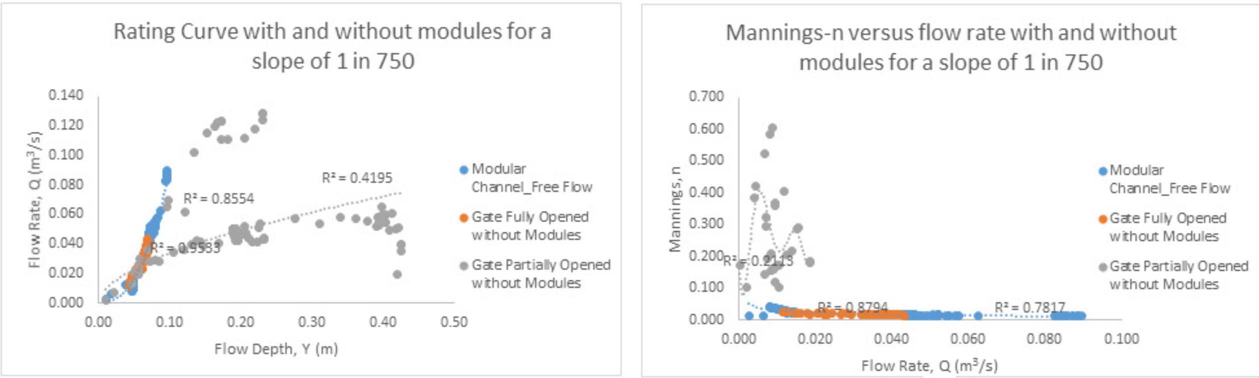

(a) **(b)**

Figure 10. (a) Rating curves (b) Manning's versus flow rate for 1 in 750 slope

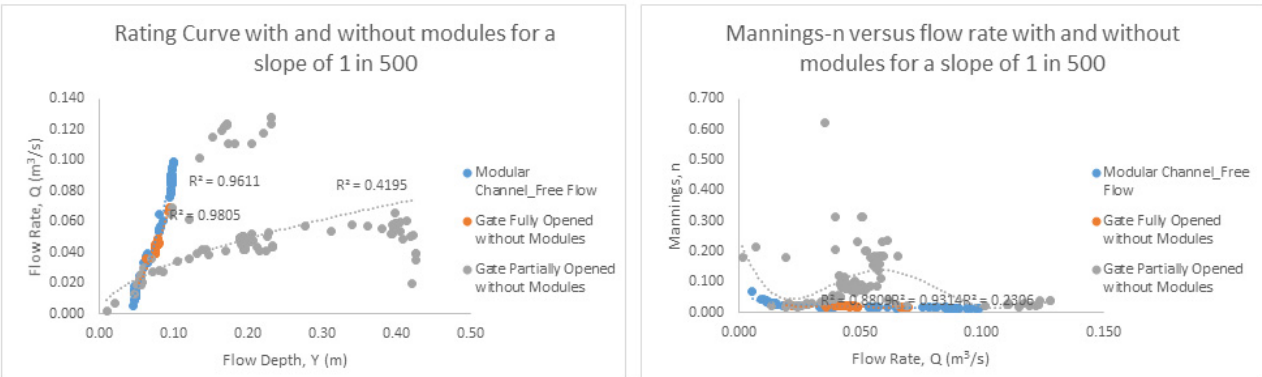

(a) **(b)**

Figure 11. (a) Rating curves (b) Manning's versus flow rate for 1 in 500 slope

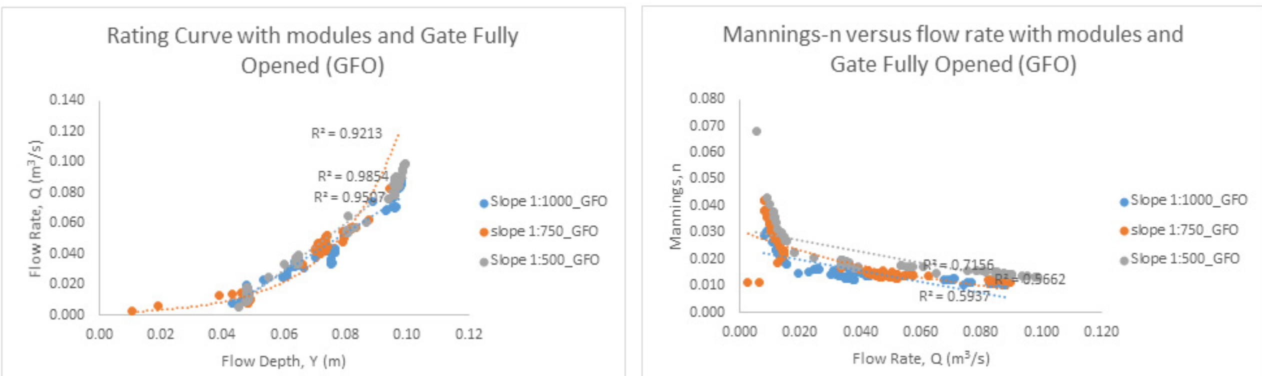

(a) **(b)**

Figure 12. Comparison of (a) Rating curves and (b) Manning's versus flow rate for all the slopes

3.4 Comparison of upstream and downstream relationships of the modular channel

Figures 13, 14 and 15 show the graphical comparison of upstream and downstream for 1/1000, 1/750 and 1/500 slopes, in terms of rating curves and Manning's versus flow rate. In each case, the rating curve for the downstream is steeper compared to that of upstream, showing that, the discharge values in the upstream were less than that in the downstream. This is as a result of the blockage effect of the module upstream of the flow direction. Conversely, the Manning's values tend to be much higher in the upstream compared to the downstream, and this is true for all the slopes.

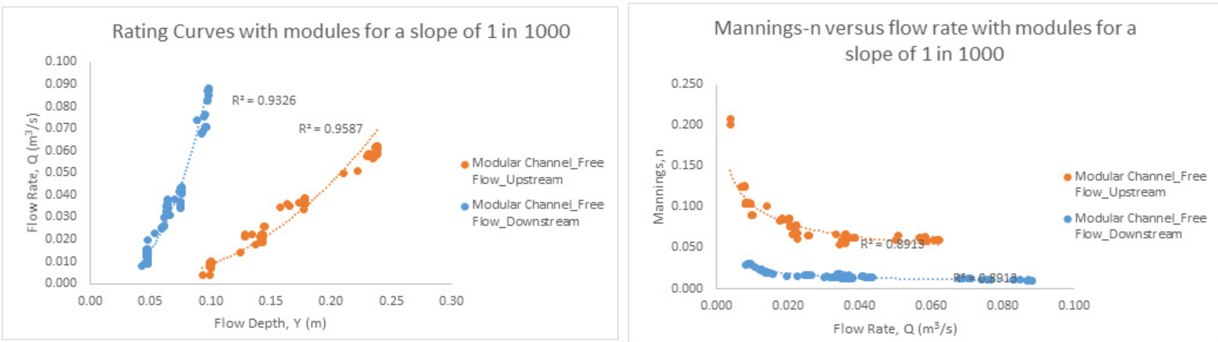

(a) (b)

Figure 13. Comparison of (a) Rating curves (b) Manning's versus flow rate for 1 in 1000 slope

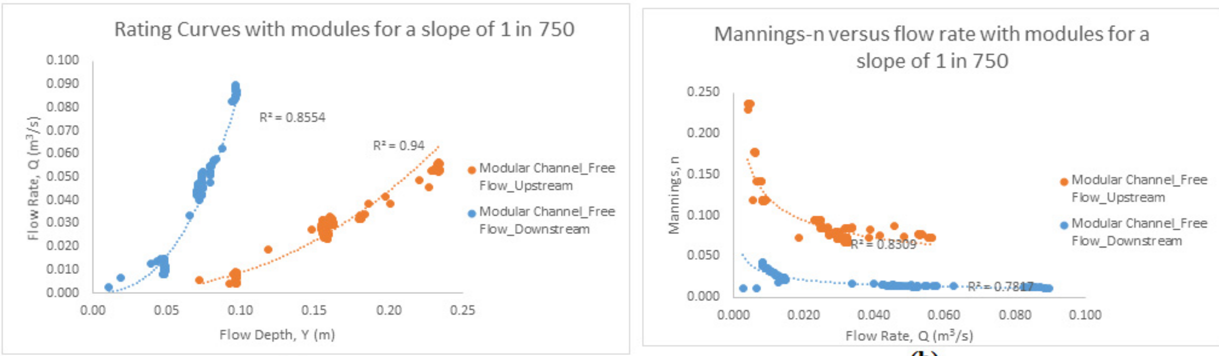

(a) (b)

Figure 14. Comparison of (a) Rating curves (b) Manning's versus flow rate for 1 in 750 slope

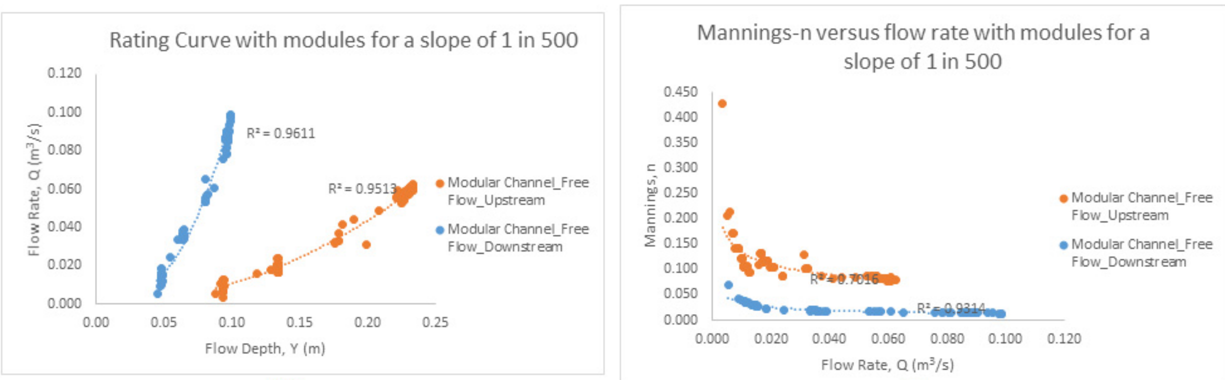

(a) (b)

Figure 15. Comparison of (a) Rating curves (b) Manning's versus flow rate for 1 in 500 slope

4 CONCLUSIONS

From the experimental results obtained, it follows that subsurface module tested herein is able to lower the average discharge of the upstream in the range of 30.03% to 37.49%, which designate flow attenuation has occurred as the water moves from upstream to downstream end of the module. Also, this shows improvement compared to the previous studies by (Hin et al., 2010). Hence, the newly designed module is recommended for use in drainage systems for sustainable stormwater management. Lastly, further study on subsurface drainage module to investigate flow parameters together with dissolve oxygen (DO) is required in order to have comprehensive data and a reliable approach for the eco-hydraulics of flow through modular channels.

ACKNOWLEDGEMENTS

The research reported herein is funded by Ministry of Education under HiCOE's niche area Sustainable Urban Stormwater Management, River Engineering and Urban Drainage Research Centre (REDAC), Universiti Sains Malaysia (No. 311.PREDAC.4403901). The researcher firstly would like to thank Universiti Teknologi Petronas for fellowship award to undertake the post graduate study.

REFERENCES

Ab. Ghani, A, Zakaria, N.A., Abdullah, R., Yusof, M.F., Mohd Sidek, L., Kassim, A.H. & Ainan, A. (2004). Bio-Ecological Drainage System (BIOECODS): Concept, Design and Construction. *Internariond Conference on HydroScience and Engineering*, Brisbane, Australia.

Abida, H., Sabourin, J.F. & Ellouze, M. (2007). ANSWAPPS: Model for the analysis of grass swale-perforated pipe systems. *Journal of Irrigation and Drainage Engineering,* 133(3), 211-221.

Ahmed, Z., White, T. & Kuczek, T. (1997). Comparative Field Performance of Subdrainage Systems. *Journal of Irrigation and Drainage Engineering,* 123(3), 194-201.

Barber, M.E., King, S.G., Yonge, D.R. & Hathhorn, W.E. (2003). Ecology Ditch: A Best Management Practice for Storm Water Runoff Mitigation. *Journal of Hydrologic Engineering,* 8(3), 111-122.

Chiu, T.-F. & Shackelford, C. D. (2000). Laboratory Evaluation of Sand Underdrains. *Journal of geotechnical and geoenvironmental engineering,* 126(11), 990-1001.

Choo, K.L. (2011). Determination of Flow Resistance in Modular Open Channel. *MSc Thesis*, Universiti Sains Malaysia.

Chow, V. T. (1959). *Open Channel Hydraulics*. New York: McGraw-Hill.

Hin, L.S., Choo, K.L., Zakaria, N.A., Aminuddin, A.G. & Kiat, C.C. (2010). Subsurface Drainagemodule Performance Study in Managing Urban Stormwater (Case Study: Taiping Health Clinic Type 2). *World Engineering Congress 2010: Conference on Natural Resources and Green Technology, Kuching, Sarawak, Malaysia.*

Kee, L.C., Zakaria, N.A., Lau, T.L., Chang, C.K. & Ab. Ghani, A. (2011). Determination of Manning's N for Subsurface Modular Channel. R*ivers 2011 Penang, Malaysia.*

Lai, S.H., Kee, L.C., Zakaria, N.A., Ab. Ghani, A., Chang, C.K. & Leow, C.S. (2009). Flow Pattern and Hydraulic Characteristic for Subsurface Drainage Module. *International Conference on Water Resources (ICWR 2009), Bayview Hotel, Langkawi, Kedah, Malaysia.*

Sidek, L.M., Tak, E.K., Ab. Ghani, A., Zakaria, N.A. & Abdullah, R. (2002). Bio-Ecological Drainage Systems (Bioecods): An integrated approach for urban water environmental planning. *Seminar on Water Environmental Planning: Technologies of Water Resources Management*.

Zakaria, N.A., Ab Ghani, A., Abdullah, R., Mohd. Sidek, L. & Ainan, A. (2003). Bio-Ecological Drainage System (BIOECODS) for Water Quantity and Quality Control. *International Journal of River Basin Management,* 1(3), 237-251.

QUANTIFYING THE ROLE OF VEGETATION IN DISASTER RISK REDUCTION MEASURES, FROM ACADEMIC RESEARCH TO PRACTICAL IMPLEMENTATION OF GREEN INFRASTRUCTURES

W. ELLIS PENNING[(1)]

[(1)] Deltares, Boussinesqweg 1, 2600 MH Delft, The Netherlands,
ellis.penning@deltares.nl

ABSTRACT

Globally, there is an increasing number of applications of nature based solutions for disaster risk reduction. These measures can include, for example, the restoration of mangrove forests, saltmarshes and coastal swamps to reduce coastal erosion and wave impact during extreme events. Besides, flood risk reduction in riverine systems benefits from nature based management solutions such as the ‘Room for the River’ type of measures and increases the capacity for water storage in floodplains and adjacent areas. In cities, green infrastructures such as bioswales, instream wetlands and green roofs are also showing their use in alleviating challenges related to water management. All these natures based strategies have in common that vegetation is part of the solution. In order to be assured that the solution is functional both in the current situation and throughout its life time, it is needed to better understand the dynamics of this vegetation and the influence of the vegetation on the hydrodynamics and morphodynamics in the area of interest. A proper quantification of vegetation and its interaction with hydrodynamics and sediment dynamics is thus needed, both in time and space. The first step in this process is commonly done in laboratory studies using flume studies and is linked to model development to be able to upscale and quantify the expected effect of this vegetation on flow and morphodynamics. Validation using field data is another valuable source of data to help in improving model development, as vegetation-related processes are difficult to be scaled down to laboratory settings. Challenges arise in taking the step from this academic research to day-to-day management and implementation of this knowledge in practice for disaster risk reduction. However, ensuring a clear dialog between science and practitioners can overcome the potential pitfalls in the process of implementing Nature Based Solution. In this presentation, examples are used from around the world for both coastal and inland solutions in which vegetation was used to reduce flood-related risks and how the functioning of the vegetation for this reduction was quantified. Linking the need for academic research to how this knowledge can be used in day-to-day water management is discussed, with an emphasis on green solutions for flood related disaster risk reduction.

Keywords: Green Infrastructure (GI); green solution; morphodynamics; room for the river; disaster risk reduction.

REFERENCES

Baptist, M.J., Penning, W.E., Duel, H., Smits, A.J.M., Geerling, G.W., Van der Lee, G.E.M. & Van Alphen, J.S.L. (2004). Assessment of the Effects of Cyclic Floodplain Rejuvenation on Flood Levels and Biodiversity along the Rhine River. *River Research and Applications*, 20(3), 285–297, http://doi.org/10.1002/rra.778.

Baptist, M.J., Babovic, V., Rodríguez Uthurburu, J., Keijzer, M., Uittenbogaard, R.E., Mynett, A. & Verwey, A. (2007). On Inducing Equations for Vegetation Resistance. *Journal of Hydraulic Research*, 45(4), 435–450.

Baptist, M.J., Haasnoot, M., Cornelissen, P., Icke, J., Van Der Wedden, G., De Vriend, H.J. & Gugić, G. (2006). Flood Detention, Nature Development and Water Quality along the Lowland River Sava, Croatia. *Hydrobiologia*, 565(1), 243–257, http://doi.org/10.1007/ s10750-005-1917-3.

Blackwell, M.S.A. & Maltby, E.E. (2005). *EcoFlood Guidelines: How to Use Floodplains for Flood Risk Reduction. Ecosystems*, http://levis.sggw.waw.pl/ecoflood/.

Cohen-Shacham, E., Walters, G., Janzen, C. & Maginnis, S. (2016). *Nature-Based Solutions to Address Global Societal Challenges*, International Union for Conservation of Nature, Gland, Switzerland, 97, http://dx.doi.org/10.2305/IUCN.CH.2016.13.en.

Geerling, G.W., Kater, E., van den Brink, C., Baptist, M.J., Ragas, A.M.J. & Smits, A.J.M. (2008). Nature Rehabilitation by Floodplain Excavation: The Hydraulic Effect of 16 Years of Sedimentation and Vegetation Succession along the Waal River, NL. *Geomorphology*, 99(1–4), 317–328, http://doi.org/10.1016/j.geomorph.2007.11.011.

Johnson, M.F., Thomas, R.E., Dijsktra, J.T., Paul, M., Penning, W.E. & Rice, S.P. (2014). *Using Surrogates, Including Scaling Issues, in Laboratory Flumes and Basins.* In: Frostick, L.E., Thomas, R.E., Johnson, M.F., Price, S.P., McLelland, S.K. (eds). Users Guide to Ecohydraulic Modelling and Experimentation: Experience of the Ecohydraulic Research Team (PISCES) of the HYDRALAB Network CRC Press/Balkema, Leiden, The Netherlands, IAHR Design Manual. 23-41.

McKenna, D., Krüger, I. & Hinzmann, M. (2015). *Coastal Protection and Sustainable Urban Drainage Systems – Nature-Based Solutions*. ReCreate Policy Brief No. 4, www.recreate-net.eu.

Möller, I., Kudella, M., Rupprecht, F., Spencer, T., Paul, M., van Wesenbeeck, B. K. & Schimmels, S. (2014). Wave Attenuation over Coastal Salt Marshes under Storm Surge Conditions. *Nature Geoscience*, 7(10), 727–731, http://doi.org/10.1038/ngeo2251.

Narayan, S., Beck, M.W., Reguero, B.G., Losada, I.J., van Wesenbeeck, B., Pontee, N., Sanchirico, J.N., Ingram, J.C., Lange, G.-M. & Burks-Copes, K.A. (2016). The Effectiveness, Costs and Coastal Protection Benefits of Natural and Nature-Based Defences. *PloS One*, 11(5), http://doi.org/10.1371/journal.pone.0154735.

Penning, W.E. & Duel, H. (2004). Water Storage: New Solutions for Water Surplus and Shortage in a Small Engineered Country? *Journal of Water and Land Development*, 8, 63–74.

Smolders, S., Plancke, Y., Ides, S., Meire, P. & Temmerman, S. (2015). Role of Intertidal Wetlands for Tidal and Storm Tide Attenuation along a Confined Estuary: A Model Study. *Natural Hazards and Earth System Sciences*, 15(7), 1659–1675, http://doi.org/ 10.5194/nhessd-3-3181-2015.

Vuik, V., Jonkman, S.N., Borsje, B.W., Suzuki, T., Kratzer, I. & Bouma, T.J. (2016). Nature-Based Flood Protection: The Efficiency of Vegetated Foreshores in Reducing Wave Loads on Coastal Dikes. *Coastal Engineering*, 116, 42–56, http://doi.org/10.1016/j.coastaleng.2016.06.001.

Vandenbruwaene, W., Temmerman, S., Bouma, T.J., Klaassen, P.C., De Vries, M.B., Callaghan, D.P., van Steeg, P., Dekker, F., van Duren, L.A., Martini, E., Balke, T., Biermans, G., Schoelynck, J. & Meire, P. (2011). Flow Interaction with Dynamic Vegetation Patches: Implications for Biogeomorphic Evolution of a Tidal Landscape. *Journal of Geophysical Research: Earth Surface*, 116(F1), http://doi.org/10.1029/2010JF001788.

Van Wesenbeeck, B.K., de Boer, W., Narayan, S., van der Star, W.R.L. & de Vries, M.B. (2016). Coastal and Riverine Ecosystems as Adaptive Flood Defenses under a Changing Climate. *Mitigation and Adaptation Strategies for Global Change*, 1–8, http://doi.org/ 10.1007/s11027-016-9714-z.

World Business Council for Sustainable Development (WBCSD). (2017). *Incentives for Natural Infrastructure*, www.wbcsd.org.

Zong, L. & Nepf, H. (2010). Geomorphology Flow and Deposition in and around a Finite Patch of Vegetation. *Geomorphology*, 116(3–4), 363–372, http://doi.org/10.1016/j.geomorph. 2009.11.020.

